

**Implications of leaf anatomy and
stomatal responses in the *Clusia* genus
for the evolution of Crassulacean Acid
Metabolism**

To those who believe in science as a tool for a better future

Declaration

I hereby certify that this thesis is the result of my own investigations and that no part of it has been submitted for any degree other than the Doctor of Philosophy at the University of Newcastle upon Tyne. All references to the work of others are duly acknowledged.

V. Andrea Barrera Z.

Victoria Andrea Barrera Zambrano

Table of Contents

Acknowledgments	11
Abbreviations	12
Abstract	15
Chapter 1: Introduction	16
1.1 The Clusia genus	17
1.2 CAM evolution.....	22
1.2.1 Evolution of CAM in Clusia.....	23
1.3 Crassulacean Acid Metabolism.....	25
1.3.1 Carbohydrate metabolism and enzyme control in the CAM pathway	29
1.3.2 Circadian control and plasticity of the CAM pathway	31
1.3.3 Water Use Efficiency	35
1.3.4 Leaf anatomy	36
1.3.4.1 Stomatal size and density and functions	38
1.4 Photoreceptors.....	40
1.4.1 Cryptochromes (cry)	40
1.4.2 Phototropins (phot)	42
1.4.3 Phytochromes (phy)	44
1.4.4 Photoreceptors and the circadian clock.....	46
1.5 Aims of thesis and hypotheses to be tested.....	47
Chapter 2: Functional leaf anatomy of Clusia.....	48
2.2 Materials and Methods.....	51
2.2.1 Plant Material	51
2.2.2 Gas exchange profiles	55
2.2.3 Leaf anatomy and stomatal characteristics	55
2.2.4 Protein extraction and western blotting.....	58

2.2.4.1 Protein extraction	58
2.2.4.2 Discontinuous SDS – PAGE.....	58
2.2.4.3 Western blotting	59
2.2.5 Immuno-labelling for PEPC and Rubisco in leaf sections	60
2.2.6 Statistical Analysis	61
2.3.1 Gas exchange profiles	62
2.3.1.1 Degree of CAM and relationship to specific leaf area (SLA) and instantaneous water use efficiency (WUE)	62
2.3.2 Leaf Anatomy.....	69
2.3.2.1 Leaf tissue characteristics and implications for the degree of CAM	69
2.3.2.2 Stomatal size and density and photosynthetic mode.....	78
2.3.3.1 Abundance of PEPC and Rubisco proteins	85
2.4 Discussion.....	87
2.4.1 Leaf anatomy and implications for the degree of CAM in Clusia	87
2.4.2 Anatomical traits and implications for internal CO ₂ conductance.....	89
2.4.3 Localization of carboxylases	90
2.4.4 Stomatal size and density and photosynthetic physiology in Clusia.....	91
Chapter 3: Stomatal Responses to Light in C ₃ and CAM species of Clusia	93
3.1 Introduction	93
3.2 Materials and methods	96
3.2.1 Gas exchange under different light regimes.....	97
3.2.2 Speed of response of stomata to changes in light intensity.....	97
3.3 Results	98
3.3.1 Gas exchange profiles under different light regimes	98
3.3.2 Speed of response of stomata to light	107
3.3.3 Stomatal guard cell chloroplasts	110
3.4 Discussion	111

3.4.1. Circadian control of stomatal conductance is more robust in the CAM Clusia compared to the C3 Clusia	111
3.4.2. Circadian control of stomatal conductance is mediated via photosynthesis and by photoreceptors in Clusia.....	112
3.4.3. Water use efficiency is altered under constant light regimes in CAM Clusia (<i>C. rosea</i>)	115
3.4.4 Stomata of the CAM Clusia responded faster to changes in PFD imposed during the photoperiod compared to the C3 Clusia.....	116
Chapter 4: Circadian regulation of the expression of photoreceptors in a C3 and CAM species of Clusia.....	118
4.1 Introduction	118
4.2 Materials and methods	122
4.2.1 Plant material	122
4.2.2 Experimental set up: Light Treatments	122
4.2.3 Genes selection and primers design	122
4.2.4 RNA extraction	124
4.2.5 Sequencing of photoreceptors	126
4.2.6 Reverse Transcriptase Polymerase Chain Reaction (RT-PCR)	127
4.2.7 Real time PCR.....	129
4.2.8 Titratable acidity	131
4.3 Results	132
4.3.1 DNA sequences of photoreceptors.....	132
4.3.2 Gene expression	133
4.3.2.1 Phot1.....	133
4.3.2.2 Phot2.....	133
4.3.2.3 Cry 2.....	133
4.3.2.4 PhyA.....	134
4.3.4 Real time PCR.....	139
4.3.5 Titratable acidity	141

4.4 Discussion	144
4.4.1 Transcript abundance of phot1 and phot2	144
4.4.2 Transcript abundance of photoreceptors implicated in transducing light inputs to the circadian clock.....	146
4.4.3 Quantification of photoreceptor abundance and responses to light using real time PCR	148
4.4.4 CAM expression in detached leaves under contrasting light regimes	149
Chapter 5: General Discussion.....	151
5.1. Leaf anatomical traits are related to the magnitude of CAM in Clusia.....	151
5.2 Genome size and correlation with anatomical traits in Clusia.....	152
5.3 Circadian control of stomatal conductance is more robust in CAM than in C3 Clusia plants and is mediated via photoreceptors rather than via metabolism.....	155
5.4 Circadian control of photoreceptors may represent a point of divergence between C3 and CAM in Clusia	158
5.5 Other findings related to the main hypotheses of the thesis	159
5.5.1 Vein density.....	159
5.4 Technical challenges encountered in studying Clusia.....	163
5.5 New perspectives and further experiments	165
5.6 Final conclusions – key findings of the thesis.....	169
Appendix 1: Gas exchange measurements.....	171
Appendix 2: Image J - How to estimate IAS and Lmes/area	174
Appendix 3: Stomata dimensions.....	175
Appendix 4: Calculated values for Stomatal conductance GH_2O	182
Appendix 5: Vein density estimation (adapted from McKown and Dengler, 2009).183	
Appendix 6: Collection and fixation of plant material for chromosome counting ..	184
References	185

Table of figures

Figure 1.1 Different habitats of <i>Clusia</i>	19
Figure 1.2 Different habits of <i>Clusia</i>	20
Figure 1.3 Scheme of basic features of photosynthetic physiotypes in CAM plants. .	21
Figure 1.4 Diagram describing the crassulacean acid metabolism pathway in a mesophyll cell.....	26
Figure 1.5 Phases of the CAM cycle described first by Osmond (1978).....	28
Figure 1.6 Scheme of a circadian system showing three components of the clock	32
Figure 1.7 Diagram showing how PEPC is under circadian control in CAM plants. .	35
Figure 1.8 Scheme of how cryptochrome responds to light and is involved in circadian processes.....	42
Figure 1.9 Scheme of how phototropins are involved in stomatal opening..	44
Figure 1.10 Scheme of how phytochrome responds to light and is involved in circadian processes.	45
Figure 2.1 Phylogenetic tree based on ITS sequences showing relations within the genus <i>Clusia</i>	54
Figure 2.2 Equation used to calculate theoretical stomatal conductance.	57
Figure 2.3 Gas exchange curves showing 24h net CO ₂ uptake for eight species of <i>Clusia</i>	65
Figure 2.4 Relationships between specific leaf area and the magnitude of CAM (percentage of CO ₂ taken up during phase I). SLA and WUE and the magnitude of CAM and WUE for eight species of <i>Clusia</i>	68
Figure 2.5 . Transverse leaf sections of eight species of <i>Clusia</i> under light microscope.....	71
Figure 2.6 Relationships between the magnitude of CAM expressed as % of CO ₂ taken up at night and: a) number of cell layers at the palisade and spongy mesophyll, water storage parenchyma and lower epidermis, b) Palisade mesophyll depth, c) Spongy mesophyll depth and d) Percentage of total mesophyll occupied by WSP for eight species of <i>Clusia</i>	72
Figure 2.7 . Relationship between tissue depth of spongy mesophyll, palisade mesophyll and WSP and number of cell layers and Cell size, for eight species of <i>Clusia</i>	73
Figure 2.8 . Relationships between magnitude of CAM and cell size and photosynthesis type and cell size of spongy and palisade mesophyll, water storage parenchyma and stomatal guard cells for eight species of <i>Clusia</i>	75
Figure 2.9 . Variation in percentage of internal air space and the decrease in length of mesophyll exposed to air as the magnitude of CAM increased, for eight species of <i>Clusia</i>	77
Figure 3.1 . Net CO ₂ uptake and stomatal conductance gH ₂ O for <i>C. rosea</i> and <i>C. multiflora</i> . under 24 h constant white light,.....	100
Figure 3.2 . Net CO ₂ uptake and stomatal conductance gH ₂ O for <i>C. rosea</i> and <i>C. multiflora</i> under 24 h constant red light	101
Figure 3.3 . Net CO ₂ uptake and Stomatal conductance gH ₂ O for <i>C. rosea</i> and <i>C. multiflora</i> under 24 h constant dark, and under 24 h constant high level blue light	102
Figure 3.4 Net CO ₂ uptake and Stomatal conductance gH ₂ O for <i>C. rosea</i> and <i>C. multiflora</i> under 24 h constant dark, and under 24 h constant low level blue light	103

Figure 3.5 Net CO ₂ uptake and stomatal conductance gH ₂ O for <i>C. rosea</i> and <i>C. multiflora</i> under constant 24 h red light (250 μmol m ⁻² s ⁻¹) with a background of blue light.....	104
Figure 3.6. Changes in rates of net CO ₂ uptake and stomatal conductance for <i>C. rosea</i> after an external light source was turned on and turned off	108
Figure 3.7. Changes in rates of net CO ₂ uptake and stomatal conductance for <i>C. multiflora</i> after an external light source was turned on and turned off	109
Figure 3.9 Pictures of epidermal peelings from the abaxial leaf surfaces of eight <i>Clusia</i> species under fluorescence microscope	111
Figure 4.1. Setting the threshold (C _T) in a real time PCR	130
Figure 4.2. Electrophoresis gels showing transcript abundance of Phototropin 1 at five different times under different light treatments for <i>C. rosea</i> and <i>C. multiflora</i>	135
Figure 4.3. Electrophoresis gels showing transcript abundance of Phototropin 2 at five different times under different light treatments for <i>C. rosea</i> and <i>C. multiflora</i>	136
Figure 4.4 Electrophoresis gels showing transcript abundance of Cryptochrome 2 at five different times under different light treatments for <i>C. rosea</i> and <i>C. multiflora</i>	137
Figure 4.5. Electrophoresis gels showing transcript abundance of Phytochrome A at five different times under different light treatments for <i>C. rosea</i> and <i>C. multiflora</i>	138
Figure 4.6. Relative change in the transcript abundance of Phototropin 1 and Phytochrome A, at different times of the day under a regular dark/light cycle in <i>C. rosea</i> and <i>C. multiflora</i>	141
Figure 4.7. Leaves of <i>C. rosea</i> and <i>C. multiflora</i> after 48 h in constant darkness. ...	142
Figure 4.8. Titratable acid content for <i>C. multiflora</i> and <i>C. rosea</i> at five points over 24 hours cycles under different light regimes	143
Figure 5.1. Positive relationship between stomatal guard cell size and 2G DNA amount for eight species of <i>Clusia</i>	154
Figure 5.2. Chromosome preparation of <i>C. multiflora</i> and <i>C. rosea</i> by Jaume Pellicer (Dec. 2010).....	155
Figure 5.3. Mean values and errors bars at 95% CI of primary vein density and secondary vein density for leaves of <i>C. rosea</i> and <i>C. multiflora</i>	160

Table of tables

Table 2.1. The percentage of net CO ₂ taken up during the day and night during a 24 hour cycle, by each of the study species.....	66
Table 2.2 Water use efficiency, CO ₂ uptake and transpiration for eight species of <i>Clusia</i> with different degrees of CAM.....	67
Table 2.3. Mean and standard errors of the depth and number of cell layers of spongy and palisade mesophyll tissues, water storage parenchyma and lower epidermis for the eight species of study.....	73
Table 2.4. Mean cell size and standard errors of spongy and palisade mesophyll, water storage parenchyma and stomatal guard cells across eight <i>Clusia</i> species.....	75
Table 2.6 Correlation matrix of physiological and anatomical traits, using mean values for the eight species of <i>Clusia</i>	84
Table 3.1. Distance in hours for peaks of net CO ₂ uptake and stomatal conductance under different light regimes.	105
Table 3.2 Water use efficiency for a 24 h period, CO ₂ uptake and transpiration for <i>C. rosea</i> and <i>C. multiflora</i> under different light regimes.....	106
Table 3.3. Rates of stomatal opening after the light was turned on and stomatal closing after the light was turned off during natural dark and natural light for <i>C. rosea</i> and <i>C. multiflora</i>	110
Table 4.1. DNA sequences of genes coding for four photoreceptors Cryptochrome 2, Phototropin 1, Phototropin 2 and Phytochrome A, and housekeeping Elongation factor α	123
Table 4.2 Primers used to amplify DNA fragments of four genes encoding for photoreceptors (Cryptochrome 2, Phototropin 1 – 2 Phytochrome A) and the housekeeping Elongation factor α in <i>C. rosea</i> and <i>C. multiflora</i>	124
Table 4.3 Amount of reagents comprising the homogenization buffer used for RNA extraction.....	125
Table 4.4. Composition of the buffers comprising the kit QIAGEN® Plasmid Purification used for the plasmid extraction.....	127
Table 4.5. DNA sequences obtained using a pair of primers designed based on EST data base for <i>Clusia</i> , for four genes encoding for cry2, phot1, phot2, phyA, for <i>C. rosea</i> and <i>C. multiflora</i>	132
Table 4.6 Time of the highest expression for four photoreceptors: Cryptochrome 2, Phototropin 1-2, Phytochrome A under different light regimes for <i>C. rosea</i> and <i>C. multiflora</i>	139

Acknowledgments

The first person who I want to thank is my supervisor Dr. Anne Borland who always believed in me, I'm very grateful for her guidance, advice, support and the long meetings we had every month trying to understand something else about *Clusia*.

Thanks also to Tahar Taybi, my second supervisor, for his guidance with the molecular work and his patience helping me with the real time PCR machine. Thanks a lot to all the people in the school of biology who supported me, giving me a hand and also the opportunity to do some demonstrations to be able to continue with my PhD. I met nice people and had a wonderful experience teaching at the University. I am also grateful to Sue Patterson for her company, her counsel and for always being supportive and resourceful; I'm glad I had the opportunity to have her in the group until my last day of experiments.

I want to thank some other people who collaborated with me in this thesis, the people in the electronic microscopy unit at Medical school, for helping me with the anatomical part of the study, also to Gordon Beakes for his help with the microscope, to Dr. Enrique Olmos and Dra. Nieves Fernandez for making me feel at home during my short stay in CSIC in Murcia, doing the Immuno-gold enzyme-assays. Thanks to Dr. Tracy Lawson for coming to Newcastle and sharing with us several discussions about stomata.

This thesis wouldn't be possible without the love and support of my parents Alberto and Mercedes and my sister Maria Paula who stay present every day through the distance. This is the result of their constancy and the confidence they had always given me. I'm very thankful to Julian Palomino for being with me from the beginning to the end of this work, for his academic advice, his company and creativeness to make our life joyful everyday, for his strength which kept me going during these four years.

Finally, I'm very grateful to all those people who made my life easier and happier in Newcastle, the people who I jogged with, the people who worked with me in the Baltic, especially Wendy, she has part on this! and the rest of my friends, Pat, Jaime, Gerardo, Georgina for all the moments in this city.

This thesis was funded by Colfuturo, NUIPS, and the School of Biology of Newcastle University.

Abbreviations

ABA	Abscisic acid
AcetylCoA	Acetyl coenzyme A
AS	Ascorbate
ADP	Adenosine 5'-diphosphate
ATP	Adenosine 5'-triphosphate
ATPase	Adenosine 5'-triphosphatase
Bicine	N, N-bis-(2-hydroxyethyl)glycine
BSA	Bovine serum albumin
C3	Photosynthesis with primary fixation of CO ₂ catalysed by RuBisCO
C4	Photosynthesis with primary fixation of CO ₂ catalysed by PEPC
CAB	Chlorophyll-a/b binding protein
CAM	Crassulacean acid metabolism
cDNA	Complimentary DNA
Chl	Chlorophyll
Ci	Internal CO ₂ concentration (in the intercellular space)
Cry	Cryptochrome
CTAB	Cetyl trimethyl ammonium bromide
CuSOD	Copper-conjugated superoxide dismutase
DEPC	Diethylpyrocarbonate
DHAS	Dehydroascorbate
DNA	Deoxyribonucleic acid
dNTP	Deoxynucleotide triphosphate
DTNB	5-5 dithio bis 2 nitro benzoic acid
DTT	Dithiothreitol
EDTA	Ethylenediamine tetracetate
EF α	Elongation factor alpha
EST	Expressed sequence tag
FAD	Flavin adenine dinucleotide
FeSOD	Iron-conjugated superoxide dismutase
FW	Fresh weight
GDP	Guanidine 5' diphosphate
Gs	Theoretical stomatal conductance
HEPES	4-(2-hydroxyethyl)-1-piperazineethanesulfonic acid

IAS	Intercellular air space
Lmes/IAS	Surface area of mesophyll exposed to intercellular airspace
LOV	Light oxygen voltage
LWGB	Lower gel buffer (polyacrylamide gel electrophoresis)
MiF	<i>C. minor</i> forward library
MiR	<i>C. minor</i> reverse library
MnSOD	Manganese-conjugated superoxide dismutase
mRNA	Messenger RNA
MuF	<i>C. multiflora</i> forward library
MuR	<i>C. multiflora</i> reverse library
NAD⁺	Nicotinamide adenine dinucleotide (oxidised)
NADH	Nicotinamide adenine dinucleotide (reduced)
NADP⁺	Nicotinamide adenine dinucleotide phosphate (oxidised)
NADPH	Nicotinamide adenine dinucleotide phosphate (reduced)
NP40	Nonidet P-40
NPQ	Non-photochemical quenching
NPQ4	The gene that encodes PsbS
O₂	Singlet oxygen
OAA	Oxaloacetate
OH·	Hydroxyl radical
PCR	Polymerase chain reaction
PEG	Polyethylene glycol
PEP carboxykinase	Phosphoenolpyruvate carboxykinase(EC 4.1.1.49)
PEP carboxylase kinase	Phosphoenolpyruvate carboxylase kinase (EC 2.7.1.-)
PEPC	Phosphoenolpyruvate carboxylase (EC 4.1.1.31)
Pr	Conformational state of phytochrome where it absorbs red light
Pfr	Conformational state of phytochrome where it absorbs far red light
Phot	phototropin
phy	phytochrome
Pi	Inorganic phosphate

PP2A	Protein phosphatase 2A
PPFD	Photosynthetic photon flux density
PSI	Photosystem I
PSII	Photosystem II
PVP	Polyvinylpyrrolidone
Pyr	Pyruvate
RNA	Ribonucleic acid
ROS	Reactive oxygen species
rRNA	Ribosomal RNA
RT-PCR	Reverse transcription polymerase chain reaction
RuBisCO	Ribulose 1,5-bisphosphate carboxylase/oxygenase (EC 4.1.1.39)
RuBP	Ribulose 1,5-bisphosphate
RWC	Relative water content
SDS	Sodium dodecyl sulphate
SOD	Superoxide dismutase
TBS	Tris-buffered saline
TBST	Tris-buffered saline + Tween-20
TEMED	N,N,N',N'-tetra-methyl-ethylenediamine
Tm	Annealing temperature for PCR (°C)
TOC1	Timing of CAB expression 1
Tris	2-amino-2-(hydroxymethyl)1,3 propanediol
UPGB	Upper gel buffer (polyacrylamide gel electrophoresis)
UV	Ultraviolet
VPD	Vapour pressure deficit
WUE	Water use efficiency
X-gal	5-bromo-4-chloro-3-indolyl-beta-D-galactopyranoside
ZnSOD	Zinc-conjugated superoxide dismutase
δ13C	Carbon isotope ratio (%)
φPSII	Quantum yield of photosystem II

Abstract

The tropical genus *Clusia* which contains species with C3, Crassulacean acid metabolism and C3/CAM properties is an interesting model to dissect anatomical, physiological and molecular traits that underpin the evolution of CAM photosynthesis. About 7 % of higher plants perform CAM, a specialised photosynthetic pathway, characterized by CO₂ uptake during the night mediated via the enzyme phosphoenolpyruvate carboxylase (PEPC) and keeping stomata shut for much of the day. CAM confers high water use efficiency (WUE) and has long been considered an adaptation to drought stress and high irradiance. In some species like *Clusia* CAM facilitates remarkable photosynthetic plasticity in dealing with changing environments. Thus, CAM plants are important and challenging model organisms for investigating plant responses to global climate change and for examining the anatomical and physiological traits that underpin enhanced water use efficiency.

In this thesis strong relationships were found between the magnitude of CAM photosynthesis in eight species of *Clusia* (*C. hilariana*, *C. alata*, *C. rosea*, *C. lanceolata*, *C. aripoensis*, *C. grandiflora*, *C. tocuchensis* and *C. multiflora*) and six leaf anatomical traits (stomatal size, stomatal density, % intercellular air space, length of mesophyll exposed to air space, cell size and specific leaf area) . These relationships point to leaf anatomical features as important in the evolution of CAM, and also have implications for the behaviour of stomata and their response to light. It was found that CAM species of *Clusia* have lower densities of larger stomata compared with C3 species of *Clusia*. The CAM species of *Clusia* still maintain a high WUE and it was hypothesised that this was a consequence of robust circadian control of stomatal conductance which was maintained under different light regimes.

To examine the response of CAM stomata to contrasting light regimes and to test if circadian oscillations in stomatal conductance are disrupted under different wavelengths of light, gas exchange measurements were recorded during 48 hours under constant light regimes (either white light, blue light, red light or darkness) for *C. rosea* a constitutive CAM plant, and *C. multiflora*, a constitutive C3 plant. It was found that the species responded differently to variation in light regimes and the response of stomata to blue light in the CAM *Clusia* had not been lost, as proposed by previous workers. The larger stomata of *C. rosea* responded faster to changes in light intensity during the photoperiod compared with those of *C. multiflora*, but this did not happen during the night. It was hypothesised that the kinetic responses of the CAM stomata might be important for optimising carbon gain and reducing water loss under changing environmental conditions at the start and end of the day.. Furthermore, circadian control of stomatal conductance was found to be mediated by both photoreceptors and metabolism, including photosynthesis and carbohydrate metabolism in CAM and C3 *Clusia* plants.

A molecular approach was taken to probe the mechanisms underpinning the contrasting responses to light. The differential transcript abundance, of photoreceptors involved in stomatal opening (phototropin 1 and phototropin 2) and circadian regulation (cryptochrome 2 and phytochrome A) was examined for *C. rosea* and *C. multiflora* under different constant light regimes using semi-quantitative reverse transcription- PCR and Real Time PCR. Diel expression patterns of phototropins were found to differ between the C3 and CAM species in terms of transcript abundance, the level of control exerted by circadian clock over the transcripts and the response of transcripts to different light regimes. It was concluded that stomatal responses to light in *Clusia* species must be mediated by a coordinated labour of different photoreceptors to exert control over water loss and CO₂ assimilation.

Further work is required to assess the expression and regulation of photoreceptors at the stomatal guard cell level. Having more knowledge regarding the function of stomata in CAM plants and their implications for WUE should help inform efforts for improving the water use of crop species in the light of environmental challenges such as desertification and global warming.

Chapter 1: Introduction

Plants are marvellous organisms, capable of making their own energy and handling biotic and abiotic surroundings using complex and diverse mechanisms to cope with the sessile condition. Photosynthesis, the action by which plants and other autotrophic organisms take CO₂ and light to produce O₂ and carbohydrates is the main process by which light impacts on the food web in the form of chemical energy. Plants take up and assimilate CO₂ by three different pathways, namely C₃, C₄ and crassulacean acid metabolism (Borland and Griffiths, 1992; Borland et al., 1992; Borland AM) Approximately 90% of all plants perform C₃ photosynthesis, characterized by the uptake of carbon during the day which is fixed by ribulose 1-5 biphosphate carboxylase oxygenase (RuBisCO) and processed via the Calvin cycle, using ATP and NADPH produced through the light reactions of photosynthesis (Sharrock and Clack, 2002). Only about 6 % of higher plants perform CAM photosynthesis (Winter and Smith, 1996). This is a specialised photosynthetic pathway, and has long been considered an adaptation to drought stress and high irradiance. CAM is characterized by CO₂ uptake during the night that is mediated via the enzyme phosphoenolpyruvate carboxylase (PEPC) (Borland and Griffiths, 1992). The 4-C organic acid that is produced is subsequently decarboxylated during the day to provide CO₂ for processing by the Calvin Cycle via Rubisco whilst the stomata remain closed. Despite their relatively small economical importance compared to C₄ and C₃ plants and low representation compared to C₃, CAM plants exhibit huge physiological plasticity (Lüttge, 2006). Some CAM species are capable of showing high productivity under certain conditions, including semi-arid environments (Burger, 2008). CAM plants present a high water use efficiency (WUE) which can be three times higher that of C₄ species and six times higher than for C₃ plants (Borland et al., 2009). The economic importance of some CAM species such as pineapple (*Ananas comosus*) and *Agave* (*Agave tequilana*) in desert regions is of considerable importance (FASTAT 2005 in Borland et al 2009). Some CAM species have been reported to possess remarkable photosynthetic plasticity in dealing with changing environments. It is well known that CAM plants fix atmospheric CO₂ at night, but there is a wide spectrum of photosynthetic responses, ranging from no net CO₂ uptake at all over a 24 h light/dark cycle (CAM-idling), day-time net CO₂ uptake under well-watered conditions but induction of CAM under drought and salinity (inducible CAM) and nocturnal net CO₂ uptake under a range of environmental conditions (constitutive CAM) (Figure 1.1). This photosynthetic plasticity underpins the

capacity of CAM plants for surviving and growing in arid and semi-arid environments, and thus renders CAM plants as important and challenging model organisms for investigating plant responses to global climate change.

The purpose of this thesis is to advance knowledge of the functioning of CAM photosynthesis from an integrated anatomical, physiological and ecological point of view. The tropical genus *Clusia* which contains species with C3, CAM and C3/CAM properties is an interesting model to dissect out anatomical, physiological and molecular traits that underpin the evolution of this photosynthetic pathway. In particular, this thesis will examine first the functional anatomical characteristics of the leaf and its relationship with the magnitude of CAM, with the purpose of answering the question if leaf anatomy, in particular succulence, has implications in the gas exchange in *Clusia*. A further important component of leaf anatomy directly related with gas exchange is stomatal size and density. This thesis will look at regulation of stomata in response to light and will address the issue of the extent to which this regulation is mediated by circadian control, comparing responses in C3 and CAM species of *Clusia*. A key aim is to evaluate if there is a stronger circadian control of stomata in the CAM compared to the C3 species (based on previous reports of the importance of the circadian clock for optimizing the operation of CAM) and to assess if this is related to the use of carbon and water in the two photosynthetic types.

1.1 The *Clusia* genus

Clusia is a tropical genus of dicotyledonous trees comprising around 300 species and is one of the largest genus of the family Clusiaceae (Pipoly, 1998). *Clusia* belongs to the subfamily Clusiodeae and tribe Clusiae and success of the genus may be due to evolutionary important traits such as epiphytism, resiniferous flowers, invasion of mountains habitats and photosynthetic diversification (Lüttge et al., 2007). *Clusia* is the only genus with trees that present CAM (Grams et al., 1997). Several species of this genus have remarkable photosynthetic plasticity, performing obligate C3, C3/CAM intermediacy and obligate CAM photosynthesis (Brulfert et al., 1975; Lüttge, 2006). Moreover, *Clusia* is ecologically successful, being found in a wide variety of habits (ie: lianas, epiphyte, shrubs and trees) and habitats. The genus is widely distributed over central and South America, extending from the Bahamas at the north to the state of Rio Grande du sul in Brazil in the south. Distribution of the genus varies from high altitudes (3500 m) in the Andes to low Amazonian forests and pacific zones,

including the Guyana highlands and Caribbean islands (Lüttge et al., 2007) demonstrating the ecological and physiological plasticity and high adaptability to different environments. Species of *Clusia* are present in habitats ranging from tropical rain forest to coastal places, and occupy diverse sites that include rocky sites, savannas, restingas, dry forests, paramos, as well as canopy niches as epiphytes (Scarano et al., 2005; Lüttge, 2008; Scarano, 2009). Within *Clusia* there is a considerable diversity at the morphological level, even although all the species within the genus have succulent and leathery leaves, with petiole and white or yellow latex. Whilst leaves tend to show similar shape across the genus, leaf and tree sizes can vary markedly (Lüttge, et al. 2007). *Clusia* species also show differences in floral morphology, size and pollinator rewards, as nectar and resin; fruits are less variable, being all fresh capsules with seven septum and different sizes with one to many seeds per carpel, generally covered with a coloured aril. Several life forms have been identified and individual species may exist as trees, shrubs, epiphytes or hemi-epiphytes, probably reflecting the physiological plasticity in photosynthetic characteristics which might be crucial to the success of the genus (Lüttge, 2006, 2008).

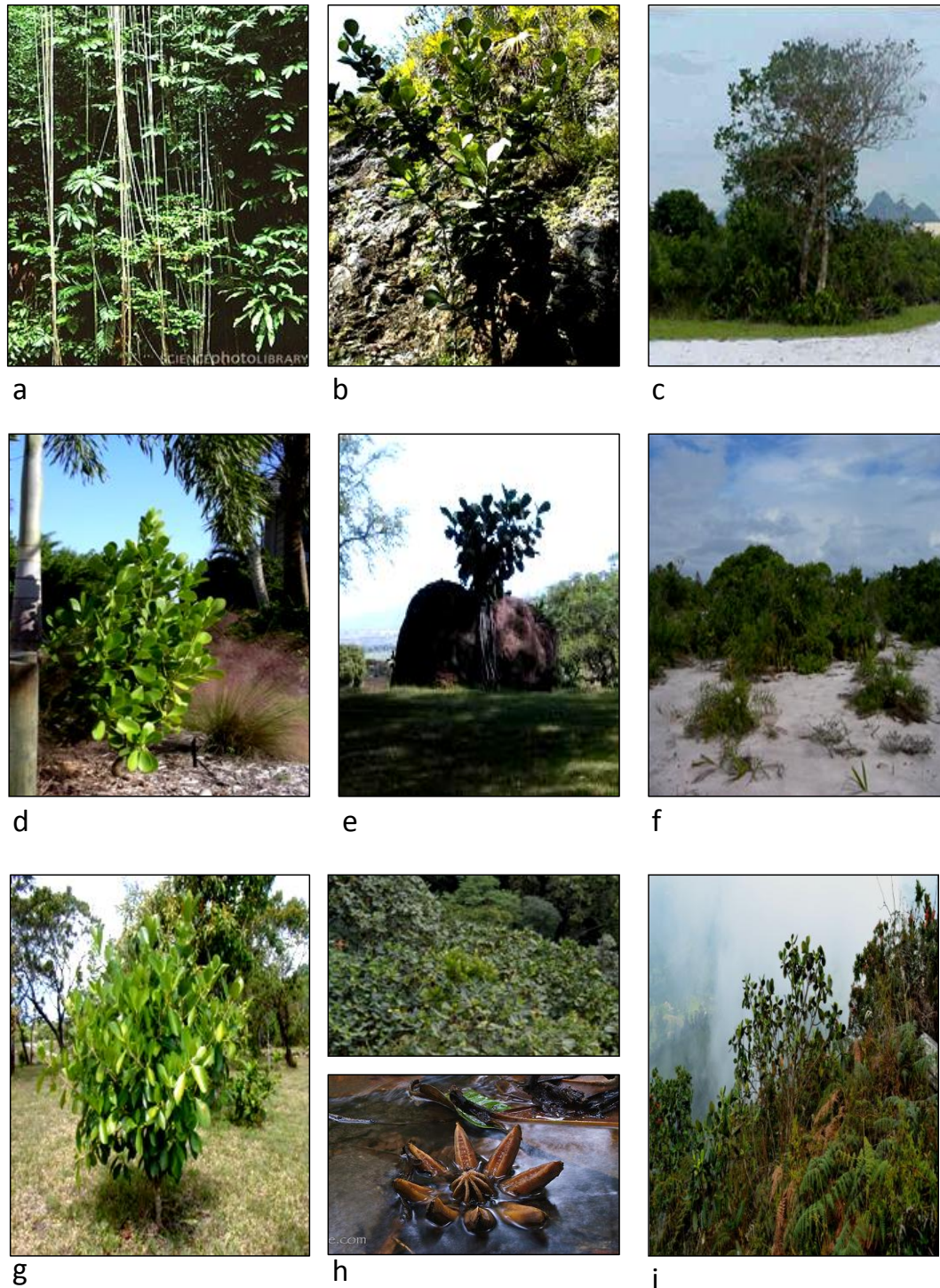


Figure 1.1 Different habitats of *Clusia* **a.** *Clusia* sp at tropical rain forest in Costa Rica, **WILLIAM ERVIN/SCIENCE PHOTO LIBRARY** **b.** *Clusia* sp in a rocky habitat, **c.** *C. hilariana* in a restinga in Brazil <http://www.casaecia.arq.br/restinga.htm>, **d.** *C. rosea* in a coast of Florida <http://www.hear.org/starr/images/image/?q=031108-0312&o=plants>, **e.** *C. rosea* growth on a rock in Hawaii. **f.** *Clusia* sp in a restinga in Brazil, **g.** *Clusia* sp in a savanna in Panama. **h.** fruit of *Clusia* in mountain forest <http://www.flickr.com/photos/primevalnature/2791979950/> **i.** tree of *Clusia* sp in a mountain forest in Colombia.

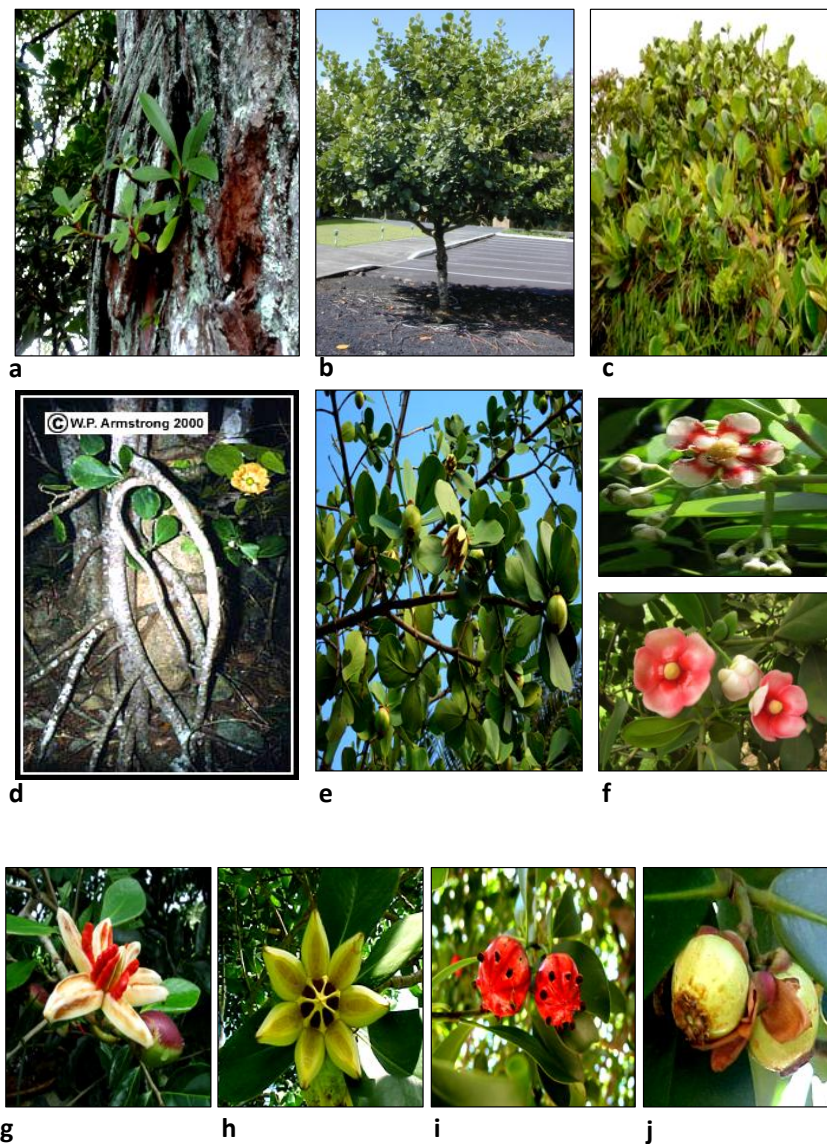


Figure 1.2 Different habits of *Clusia* **a-e**. **a**. *C. rosea* saplings in Hawaii, **b**. *C. rosea* tree in Hawaii <http://www.hear.org/starr/images/image/?q=041018-0031&o=plants> , **c**. *Clusia* sp in a mountain forest, **d**. *C. rosea* in a forest of Virgin Islands <http://waynesword.palomar.edu/ploct99.htm>. **e**. *C. rosea* in a mountain forest <http://www.beautiful-tropical-gardens.com/autograph-tree.html>. **f**. flowers of *C. uvitana* and *C. hilariana* (www.luisbacher.tk). **g**. fruit of *Clusia* cf *pratensis* <http://ntsavanna.com/clusia-the-autograph-tree/>. **i**. fruits of *C. lanceolata* <http://www.flickr.com/photos/mariasg/315224936/>. **H**. open, **j**. closed fruits of *C. rosea* http://www.cybertruffle.org.uk/vinales/eng/clusia_rosea_ok.htm.

In addition to its phenotypic and ecological plasticity the *Clusia* genus shows a remarkable plasticity in their use of photosynthetic CO₂ assimilation (Figure 1.3), and many

species are able to switch between C3 photosynthesis and CAM (Ball et al., 1991, 1991; Borland and Griffiths, 1992; Borland et al., 1992). Among *Clusia* there are species that perform C3 photosynthesis exclusively and others which can use CAM under stressful conditions, a situation known as facultative CAM. Species that perform CAM can present variations in expression of the pathway: CAM idling describes the situation where stomata are closed during night and day and CO₂ from respiration is re-fixed in the night and recycled to carbohydrate during the day. CAM cycling is where net CO₂ is taken up and fixed during the day and CO₂ from respiration is re-fixed by PEPC during the night and used to make organic acids which are stored overnight. Several *Clusia* species exhibit constitutive CAM under all environmental conditions (Luttge 2006). Physiological and ecological plasticity and a diversity of life forms have made *Clusia* the focus of much research after the CAM pathway was found in the genus (Tinoco and Vazquez-Yanez 1983; Ting 1985). *Clusia* is also an ideal model to study the evolution of CAM in closely related plant species.

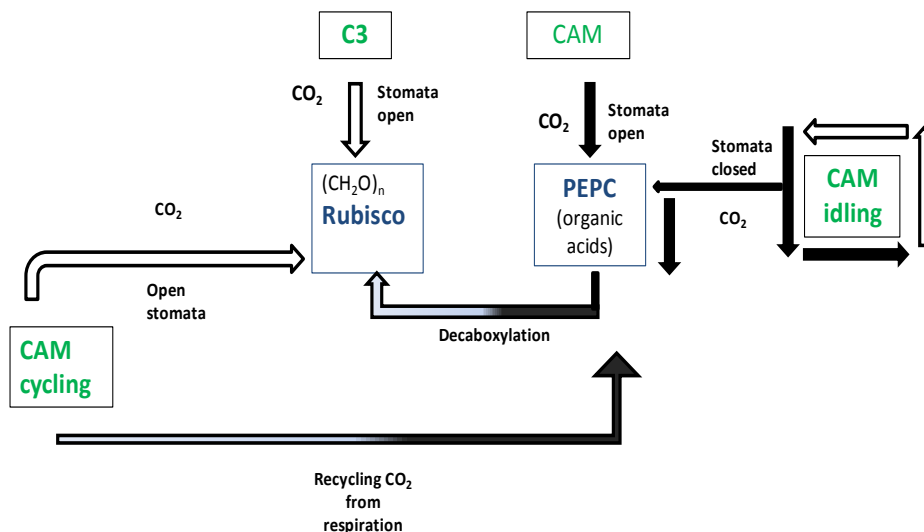


Figure 1.3 Scheme of basic features of photosynthetic physiotypes in CAM plants represented in green: CAM, CAM cycling, full CAM and CAM idling. There are also switches between C3 and CAM in C3/CAM intermediates (a phenomenon also referred to as facultative CAM). Black arrows represent processes occurring at night and white arrows indicate processes occurring during the day. Modified from Luttge (2006).

1.2 CAM evolution

The most common and primitive pathway of photosynthesis is the C₃ pathway (Cerling et al., 1993). There is strong support that the evolution of the photosynthetic adaptation of CAM (Bowler et al., 1994) has progressed from C₃ to C₃-CAM intermediates through to constitutive CAM (Motomura et al., 2008; Silvera et al., 2009). CAM is a taxonomically widespread photosynthetic pathway that has evolved in plants found in both CO₂ and water limited environments. CAM is found in nearly 7% of vascular plants within 35 families (Smith and Winter, 1996; Holtum et al., 2007). Most CAM plants inhabit semi-arid zones, places with seasonal drought and some aquatic environments. However, CAM species are also established in other habitats that include moist montane forest and canopies of tropical forest, which provides evidence of the ecological significance of photosynthetic plasticity (Dodd et al., 2002). Epiphytes are important components of CAM plants which are found in canopies of tropical forest (Lüttge, 2004) where the availability of water is usually low and irradiance is high. A substantial component of the biomass of tropical forests is made up of epiphytes comprising numerous species of orchids and bromeliads, most of which are CAM plants (Benzing, 1987; Lüttge, 2004; Zotz, 2004). Epiphytic and terrestrial specimens of the *Clusia* genus are also found in this habitat.

It has been suggested that the C₄ and CAM pathways have a less ancient evolutionary origin than the C₃ pathway (Cerling et al., 1993; Ehleringer and Cerling, 1998) and might coincide with the stabilization of arid regions in the last five million years (Landrum, 2002; Arakaki et al., 2011). There is no strong fossil evidence of the presence of CAM photosynthesis previous to 40,000 years ago (Troughton, 1974), even though it has been proposed that the pathway arose during the Cretaceous or Triassic in isoetes and cycads (Griffiths, 1992). Early CAM evolution in Isoetes during the Permian (250 to 310 Ma of years ago) may coincide with the presence of an atmosphere with low concentrations of CO₂ ((Berner, 1994; Laws, 2001). Evidence based on paleosol carbonate and fossilised teeth of mammals that point to the diversification of C₄ grasses in the old world as in the new world late Miocene, 4–7 Ma years ago suggest a change in climatic conditions. This was very likely a decrease in CO₂ levels (probably below a threshold efficient for C₃ photosynthesis 400 – 500 p.p.m.v) which favoured the expansion of C₄ over the C₃ species (Cerling T. E. , 1993; Cerling et al., 1993) and the emergence of other photosynthetic pathways as C₃/CAM and CAM. Also, Ramirez et al (2007) provided data that suggested that the two large sub-families of orchids (Orchidoideae and Epidendroideae), which contain epiphytes that perform CAM diversified during a period of

aridification and decreasing CO₂ concentrations in the Tertiary (Pearson and Palmer, 2000). Past research summarized in Ehleringer and Monson (1993; Pearson and Palmer, 2000) has suggested multiple origins within families and even within genera of the CAM pathway. Landrum *et al* (2002) pointed out that the establishment of arid regions and accelerated evolution of succulent plants in those “arid islands” caused a strong selective pressure that originated in exclusive succulent plants with C₄ and CAM photosynthesis. Also a recent work concludes that the major diversification of Cactus occurs in the late Miocene and beginnings of the Pliocene, coinciding with the diversification of other succulent as Agaves in America with two diversifications during the same period (8-6 Ma and 3-2.5 Ma), and Ice plants in Africa about 8.7-3.8 Ma ago. In summary all origins of succulents have been reported within the same frame of time late Miocene – Pliocene (11 – 2 Ma) coinciding with the establishment of several extent desert ecosystems (Arakaki et al., 2011) Recent work of Silvera et al (2009) also found multiple independent origins and several reversals of CAM within the family Orchidaceae. In addition, epiphytism and the CAM pathway have been correlated during evolutionary time (Crayn et al., 2004). A relationship was found between epiphytism and CAM photosynthesis in two subfamilies of bromeliads: Tillandsioideae, in which the C₃ pathway was ancestral and CAM developed later in the most tough epiphytes and Bromelioideae, where CAM photosynthesis seems to precede epiphytism. Also, following radiations in less dry habitats reversals to C₃ photosynthesis were observed in bromeliads, suggesting great physiological flexibility to overcome the presumable extra cost of CAM (Shorrocks unpublished). Ehleringer and Monson (1993) summarized several works about CAM evolution showing that the CAM pathway has multiple origins within families and even within genera. That is the case of *Clusia* (Vaasen et al., 2002), a tropical genus where C₃ photosynthesis does not appear as an ancestral character (Gehrig et al., 2003), and 2 gains and 10 loss of CAM are revealed by the phylogenetic tree based on ITS sequences (Gustafsson and Bittrich, 2002; Gehrig et al., 2003).

1.2.1 Evolution of CAM in *Clusia*

Relatively few robust phylogenies have been conducted to understand the evolution of CAM within *Clusia*. Studies using ITS sequences (Gustafsson and Bittrich, 2002) were first conducted as a means of overcoming difficulties with taxonomy of the group and for comparing morphological and molecular characteristics. Using this approach, no evident group-specific evolution of CAM within the genus was found for the 17 *Clusia* species studied. However,

succeeding numbers of studies in this area have concluded that ITS sequences are useful and trustable markers for phylogenetic studies in Clusiaceae. Several authors found a classification of those 17 species in three main groups, (Lüttge, 2006; Winter et al., 2008), i.e: the *Clusia flava* group, the *Clusia minor* group and the *Clusia multiflora* group. CAM was found only in the *C. flava* and *C. minor* groups supporting the hypothesis of multiple independent origins of CAM (Gehrig et al., 2003). Also, *C. multiflora* an obligate C3 species ($\delta^{13}\text{C} \pm 26.2$; (Grams et al., 1998)), and the *C. multiflora* group is not placed at the bottom of the phylogenetic tree for the genus and seems not to be the origin of the CAM or C3/CAM in the family, again reaffirming the several gains of CAM (Vaasen et al., 2002). Raven (1996) considered the origin of CAM a recent event so the loss of CAM in *C. multiflora* after the presence of CAM in the whole genus is less probable than the suggestion that CAM has never evolved in the *C. multiflora* group (Vaasen et al., 2002). This idea is concordant with the finding of nearly 30 distinct origins of the C4 pathway identified in individual families (Sage, 2001). Indeed recently Vaasen et al. (2006) studied the presence of different isoforms of phosphoenol pyruvate carboxylase (PEPC), one of the key enzymes in the CAM pathway, in the genus *Clusia* and found 3 different isoforms in a constitutive CAM species *C. hilariana*, one of those also present in an intermediate C3/CAM *C. minor* and constitutive C3 *C. multiflora*. This isoform is then considered a housekeeping protein that also supports the CAM photosynthesis in the intermediate species, the other two isoforms present in *C. hilariana* could be considered as one CAM specific isoform and an isoform related with a PEPC presence in the roots. Phylogenetic analysis based on the comparisons of amino acid sequences of PEPC, identified two groups within the genus, one group containing the housekeeping isoform, and another with the CAM isoform. In contrast, other CAM plants such as *M. crystallinum* and *Kalanchoë blossfeldiana* possess additional isoforms of PEPC that are different to the housekeeping PEPC (Cushman et al., 1989; Cushman and Bohnert, 1996). Having in mind that these species are inducible CAM plants without the possibility of reversion to C3, it is very likely that the use of the C3 PEPC isoform in the genus *Clusia*, confers the capacity to switch between C3 and CAM photosynthesis in both directions. Finally, polyphyletic evolution of CAM at family level and within the genus *Clusia*, might be possible because there are no unique enzymes required specifically for CAM photosynthesis (Vaasen et al., 2002; Gehrig et al., 2003; Vaasen et al., 2006).

Other studies have intended to elucidate phylogenetic relationships within the *Clusia* genus using morphological and ecological features. Vargas-Soto et al., (2009) reported the non-existent correlation between epiphytism and CAM photosynthesis in *Clusia* in Mexico, unlike the situation reported for Orchids (Silvera et al., 2009) and two subfamilies of bromeliads (Crayn

et al., 2004). However, the same authors found that even although there were less species of *Clusia* in Mexico than in Panama, the percentage of *Clusia* plants performing CAM was higher in Mexico, probably due to the more arid habitats and lower altitudes where the Mexican plants were recorded. Negative relationships between altitude and the CAM pathway have been also reported for *Clusia* in Venezuela and Panama (Diaz et al., 1996; Holtum et al., 2004), and in orchids in Panama (Silvera et al 2009). Medina et al. (2006) discovered a positive relationship between *Clusia* species groups clustered by morphological and molecular characteristics with those groups clustered on the basis of wax composition in leaves. However, relatively few species were used in the study so robust conclusions on the significance of this relationship are not possible (Medina et al., 2006). This thesis will evaluate the possible relationships between morphological characters of the leaf and the performance of CAM photosynthesis in closed related species to corroborate previous works with other CAM plants.

1.3 Crassulacean Acid Metabolism

Crassulacean acid metabolism is a specialised photosynthetic pathway characterized by CO₂ uptake during the night when the temperature is lower than during day and hence the water loss from leaves is less than rates of evapo-transpiration that are typically measured during the day. CO₂ taken up in the dark is fixed by the enzyme phosphoenolpyruvate carboxylase (PEPC), producing malic acid which is stored in large central vacuoles within the leaf cells. The next day, behind closed stomata and therefore in the absence of leaf net gas exchange with the atmosphere, the acids are mobilized and decarboxylated generating CO₂ to be refixed by Rubisco and assimilated via the Calvin cycle (Lüttge, 2006 Figure 1.2). The day/night metabolic processes that comprise CAM can be summarised as four main phases, I to IV as shown in Figure 1.5. Osmond (1978) reported the occurrence of these four phases for the first time. Phase I entails nocturnal net CO₂ uptake that reacts with PEP to form oxaloacetate (OAA), this reaction is mediated by PEPC. OAA is then converted to malate which is pumped into the vacuole by means of a proton ATPase and stored in the form of malic acid (Fig. 1.4). Phase II starts at dawn, during this time PEPC activity is reduced and RubisCo activity starts to increase. During phase III, stored malate is decarboxylated to generate CO₂ behind closed stomata and this CO₂ is fixed by RubisCo. In phase IV, RubisCo activity is high, doing the direct fixation of atmospheric CO₂. The sugars produced during phase IV are mostly exported from source tissues and mainly used

for plant growth (Borland et al., 1996; Osmond, 1999; Borland et al., 2000; Borland and Dodd, 2002).

Several CAM plants possess the capacity to perform a range of photosynthetic patterns, varying from C3 to CAM in different degrees. CAM plants can be separated into obligate CAM and inducible CAM based on their responses to environmental stressors including drought and salinity (Borland and Griffiths, 1990). Obligate CAM plants normally take most (over 70%) of the carbon up at night, even under non-stressful conditions whereas facultative CAM only take up CO₂ at night after induction of the pathway in response to stress. Within the CAM performances are the variations of CAM idling and cycling described above (see Fig.1.3).

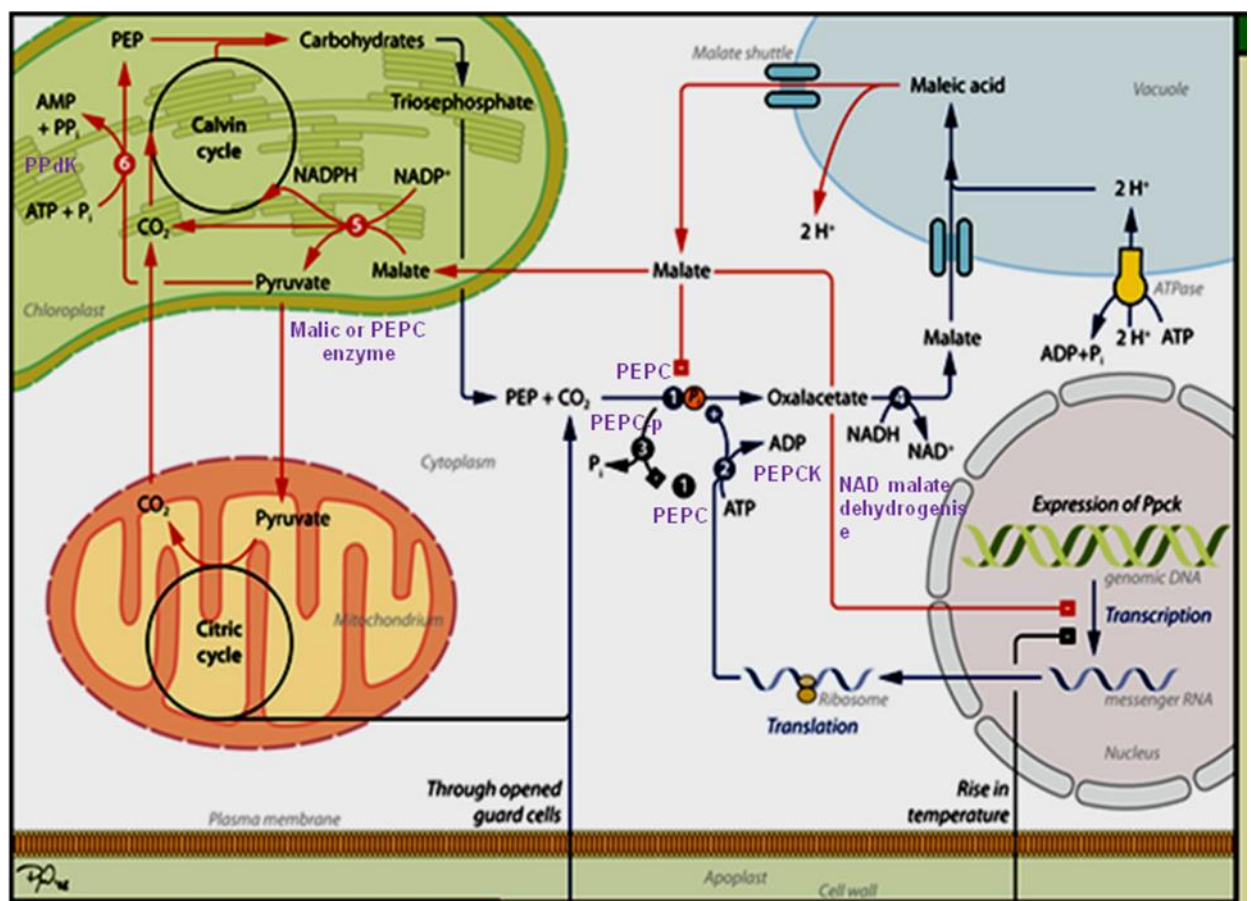


Figure 1.4. Diagram describing the crassulacean acid metabolism pathway in a mesophyll cell. Blue arrows represent reactions during the dark, red arrows represent reactions during the light, main enzymes are in purple. CO₂ enters the cell during the night through open stomata and in the cytoplasm reacts with phosphoenol pyruvate with the intervention of phosphoenol pyruvate carboxylase which has been phosphorylated by phosphoenol pyruvate carboxylase kinase. From this reaction oxaloacetate is produced and converted to malate by NAD malate dehydrogenase (4). Malate is then

stored in the vacuole as malic acid and the next morning released to the cytoplasm and transported to the chloroplasts to be decarboxylated by malic enzyme (5) and produce pyruvate and CO₂, the latter product enters the Calvin cycle where trioseP and carbohydrates are produced. Carbohydrates are broken down at night to produce phosphoenol pyruvate again during the following night. Pyruvate produced from the decarboxylation of malic acid with the intervention of pyruvate phosphate dikinase, is degraded in the mitochondria during the citric acid cycle, and pyruvate is metabolised to recover phosphoenol pyruvate. Regulation of PEPC kinase production is also shown at bottom right: transcription is inhibited by excess of malate in the cytoplasm and through downregulation of PEPC transcription during the day time (increase in temperature and/or circadian control). Modified from <http://en.wikipedia.org/wiki/File:CAM.png> based on (Nimmo, 2003; Borland and Taybi, 2004; Hartwell, 2005)

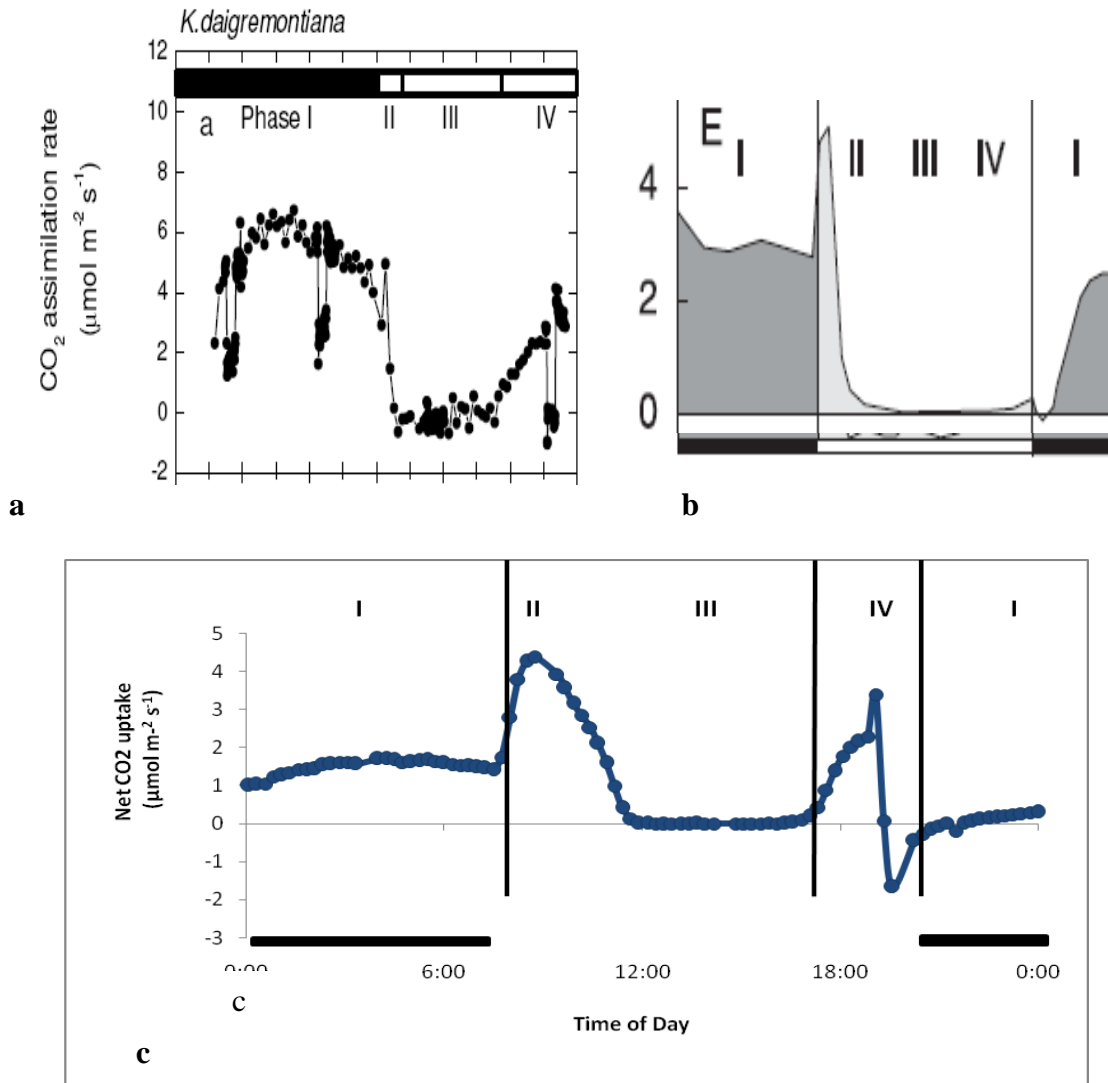


Figure 1.5 Phases of the CAM cycle described first by Osmond (1978). Phases are indicated at the top of the figure: Phase I corresponds to the dark period when stomata are open and CO₂ enters the cell and is taken up by PEPC. Phase II occurs during the start of the day, stomata are still open and PEPC activity starts to decline and Rubisco activity to increase. The graphs show net CO₂ uptake (µmol m⁻²s⁻¹) over a period of 24 h for a) *K. daigremontiana*, a typical CAM plant, with a extended phase I (figure taken from (Von Caemmerer and Griffiths, 2009). b). A typical strong CAM plant *Clusia alata* with an extended phase I, and a large proportion of CO₂ uptake during phase II, but during a short period of time, (figure modified from (Lüttge, 2006), and c). *Clusia rosea* a constitutive CAM plant with a extended phase II and considerable phase IV representing important contributions (42.14 % and 47.05 % of total) to net CO₂ uptake during the diel cycle. Phase III corresponds to the middle part of the light period, stomata are closed and CO₂ from malate decarboxylation is being incorporated by Rubisco into the Calvin cycle. During Phase IV at the end of the light period, when there is a depletion in concentrations of internal CO₂ and stomata are open again to take more CO₂, during this phase PEPC activity starts to increase and Rubisco activity to decrease. Phases are based on CO₂ assimilation; also there is a variation in the

duration and expression of the four phases depending on the species and environmental conditions

1.3.1 Carbohydrate metabolism and enzyme control in the CAM pathway

Carbon flow pathways and their associated energetic balance in CAM are still to be completely elucidated (Winter and Smith, 1996). However, carbohydrate turnover is a central component determining the magnitude of CAM, and it also signifies a constraint for growth and productivity (Borland and Dodd, 2002). It has been thought that minor amounts of carbohydrates are mobilized at night and that the growth of CAM plants is supported by the differentiated translocation of soluble sugars produced during phase IV (Winter et al., 1985). Nevertheless, in some CAM species net export of carbohydrates occurs during the day as well as during the night (Borland and Dodd unpublished observations). A method to make possible the control of carbohydrate metabolism in CAM plants might be the partitioning of carbohydrates derived from C3 and C4 carboxylation, for growth and CAM photosynthesis separately (Borland et al., 1994; Dodd et al., 2002)

CAM plants show exceptional plasticity for adjusting the proportion of CO₂ taken up directly via PEPC and Rubisco, depending on internal metabolic requirements and responding to external environmental factors (Borland et al., 2000; Cushman and Borland, 2002). Some works (Adams et al., 1998; Borland and Dodd, 2002; Borland and Taybi, 2004) have reported the partitioning of C4 and C3 into discrete transport and storage pools of soluble sugars. In *Clusia minor* soluble sugars derived from C3 and C4 metabolism are used in a discriminate way for CAM photosynthesis and non-photosynthetic processes (Borland and Taybi, 2004). In *M. crystallinum* after the induction of CAM via salinity a reduction of 28% in total daily carbon input was noted, (Borland and Dodd 2002). Moreover, primary leaves which are developed under C3 photosynthesis pathway are devoted to rapid growth using the carbohydrate accumulated as a starch, with the purpose of producing axillary succulent leaves with a higher turnover of soluble sugars, able to perform CAM photosynthesis and support growth during dry periods (Adams et al., 1998). In another study, Winter and Smith (1996) reported that 20% of leaf dry weight may be devoted to generate PEP for nocturnal C4 carboxylation. In addition, patterns of gene expression of enzymes implicated in starch degradation (i.e α and β amylases, starch phosphorylase, glucanotransferase) followed a diel rhythm after CAM induction. Peaks in transcript abundance of genes implicated in starch degradation precede the timing of maximum

expression of PEPC kinase (Dodd et al, 2002; Borland, Dodd and Griffiths unpublished observations), suggesting that the circadian control of starch metabolism may be responsible for the tight regulation of carbohydrate breakdown and PEPC activation at night (Dodd et al., 2002). With this in mind it has been hypothesized in this work that CO₂ uptake should be also implicated in this regulation perhaps through the control of stomata which are the first window for gas exchange. This thesis will test the response of stomata to light, the most important input signal of circadian clocks with the purpose of investigating the implications of circadian control over stomatal function in CAM plants.

In *Clusia minor* (C3/CAM intermediate) and *Clusia rosea* (constitutive CAM), Borland and Dodd (2002) observed a distinct partitioning of C3 and C4-derived carbohydrates for photosynthetic and non-photosynthetic processes. Soluble sugars were accumulated early after sunrise in *C. minor* and 4 hour after sunrise in *C. rosea*, whilst accumulation of starch occurred at the end of the day in *C. minor* and over the day in *C. rosea*. Thus, the pattern of carbohydrate mobilization and storage is opposite in both species, and accumulated starch presented a more C3-like isotopic signature whereas soluble sugars for organic acid turnover had a more C4-like signatures, suggesting a strategy to assure reproduction independently of the level of CAM, a crucial factor to determine the success of *Clusia* in different habitats. Finally, carbon isotope signatures revealed the greater contribution from carbon fixed by PEPC in *C. rosea* than in *C. minor*.

In summary, it has been described that nocturnal degradation of carbohydrate in CAM plants generates PEP, the 3C carbon substrate, for PEPC. Day/night turnover of organic acids is a matter of a synchronized control of the enzymes involved in decarboxylation (i.e.: NADmalic enzyme, NADP malic enzyme or PEPC, this last has been reported the predominate decarboxylase in *Clusia* (Black et al., 1996)). The CO₂ plus 3-C compound produced from decarboxylation contributes to C3 photosynthetic metabolism and growth. However, induction by environmental factors of increases in the rate of organic acid degradation is not always accompanied by correspondent changes in the activity of decarboxylases (ie: *Sedum* (Brulfert et al., 1988; Conti and Smirnoff, 1994) and pineapple (Borland unpublished observations)) suggesting that malic acid efflux from the vacuole rather than decarboxylation is the key rate-limiting step in the day-time processes of CAM and it is also possible that changes in the rate of day-time acid breakdown are reached by post-translational modifications of decarboxylating enzymes (Dodd et al., 2002).

1.3.2 Circadian control and plasticity of the CAM pathway

Circadian rhythms are internal pulses that occur in all organisms and persist upon changes in environmental conditions. The plant circadian clock is believed to underpin adaptive fitness (Pittendrigh, 1981; Edmunds, 1988; Johnson et al., 1998). Normally, circadian rhythms are internal and persist even when the environmental cues change, demonstrating the capacity of the organisms to measure the time and use this information to control metabolic processes (McClung, 2000). Maintenance of the circadian clock might be a trait related to the adaptive fitness, since it occurs across broad taxonomic ranges, however that hypothesis is difficult to prove (ie: experiments with *Synechococcus sp.*; (Johnson and Golden, 1999).

In theory, circadian rhythms continue in the absence of changes in external time cues, but are able to entrain to ambient conditions. Moreover, abrupt or continuous long term changes in temperature or light can shift the phase of the clock (Pittendrigh, 1981; Johnson et al., 1992).

Circadian systems have three components: an input pathway that provides information from the ambient environment to the clock, an oscillator which encloses the mechanism itself and an output that contains the information from the oscillator and controls other metabolic process in the organisms (McClung, 2000) (Figure 1.6). It has been suggested that the oscillator works via negative feedback, the accumulation of the products from the genes controlled by the clock serve as an inhibitor and regulator of the clock and the best-characterized input to the circadian clock is light (McClung, 2000).

In higher plants circadian clocks control several processes such as flowering time, hypocotyl elongation, leaf movements, and CO₂ fixation in CAM (McClung, 2000). Several genes have been reported as regulated by circadian rhythms (Kreps and Kay, 1997; Fejes and Nagy, 1998). Some of these genes are involved in photosynthesis and present circadian patterns of transcript abundance (Giuliano et al., 1988; Sharrock and Quail, 1989; Martinocatt and Ort, 1992; Pilgrim and McClung, 1993; Salvador et al., 1993; Clack et al., 1994; McClung, 1997; Nakahira et al., 1998; Piechulla, 1999). Others are implicated in gas exchange and stomatal movements (Gorton et al., 1993; Webb, 1998). For example Hennessey and Field reported a circadian regulation of Calvin Cycle in beans (Hennessey and Field, 1991). One of the best known circadian rhythm is the CO₂ metabolism in CAM (Wilkins, 1992; Lüttge, 2000). The system of post-transcriptional circadian regulation is the activation of PEPC through PEPC Kinase in CAM plants has been described by (Nimmo, 1998) and will be explained in more detail in a later section (see also Figure 1.7).

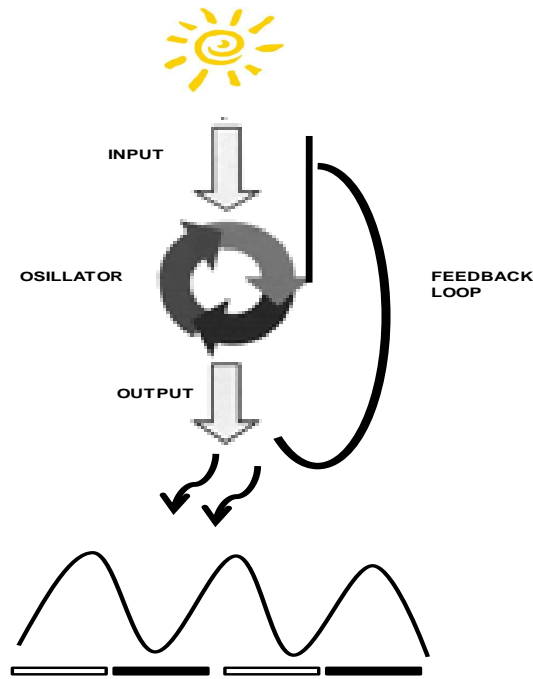


Figure 1.6 Scheme of a circadian system showing three components: an input pathway that provides information from the ambient environment to the clock, which in this case is light, an oscillator which encloses the mechanism itself and an output that contains the information from the oscillator and controls other metabolic process in the organisms generating cyclical patterns. It has been suggested that the oscillator works via negative feedback (McClung, 2000). Figure modified from (Devlin, 2002)

In general, the expression of CAM as mentioned before is highly variable and responds to environmental conditions such as temperature, water, light and salinity. Given that CAM plants frequently inhabit stressful conditions, the capacity for adapting to changing and limiting environments might be essential for survival (Dodd et al., 2002). For example, plasticity in the performance of the four phases of CAM is an ubiquitous character in most CAM plants (Dodd et al., 2002), with few exceptions (Nobel, 1988; Kluge et al., 1992; Kluge et al., 2001). Even the less plastic CAM species will respond to environmental change, regulating the expression of the day-night phases, ie: *Kalanchoe daigremontina* exhibits four phases of CAM under well watered conditions but after drought stress phase IV is lost and phase I is reduced (Griffiths et al., 2002).

Within plants performing CAM photosynthesis, C3-CAM intermediates probably exhibit the greatest photosynthetic plasticity (Ting, 1985; Kluge et al., 2001), and those species have an intrinsic capacity to induce CAM upon changing environmental conditions, especially water availability. A very well documented example of this is *Clusia minor*, showing an

exceptional capacity for the magnitude and reversibility of CAM induction upon changes in VPD on opposite leaves of the same plant (Schmitt et al., 1988).

Temporal separation of CO₂ uptake in CAM requires tight metabolic control over the diel phases, to avoid futile carbon cycle, but also a flexible mechanism that allows the plants to respond to changes in environmental conditions (Dodd et al., 2002). This strict metabolic control occurs via the carboxylation enzymes. PEPC kinase is regulated by endogenous rhythms (Carter et al., 1991; Hartwell et al., 1996), and at the level of transcription and activity, controlling the rate of nocturnal CO₂ uptake, and consequently the overnight accumulation of malate. PEPC is regulated by reversible phosphorylation so that during the day PEPC is dephosphorylated and inhibited by malate (Nimmo et al., 1984; Nimmo et al., 1986; Grams et al., 1997) whilst at night, the protein is phosphorylated thus releasing malate inhibition (Nimmo, 2003). Rubisco may also be regulated through the transcription of an effector, rubisco activase, the activity of which depends on the rate of photosynthetic electron transport to the reduction of the large subunit via ferredoxin-thioredoxin reductase (Zhang and Portis, 1999). The regulation of Rubisco is also influenced by its substrate, ribulose 1-5 bi-phosphate. Both enzymes responsible for carboxylation in CAM species are partially regulated by endogenous rhythms which persist even when the environmental cues change. However, these rhythms are entrainable to ambient conditions and abrupt or continuous long term changes in temperature or light can shift the phase of the clock (Pittendrigh, 1981; Johnson et al., 1992). The plasticity of the CAM pathway must be achieved whilst maintaining a balance between carboxylation and decarboxylation reactions to lessen futile carbon turnover during the diel cycle and overcome the energetic costs of CAM photosynthesis without compromising productivity (i.e: figures for *Agave tequilana* indicate production of up to 50 Mg dry biomass ha⁻¹ year⁻¹, *Ananas comosus* produces up to 86 Mg fruit ha⁻¹ year⁻¹ and *Opuntia. ficus-indica* of 47–50 Mg ha⁻¹ year⁻¹ (in Borland et al 2009; Borland and Taybi 2004).

From the molecular point of view, recent work from Boxall and co-workers have characterized eight genes (CCA1, LHY, TOC1, ELF3/4, ZTL, FKF1, GIGANTEA) involved in circadian control in the inducible CAM plant *M. crystallinum*, based on *Arabidopsis* databases (Boxall et al., 2005). This study was the first to report that PEPCK transcript levels were delayed by 6 hours with respect to the peak observed under constant light conditions in the CAM mode. Also, the possible association with CCA1/LHY and TOC1 oscillations, suggested that the output pathway that links PEPCK with the central clock includes a component subjected to phase delay from the basic oscillator under constant light in CAM. The same work reported that CCR1/2

oscillations damp very quickly once CAM has been induced by salt stress and transferred to constant light, and this damping did not occur in the C3 mode, where the rhythms were very robust. This result suggests that circadian regulation of CCR1/2 is lost in salt stressed CAM induced plants (Boxall et al., 2005). In addition, CCA1 and LHY oscillations did not change after the induction of CAM, and the rhythms for CAB were kept as well. However, the amplitude of the oscillations decreased due to the repression of CAB, possibly as a consequence of the salt stress or due to the presence of a repressor protein binding to CAB to down-regulate its expression in CAM. Furthermore, TOC1 and LHY were under circadian control in a similar way to that in *Arabidopsis* and ELF4/3, FKF1, ZTL and GIGANTEA presented circadian rhythms during both C3 and CAM modes of photosynthesis. However, ZTL showed oscillations in *M. crystallinum* unlike *Arabidopsis* probably due to the evolutionary divergence (7 million of years between them) of the two orders (*Arabidopsis* – Brassicales and *Mesembryanthemum*-Caryophyllales (<http://www.flmnh.ufl.edu/deeptime>)). All the work by Boxall and co-workers described above have given a first insight to the molecular bases of circadian control in CAM, demonstrating that the clock in *M. crystallinum* is well compensated against abiotic stress (NaCl) and through developmental changes, giving more evidence of the importance of the robustness of circadian clocks in the adaptation and success of CAM plants and its implication in the avoiding of futile carbon cycles (Borland and Taybi 2004). PEPC and PEPC kinase are the key enzymes of CAM photosynthesis and it has been demonstrated that both are under circadian control in *Kalanchoe*, *A. thaliana*, *M. crystallinum* and *Clusia* (Taybi et al., 2004; Boxall et al., 2005; Hartwell, 2005). In *Clusia*, day/night differences have been found in the transcript abundance of PEPCK between weak CAM *C. aripoensis* and constitutive C3 *C. multiflora* with respect to C3/CAM *C. minor* and constitutive CAM *C. Rosea*. The first two species presented high levels of PEPCK during the day and night whereas the latter two species showed low levels of transcripts of PEPCK during the day but similar levels to the first (weak CAM and C3) during the night (Taybi et al., 2004). This result highlights the importance of circadian regulation over the key enzymes that underpin the capacity for CAM photosynthesis in *Clusia*.

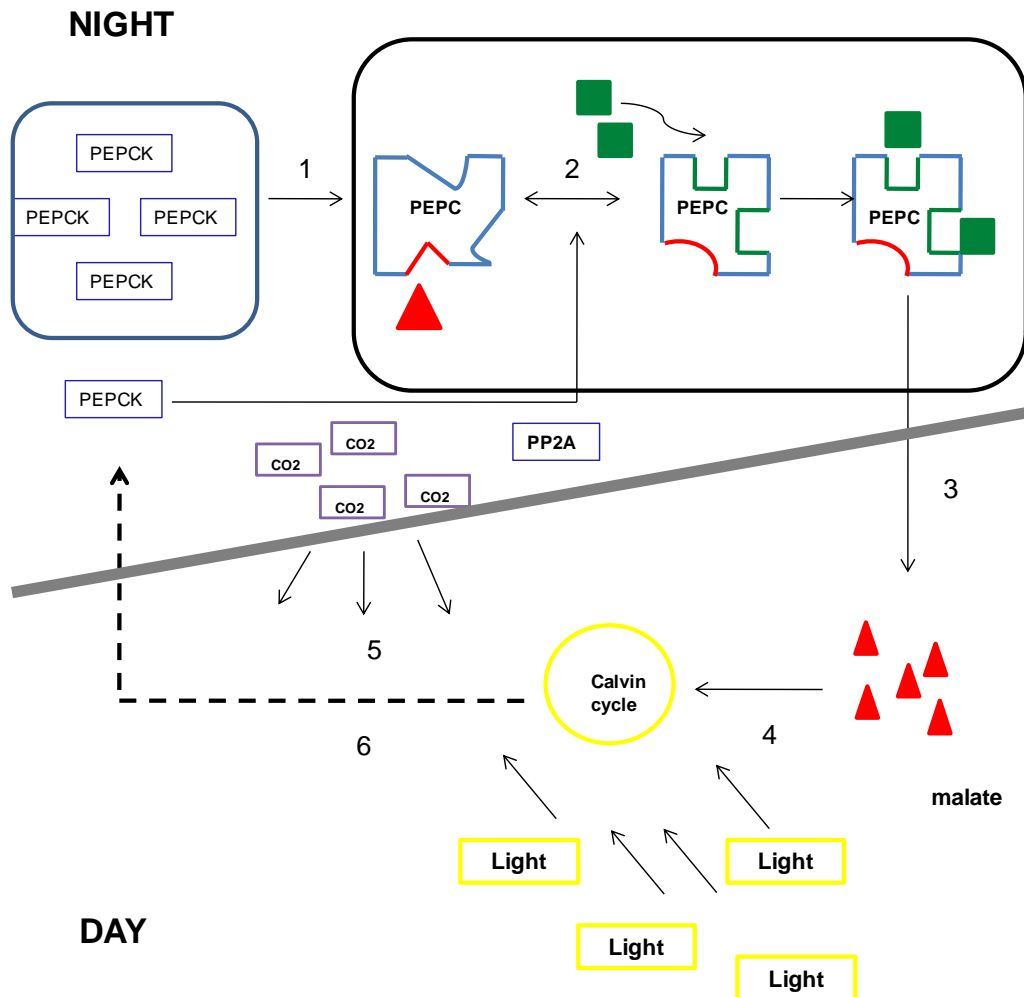


Figure 1.7 Diagram showing how PEPC is under circadian control in CAM plants during the night when levels of PEPC kinase are high, PEPC is activated by phosphorylation (Yulin LI1) making the enzyme less sensitive to malate (inhibitor- red triangle) and more sensitive to the effectors glucose 6 phosphate and triose phosphate (green boxes). PEPC kinase transcription which is under circadian control determines the phosphorylation of PEPC. A reversible, dephosphorylation (Yulin LI1) is regulated by phosphatase 2A during the diel cycle. Accumulation of malate during the day is followed by decarboxylation (4) and photosynthesis driven by light; stomata are open again by the end of day in response to the drop in internal CO₂ concentrations and net CO₂ uptake takes place (5), then PEPC kinase transcription (6) starts again to activate the necessary levels of PEPC during the night for CAM.

1.3.3 Water Use Efficiency

One of the greatest physiological benefits of CAM photosynthesis is high water use efficiency (Osmond, 1978; Nobel, 1988). WUE is defined as the ratio of moles of CO₂ fixed and assimilated to moles of water lost by transpiration and this parameter is high in CAM plants due

to the opening of stomata during the dark period, when the temperature is lower and humidity higher, causing less transpirational water loss (Lüttge, 2006). Certainly, values of WUE about 5–16 mmol CO₂ per mol of H₂O on an annual basis which are 4 to 10-fold higher than C3 (Borland et al., 2009) and 3 to 6-fold higher than C4 have been reported (Black, 1973; Lüttge, 2004). Because of the high water use efficiency in CAM plants and the high presence of succulents in arid habits, it is thought that most CAM species should be found in deserts or very dry places. However just about 1800 CAM species inhabit these type of environments whilst nearly 10,000 species of CAM epiphytic orchids and bromeliads inhabit rainforests (Lüttge, 2000) where they can be subject to variable and potentially limiting water supply in a semi-exposed canopy (Zotz and Hietz, 2001). WUE must be a defining trait in the evolution (Gil, 1986; Lüttge, 2006) and success of CAM plants. Although high WUE is in general due to the opening of stomata during the night, it is strongly related with the four phases of CAM. Lee et al. (1989) reported distinctive values of WUE for *C. rosea* during the day and night phases (i.e. phase II 7.62 mmol CO₂/mol H₂O, Phase IV 9.78 mmol CO₂/mol H₂O Phase I 22.9 mmol CO₂/mol H₂O) whilst in *Kalanchoe-daigremontiana* under drought, day phases II and IV are suppressed (Smith and Luttge, 1985; Lüttge, 1987; Lee et al., 1989).

Furthermore, CAM plants are good at dealing with water stress, not just because of their high WUE efficiency, but also due to anatomical features such as the possession of large vacuoles to store organic acids and water which are also responsible for tissue succulence. Long term water storage involve tissues such as hydrenchymas, epidermal bladder cells (as in *M. crystallinum*: Haberlandt, 1904) and water storage parenchyma (*Peperomia* and bromeliads (Gibeaut and Thomson, 1989; Lee et al., 1989)). All these anatomical features and also stomatal characters and function will be studied in this thesis and related with the WUE capacities across eight *Clusia* species with different degree of CAM photosynthesis and a range of WUE in an effort to elucidate more factors that can be implied in CAM evolution.

1.3.4 Leaf anatomy

Despite the variation and plasticity in the metabolic traits between and within CAM species, plants with this photosynthetic specialisation share a number of anatomical characteristics. Succulence is required for the operation of CAM and is characterized by the possession of large undifferentiated leaves that possess large cells containing a central vacuole (Gibson, 1982; Smith et al., 1996; Winter and Smith, 1996) for the nocturnal storage of organic

acids and water (Borland et al., 1998). Succulence is generally accompanied by an increase in mesophyll cell size which leads to a low internal air space, as a result of the tightly packed cells. The reduction in the internal air space and surface of the mesophyll cells exposed to air might cause constraints in the diffusion of CO₂ from stomatal to carboxylation sites or also may be a mechanism for enhancing CO₂ concentration within the leaf and thereby enhancing photosynthetic efficiency (Maxwell, 1997; Borland et al., 2000). However, leaf thickness and succulence is a very plastic character and within the family of Crassulaceae the magnitude of CO₂ fixation during the night is associated with the thickness and succulence of the leaf (Teeri et al., 1981; Kluge et al., 1991; Kluge et al., 1993). Also, a study with 18 CAM plants belonging to 13 families and six C3 and four C4 plants found an association with the degree of succulence and the internal air space and length of mesophyll exposed to air, being lower in the CAM plants (Nelson et al., 2005). In addition, investigations with *Kalanchoe piñata* have demonstrated that thinner leaves are more plastic and behave like C3 species, whilst in contrast related species with thicker leaves have more constraints to CO₂ diffusion constraints (Maxwell, 1997) and are less photosynthetically plastic, depending on predominant uptake of CO₂ at night (Maxwell unpublished observations).

The leaves of most succulent CAM species possess an undifferentiated mesophyll (Nelson and Sage 2005) but this pattern is not followed by the leaves of *Clusia* which possess clearly differentiated palisade and spongy mesophyll tissues along with an adaxial layer of water storage parenchyma (WSP; Borland et al., 1998). These morphological traits raise the question if CAM photosynthesis requirements of succulence are revealed in the cell size and thickness of the different layers in the mesophyll (i.e. palisade, spongy and WSP). Moreover, does such leaf differentiation in *Clusia* confer a higher degree of photosynthetic plasticity to the plants and influence the magnitude of CAM expression by impacting on leaf CO₂ diffusion? If there is a negative implication for CO₂ diffusion due to the low internal air space in the mesophyll, any other mechanism might exist to counteract the low CO₂ diffusion. Detailed implications of low CO₂ diffusion in CAM plants have been proposed by other authors in previous studies (Evans et al., 1994; Maxwell, 1997; Nelson et al., 2005; Griffiths et al., 2007) and will be discussed in detail in chapter 2. A further important trait relating to leaf anatomy and implicated in CO₂ diffusion is stomatal conductance, raising the question if leaf anatomical traits show any relationship with stomatal size and density in CAM plants.

1.3.4.1 Stomatal size, density and functions

Stomata are the first window for gas exchange in leaves and they are the key structures responsible for the control of CO₂ uptake and water loss via transpiration. Variations in stomatal morphology, distribution patterns and behaviour will impact on water use efficiency (Radoglou and Jarvis, 1990; Ceulemans and Mousseau, 1994) and photosynthetic efficiency. Regulation of leaf gas exchange strongly depends on the balance of stomatal functioning for controlling water and CO₂ demands during photosynthesis (Buckley, 2008) and structural adaptations and coordinated movements of stomata are key to carbon and water use strategies in plant species. There is a broad diversity of stomatal morphology in vascular plants which is expected to be related with functionality (Franks and Farquhar, 2007). There are several examples of plasticity in stomatal density within species as a consequence of changes in atmospheric CO₂ concentrations (Woodward et al., 2002; Hetherington and Woodward, 2003) and drought (Cutter, 1977; Quarrie and Jones, 1977). Also, the ecological and evolutionary success of grasses in arid and semi-arid regions as well as during periods of aridification has been attributed in part to the large morphological diversity and dynamic performance of stomata (Hetherington and Woodward, 2003). Gay and Hurd (1975) showed higher stomata densities in Tomato leaves of plant growing under high light. Also, Ticha (1982) and further Casson and Gray (2008) reported the significant influence of the environment on stomatal development showing that CO₂ concentrations and light intensity control stomatal frequency in developing leaves. It is clear that there is a strong relationship between environmental conditions and stomatal size and density, and the responses are variable between species. Previous works have reported lower stomatal densities in more succulent plants, which are expected to tolerate drought (Sayed, 1998; Lüttge et al., 2007). Beaulieu et al. (2008) have shown that in general, larger cells are a consequence of a larger genome, and there is a theory supporting that CAM evolution involved genome duplication (Cushman, 2001). Thus, large stomata may be a result of the predicted larger genomes of CAM species compared to closely related C3 species which will have implications for the control of gas exchange, perhaps presenting higher rates of water loss and/or CO₂ fixation. Circumstances which might signify a pressure to evolve CAM photosynthesis could be to provide a strategy to respond faster to changes in environmental conditions (Assmann and Wang, 2001; Franks and Farquhar, 2007). To this end it is important to outline how stomata operate in the context of CAM photosynthesis, with high WUE and possible constraints in CO₂ diffusion.

1.3.4.1.1 Stomatal functioning and responses to light

The internal signals that are generated in response to external environmental factors result in the accumulation of K^+ ions in the guard cells surrounding the pore. The accompanying osmotic changes lead to swelling of the guard cells and opening of the stomata (Shimazaki et al., 2007). Stomatal opening occurs in response to red and blue light (Kuiper, 1964; Assmann and Shimazaki, 1999) in two ways. One of the most accepted hypothesis is that red light which drives photosynthesis in the guard cells and which causes CO_2 depletion may act indirectly as a signal for stomatal opening (Sharkey and Raschke, 1981; Roelfsema and Hedrich, 2005). However, some studies demonstrated that there are more than one mechanism responsible of stomatal opening in reaction to CO_2 in C3 plants. One dependent of electron transport during photosynthesis and the other might occur in the dark, being independent of photosynthesis (Messinger et al., 2006). Lawson et. al, (2008) showed that plants of tobacco with a reduction in the Calvin cycle regeneration capacity presented greater stomatal conductances under red light at different C_i , suggesting that primary stomatal responses to light are not only dependant of photosynthetic capacity of guard and mesophyll cells, as it was demonstrated previous in the same plants (von Caemmerer et al., 2004).

Blue light may elicit a direct response in stomata by activating the plasma membrane H^+ -ATPase (Kinoshita et al., 2001; Briggs and Christie, 2002) and driving K^+ uptake by the guard cells (Figure 1.8). Pigments and photoreceptors which absorb blue light have been implicated in the process of stomatal opening (Horwitz and Berrocal, 1997) and zeaxanthin has been the subject of several works recognizing its implications in the blue light reponse of stomata (Zeiger and Zhu, 1998; Zeiger et al., 2002; Talbott et al., 2003). However, other authors have reported no alterations in stomata response to light in the Arabidopsis zeaxanthin mutant *npq1-2* (Eckert and Kaldenhoff, 2000) and important roles of phototropins in the stomatal opening in response to blue light (Kinoshita et al., 2001)

Most of the studies on stomatal responses to light have been conducted using C3 plants, showing the correlation of stomatal opening stimulated by blue light and levels of guard cell zeaxanthin. This pigment forms part of the xanthophyll cycle in chloroplasts where it is converted from violoxanthin and xanthophylls after high light irradiation, and serves as a photoprotective mechanism, absorbing mainly blue light (Quinones et al., 1996). However,

relatively little is known about the responses of stomata of CAM plants to light. Considering the importance of stomata in controlling gas exchange and preservation of water a key aim of this thesis will be to evaluate the responses of stomata to light signals in a C3 and a CAM species of *Clusia*.

Since stomata of CAM plants are open during the dark period, it is intriguing to establish if the response to light still remains in the guard cells. Some studies have reported the loss of stomatal response to blue light but not to red light in *M. crystallinum* and *Portulacaria afra* after induction of CAM (Lee and Assmann, 1992; Tallman et al., 1997). Responses to far red light have been detected in the CAM orchid *Papiphelidum* which lacks chloroplasts in guard cells, suggesting the involvement of an important photoreceptor related to the maintenance of circadian rhythms, (i.e. Phytochrome A), in stomatal movements in CAM plants (Talbot et al., 2002).

Stomatal movements in CAM plants might be controlled through the circadian clock. Since internal CO₂ concentrations depend on PEPC and PEPC kinase activity, and these enzymes are subject to circadian oscillations, the control of CO₂ uptake by stomata might be highly coordinated with the transcription of PEPC kinase as described previously in this introduction. Thus, in summary stomatal movements in CAM plants can be the response of two main signals which are not mutually exclusive and actually act together: the direct light response of photoreceptors involved in circadian control and the response to internal CO₂ concentrations driven by enzymes subjected to circadian regulation.

1.4 Photoreceptors

Photoreceptors are light sensitive proteins able to sense and respond to light, and are present across all living organisms. There are two important families of photoreceptors in plants, cryptochromes and phototropins, which are responsible for phototropism, hypocotyls elongation, chloroplast movements, stomatal opening, and circadian control in response to light (Kendrick, 1994).

1.4.1 Cryptochromes (*cry*)

Cryptochromes are flavoproteins with a single molecule of flavin adenine dinucleotide (FAD) non-covalently bound to the protein, and an N-terminal photolyase (PHR) bound to a light harvesting chromophore which in *Arabidopsis* can be either dezaflavin or pterin; the first

confers absorption to the blue light and the second to the UV-A (Sancar et al., 2000). Although it is still not clear which is the specific chromophore in cryptochrome 1 (Cry1) found in *Arabidopsis*, it seems more likely to be dezaflavin (Ahmad and Cashmore, 1993). Apart from Cry 1, Cry 2 has also been described in plants. Cry 2 has a very similar structure (figure 1.8) and function to cry1 but contains a different C-terminal (Lin et al., 1996). Both cry 1 and cry 2 are phosphorylated by blue light but not by red light (Lin et al., 1998). Some works with mutants have demonstrated that cry 2 differs to cry 1 in this sensitivity to a very weak blue light opposite to cry 1 (Briggs and Huala, 1999). Though some properties of cry 1 and cry 2 are related, there are also distinct roles for these gene products (Cashmore, 1998). Cry 2 seems to have an important role in photoperiodism, especially in flowering (Briggs and Huala, 1999) and its effect in photoperiod timing might be via facilitating mediated signalling rather than a direct signal to the oscillator (Somers et al., 1998). Mao et al. (2005) suggested the involvement of both cry 1 and cry 2 together with phototropins (Pho1 and Pho 2) in the stomatal opening response to blue light in *Arabidopsis*. This blue light induction of stomatal opening by cryptochromes might be mediated by a negative regulation of another protein COP1 (Shalitin et al., 2002; Mao et al., 2005). However, the specific involvement of cry 2 in stomatal opening has not been studied, and due to its importance in circadian control, its sensitivity to low blue light (present at dawn and dusk) and the fact that it was reported for *Clusia* in the EST data base (Sorrock 2009) the transcript abundance of this gene and its response to light will be studied in this thesis.

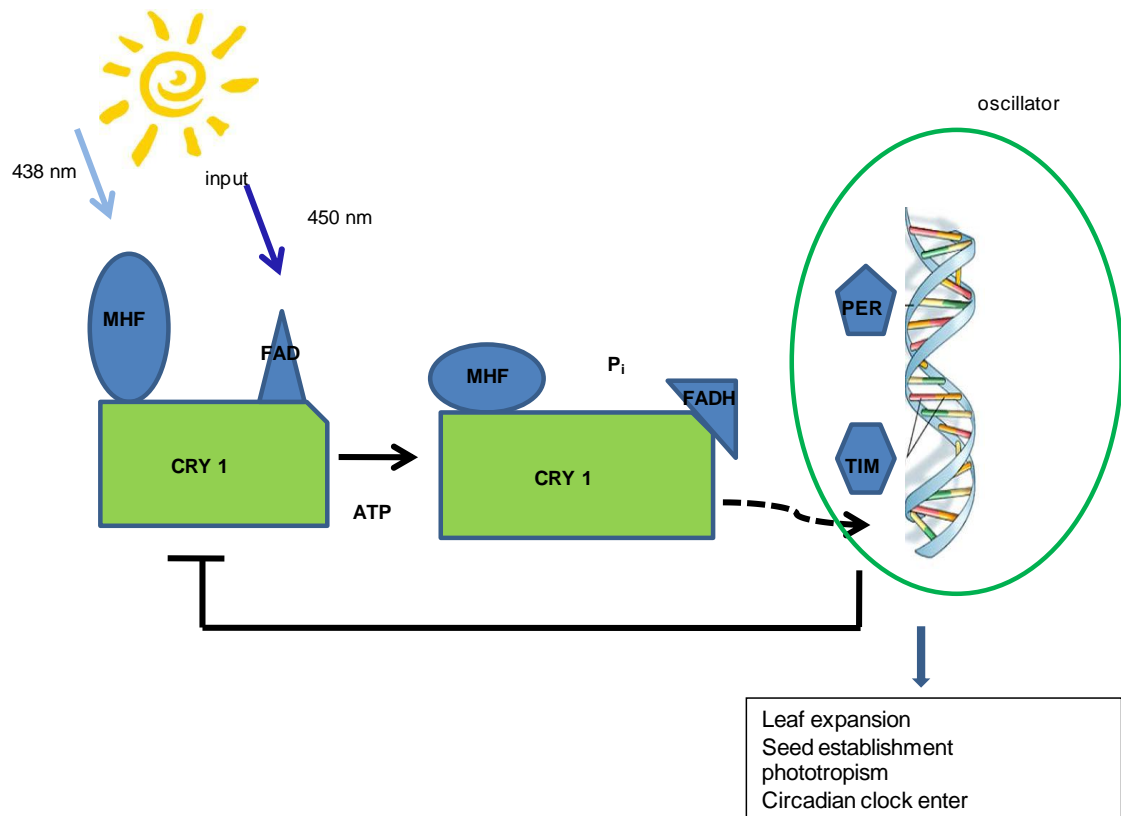


Figure 1.8 Scheme of how cryptochrome responds to light and is involved in circadian processes. Cryptochrome is a flavoprotein with two chromophores 5,10-methenyltetrahydropholic acid (MHF) and flavin (FAD) which absorb blue light at different wavelengths. After the absorption of light the molecule is phosphorylated generating the transcription of genes involved in time control (TIM) and periodical process (PER), which correspond in the diagram to the oscillator, enclosed in a green circle, controlling the dephosphorylated state of the cryptochrome by negative feedback. Output processes include leaf expansion, seed establishment, phototropism and the time sensing to enter the clock. Figure based on (Devlin, 2002).

1.4.2 Phototropins (phot)

Phototropins are blue light receptors controlling responses related to growth and photosynthesis in plants and other living organisms (Christie, 2007). Phototropins are made up of two parts: an activated serine/threonine kinase and a photosensitive domain at the N-terminal. The N-terminal has domains: LOV1 and LOV2 (light, oxygen, voltage) which bind to the cofactor FMN (flavin mononucleotide). Photo-excitation of the LOV domains by blue light escort the autophosphorylation of the phototropin (Christie et al., 1998; Sakai et al., 2001).

An extensive work about the functioning of LOV domains has been published (see Christie 2007 review); however a brief description is presented here. In darkness LOV domains

are non-covalently bound to flavin mononucleotide (FMN) and absorb light near to the 447 nm (Christie et al., 1998; Salomon et al., 2000; Suetsugu et al., 2005). After illumination a covalent bond is formed between the flavin and cysteine which in turn is converted to alanine or serine losing its photochemical reactivity (Salomon et al., 2000) and becomes sensitive to light near to 390nm. This reaction is reversible in darkness (Salomon et al., 2000; Swartz et al., 2001; Kasahara et al., 2002) (Figure 1.9).

Structures of LOV1 and LOV2 are almost identical but present differences in quantum efficiencies and kinetics (Salomon et al., 2000; Kasahara et al., 2002), suggesting different roles in light sensing between them, which might confer the same properties to phot 1 and phot 2. Also, LOV domains are implicated in the recovery from darkness in phot 1 which is 10 times slower than in phot 2 (Kagawa et al., 2004; Kasahara et al., 2004).

Phototropins are widely present in all higher plants. In *Arabidopsis* phot 1 and phot 2 have been described (Briggs and Christie, 2002; Celaya and Liscum, 2005). Work with mutants has demonstrated partially overlapping functions of both phototropins and other responses of plants to light that include chloroplast movements which improve capture or avoidance of light (Christie, 2007). Both phot 1 and phot 2 induce stomatal opening and some studies report equal contribution of both (Kinoshita et al., 2001), but differences in the response might occur according to the differential sensitivity to light intensities. It has been described in *Vicia faba* that phot 1 in guard cells binds a 14-3-3 protein after autophosphorylation (Kinoshita et al., 2003) of Ser³⁵⁸ situated between LOV1 and LOV2 (also in oat Ser³²⁵). This process occurs in response to blue light (Salomon et al., 2003) and indicates the involvement of the interaction between phototropins and H⁺-ATPase in guard cells since H⁺-ATPase are directly implicated in the changes in guard cell turgor causing stomatal opening or closure (Zeiger and Hepler, 1977).

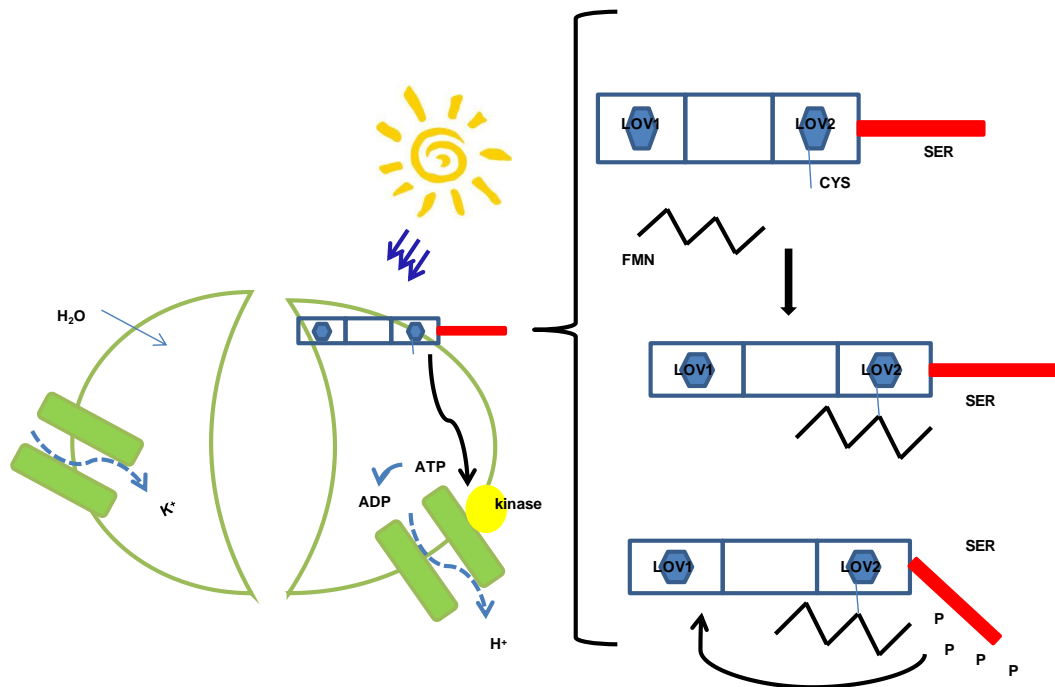


Figure 1.9. Scheme of how phototropins are involved in stomatal opening. Phototropins have two LOV domains (blue circles) and a serine domain (red box), blue light activates the LOV2 domain making the cysteine terminal available to form a covalent bond with the flavo-mononucleotide (FMN). This generates a conformational change in the molecule and autophosphorylation of the photoreceptor (Christie, 2007). As a consequence, the ATPase channels at the guard cell membrane are activated mediated by the kinase, a depolarization of the membrane occurs due to the exit of H^+ ions and entrance of K^+ ions and water, so that turgor pressure inside the guard cell increases and the stomata are open. Figure modified from (Christie, 2007; Shimazaki et al., 2007).

1.4.3 Phytochromes (*phy*)

Phytochromes are another family of photoreceptors that are sensitive to red and far red light. Phytochromes are chromophores with a single bilin molecule (biological pigments) which is composed by an open linear chain of four pyrrole rings (heterocyclic aromatic organic compound; (Quail et al., 1995). Phytochromes can be at the ground state Pr, which absorbs red light (650-670 nm). Once red light is absorbed the pigment undergoes a conformational change to the Pfr state when it absorbs far red light (705-740 nm). These reactions are reversible after the correspondent illumination (Hillman and Koukkari, 1967; Abe et al., 1985; Shimazaki and Pratt, 1985; Tokuhiya et al., 1985) (Figure 1.10). Within the phytochrome family five members

have been identified in *Arabidopsis* (Phy A, Phy B, Phy C, Phy D, Phy E) (Sharrock and Quail, 1989; Clack et al., 1994) and Tomato *Lycopersicon esculentum* (Alba et al., 2000). The five phytochromes are found to belong to two types: the photolabile type I and the light stable type II, Phy A corresponds to type I, Phy B and Phy C are intermediate and Phy D and Phy E are more light stable being part of the type II (Hillman and Koukkari, 1967; Abe et al., 1985; Shimazaki and Pratt, 1985; Tokuhisa et al., 1985).

Phy A is the most abundant in etiolated seedlings and perhaps with phy B is the most studied of the phytochromes (Hall et al., 2001). Phy A plays a role in the promotion of germination (Shinomura et al., 1994), shade avoidance (Johnson et al., 1994), flowering time (Johnson et al., 1994; Reed et al., 1994) and circadian clock entrainment (Somers et al., 1998).

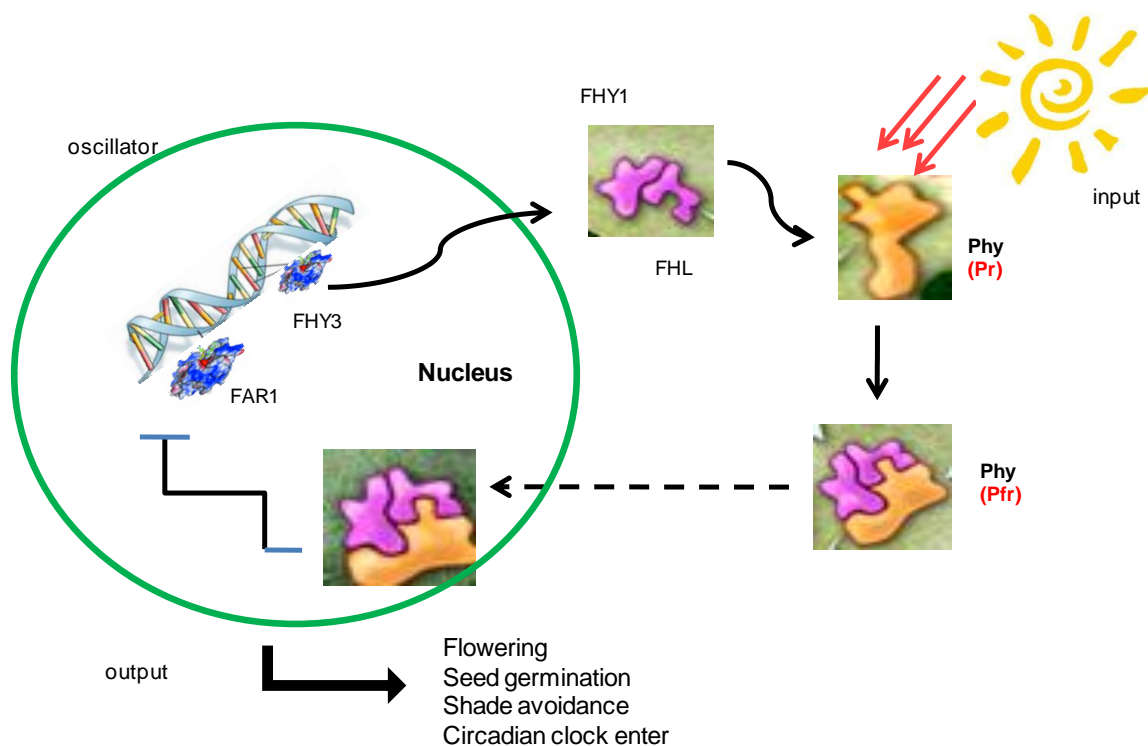


Figure 1.10. Scheme of how phytochrome responds to light and is involved in circadian processes. Two proteins FHY3 (Far red elongated hypocotyls) and FAR (Far red impaired response) bind the DNA leaving the production of FHY1 (Far red elongated hypocotyls) and FHL (Far red elongated hypocotyls like). Phytochrome is a molecule sensitive to red and far red light, changing its conformational change becoming available for the FHY1 and FHL. With this conformation the PHYA is imported to the nucleus where it initiates different responses of plants to light (flowering, seed germination, shade avoidance and circadian clock enter). The oscillator in this case is composed by negative feedback of the transcriptional control of the PHYA which regulates the production of the two proteins FHY3 and FAR and possible other still

unknown. Figure based and modified from Illuminating Study Reveals How Plants Respond to Light." PHYSSorg.com. 23 Nov 2007.<http://www.physorg.com/news115053032.html>

1.4.4 Photoreceptors and the circadian clock

As mentioned above the most important environmental factors to entrain circadian clocks are light and temperature. Photoreceptors play an essential role in sensing and translating the signal perceived from light to the central oscillator (Toth et al., 2001). Cryptochrome and phytochrome have been shown to be involved in that mechanism (Somers et al., 1998; Devlin and Kay, 2000). Some previous works (Ahmad and Cashmore, 1993; Clack et al., 1994; Lin et al., 1998) have reported no changes in the mRNA accumulation of phytochromes and cryptochromes in response to light. On the other hand, more recent investigations have demonstrated that the expression of PhyB is under circadian regulation (Kircher et al., 1999). cry1 and cry2 have also shown circadian rhythms under constant light in *Arabidopsis* (Harmer et al., 2000). Furthermore, Toth and co-workers (2001) demonstrated as well that all cryptochromes and phytochromes (except PhyC) are under circadian regulation at the level of mRNA accumulation and their expression is influenced by light. Under constant light cry2 and PhyC promoters were up-regulated and cry2, PhyA and PhyB were down-regulated. Also, the same work reported similarities in the expression patterns of cry2 and PhyA which showed similar amplitude phase, similar oscillation rhythms, down-regulation by light and sensitivity to low light intensities for both. In addition, Hall and co-workers (2001) showed that PhyA expression is under circadian regulation by red light and the rhythm of the expression damps under constant dark (Figure 1.10).

There is still some debate that phytochromes are directly implicated in circadian rhythms. For instance, it has been reported that the expression of CAB (chlorophyll A/B binding protein) is regulated by light through phytochromes (Hall et al., 2001). Also, Zhong et al. (1997) suggested the association of PhyA and Cry1 in the circadian expression of CAT3 (Catalase 3) in *Arabidopsis*.

The expression of PhyB is influenced by rhythmic output signals coming from the oscillator feedback on the light input pathway (Hall et al., 2001), and the regulation of PhyA might be an outloop from the circadian output on the input pathway (Lakin-Thomas, 2000; McWatters et al., 2000; Hall et al., 2001). Also, it seems that the circadian control of

phytochrome does not occur in all plant species (Hall et al., 2001; Nasy and Millar unpublished observations) or with the same pattern in all plant tissues (Hall et al., 2001).

1.5 Aims of thesis and hypotheses to be tested

Clusia has been demonstrated to show unprecedented photosynthetic plasticity in terms of ability to regulate the amount and duration of CO₂ uptake over the day and night. In this thesis I will take a morphological, physiological and molecular approach to understand how CAM has evolved in this tropical genus. Specifically, I will establish if there are any implications of leaf anatomy in the performance and evolution of CAM, and I will examine how anatomical and physiological features might counteract the diffusive difficulties inherent to the pathway. In addition, stomatal responses to light will be compared in a constitutive CAM plant *C. rosea* and a constitutive C3 plant *C. multiflora* as a means of learning more about the role of photoreceptors in the circadian control of CO₂ uptake and transpiration. For that purpose the following hypotheses will be addressed in this thesis:

H₁: Leaf anatomical traits are related to the magnitude of CAM

H₂: The circadian control of stomatal conductance is more robust in CAM than in C3 *Clusia* plants and is mediated via photoreceptors rather than via metabolism (photosynthesis)

H₃: Patterns of transcript abundance of phot 1 and phot 2 will be different in *C. multiflora* and *C. rosea* under 12h dark/12h light cycles and will present changes in response to different light regimes

H₄: Circadian expression of photoreceptors will be more robust in *C. rosea* than in *C. multiflora*.

H₅: The amplitude of circadian oscillations in the transcript abundance of *cry2* and *phyA* will be more responsive to the imposition in different light regimes in the CAM compared to the C3 *Clusia*

Chapter 2: Functional leaf anatomy of *Clusia*

2.1 Introduction

A general trait pertaining to the leaf anatomy of plants with crassulacean acid metabolism (Bowler et al., 1994) is succulence which is generally characterised by large undifferentiated chlorenchymatous cells, each of which is dominated by a large central vacuole. The extensive vacuolar storage capacity of CAM leaves permits overnight accumulation of malic acid and also enhances the storage of water (Borland et al., 1998). Positive relationships have been demonstrated between succulence and the magnitude of CAM expression and between leaf thickness and CAM-like ^{13}C discrimination in diverse phylogenetic lineages (Teeri et al., 1981; Winter et al., 1983; Borland et al., 1998; Holtum et al., 2004; Griffiths et al., 2007; Vargas-Soto et al., 2009). Given that leaf succulence and thickness are often linked with general adaptation to water-limited habitats, it has been suggested that possession of this anatomical trait might have predisposed ancestral CAM taxa towards the evolution of this photosynthetic specialisation in water-limited habitats (Sage, 2002).

It has been proposed that *Clusia* species are adapted to drought and high irradiance through the use of CAM and that this is associated with the degree of leaf succulence (Borland et al., 1998). However, unlike the largely undifferentiated leaf anatomy that is typical of most CAM species (Nelson et al., 2005), the leaves of *Clusia* possess clearly differentiated palisade and spongy mesophyll tissues along with an adaxial layer of water storage parenchyma (WSP) (Borland et al., 1998). *Clusia* species vary in terms of leaf thickness/succulence and in addition show different levels of CAM both within and between species, which could confer more or less adaptability to environmental limitations. We do not fully understand how the morphological and physiological characteristics of leaves of *Clusia* contribute towards adaptation and acclimation to water-limited conditions or indeed if certain leaf characteristics predispose or constrain *Clusia* species to show different degrees of CAM. Observations on a range of taxonomically diverse CAM species have implied that thicker, more succulent leaves have less air space between mesophyll cells (Maxwell; Maxwell, 2002; Brodribb and Holbrook, 2003; Nelson et al., 2005) and a reduction in the surface of mesophyll exposed to air (Lmes/area) (Nelson and Sage, 2008). Such observations raise the question of how the CAM requirement for succulence is reflected by the relative

thickness and cell size of the different tissues (i.e. palisade, spongy and WSP) in *Clusia* leaves and how this might influence genotypic differences in both the magnitude and plasticity of CAM expression by impacting on leaf CO₂ diffusion.

Several hypotheses have been proposed about characteristics and mechanisms that succulent CAM species possess to counteract the possible diffusional limitations imposed by tightly packed cells in the leaf. Reduced internal air space of leaves performing CAM can increase resistance to CO₂ flux (Nelson et al., 2005). The hypothesis is that this trait reduces internal CO₂ conductance and could thus limit the efflux of respiratory CO₂ at night. Recapture of respiratory CO₂ at night is thought to have been an early step in the evolutionary process by which CAM evolved from C₃ photosynthesis. A low internal conductance to CO₂ would also minimize CO₂ efflux from leaves during the day-time decarboxylation processes of CAM so a low internal CO₂ conductance could be seen to maximize the photosynthetic efficiency of CAM species that rely on dark CO₂ uptake (Phase I) for the majority of net carbon gain (Griffiths et al., 2007). In contrast, it has been hypothesised that reduced internal CO₂ conductance may reduce photosynthetic efficiency in CAM plants which rely heavily on late afternoon (Phase IV) direct atmospheric uptake of CO₂, because diffusion through the tightly packed mesophyll limits carbon availability for Rubisco (Evans et al., 1994; Maxwell, 1997; Nelson et al., 2005). This has prompted the suggestion that low intracellular air space (IAS) could be a selection pressure promoting CAM efficiency, particularly in constitutive CAM species which rely heavily on dark CO₂ uptake for carbon gain rather than an inevitable consequence of large cells with storage capacity for malic acid and water (Maxwell, 1997). In contrast, it might be hypothesised that a low IAS is a disadvantage for facultative CAM species which show plasticity in adjusting net CO₂ uptake during the nocturnal and day-time phases of CAM. Such hypotheses imply that differences in leaf succulence and IAS might predispose closely related species to different degrees of CAM. A further unresolved question in terms of leaf diffusional constraints to CO₂ exchange in CAM plants concerns stomatal conductance. Thus, is there any relationship (positive or negative) between internal leaf diffusion, succulence and stomatal density/index?

The aim of this chapter was to investigate the question of whether or not genotypic variation in the plasticity of CAM in *Clusia* is reflected in anatomical attributes that influence the diffusion and conductance of CO₂ and H₂O through leaves. From an evolutionary context we also sought to establish if there is a particular leaf anatomy that might predispose *Clusia* species towards CAM expression. Recent phylogenies of *Clusia* reveal that CAM has two independent origins within the family (i.e. first time in a group of sections: section Chlamydoclusia (containing *C. rosea* and *C. grandiflora* (reversal), section Ploianthera (containing *C. hilariana* and *C. lanceolata*), The Omphalanthera complex

(containing *C. ariipoensis*), The Flava group, and section Cordylandra and second time in section Retinostemon and nine reversals, suggesting that CAM is a homoplasious character (Figure 2.1) (Gehrig et al., 2003). It does not appear that C₃ photosynthesis was the origin of CAM within *Clusia* since *C. multiflora* which is an obligate C₃ species, does not appear at the base of the phylogeny and actually is found in the most derived grouping of *Clusia* species, many of which are also proposed to exhibit C₃ characteristics (Vaasen et al., 2002; Gehrig et al.; Holtum et al., 2004). Perhaps even more intriguing is the observation that this obligate C₃ *Clusia* species is extremely drought tolerant, a trait usually associated with CAM (Herzog et al., 1999). This poses the question as to whether or not the leaves of C₃ *Clusia* species possess anatomical features that are incompatible with CAM yet confer adaptation to water limitation. Further, is leaf anatomy in *Clusia* defined more by phylogenetic position rather than photosynthetic characteristics?

In order to address the questions posed above, the following hypotheses were constructed:

H₁. Specific leaf area is inversely related to the magnitude of CAM

P₁: *Clusia* species with a higher degree of CAM assessed as percentage of CO₂ taken during phase I will present a lower specific leaf area and a higher WUE (Winter and Holtum, 2002; Lüttge, 2006); (Winter et al., 2005)

H₂ The degree of CAM is positively related to cell size and negatively related to IAS and length of mesophyll surface exposed to air (Lmes/area) in *Clusia* species.

P₂: All tissue types within the leaves of CAM species of *Clusia* will have larger cells than the C₃ species in order to accommodate vacuoles for malic acid storage and this will present lower values of IAS and Lmes/area, due to tighter cell packaging in the CAM species.

H₃: The presence and relative abundance of PEPC and Rubisco vary through different layers of the leaf mesophyll in different photosynthetic categories of *Clusia* species.

P₃: It is predicted that Rubisco will be found in higher abundance in the palisade cells than in the spongy mesophyll in all *Clusia* species since this will confer greater availability of PAR for photosynthesis. In contrast, the abundance of PEPC is predicted to be higher in the spongy than in the palisade mesophyll of CAM species, because proximity to the sub-stomatal cavities could maximise the draw-down of CO₂ into the leaf and help to overcome the constraints imposed by low IAS to CO₂ diffusion.

H₄: The degree of CAM in *Clusia* species shows a positive relationship with stomatal density and/or pore area.

P₄ : Previous studies have indicated that, in general, more succulent species show lower stomatal density than less succulent species (Sayed, 1998; Lüttge et al., 2007). However, it is also possible that to counteract low CO₂ diffusion from the sub-stomatal cavity to Rubisco carboxylation sites, succulent plants have higher stomatal densities and/or larger stomatal apertures, features directly implied in CO₂ conductance (Lawson et al., 1998; Lawson et al., 1998).

2.2 Materials and Methods

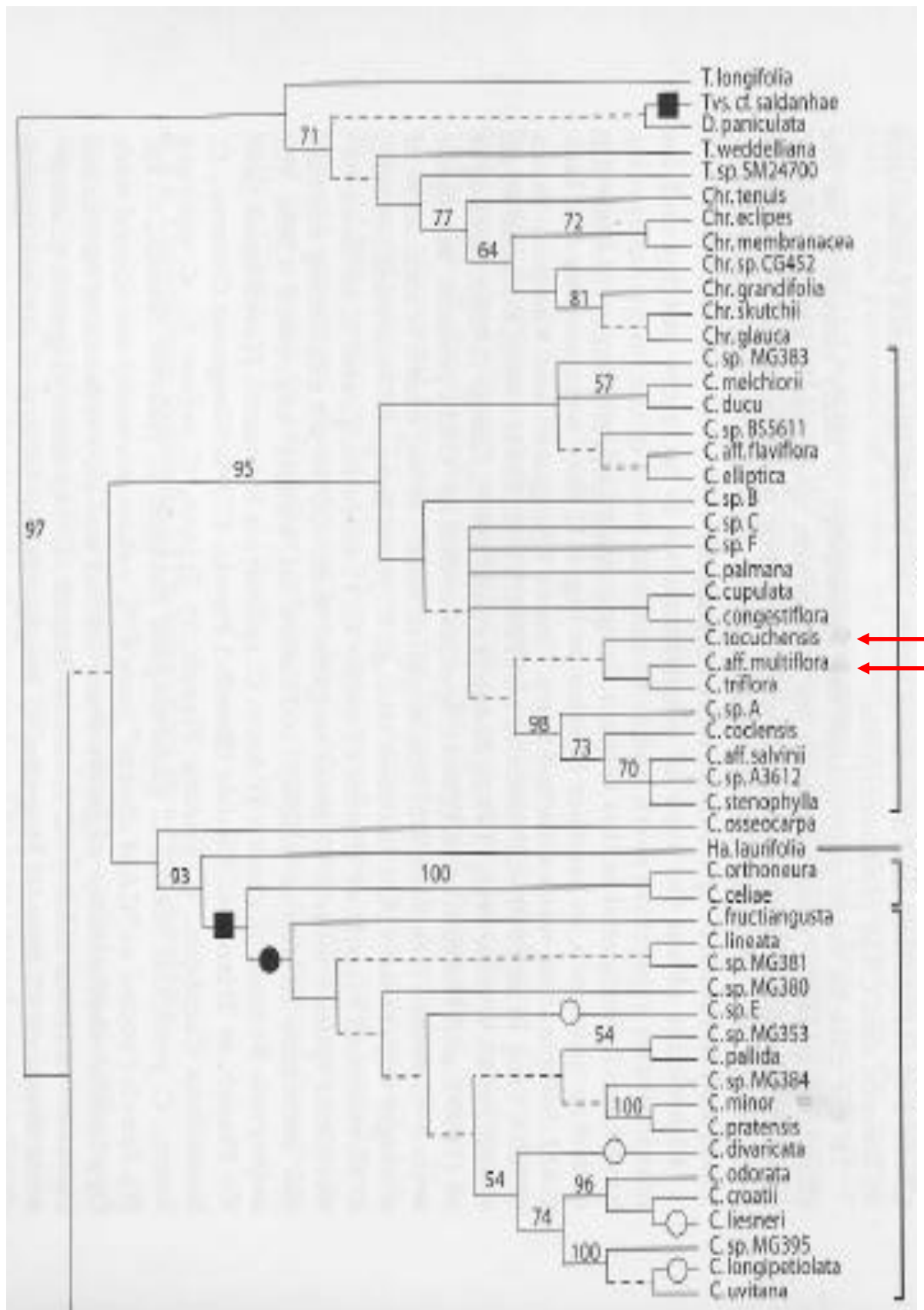
2.2.1 Plant Material

The species chosen for this work were based on the degree of leaf thickness, previous reports of CAM activity and position in phylogenetic trees (Vaasen et al., 2002; Gehrig et al., 2003; Holtum et al., 2004). Species included were: *C. multiflora* H. B. K. an obligate C₃ species (Grams et al., 1998), found growing in Venezuela (Herzog et al., 1999) and reported in Central and South America; *C. tocuchensis* Britton 1921, reportedly an obligate C₃ species (Lüttge, 2007) found in Trinidad & Tobago Islands and considered an endangered species (Van den Eynden et al., 2008); *C. lanceolata* Camb., a weak C₃/CAM intermediate species (Roberts et al., 1996; Luttge, 1999), with less thick leaves compared to the other species of study and reported to be found mainly in Brazil; *C. aripoensis* Britton 1923, an intermediate C₃/CAM species (Borland et al., 1998) found in Trinidad & Tobago and considered an endangered species (Van den Eynden et al., 2008); *C. hilariana* Schlecht. described as a CAM species found in South America (Franco et al., 1999) with succulent leaves; *C. alata* Pl et Tr 1860 considered to be a strong constitutive CAM species with very thick leaves (Luttge, 1999), and found in Central and South America; *C. rosea* Jacq 1760 distributed at the tropics in North, Central and South America and considered a constitutive CAM species. (Lüttge, 2007) and *C. grandiflora* Splitg 1842, reported in French Guyana, Suriname and Venezuela, considered a C₃ species that has lost CAM (figure 2.1) (Gehrig et al., 2003).

It is important to note that these *Clusia* species (except *C. multiflora*) have been reported to present different degrees of CAM under diverse growing conditions and previous studies have failed to agree on the potential of CAM expression in these different species. Thus, all species described above

were analysed for CAM expression by monitoring diel gas exchange patterns under identical controlled conditions.

Cuttings of each species were taken from plants growing at Moorbank Botanic Garden, Newcastle University. Rooted cuttings between 2-3 years old and about 80cm -100cm in height were taken from Moorbank to a growth chamber with a 12 hour photoperiod, 65-75% relative humidity, $300 \mu\text{mol m}^{-2}\text{s}^{-1}$ light intensity at plant height and day/night temperature of 27/18 °C. The plants were maintained under these conditions for 2-4 weeks for acclimation before gas exchange measurements and anatomical studies commenced.



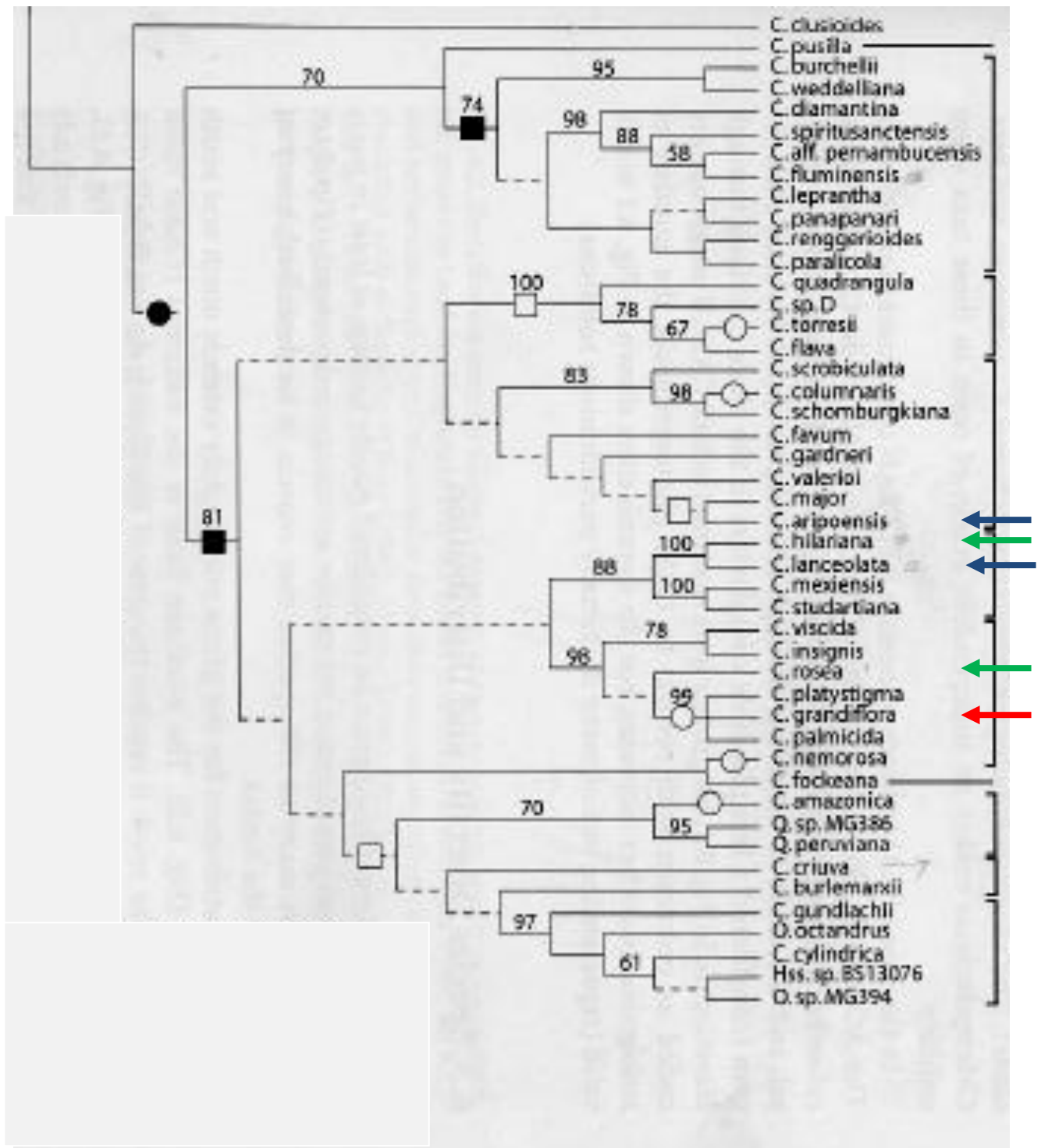


Figure 2.1. Phylogenetic tree based on ITS sequences showing relations within the genus *Clusia* (taken from (Gehrig et al., 2003) Gustafsson and Bittrich 2003). Circles represent CAM photosynthesis (black = gain, white = loss). Data are based on $^{13}\text{C}/^{12}\text{C}$ ratios, and thus mean that weak CAM cannot be excluded with certainty (Gustafsson and Bittrich, 2002). *C. multiflora*, *C. tocuchensis* are placed at the most derived positions of the phylogeny, with C3 photosynthesis. *C. aripoensis*, *C. hilariana*, *C. lanceolata* and *C. rosea* are more basal, presenting CAM photosynthesis. *C. grandiflora* shows a loss of CAM photosynthesis. Red arrows show C3 species, blue

arrows C3/CAM and green arrows CAM species. *C. alata* is not showed in this phylogeny but in another phylogenetic tree from (Vaasen et al., 2002) *C. alata* appears next to *C. minor*.

2.2.2 Gas exchange profiles

Net CO₂ uptake was measured using a compact mini cuvette system, Central Unit CMS-400 with BINOS- 100 infra-red gas analyzer, working in an open format. A fully expanded leaf was clamped in the cuvette, ensuring it received full light within the growth chamber. Temperature and relative humidity of the cuvette were set to track environmental conditions within the growth room. Data for net CO₂ uptake, evapo-transpiration and conductance to water and CO₂ were recorded every 15 minutes. The measurements were made at CO₂ ambient concentrations of 360 μmol mol⁻¹ CO₂ and also under CO₂-free air to measure maximum stomatal pore aperture and conductance. The gas flow through the cuvette was maintained between 400 and 500 ml min⁻¹ to avoid water condensation inside the cuvette. The leaf was maintained inside the cuvette for at least 48 hours to get a complete 24 h gas exchange profile. Data were analysed using DIAGAS software based on the area of leaf inside the cuvette (variable depending on the leaf size). Net CO₂ uptake was determined using the difference in CO₂ mole fractions between gas entering and leaving the cuvette (for detail of .BINOS mechanism and calculations see appendix 1) Data were plotted against time of the day.

2.2.3 Leaf anatomy and stomatal characteristics

Leaf thickness plays an important role in plants and is directly related to resource-use strategies that include quantity of light absorbed and amount/rate of CO₂ diffusion through the mesophyll to perform photosynthesis and invest in growth (ie: leaf thicknes is negative realted with growth and photosynthesis and a relationship between construction costs and longevity of the leaf have been related with thicker leaves) (Vile et al., 2005); as mentioned above leaf thickness also appears to be a functional trait in CAM plants. However, leaf thickness is a difficult feature to assess, due to the different components of the leaf (cuticle, hairs, spines) and the relatively small dimensions involved (Vile et al., 2005). Succulence is a diagnostic trait of CAM plants that directly influences leaf thickness however some authors (Vendramini et al., 2002; Vile et al., 2005) have suggested other measurements which are better indicators of leaf thickness compared to succulence. Such measurements include specific leaf area (SLA), leaf water content (LWC) (Witkowski and Lamont, 1991; Garnier and Laurent,

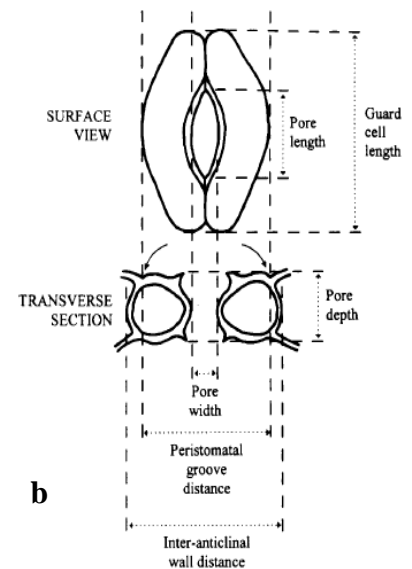
1994; Shipley, 1995; Cunningham et al., 1999; Pyankov et al., 1999; Wilson et al., 1999), all in (Vendramini et al., 2002) and leaf dry matter content (LDMC) (Vile et al., 2005). SLA is a good indicator of resource use (Yulin LI, 2005) and leaf tissue density (Garnier and Laurent, 1994), is a better predictor of resource strategies in succulents, and is probably the most useful leaf anatomical measurement for inclusion in large comparative databases (Vendramini et al., 2002). For these reasons, specific leaf area (SLA) = leaf area (cm²) / dry weight (g) was used as a surrogate measure of succulence in the present study. Leaf discs were punched from three different plants of each *Clusia* species and fresh weight was recorded, the same discs were dried at 70 °C for three days and dry weight record using a Sartorius balance.

The leaves of *Clusia* are hypostomatous (Barrera, unpublished observations) so to measure stomatal characteristics, impressions of abaxial surface of the leaf at the mid part of each side of the main vein, were taken using Xantropen VL plus silicone impression material and hardener (Beyer Dental Leverkusen, Germany) with a mixture of approximate ratio 10:1 smeared over approximate a 15% of the leaf (Weyers and Johansen, 1985). After polymerization, the material was detached and cut in several pieces of 1cm², a positive image made by applying clear nail varnish. Once dry the nail varnish was peeled off and placed on a microscope slide (Weyers and Johansen, 1985). Stomatal impressions were made for 2-3 leaves of 2 plants per species and at different times of the day, to cover a range of stomatal opening states under ambient CO₂ and under CO₂ free air (to get maximal stomatal aperture). Several pictures were taken per species under the light microscope (Leica DM RB) in order to cover different parts of the same leaf. At least 25 stomata per leaf were measured in terms of stomatal dimensions and in average 51.76 areas of 1.65 mm² were used to estimate stomatal density and stomatal index. Stomatal dimensions (pore width, pore length, peristomatal groove distance (was measured because has been proposed as a surrogate measure of pore aperture and it is usefull in case pore aperture are diiult to see), and guard cell distance (Figure 2.2) were measured under 40x magnifications and stomatal density was measured under 10x magnifications. All the images were analysed using J image software.

Based on stomatal dimensions (maximal pore aperture based on an elliptical shape where aperture is 2/3 of mean pore lenght), mean depth and density, the theoretical stomatal conductance (GH₂O) was estimated using the equation given below (Lawson et al., 1998):

$$G_s = \frac{(\text{mean formula mass of air}) \times (\text{effective diffusion coefficient}) \times (\text{Stomatal density}) \times (\text{pore area})}{(\text{pore depth}) + (\text{end correction})}$$

a.



b.

Lawson et al. 1998

Figure 2.2. a. Equation used to calculate theoretical stomatal conductance, mean formula of air was taken as 40.9 mol m^{-3} at 25°C , effective diffusion coefficient for water vapour in air is $2.49 \times 10^{-5} \text{ m}^2 \text{ s}^{-1}$ at 25°C (Jones, 1992). Pore area was calculated assuming the pore as an ellipse with a constant minor axis, pore length, at different apertures, and maximal aperture (equal $2/3$ of pore length) as major axis. Finally an end correction = $(\text{pore area} / \pi)^{0.5}$ (Nobel, 1991) was applied. b. diagram showing the anatomical features measured for stomata.

To study internal leaf anatomy, transverse sections of 2-3 leaves of each species were made, following the methodology of (Morison et al., 2005). Small sections of leaf (approximately 2-3 mm wide by 8-10mm long) were cut using a razor blade, vacuum infiltrated with 5% glutaraldehyde and left overnight at 5°C . The leaf pieces were subsequently passed through a dehydration/wash series of 20%, 30%, 50%, 70% and 90% ethanol, ending with 2 washes in 100% ethanol and left overnight at 5°C . Each leaf piece was then placed in a capsule (Agar Scientific Ltd, 66a Cambridge Road, Stansted, Essex CM24 8DA Cat. No. G292-00 Size 0 Gelatine Capsules) and resin (Sigma LR white acrylic resin; L9774-100G) was added. A capsule lid was attached and the entire capsule was placed in an oven at 65°C overnight in order to polymerize the resin. The capsules were labelled and stored at room temperature until sectioning. Sections of $1 \mu\text{m}$ thick were cut using an ultra-microtome, placed on a microscope slide, stained with toluidine blue then heated gently in order to bond sections to the slide and then a cover slip was placed on top. Pictures of each section were taken under 5x, 10x and 40x magnifications in order to measure mesophyll thickness, (i.e. depth of each mesophyll layer and of

water storage parenchyma), cell size (i.e area), Internal air space (IAS) and Length of mesophyll exposed to air per area unit (Lmes/area) and pore depth respectively with the help of Image J software (Appendix 2, gives details of the use of Image J for these measurements).

2.2.4 Protein extraction and western blotting

2.2.4.1 Protein extraction

Samples from two leaves of three different plants of each species were taken during the morning, under well watered conditions and after nine days of drought in the case of *C. lanceolata*, *C. aripoensis*, and *C. grandiflora*. All leaves sampled were mature, fully expanded and without visible signs of senescence. Where possible, leaves were sampled at the same branch position, having similar incident photon flux densities. Immediately after sampling, tissue was snap frozen in liquid nitrogen then stored at -80°C. Approximately 200mg of frozen leaf tissue (mid-vein removed) was ground in 500 µl of extraction buffer pH 10.3 composed of 450 mM bicine, 50mM CAPS (cyclohexylamino-propanesulfonic acid), 1% PEG (Polyethylene Glycol) 6000. The slurry was poured into a 1.5 ml eppendorf tube, the lid was pierced and the tube was snap frozen in liquid nitrogen. After thawing, the tubes were spun at 15700g (13000 rpm) for 5 min at 5°C. Exactly 200 µl of the supernatant was added to 800 µl of 80% cold acetone at 5°C in a 1.5ml eppendorf, the lid was pierced and the tube was snap frozen in liquid nitrogen. After thawing, samples were spun at 15700g for 7 min at 5°C. The acetone was poured off and discarded, the remaining protein pellet was re-suspended in 100 µl of 'blue water'. 'Blue water' comprised: 0.0756g Tris base, 1 ml glycerol, 5 ml 10% SDS, 0.5 ml mercaptoethanol, 100 µl of 0.02% bromophenol blue, 25 µl (1M) DTT (dithiothreitol), 50 µl (10%) SDS (sodium dodecyl sulphate) in total volume of 10 ml. Finally the samples were boiled for 2 min.

2.2.4.2 Discontinuous SDS - PAGE

Proteins were separated by molecular mass, using polyacrylamide gel electrophoresis (SDS-PAGE; (Laemmli, 1970) with Vertical Mini-Protean II™ gel system (Bio-Rad Laboratories Ltd, Hemel Hempstead, Hertfordshire) which uses gels that are 0.75 mm thick, 7 cm long and 8 cm wide. Approximately 1 cm depth of 4% stacking gel composed of 1.2 ml 30% acrylamide stock, 5.6 ml H₂O, 2.25 ml 4x UPGB (pH 6.8, 15.2 g Tris, 10ml 10% SDS to 240 ml with H₂O), 54 µl 10% ammonium persulphate (APS), 9 µl N,N,N',N'-tetra-methyl-ethylenediamine (TEMED) was used to focus proteins, prior to separation in a 12% resolving gel composed of 7.5 ml 30% acrylamide stock, 6.25 ml H₂O, 4.5

ml 4X LWGB (pH 8.8, 45.4 g Tris, 10ml 10% SDS to 240ml with dd water), 100 µl fresh made 10% APS and 18 µl TEMED. Large and small glass plates were cleaned with 80% acetone prior to assembling onto casting stand. After transferring the resolving gel mix to the glass plate assemblage it was overlain with 200 µl of isopropanol. After polymerization of the resolving gel (~ 45 min), indicated by the formation of a line between isopropanol and the gel, the remaining isopropanol was poured off and the 4% stacking gel mix was poured over the surface of the polymerised separating gel. A PFTE[®] comb was inserted into the top of each gel to form the loading wells and the gel was polymerised (~30 min). The combs were removed and the assemblage remounted in the electrophoresis apparatus. For running the gel, the electrophoresis chambers were filled with ~ 600 ml of 1X running buffer. The stock 10X buffer was made with 15.15g Tris, 72g Glycine, 5g SDS in 500 ml of H₂O, pH 8.3. Prior to loading, samples were heated in a boiling water bath for 5 min to completely denature proteins. Exactly 15 µl of each sample were loaded on the same gel and 5 µl Fermentas PageRuler pre-stained protein ladder was loaded for monitoring protein separation during SDS-PAGE. Three gels were run simultaneously, one for PEPC, one for Rubisco and one for protein staining to check that comparable amounts of protein had been loaded for each of the different *Clusia* species. Samples were run at 75V through the stacking gel for ~45 min and then at 150V through the separating gel for 45-60 min until the dye band reach the bottom of gel. Gels were removed from the electrophoresis apparatus and the gel for protein staining was immersed in fixative solution composed of 80ml methanol, 14 ml 100% glacial acetic acid, 6 ml H₂O for 3 min and then stained overnight in 10 ml coomassie blue solution (40% methanol, 7% glacial acetic acid, 0.05% Coomassie brilliant blue (Raymond A. Lamb) with 2.5 ml methanol.

2.2.4.3 Western blotting

After electrophoresis, gels for blotting were soaked for 15 min in blot transfer buffer that was composed of 5.82g Tris, 2.93g glycine, 3.75 ml 10% SDS, 200 ml methanol, made up to 1L with dH₂O. Four sheets of blotting paper, of the size of the gel, were soaked in blot transfer buffer and one piece (of the same size of the gel) of PVDF (polyvinylidene difluoride) membrane (0.45 µm pore size; Immobilon-P, Millipore Corporation Bedford, USA) was soaked in 100% methanol and then in blot transfer buffer. A sandwich that was made up of two pieces of blotting paper, the membrane, the gel and two pieces of blotting paper on the top was placed over the anode plate of the blot transfer apparatus (Bio-Rad); air bubbles were eliminated by rolling a glass test tube over the assembled sandwich which was then covered with the cathode plate of the transfer apparatus. Protein transfer was conducted at 10v for 30 min.

After removal from the blot transfer apparatus, membranes were immersed overnight in 10X Tris Buffered Saline (TBS) that was composed of 1.5M NaCl and 100mM Tris pH 7.5. The membrane was subsequently immersed in Ponceau S solution (in 5% acetic acid, Sigma-Aldrich) to ensure complete protein transfer, then the membrane was blocked in 5g skimmed milk powder in 100 ml of 1X TBS, for 60 min. Antibodies for PEPC (raised against the purified enzyme from *Panicum miliaceum* and provided by Professor Jean Vidal) and Rubisco small sub unit (SSU raised against the purified enzyme from tobacco in rabbit, provided by Dr. M.A.J. Parry, Crop Performance and Improvement, Rothamsted Research, UK) were added to the membranes in a 1:3000 dilution in 5% milk, for 60 min. Then, two x 10 min washes in TBST (0.1% Tween 20 in TBS) were given and one 10 min. wash in 1x TBS followed. After this, a secondary antibody (10ul made up in 10 ml blocker milk solution; Sigma A6154, goat ant-rabbit IgG) was added for 60 min. Finally, three x 10 min. washes in TBST were given. During the incubation and wash steps, the membrane was agitated on a shaker. To visualize PEPC and Rubisco SSU, the membrane was soaked in a mixture of 3ml ECL (GE-Health Suppliers) reagent 1 and 3ml ECL reagent 2 for 1 min. Then the membrane was placed on a clean piece of acetate film on a film cassette and taken to the dark room where photographic film (Kodak Biomax-XAR) placed on the cassette and developed after 5 min. Film was developed using Kodak developer and fixer reagents prepared according to the manufacturer's instructions

2.2.5 Immuno-labelling for PEPC and Rubisco in leaf sections

To localise and determine the relative abundance of PEPC and Rubisco in palisade and spongy mesophyll cells, transverse sections of leaves of *C. aripoensis* and *C. rosea* were taken. Leaf pieces (strips of approximately 1 cm length and 0.2 cm width) were fixed in 0.5% glutaraldehyde plus 2.5% paraformaldehyde in sodium buffer 0.1 M pH 7.2 for 90 min at 4°C. Three washes of 15 min each, in sodium phosphate buffer 0.1 M pH 7.2 were given at 4°C. Dehydration with ethanol was carried out and consisted of 30 min washes in 35%, 50%, 70%, 96% ethanol and three (30 min each) washes in 100% ethanol, at room temperature. For embedding, the dehydrated leaf pieces were submersed for 60 mins in 75% ethanol + 25% LR whiteTM white resin medium grade (ref 14381 Electron Microscopy Science). The leaf pieces were then transferred to 50% ethanol + 50% LR white resin for 60 min, 25% ethanol + 75% LR whiteTM resin for 60 min, 100% LR white resin for 60 min and left in white resin overnight at

4°C. Finally polymerization¹ was carried out in an oven at 50°C for 12-18 hours, inside flat moulds under a continuous flux of N₂.

Sections of 60-70 nm thickness were cut using a Leica EM UC6 ultra-microtome, and were collected on var-coated nickel grids. For enzyme localisation, between 2-4 samples of each species were treated with 40 µl PBS (Tampon phosphate potassium) KH₂PO₄ 10 mM pH 7.4 + 150 mM NaCl and 5% BSA (Bovine Serum Albumin) for 30 min. After this, a specific antibody (the same used for western blots) was added to the gridded samples in a dilution of 1:250 in PBS and 5% BSA for 180 min. Three washes of five min each with 40 µl PBS were carried out and a secondary antibody (Goat anti-Rabbit, IgG, 10nm, Electron Microscopy Sciences) labelled with gold in a dilution of 1:100 in PBS and 40 µl 1% BSA was added for 120 min. Samples were then washed twice (5 min each) in 40 µl of PBS. Finally, five washes in MLQ (Mili-Q, water purified using an ion exchange cartridge (Millipore Corporation) fresh filter water, each for 5 min duration were made. The copper grids were left to dry at room temperature inside a petri dish with filter paper. A Philips Tecnai 12 transmission electron microscope¹ was used to examine sections and dots of gold per µm² were counted in the cytoplasm for PEPC and in the chloroplast for Rubisco, as well in the mitochondria and vacuole as a background.

Results from the Immunolabeling technique are only shown for *C. aripoensis* and *C. rosea*, due to the problems of encountering mesophyll cell damage in *C. multiflora* and *C. tocuchensis*. It is possible that the high content of phenolics and latex in the C3 *Clusia* species (K Shorrocks personal communication) impeded penetration of resin so that tissue conservation was poor in these species.

2.2.6 Statistical Analysis

Measurements of pore areas, density and index, IAS and Lmes/area for the eight *Clusia* species were grouped according to photosynthesis type, constitutive CAM, C3/CAM and constitutive C3. Anova tests were performed in case of normality and Kruskal wallis in case of non-normality. A Tukey test was performed to test for significant differences between photosynthetic groups. All statistical analyses were performed using SPSS 15.

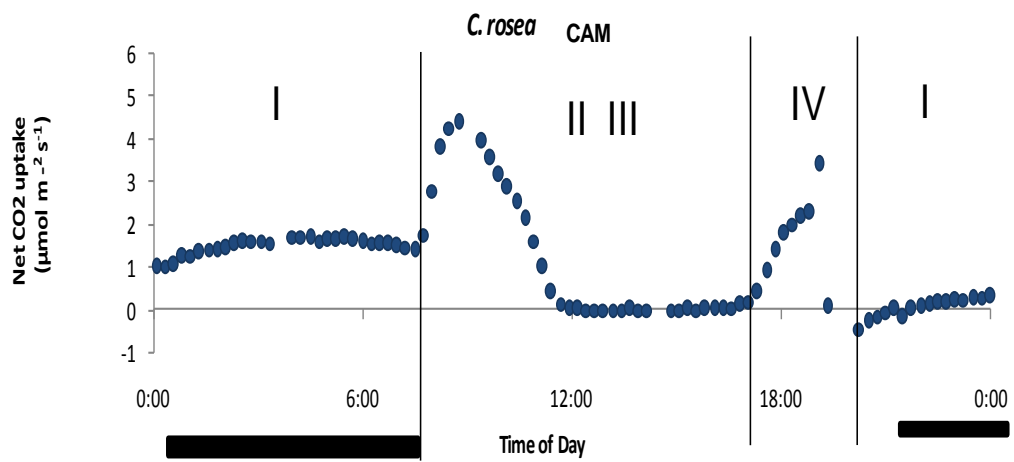
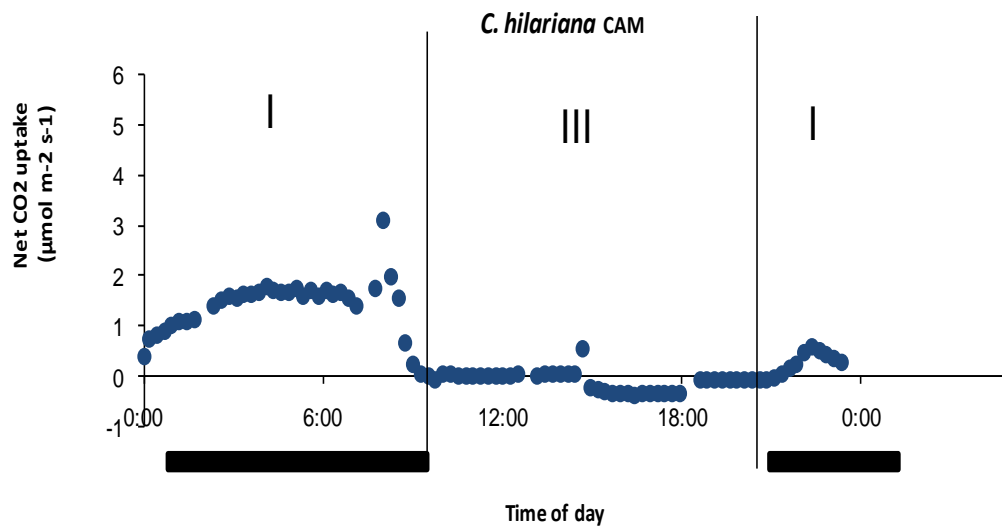
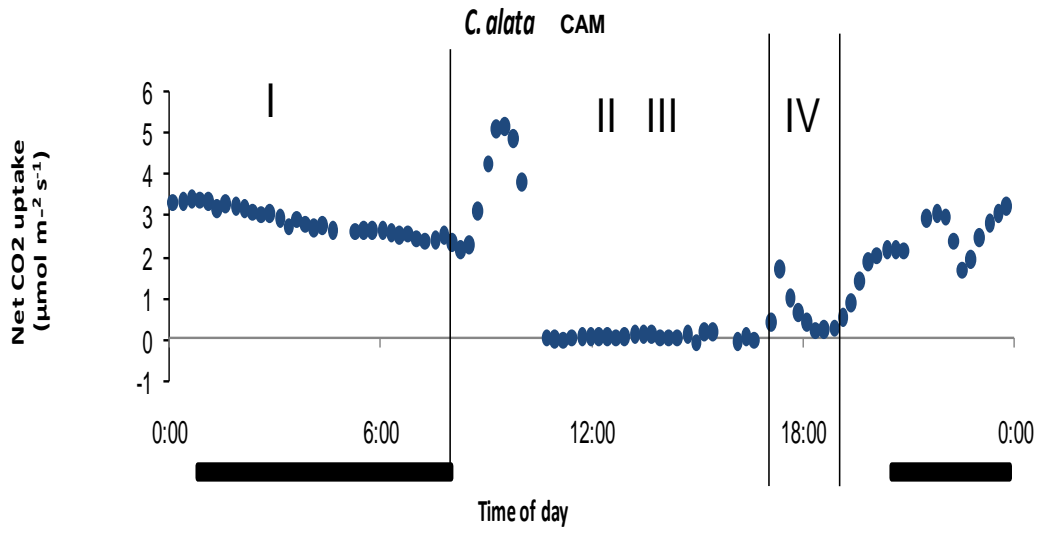
¹ This part of the work was done by Dr. Olmos and Dr Fernandez at the Department of Stress Biology and Plant Pathology, Centro de Edafología y Biología Aplicada del Segura (CEBAS-CSIC)

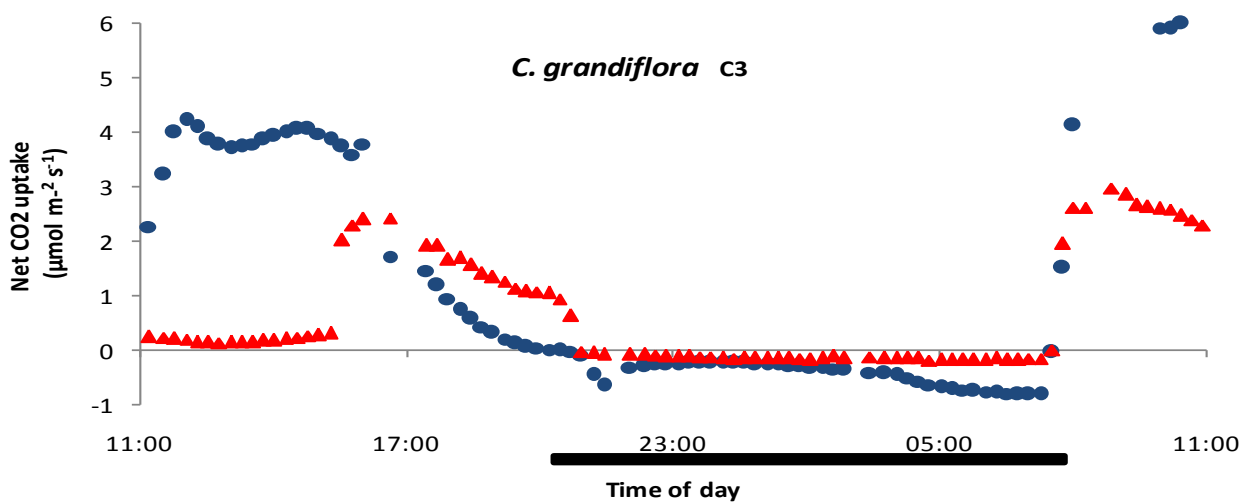
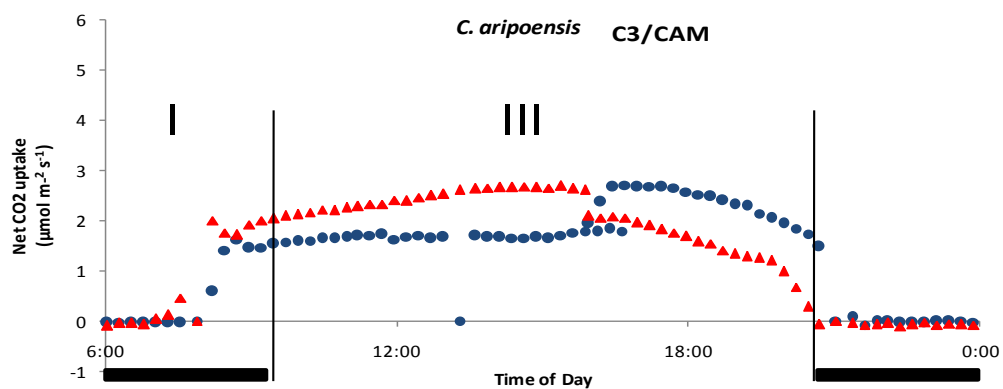
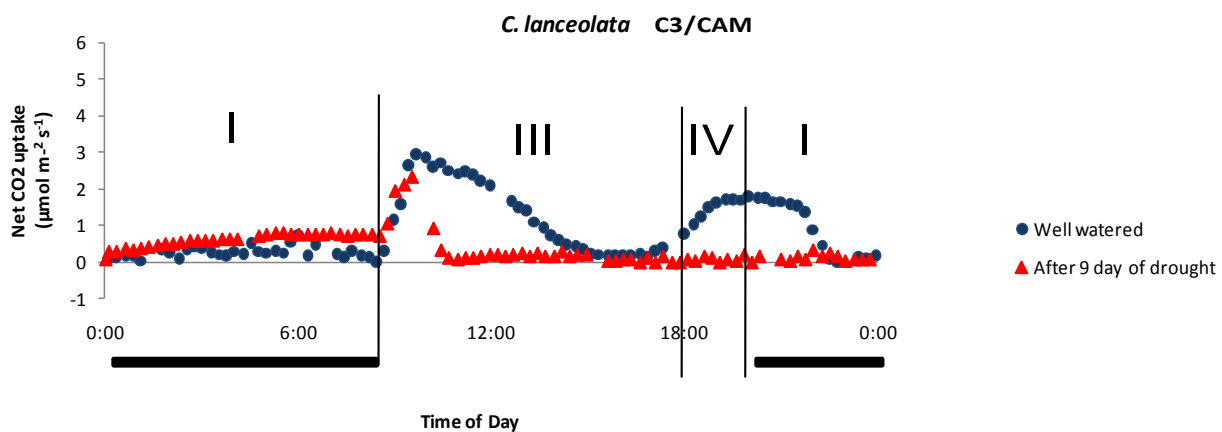
2.3 Results

2.3.1 Gas exchange profiles

2.3.1.1 Degree of CAM and relationship to specific leaf area (SLA) and instantaneous water use efficiency (WUE)

Patterns of net CO₂ uptake were measured for mature leaves of all 8 species over 24 h under ambient [CO₂] and under well-watered conditions. Measurements were also made under drought (6-9 days without water) conditions for *C. lanceolata*, *C. aripoensis* and *C. grandiflora* to check for inducible CAM in these 3 species (Figure. 2.3). Based on the amounts of net CO₂ taken up during the day and night, the species were classified as constitutive CAM, C3/CAM intermediate or constitutive C3 (Table 2.1). An inverse relationship was found between specific leaf area and the degree of CAM, measured as the percentage of CO₂ taken up during phase I ($R^2 = 0.808$; Figure 2.4 a).





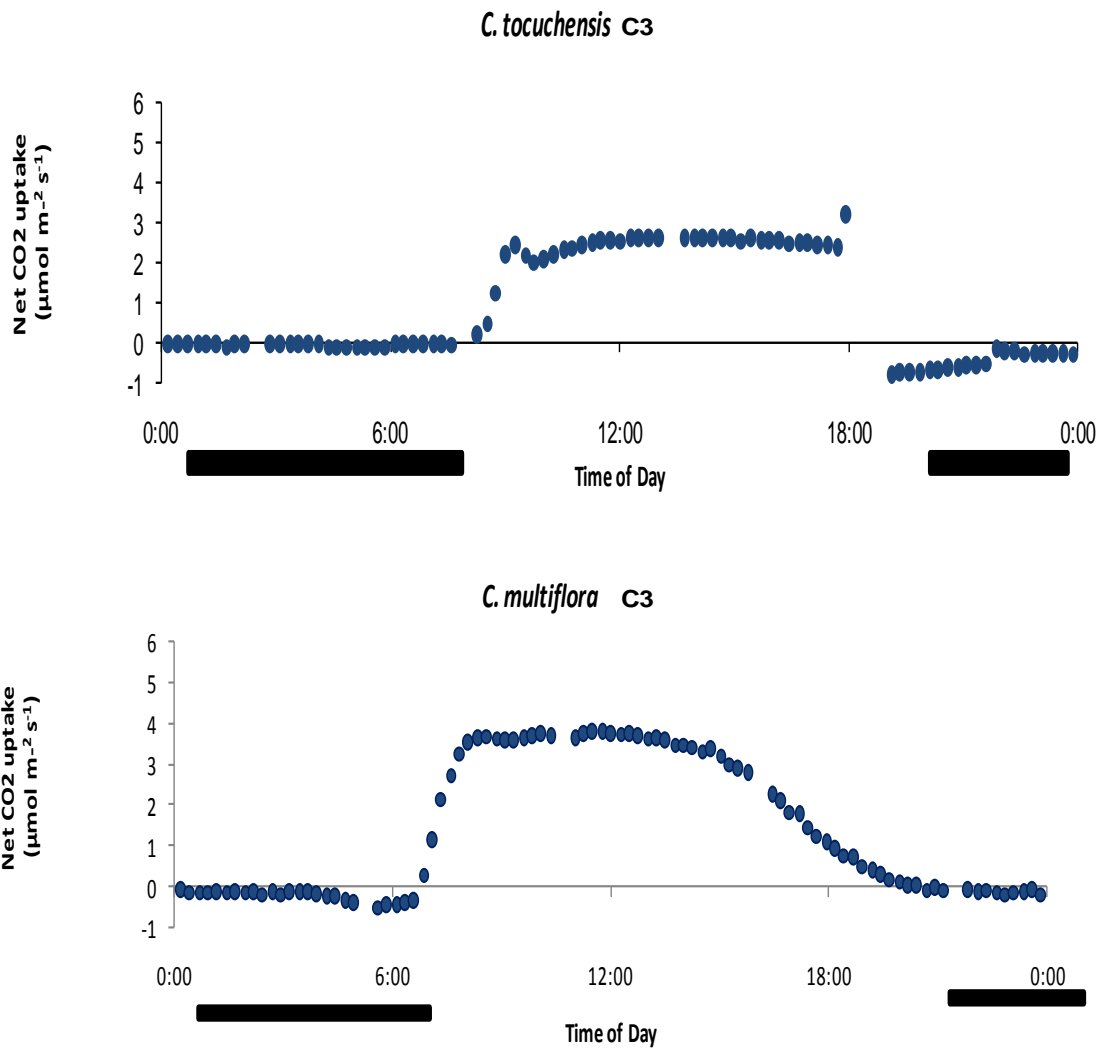


Figure 2.3. Gas exchange curves showing 24h net CO₂ uptake for eight species of *Clusia* under well watered conditions for all and under drought (for 9 days) for three species (*C. lanceolata*, *C. aripoensis* and *C. grandiflora*) to check for inducible CAM. The solid bars on the X axes represent the periods of darkness. Graphs represent at least three replicates of runs for each species.

Table 2.1. The percentage of net CO₂ taken up during the day and night during a 24 hour cycle, by each of the study species. * indicates the % CO₂ taken up after 9 days without water. Specific leaf area (SLA) showed an inverse relationship with the degree of CAM.

Species	% CO ₂ phase I	% CO ₂ Phase II	% CO ₂ phase III	% CO ₂ phase IV	Photosynthesis type	SLA (cm ²) / dry weight (g).
<i>C. hilariana</i>	93.36	15.87	-9.23	-	CAM	111.92
<i>C. alata</i>	72.33	15.5	-1.41	13.54	CAM	91.302
<i>C. rosea</i>	43.83	42.14	-33.34	47.05	CAM	117.81
<i>C. lanceolata</i> *	12.33	-	87.67	-	C3/CAM	159.04
	58.62	-	41.38	-		
<i>C. aripoensis</i> *	5.42	-	94.57	-	C3/CAM	196.35
	0.8	-	99.2	-		
<i>C. grandiflora</i> *	3.18	-	96.81	-	C3	159.78
	-11.17	-	111.17	-		
<i>C. tocuchensis</i>	-3.28	-	103.27	-	C3	196.35
<i>C. multiflora</i>	-4.82	-	104.82	-	C3	212.06

Table 2.2 Water use efficiency, CO₂ uptake and transpiration for eight species of *Clusia* with different degrees of CAM, differentiated by photosynthesis type and also SLA indicated, under well watered conditions and after eight days of drought* for *C. lanceolata*, *C. aripoensis* and *C. grandiflora*

Specie	Photosynthesis Type	SLA (cm ² /dry weight g)	24h CO ₂ uptake (mmol C ₂)	24h Transpiration (mol H ₂ O)	WUE (mmol CO ₂ /mol H ₂ O)
<i>C. hilariana</i>	CAM	111.92	0.05	0.003	22.27
<i>C. alata</i>	CAM	91.03	2.22	0.20	11.01
<i>C. rosea</i>	CAM	117.81	0.09	0.03	2.80
<i>C. lanceolata</i>	C3/CAM	159.04	1.20	0.23	5.18
*			0.51	0.02	30.95
<i>C. aripoensis</i>	C3/CAM	196.35	0.95	0.12	7.78
*			1.00	0.09	10.61
<i>C. grandiflora</i>	C3	159.78	2.06	0.77	2.69
*			0.89	0.16	5.64
<i>C. tocuchensis</i>	C3	196.35	1.65	0.73	2.26
<i>C. multiflora</i>	C3	212.06	0.12	0.05	2.40

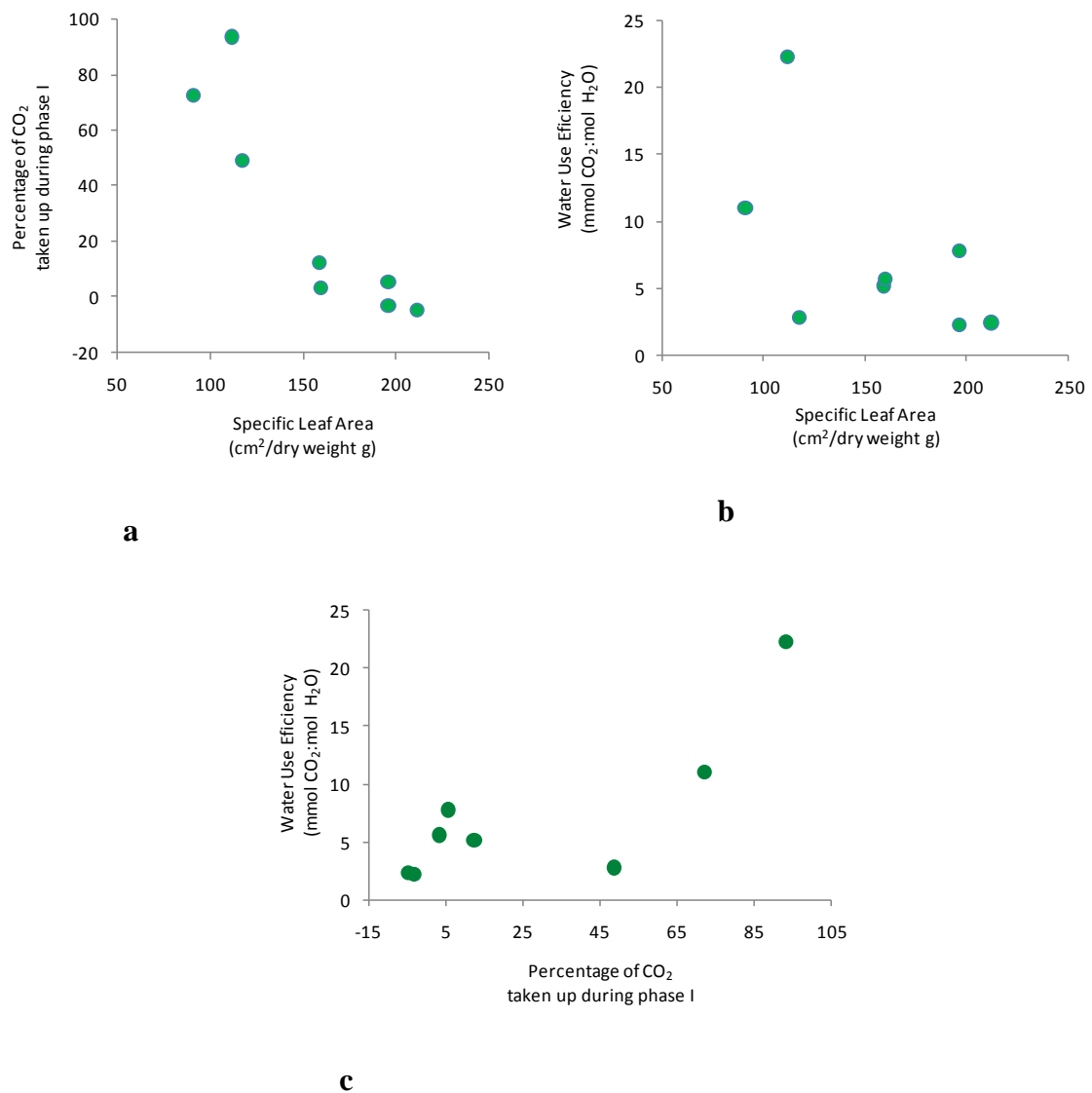


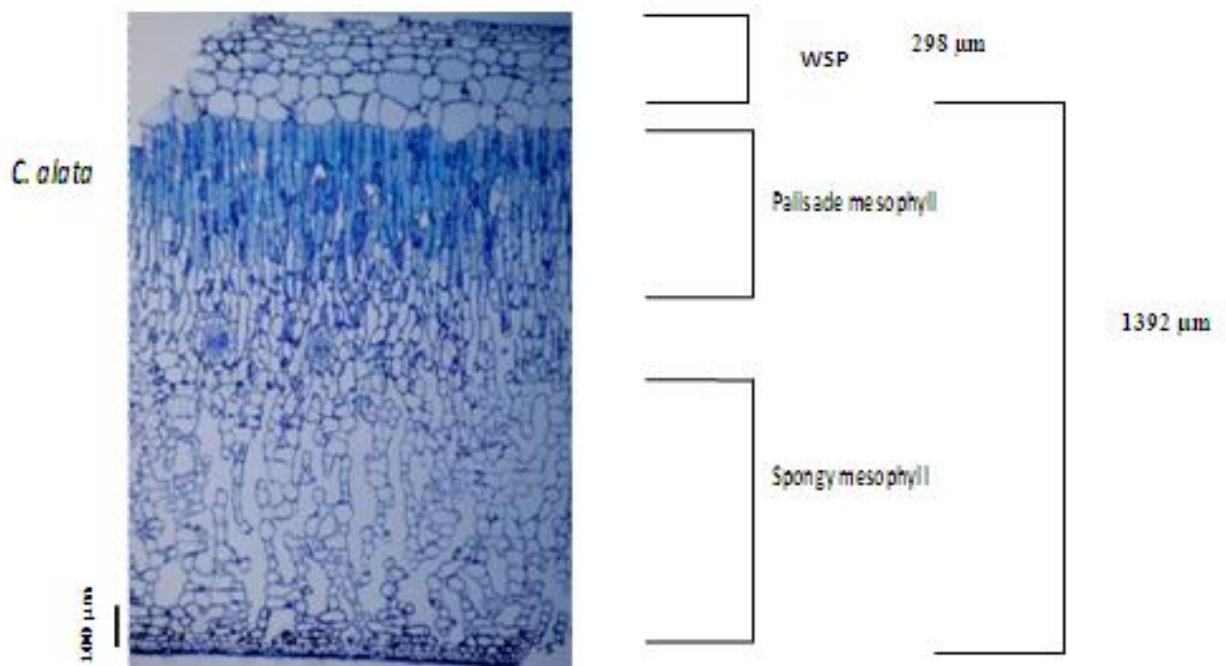
Figure 2.4. Relationships between a) specific leaf area and the magnitude of CAM (percentage of CO₂ taken up during phase I) b). SLA and WUE and c) the magnitude of CAM and WUE for eight species of *Clusia*, under well watered conditions, n = 3.

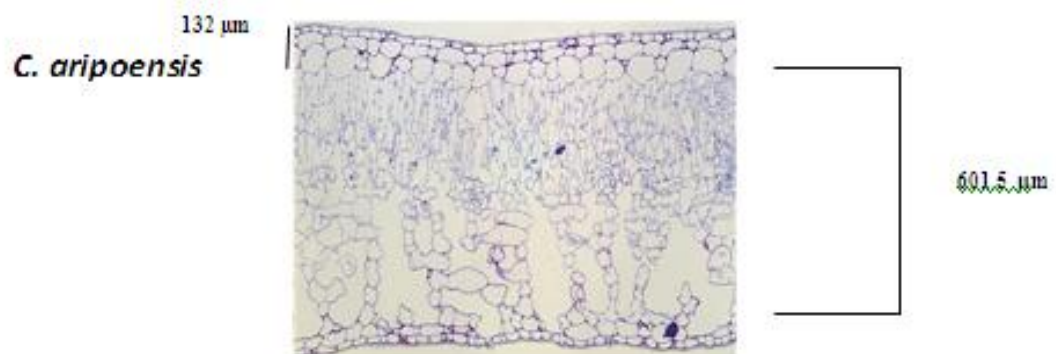
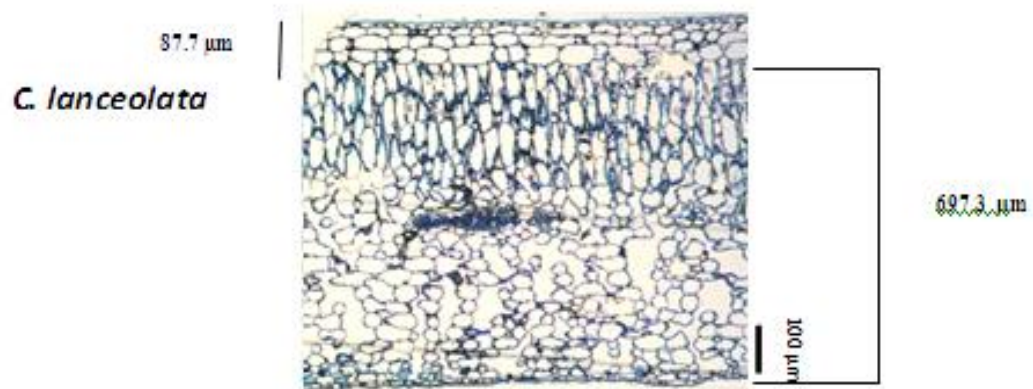
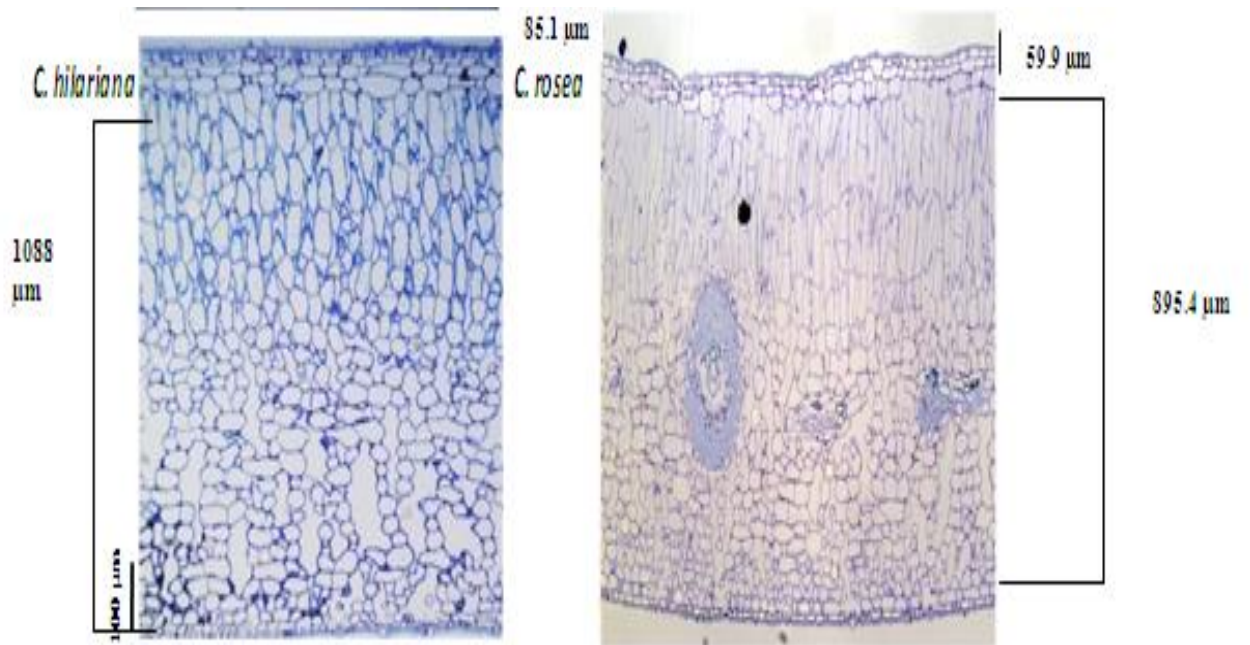
Water use efficiency (mmol CO₂/ mol H₂O) was estimated by integrating net CO₂ uptake and transpirational water loss over a 24 h light/dark cycle (Table 2.2). A close and positive relationship between WUE and the degree of CAM was found $R^2 = 0.689$ (Figure 2.4 c)

2.3.2 Leaf Anatomy

2.3.2.1 Leaf tissue characteristics and implications for the degree of CAM

Leaves of CAM plants are thicker than those of C3 and this was reiterated by the inverse relationship between SLA and magnitude of nocturnal CO₂ uptake in the eight *Clusia* species that were investigated $R^2 = 0.808$ (Fig 2.4 c). To assess the relative contributions that different tissue types made to leaf thickness, transverse sections of leaves from each of the eight *Clusia* species were taken and analysed via light microscopy (Figure 2.5). The relationships between tissue depth and the amount of CO₂ taken up at night are shown in Figure 2.6. The degree of CAM was strongly correlated with palisade ($R^2 = 0.847$) and spongy mesophyll ($R^2 = 0.752$) depth but not with WSP depth ($R^2 = 0.034$). Instead, an inverse relationship was found between the magnitude of CAM and the percentage of total mesophyll occupied by WSP ($R^2 = 0.249$). There was a strong positive relationship between the number of cell layers and the depth of each of the different tissue layers (Figure 2.7 a) i.e. ($R^2 = 0.867$ for spongy mesophyll; $R^2 = 0.477$ for palisade and $R^2 = 0.969$ for WSP). Tissue depth showed a positive correlation with cell size for the three mesophyll layers (Figure 2.7 b), however this relation was strongest in the case of WSP ($R^2 = 0.898$).





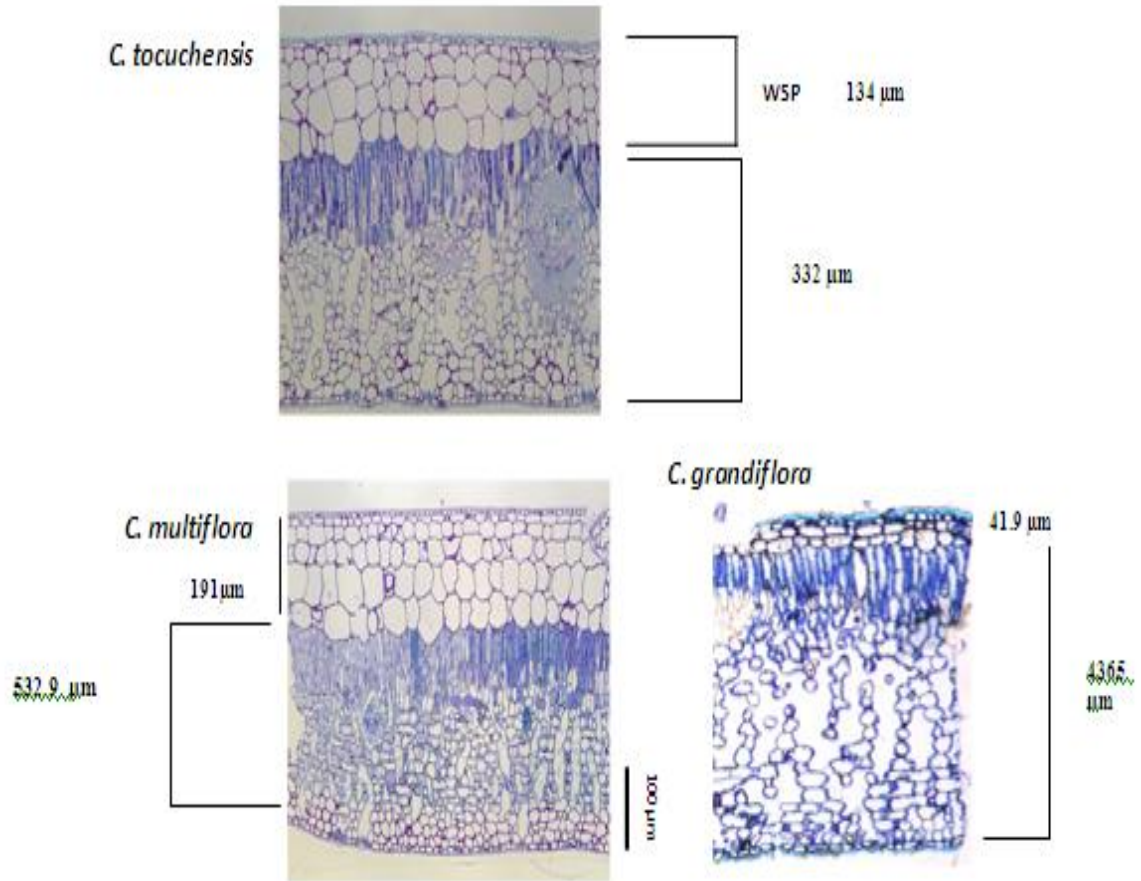


Figure 2.5. Transverse leaf sections of eight species of *Clusia* under light microscope at 5X magnification and indicating the major tissue types within the layers including WSP (water storage parenchyma), palisade mesophyll, and spongy mesophyll. Values are also given for mesophyll and WSP depth (μm). n=5

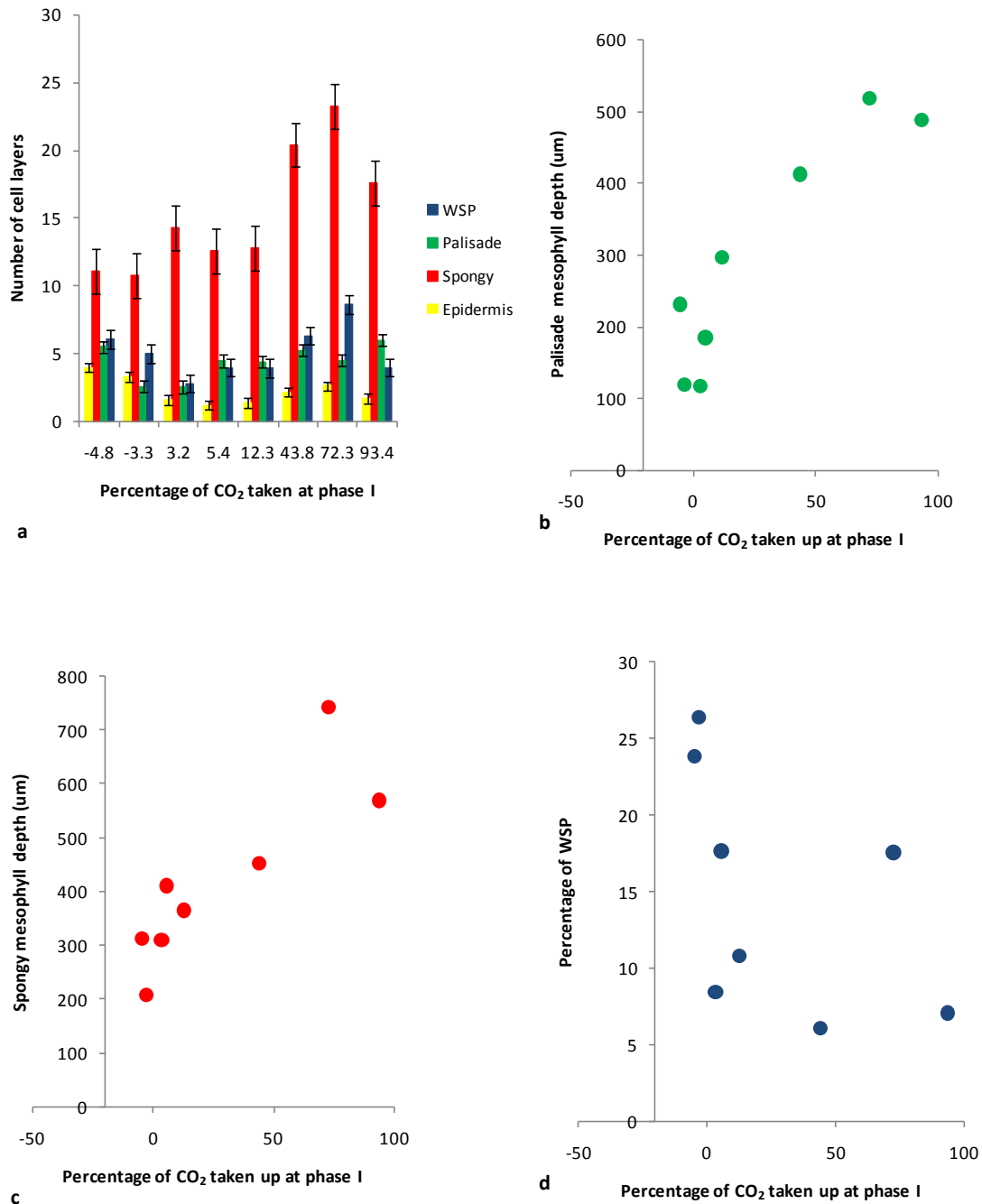


Figure 2.6 Relationships between the magnitude of CAM expressed as % of CO₂ taken up at night and anatomical features: a) number of cell layers at the palisade and spongy mesophyll, water storage parenchyma and lower epidermis, bars represent standard error; b) Palisade mesophyll depth; c) Spongy mesophyll depth and d) Percentage of total mesophyll occupied by WSP for eight species of *Clusia*. n=5

The relationship between cell size of the different leaf tissues and photosynthetic type was also assessed. There was a general trend for larger mesophyll, epidermal and stomatal guard cells in those *Clusia* species which engaged in more dark (phase I) CO₂ uptake ($X^2 = 136.75$ $p < 0.0001$; Figure 2.8 a). The palisade cells in particular were substantially larger (~3 x) in the CAM species compared to the other photosynthetic categories. The size of stomatal guard cells was calculated as pore area using the formula for an ellipsoid taking the guard cell length (see Figure 2.2 and 2.11) as a diameter.

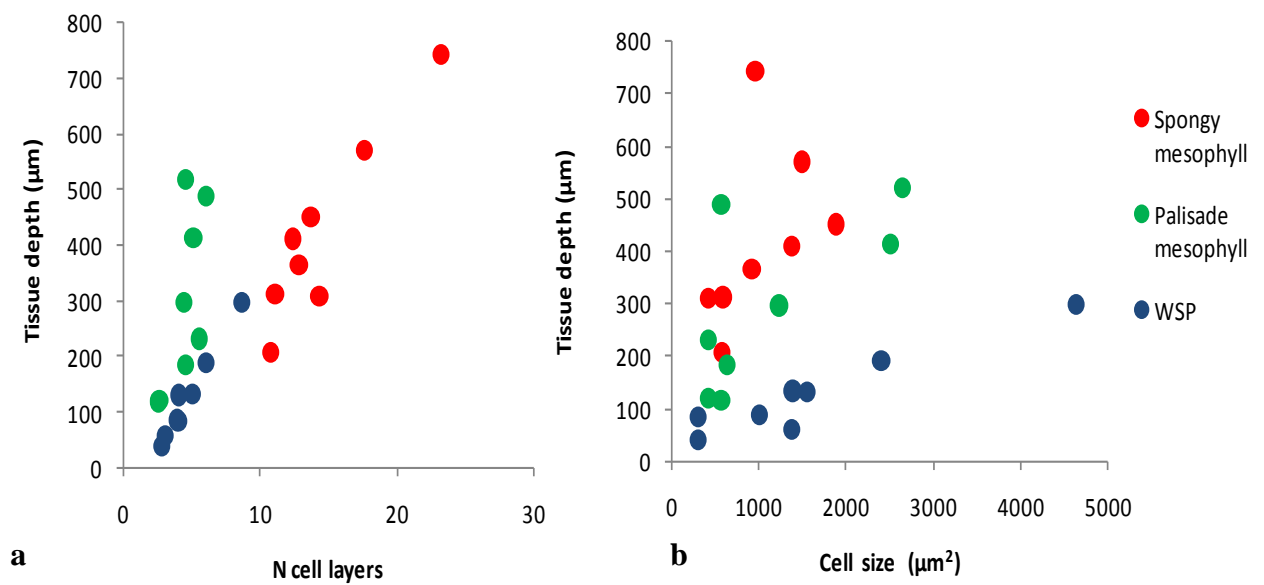
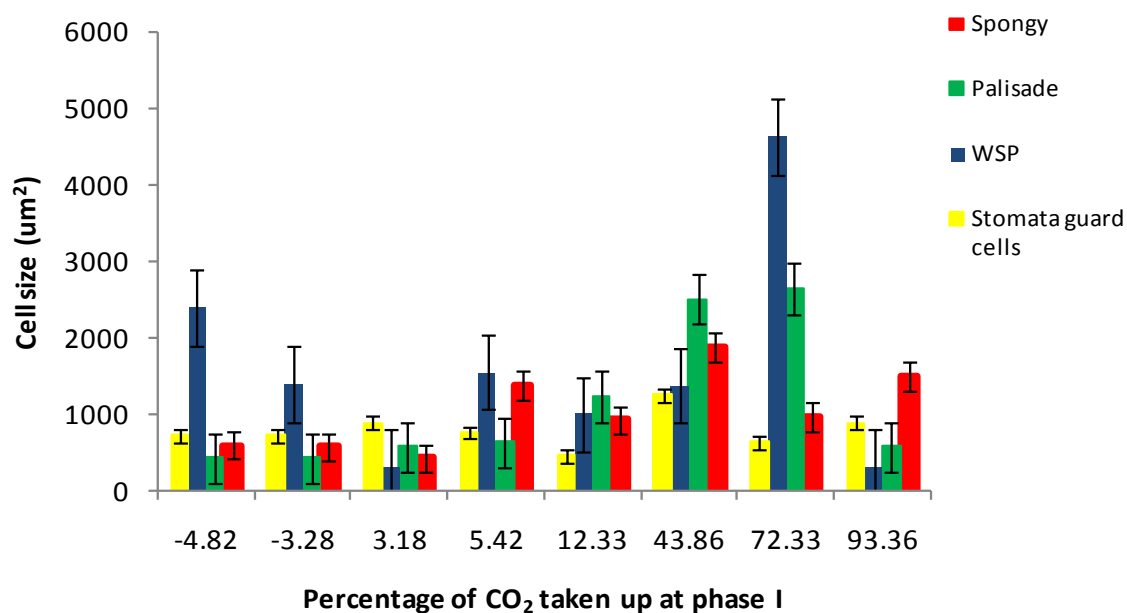


Figure 2.7. Relationship between tissue depth of spongy mesophyll, palisade mesophyll and WSP and a) Number of cell layers $n=5$ and b) Cell size (μm^2) $n=25$, for eight species of *Clusia*.

Table 2.3. Mean (n=5) and standard errors of the depth (μm) and number of cell layers of spongy and palisade mesophyll tissues, water storage parenchyma and lower epidermis for the eight species of study. The percentage of the total leaf mesophyll depth occupied by water storage parenchyma is also shown.

species	Spongy (μm)	N ^o Cell layers	Palisade (μm)	N ^o Cell layers	WSP (μm)	% WSP	N ^o Cell layers	Epidermis N ^o cell layers
<i>C. alata</i>	741.37 \pm 68.9	23.25 \pm 0.49	518.62 \pm 48.5	4.5 \pm 0.27	297.63 \pm 5.04	17.59	8.63 \pm 0.22	2.62 \pm 0.14
<i>C. hilariana</i>	569.09 \pm 87.4	17.6 \pm 0.41	488.18 \pm 75.01	6 \pm 0.33	85.07 \pm 1.62	7.09	4 \pm 0.0	1.69 \pm 0.14
<i>C. rosea</i>	451.28 \pm 60.93	13.7 \pm 1.13	412.78 \pm 54.78	5.1 \pm 0.88	59.88 \pm 2.02	6.11	3 \pm 1.01	2.6 \pm 1.02
<i>C. lanceolata</i>	364.86 \pm 32.97	12.8 \pm 0.47	296.5 \pm 26.47	4.4 \pm 0.26	87.74 \pm 1.58	10.84	3.93 \pm 0.12	1.4 \pm 0.14
<i>c. aripoensis</i>	410.44 \pm 48.13	12.37 \pm 0.26	184.66 \pm 21.3	4.56 \pm 0.15	132.02 \pm 2.37	17.67	4 \pm 0.0	1 \pm 0.0
<i>C. grandiflora</i>	308.92 \pm 44.76	14.31 \pm 0.2	117.12 \pm 16.74	2.56 \pm 1.12	41.88 \pm 2.3	8.46	2.81 \pm 0.1	1.56 \pm 0.13
<i>C. tocuchensis</i>	207.87 \pm 26.38	10.77 \pm 0.37	119.46 \pm 14.92	2.61 \pm 0.15	134.3 \pm 2.04	26.39	5 \pm 0.0	3.31 \pm 0.14
<i>C. multiflora</i>	312.09 \pm 38.2	11.07 \pm 0.51	230.88 \pm 27.6	5.5 \pm 0.84	191.26 \pm 4.35	23.82	6.07 \pm 0.81	4 \pm 0.92



a

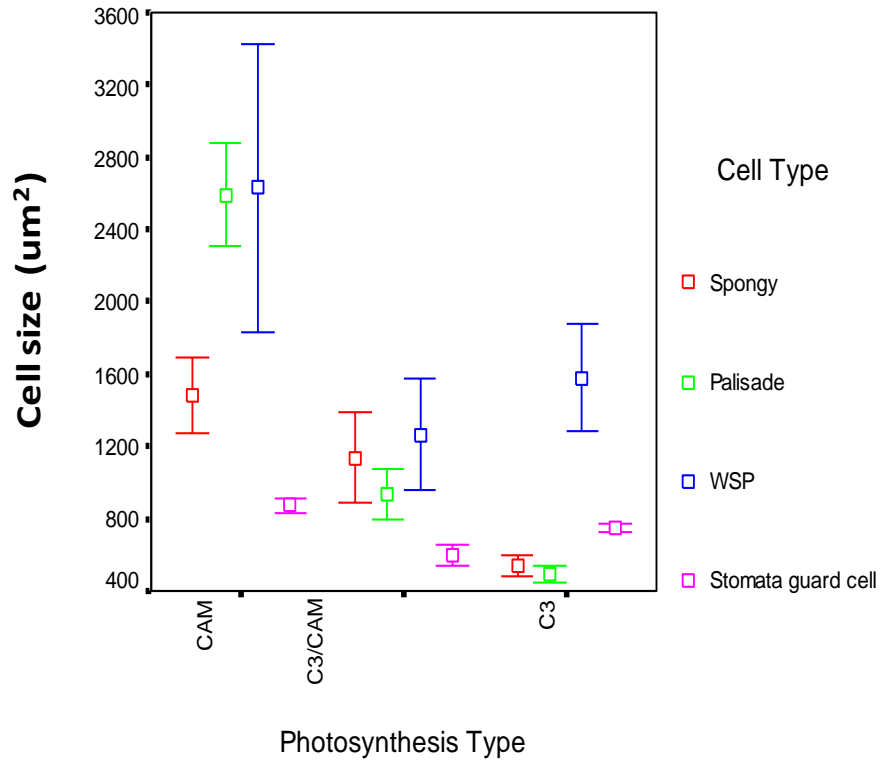
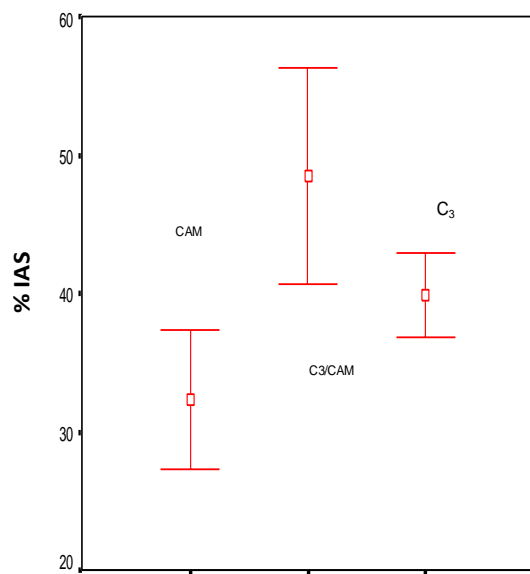


Figure 2.8. Relationships between a) magnitude of CAM (percentage of CO_2 taken up during phase I) and cell size ($n=25$) and b) photosynthesis type and cell size (measured as cell area in μm^2) of spongy and palisade mesophyll, water storage parenchyma and stomatal guard cells for eight species of *Clusia*.

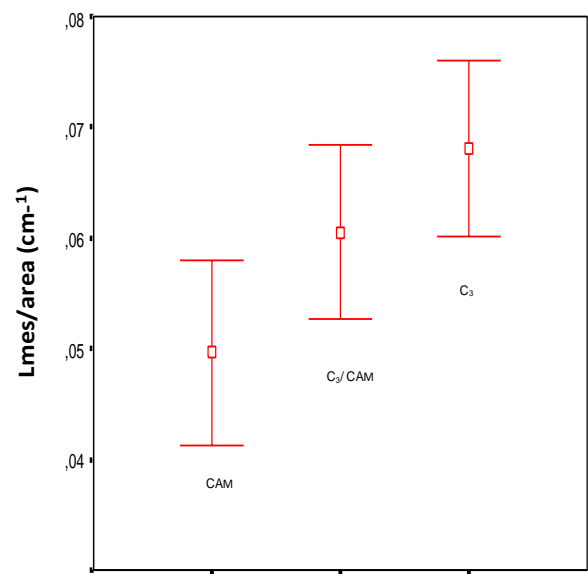
Table 2.4. Mean ($n \geq 25$) cell size (area in μm^2) and standard errors of spongy and palisade mesophyll, water storage parenchyma and stomatal guard cells across eight *Clusia* species.

Species	Spongy (μm^2)	Palisade (μm^2)	WSP (μm^2)	Guard cells (μm^2)
<i>C. alata</i>	956.45 \pm 112	2637.68 \pm 314.75	4625.25 \pm 753.88	623.93 \pm 8.95
<i>C. hilariana</i>	1491.04 \pm 112.15	565.44 \pm 36.02	300.08 \pm 39.95	879.18 \pm 14.45
<i>C. rosea</i>	1874.73 \pm 212.78	2504.88 \pm 159.21	1372.36 \pm 242.4	1248.82 \pm 39.13
<i>C. lanceolata</i>	911.08 \pm 68.28	1227.35 \pm 93.94	995.23 \pm 125.04	447.6 \pm 15.14
<i>c. aripoensis</i>	1372.12 \pm 231.8	628.8 \pm 49.72	1547.8 \pm 26.95	754.56 \pm 31.73
<i>C. grandiflora</i>	422.76 \pm 43.34	565.44 \pm 36.68	300.08 \pm 39.63	879.18 \pm 25.53
<i>C. tocuchensis</i>	571.92 \pm 56.77	424.3 \pm 41.19	1381.79 \pm 239.288	710.52 \pm 27.45
<i>C. multiflora</i>	582.42 \pm 42.56	491.29 \pm 39.67	2395.7 \pm 213	713.28 \pm 16.81

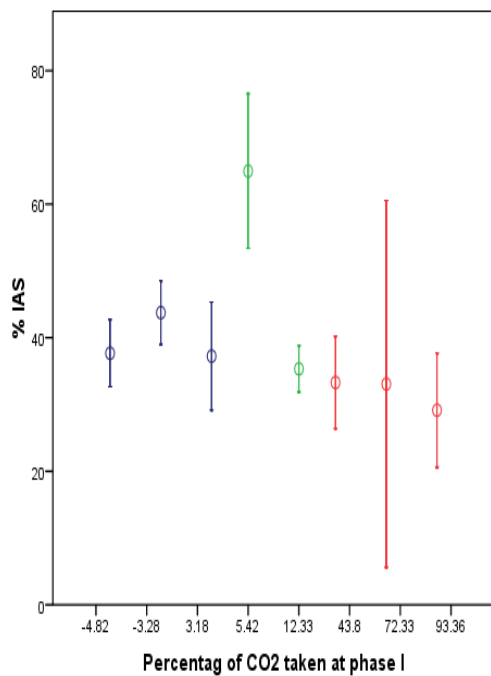
Internal air space (IAS) in the mesophyll and length of mesophyll exposed to air per unit area ($L_{mes}/area$), were also found to be related to the magnitude of CAM in the eight species of *Clusia* studied here. CAM was associated with reduced intercellular air space (IAS) and there was a significant difference in the % of IAS between constitutive CAM and C3/ CAM ($p < 0.001$) but this was not significant between constitutive CAM and constitutive C3 ($p = 0.173$) or between C3/CAM and C3 ($p = 0.081$). The area of mesophyll exposed to IAS was also related to the degree of CAM in the 8 species of *Clusia* that were examined. This difference was particularly evident between CAM species and the C3 species ($p = 0.05$) (Figure 2.9).



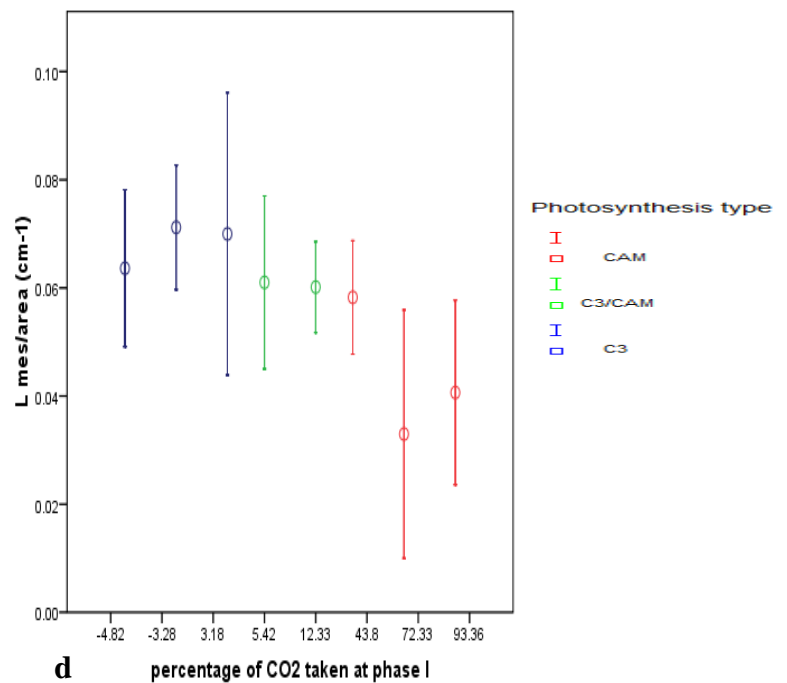
a



b



c



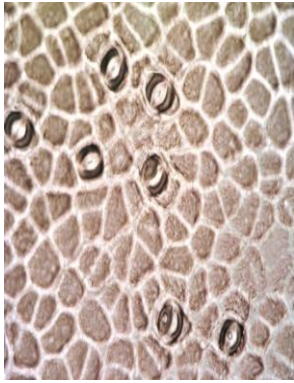
d

Figure 2.9. Variation in percentage of internal air space (a ($p= 0.05$), c) and the decrease in length of mesophyll exposed to air (b ($p<0.001$), d) as the magnitude of CAM (percentage of CO_2 taken up during phase I) increased, for eight species of *Clusia* which have been grouped according to the photosynthesis type (a, b) and without grouping (c,d). $n=5$

2.3.2.2 Stomatal size and density and photosynthetic mode

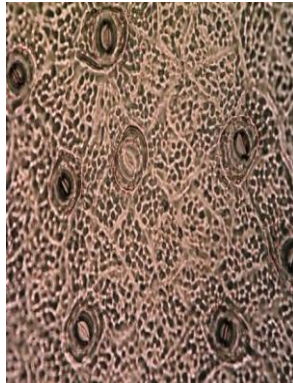
Stomatal impressions were made from the lower leaf surfaces of eight *Clusia* species and pictures taken under light microscope at 40x magnification (Figure 2.10) in order to take measurements of stomatal dimensions (Figure 2.11) and distribution (Figure 2.12).

C. alata



25 μm

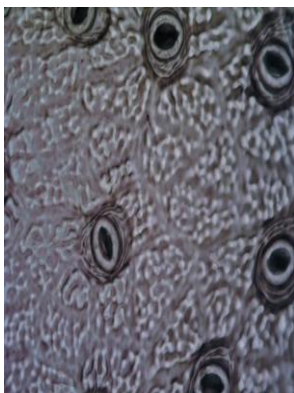
C. lanceolata



C. rosea



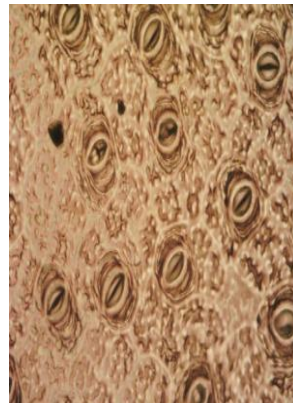
C. hilariana



C. aripoensis



C. tocuchensis



C. grandiflora



C. multiflora

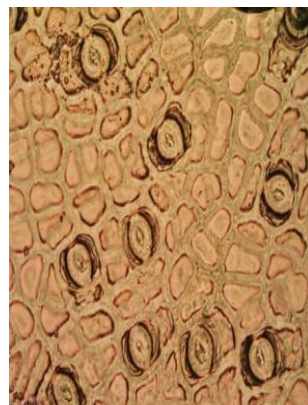


Figure 2.10. Stomatal impressions taken from the abaxial surfaces of leaves for eight species of *Clusia* under light microscope at 40x magnification.

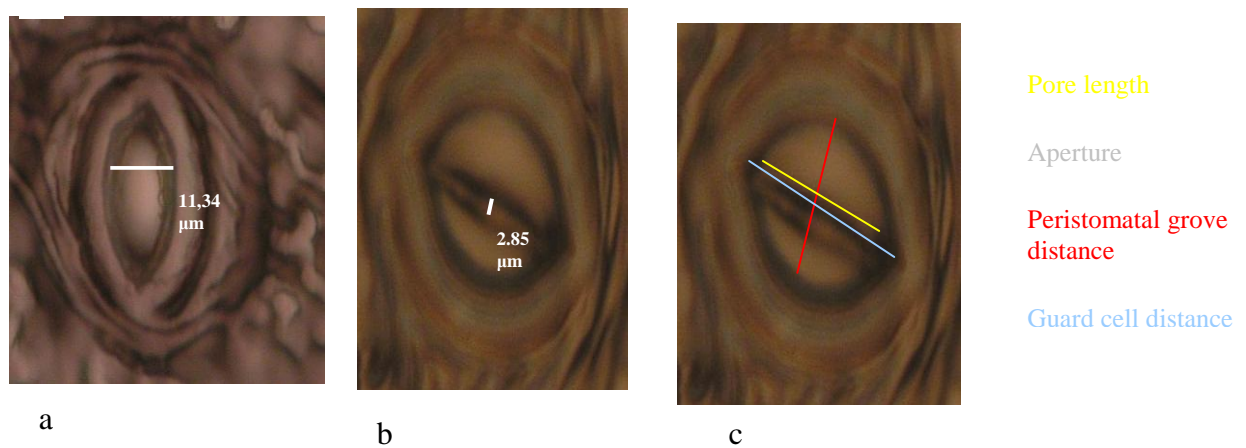


Figure 2.11. From left to right, impression of a fully open stoma (a), closed stoma (b) under light microscope at 40x magnification, indicating the measures made (c) for each stoma. Pore area is calculated using the equation: Area ellipse: $[(\text{major axis}/2) * (\text{minor axis}/2)] * \pi$. Major axis is the longitudinal length of the pore and minor axis the transversal length of pore

In general, stomatal density decreased as the magnitude of CAM (percentage of dark CO_2 uptake) increased (Figure 2.12a) There was no such relationship with stomatal index (Figure 2.12b) whilst pore area was highest in the species that conducted more CAM (Figure 2.12c; $R^2 = 0.714$). The largest pore area recorded for the C_3 *Clusia* species was noted for *C. grandiflora*, a species proposed to have lost CAM. The stomatal distribution patterns were subsequently grouped according to photosynthetic type (Figure 2.13). There was a significant difference between stomatal density of constitutive CAM species and the other species ($p < 0.001$), but not between stomatal density of the C_3/CAM intermediates and C_3 species ($p = 0.073$). A significant difference in stomatal index was noted between C_3/CAM intermediates and the rest of the species ($p < 0.001$), but was not significant between CAM and C_3 (Figure 2.13 a,b). There was also a trend to have bigger stomata (pore area) and lower stomatal densities as the degree of CAM increased (Figure 2.13c). The difference in pore area between species was significant ($p < 0.001$), due to a significant difference between pore area of constitutive CAM species and the others, but not between C_3 and the C_3/CAM intermediate species ($p = 0.877$).

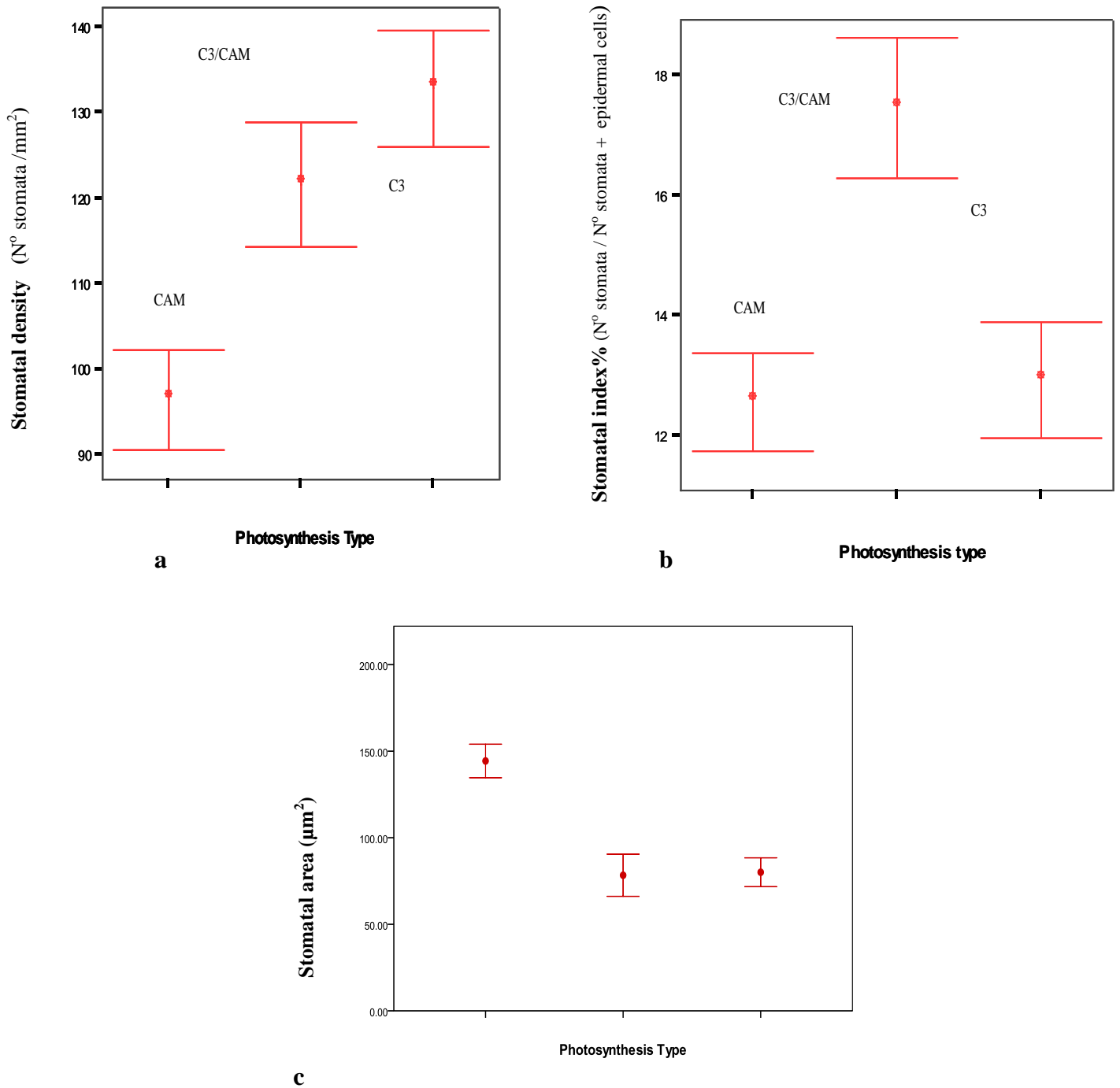


Figure 2.13. The relationships between a) Stomatal density $p < 0.001$, b) Stomatal index and c) Stomatal area $p < 0.001$, with the mode of photosynthesis for eight species of *Clusia*. bars represent \pm standard error. $n > 25$

Table 2.5. Mean (n> 25) stomatal density (Number of stomata per mm²) stomatal index (number of stomata / number of stomata plus epidermal cells) pore area (µm²), % Internal air space in the mesophyll (IAS) and length of mesophyll exposed to air per area (cm²) across eight *Clusia* species.

Species	Denisty(N stomata/mm²)	Index % (N stomata/N stomata+epidermis)	Area(um²)	% IAS	Lmes /area (cm¹)
<i>C. alata</i>	107.5	9.2	140	34.37	0.04
<i>C. hilariana</i>	74	15.2	139	30.74	0.04
<i>C. rosea</i>	103.66	14.7	122	20.83	0.042
<i>C. aripoensis</i>	128.25	16.6	72.19	61.33	0.097
<i>C. lanceolata</i>	126	18.9	66	30.88	0.055
<i>C. grandiflora</i>	133.9	21.2	139.03	37.23	0.069
<i>C. tocuchensis</i>	155.31	15.4	83.11	45.73	0.077
<i>C. multiflora</i>	118	8.9	65	41.68	0.08

The maximum measured stomatal conductance (gH₂O) of *Clusia* species was substantially lower than the stomatal conductance that was predicted (GH₂O) based on stomatal size and density (Figure 2.14). There was a slightly negative relationship between measured maximum stomatal conductance and the magnitude of CAM (Figure 2.14a). However, there was no such relationship between the magnitude of CAM and predicted stomatal conductance (Figure 2.14b)) This result suggests that there might be other features related to leaf anatomy, apart from stomatal density and size, like internal air space in the mesophyll or stomatal movements, that are responsible for the lower measured stomatal conductance in CAM plants (Figure 2.9a).

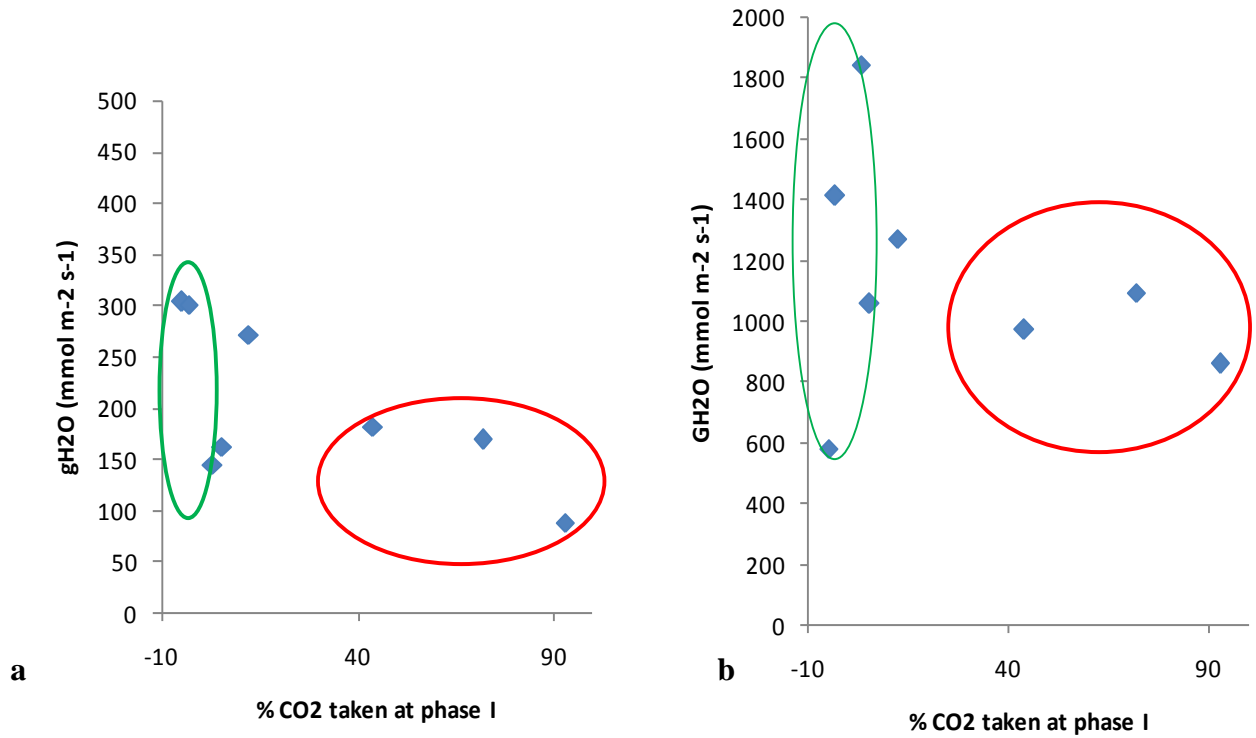


Figure 2.14. The relationship between magnitude of CAM (percentage of CO₂ taken up during phase I) and a) measured maximal stomatal conductance (gH₂O) and b) estimated maximal stomatal conductance (GH₂O) using the equation described in figure 2.2, calculating pore area based on an elliptic form taken aperture as 2/3 of pore length. Red circles enclose CAM species and green circles enclose C₃ species.

Table 2.6 correlation matrix of physiological and anatomical traits, using mean values for the eight species of *Clusia*. In red are highlighted the significant correlations

	SLA	% phase I	spongy cell depth	spongy cell layers	spongy palisade cell depth	spongy palisade cell layers	WSP depth	WSP layers	WSP cell layers	epiderm cell layers	spongy size	spongy palisade size	WSP size	guard cell size	stom density	stom index	stom area	%IAS	Lmes
SLA	1																		
% phase 1	-0.891	1.000																	
spongy depth	-0.836	0.867	1.000																
spongy cell layers	-0.854	0.812	0.932	1.000															
palisade depth	-0.859	0.921	0.896	0.776	1.000														
palisade cell layers	-0.289	0.555	0.514	0.228	0.691	1.000													
WSP depth	-0.114	0.184	0.507	0.518	0.337	0.163	1.000												
WSP cell layers	-0.183	0.246	0.517	0.565	0.383	0.142	0.985	1.000											
epiderm cell layers	0.229	-0.170	-0.193	-0.153	-0.021	0.057	0.439	0.483	1.000										
spongy size	-0.497	0.583	0.476	0.199	0.611	0.630	-0.209	-0.260	-0.312	1.000									
palisade size	-0.730	0.489	0.665	0.603	0.686	0.215	0.345	0.346	0.059	0.470	1.000								
WSP size	-0.234	0.188	0.553	0.547	0.398	0.141	0.948	0.922	0.429	-0.085	0.591	1.000							
guard cell size	-0.279	0.241	0.032	-0.050	0.156	0.164	-0.460	-0.479	0.065	0.577	0.245	-0.294	1.000						
stom density	0.684	-0.868	-0.731	-0.572	-0.855	-0.836	-0.033	-0.065	0.138	-0.643	-0.324	-0.030	-0.333	1.000					
stom index	0.110	-0.278	-0.435	-0.338	-0.470	-0.512	-0.821	-0.815	-0.716	-0.056	-0.347	-0.796	0.063	0.307	1.000				
stom area	-0.816	0.714	0.598	0.740	0.521	-0.009	-0.040	0.032	-0.168	0.224	0.407	0.036	0.478	-0.517	0.038	1.000			
% IAS	0.695	-0.517	-0.322	-0.339	-0.607	-0.267	0.220	0.108	-0.118	-0.307	-0.580	0.058	-0.349	0.506	0.023	-0.497	1.000		
Lmes	0.918	-0.820	-0.664	-0.683	-0.846	-0.350	-0.032	-0.142	0.012	-0.411	-0.665	-0.139	-0.235	0.677	0.152	-0.676	0.891	1.000	

2.3.3.1 Abundance of PEPC and Rubisco proteins

Under well watered conditions the abundance of Rubisco protein (as indicated by the blots of Rubisco small sub-unit) was found to be similar in all eight species when comparable amounts of leaf soluble proteins were loaded on gels. However, the abundance of PEPC protein was related to the level of CAM expression and was only detected in one of the C3 / CAM species (*C. lanceolata*) (Figure 2.15).

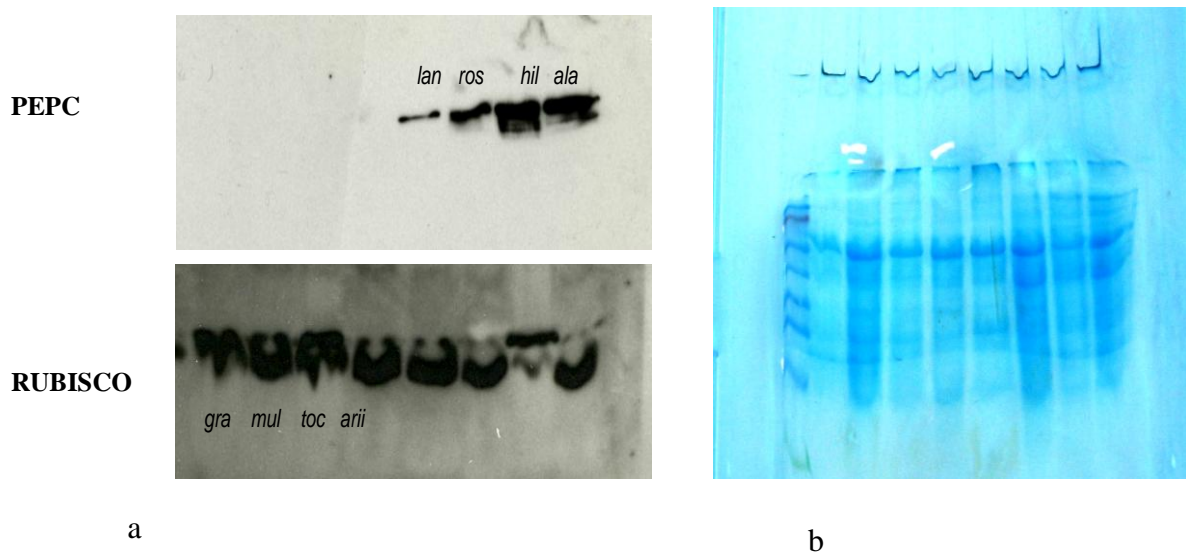
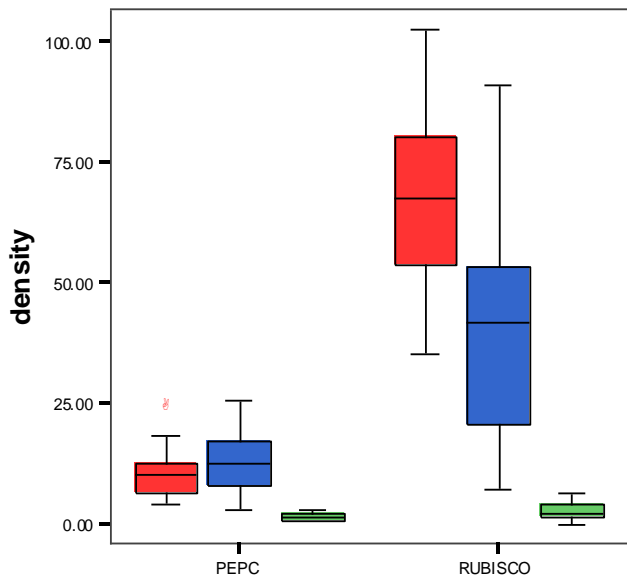


Figure 2.15 a). Abundance of PEPC and Rubisco proteins across eight *Clusia* species (from left to right *C. grandiflora*, *C. multiflora*, *C. tocuchensis*, *C. ariipoensis*, *C. lanceolata*, *C. rosea*, *C. hilariana* and *C. alata*) under well watered conditions b) Protein gel, used as a loading control, showing that comparable amounts of protein (15 μ l) were loaded for each species.

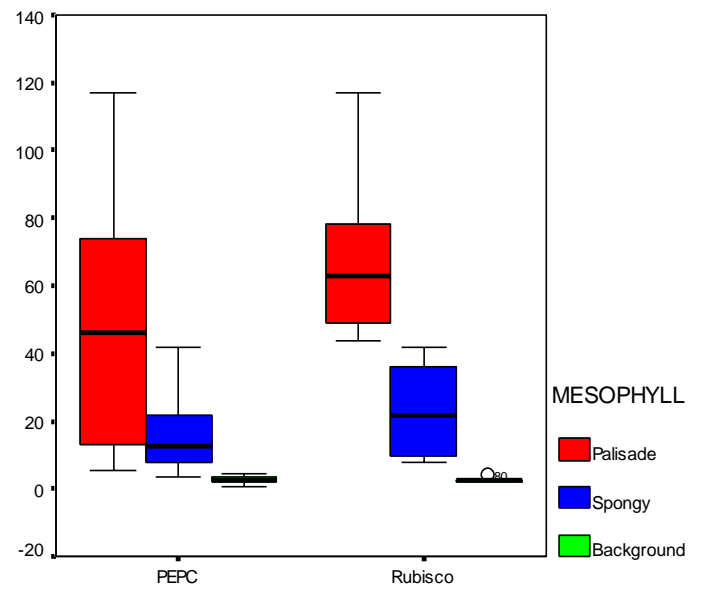
2.3.3.2 Immunolocalization of PEPC and Rubisco

The abundance of Rubisco protein was 1.5 times higher in palisade cells compared to spongy mesophyll cells in both *C. ariipoensis* ($t = 4.436$ $P < 0.0001$) and *C. rosea* ($t = 3.619$ $P = 0.001$). The abundance of PEPC was slightly higher in spongy mesophyll cells in *C. ariipoensis* compared to palisade cells but was 3 times higher in palisade cells compared to spongy mesophyll cells in *C. rosea* ($t = 6.770$

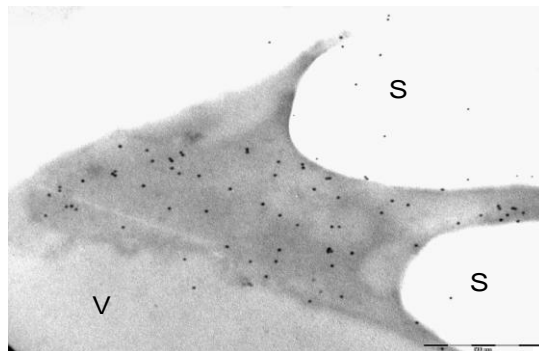
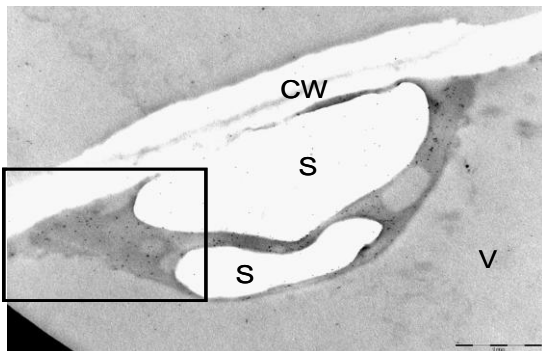
$p < 0.0001$). As expected, the abundance of PEPC protein was higher in *C. rosea* compared with *C. aripoensis*.



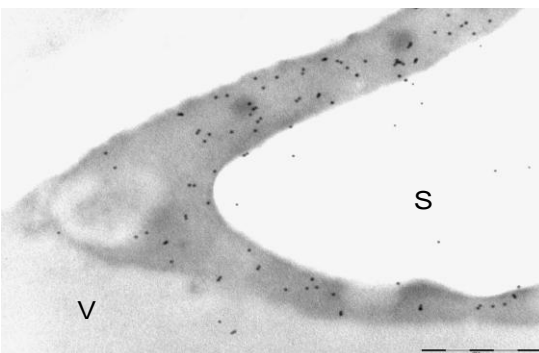
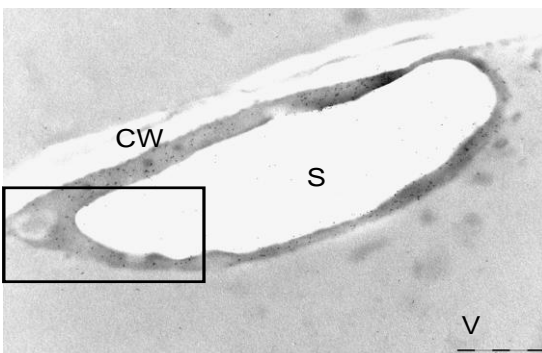
a



b



d



f

e

Figure 2.18 Immunolocalization (dark dots) of PEPC (c,d) and Rubisco (e,f) in palisade mesophyll of *C. aripoensis* by transmission electronic microscope. CW = Cell wall, S= Starch, V= Vacuole (d and f are enlargements of the corresponding area enclosed by squares).

2.4 Discussion

The aim of this study was to test 4 hypotheses relating to the functional leaf anatomy of *Clusia* with the overall objective of establishing if genotypic divergence and phenotypic plasticity in CAM within the genus was related to particular leaf anatomies.

2.4.1 Leaf anatomy and implications for the degree of CAM in *Clusia*

Succulence and leaf thickness are important anatomical traits in CAM plants, resulting from the presence of large vacuoles to store organic acids accumulated during the night and also acting as water reservoirs. Previous studies have reported positive relationships between succulence and the magnitude of CAM in a taxonomically diverse range of CAM lineages (Lüttge, 2002). Specific leaf area (SLA) is a good indicator of leaf tissue density and leaf thickness (Vile et al., 2005) and generally shows an inverse relationship with succulence (Vendramini et al., 2002). With regard to hypothesis 1, there was indeed a negative relationship between specific leaf area, and the magnitude of CAM for the eight species of *Clusia* studied (i.e. SLA was lower for those *Clusia* species which showed increased dark uptake of CO₂). Previous works have reported the higher WUE of CAM species compared with C3 species. Between the eight species of *Clusia* studied here, a strong positive relationship was found between the percentage of CO₂ taken up during phase I and WUE and a strong negative relationship was observed between SLA and WUE, which confirms previous findings and supports hypothesis 1.

In addition to serving as a surrogate and inverse measure of leaf succulence and thickness, SLA is also a good indicator of the way in which plants invest carbon and nutrients (dry biomass) in a given area of light-intercepting foliage. Species with lower SLA may be considered to incur a higher leaf-level cost for light interception (Poorter et al., 2009) and this strategy is commonly found in species that inhabit environments where drought and/or nutrient limitation hamper growth. Thus, possession of a low SLA may be a key trait that predisposed *Clusia* species towards the evolution of CAM in water and nutrient-limited habitats. At a tissue level, the lower SLA in the CAM-*Clusias* was attributed to increased cell division and larger cells for both the spongy and palisade mesophyll layers compared to

the C3 *Clusia* species. The palisade cells in particular were, on average, ~ 3 x larger in CAM compared to C3 *Clusia* species. The pronounced development of the palisade tissue in CAM-*Clusias* would be expected to increase the amount of the photosynthetic apparatus on an area basis. The immunolocalisation studies indicated that Rubisco proteins were indeed in higher abundance in the palisade compared to mesophyll cells in *Clusia* species. Enhanced development of palisade tissue is commonly found in leaves of species with low SLA and is believed to act as a strategy for improving the harvesting of light, thereby helping to offset the increased investment in biomass in thicker leaves (Smith and Hughes, 2009). That this enhancement of palisade tissue was also found in the CAM-*Clusias*, which typically inhabit open environments, could be a similar strategy for offsetting not only the costs of thicker leaves but also the increased energetic requirements of CAM.

In contrast to the close positive relationship that was established between leaf thickness and the depth of palisade and mesophyll tissues within *Clusia*, there was no such positive relationship with water storage parenchyma. In fact, the presence of a thick layer of water storage parenchyma was particularly evident in the C3 *Clusia* species *C. tocuchensis* and *C. multiflora*. The thickness of the WSP was determined principally by cell size ($R^2= 0.898$) and number of cell layers ($R^2= 0.969$). Comparisons of WSP in the genus *Peperomia* have shown that the thickness of this tissue shows a negative relationship with CAM expression (Sipes and Ting, 1985). Thus, leaves of the C3-CAM intermediate *P. obtusifolia* showed a thicker WSP (i.e. 63% of total mesophyll) compared with *P. macrostachya* a constitutive CAM species (i.e. WSP =19% of total mesophyll (Fondom et al., 2009). The same study also indicated that the drought-induced switch to CAM in *P. obtusifolia* was accompanied by a shrinkage of the WSP and palisade mesophyll but this species still presented a higher WUE compared with the constitutive CAM *P. macrostachya* under the same conditions of drought (Fondom et al., 2009). Thus, it was suggested that even when *P. obtusifolia* performed CAM, the WSP could act to conserve water. It is tempting to speculate that by acting as a means of buffering against water shortage, the thick WSP in the two constitutive C3 *Clusias* *C. multiflora* and *C. tocuchensis* (section Anadogyne of the Clusiaceae) might obviate the need for CAM. However, the presence of a thick WSP in the strong CAM species *C. alata* indicates that the presence of WSP and CAM are not mutually exclusive. It is possible that the thickness of WSP is determined more by phylogeny than photosynthetic mode since *C. grandiflora*, a C3 species within Section Chlamydoclusia of the Clusiaceae had a reduced WSP (compared to the other C3 species *C. multiflora* and *C. tocuchensis*) but which was of comparable depth to the WSP in the CAM species *C. rosea*, also located within this section.

2.4.2 Anatomical traits and implications for internal CO₂ conductance

With regard to hypothesis 2, the present study confirmed that the lower SLA of CAM *Clusias* was accompanied by a lower percentage of internal air space in the mesophyll and a reduced surface area of cells in the mesophyll exposed to air. At an anatomical level this was attributed to more and larger cells within the palisade and spongy mesophyll layers in the CAM species. Previous studies (Nelson et al., 2005) found that in taxonomically diverse CAM species (14 families including Clusiaceae) the more succulent leaves present reduced internal air space which in turn can increase resistance to CO₂ flux. The hypothesis is that reduced internal CO₂ conductance could provide higher photosynthetic efficiency to CAM plants which rely on dark CO₂ uptake (Phase I) because less CO₂ efflux at night maximizes net nocturnal carbon gain by minimizing the loss of carbon previously fixed during the day. In contrast, it has been hypothesised that reduced internal CO₂ conductance may confer reduced photosynthetic efficiency in CAM plants which rely heavily on late afternoon (Phase IV) atmospheric uptake of CO₂, because diffusion through mesophyll limits carbon availability for Rubisco (Evans et al., 1994; Maxwell, 1997; Nelson et al., 2005). Of the CAM *Clusia* species investigated here, *C. rosea* showed the most day-time net CO₂ uptake yet did not show any significant difference in %IAS or Lmes/area compared to the other CAM *Clusias*. However, it is worth highlighting that the CAM *Clusia* species investigated here showed substantially higher % IAS (mean of 30%) compared to the diverse CAM lineages investigated by Nelson and Sage (2005) where average %IAS was ~15%. Similarly, the average Lmes/area of the CAM *Clusias* (0.05 μm⁻¹) was almost 2 x higher than that of the CAM species studied by Nelson and Sage (2005). The values of % IAS and Lmes/area obtained for the CAM *Clusias* actually sit at the lower end of values measured for a range of C3 species (Nelson and Sage, 2005) suggesting that this anatomical trait may be a functional requirement of the notable phenotypic plasticity of C3/CAM engagement within *Clusia*.

In order to make an overall assessment of which anatomical traits might mediate divergence between photosynthetic categories in *Clusia*, a correlation matrix of physiological and anatomical traits was constructed (Table 2.6). Significant correlations were found between ‘CAM strength’ (i.e. % of phase I dark CO₂ uptake) and palisade mesophyll depth ($R^2 = 0.921$) and spongy mesophyll depth ($R^2 = 0.867$), each of which were primarily determined by the number of cell layers (Fig 2.8a). A significant negative correlation between CAM strength and Lmes/area ($R^2 = -0.820$) was also observed. These results imply that within *Clusia*, photosynthetic divergence is mediated via the degree of cell proliferation in the photosynthetic mesophyll tissues which impacts on Lmes/area. The inclusion of *C. grandiflora* (suggested being a reversal from CAM to C3, (Gehrig et al., 2003) in these analyses did not

alter the above interpretation, indicating the close functional relationship between leaf anatomy and photosynthetic physiology within the genus.

2.4.3 Localization of carboxylases

The reduced $L_{mes}/area$ in CAM *Clusias* imply constraints to internal CO_2 conductance compared to weak CAM and C3 species of *Clusia*. In this regard, it is important to know the arrangement of PEPC and Rubisco proteins within the leaf to test the hypothesis that localisation of the C3 and C4 carboxylases in particular leaf tissues could help to overcome internal diffusional constraints by optimising CO_2 draw-down and uptake. The magnitude of CAM in the eight species of *Clusia* examined here was related to the abundance of PEPC protein as has been shown previously for other species within the genus (Borland et al, 1998). Comparing the tissue-level localisation of PEPC protein between the strong CAM species *C. rosea* and the weak CAM species *C. aripoensis*, indicated that the enhanced PEPC abundance in *C. rosea* was largely associated with the palisade tissue which contained 3 x more PEPC protein compared to the spongy mesophyll. In contrast, PEPC protein was present in similar abundance in both palisade and spongy mesophyll tissues in the weak CAM species *C. aripoensis*. Rubisco was also present in higher abundance in the palisade cells compared to mesophyll cells in both *Clusia* species.

The immunolocalisation results obtained here for *Clusia* contrast with immunolocalisation studies in *Peperomia*. Leaves of the C3-CAM intermediate *P. camptotricha* show three well differentiated mesophyll layers (multiple epidermis (analogous to WSP), spongy and palisade mesophyll; (Nishio and Ting, 1987) in common with *Clusia* spp, but in contrast to other species that perform CAM ie. *Mesambryanthum* and *Hoya carnososa* (Nelson et al., 2005). In *P. camptotricha*, Rubisco protein was in highest abundance in the palisade mesophyll (in common with *Clusia*), but the CAM-related proteins PEPC and malic enzyme were in highest abundance in the multiple epidermis (WSP) and spongy mesophyll, which contrasts with the results obtained for the CAM-performing *C. rosea*. *Peperomia* also contrasts with *Clusia* in terms of cell size of the different leaf tissues, with CAM-performing *P. camptotricha* having bigger cells in the spongy mesophyll, presumably to accommodate increased CAM-enzyme abundance and vacuolar storage for malic acid compared with C3 performing *P. camptotricha* whilst the size of palisade cells was similar in the different photosynthetic modes (Nishio and Ting, 1987). In *C. rosea*, the higher abundance of PEPC in palisade mesophyll compared to spongy mesophyll could be positively correlated with the considerably larger palisade cells in the CAM compared to the C3 *Clusias*. In the CAM *Clusias*, larger palisade cells would be important for

accommodating CAM enzymes and large vacuoles for acid storage. In *C. rosea* the higher abundance of Rubisco in the palisade layer compared to the spongy mesophyll is probably associated with the access to light, indicating enhanced production of energy and reducing requirements for CAM-reactions in the palisade. Furthermore, co-localisation and concentration of both carboxylases in the palisade mesophyll would be envisioned to improve the efficiency of decarboxylation during the day time, allowing a direct transfer of CO₂ from malic acid breakdown to Rubisco within the same cell, thus obviating diffusional limitations to CO₂ across the leaf. This could be particularly relevant for CAM plants such as *Clusia* which generally show enhanced duration of phases II and IV compared to many other CAM species. Whilst, the well differentiated tissue layers within the leaves of *Clusia* and *Peperomia*, could be related to the physiological plasticity and capacity to switch between C3 and CAM (Kluge, 1987; Cushman and Bohnert, 1999) differences between the two genus' in terms of the relative contributions that the different mesophyll layers make to CAM functioning could reflect their different taxonomic backgrounds.

2.4.4 Stomatal size and density and photosynthetic physiology in *Clusia*

This chapter also tested the hypothesis that the potentially lower internal conductance within CAM leaves could be countered by the possession of more and/or bigger stomata on the leaves of CAM-performing *Clusia* species in comparison with C3 *Clusia* species. The correlation matrix was also queried to examine any relationships between the mode of photosynthesis and stomatal traits within *Clusia* (Table 2.6). A significant negative correlation between the magnitude of CAM and stomatal density ($R^2 = 0.868$) was revealed whilst a significant positive correlation ($R^2 = 0.714$) was noted for stomatal area and the magnitude of CAM. Thus, whilst stomata are present in lower densities in the CAM species, these species have larger guard cells and larger stomatal areas compared to the C3 species. A recent study of stomatal size and density in the leaves of *Eucalyptus globulus* growing along a rainfall gradient revealed a similar negative relationship between stomatal density and stomatal size (Franks et al., 2009). The compromise between stomatal size and density is related to the limitation of the leaf area allocated to stomata. Thus, Franks et al (2009) suggested that taking into account the leaf area limitation, there is a point when the only way to increase stomatal conductance is by decreasing stomatal size and increasing density, since increasing stomatal conductance by increasing size will require a greater percentage of leaf surface allocated to stomata and a higher change in the leaf area. In the case of *Clusia*, with the increase in leaf succulence and low leaf area:volume ratio as CAM expression is increased, this relationship might be expected. However, the results of this thesis show the opposite trend in that more succulent leaves present larger stomata in lower densities. Furthermore,

Hetherington and Woodward (2003) suggested that smaller stomata are better at improving WUE, due to their more rapid response to changes in environmental conditions such as humidity, and thus the possession of smaller stomata might have been predicted for CAM-performing *Clusias*. However, Franks et al (2009) suggest that there is an additional metabolic cost in the production of more smaller stomata for a given leaf area and it has been shown that high stomatal conductance is accompanied by high guard cell respiration rates in cotton (Srivastava et al., 1995). This extra cost could be compensated for with high CO₂ assimilation rates but only if environmental resources such as water and light are not limiting (Franks et al., 2009). Given that CAM species such as *Clusia* commonly inhabit water-limited environments and given the extra energetic costs associated with CAM, the possession of larger stomata in lower densities might be the most appropriate strategy in terms of resource use.

Calculating the theoretical maximum stomatal conductance to water, based on stomatal size and density, indicated that *Clusia* plants should lose more water (measured as a gH₂O) than they really do. The values of theoretical stomatal conductance for water vapour, obtained using the model of (Lawson et al., 1998) were much higher than those measured directly with the BINOS system. The discrepancy between theoretical and measured gH₂O was higher for CAM plants than for C3 (Figure 2.14). This result implies that low IAS, could also impact on the diffusion of water vapour from leaves (a similar result was found by Kaiser (2009)), giving an advantage for CAM plants under drought and high irradiance conditions. Larger stomata could signify a benefit for CAM plants in terms of enhancing CO₂ influx but could also lead to potentially higher water loss (modeled Gs) as in *C. rosea*. Such observations raise the question as to whether the stomata of CAM plants respond faster (open/close) than those of C3 plants, to environmental variables like light and humidity, and could this be a key factor in optimizing WUE? Assmann and Wang (2001) found that smaller stomata are more sensitive to a decrease in leaf water potential, whereas larger stomata were more sensitive to an increase in leaf water potential. Furthermore, the correlation is opposite when the width of guard cells was examined. Thus, wider guard cells might confer a higher capacity to detect decreases in humidity, which is more important in dry environments. The responses of stomata in CAM and C3 *Clusia* species to light quality and environmental perturbations will be explored in the next chapter of this thesis.

Chapter 3: Stomatal Responses to Light in C3 and CAM species of *Clusia*

3.1 Introduction

High water use efficiency and optimum carbon gain should be selected for in plants found in habitats that typically experience low humidity and soil water availability (Givnish, 1988; Chapin et al., 1993; Kozlowski and Pallardy, 2002). Stomata are directly implicated in this dual process of optimizing H₂O and CO₂ use (Assmann, 1993; Blatt, 2000) and variations in stomatal density, size and functionality might be expected to reflect the environment inhabited by the plant.

Previous studies have indicated that, in general, more succulent species which are expected to tolerate drought stress, show lower stomatal density than less succulent species (Sayed, 1998; Lüttge et al., 2007). Nevertheless, other studies have reported variable results, ie: a reduction in stomatal index in *Caltha palustris* under drought conditions (Quarrie and Jones, 1977) but no alterations in stomatal index were observed after water stress in groundnut (Clifford et al., 1995). It is clear that there is a strong relationship between environmental conditions and stomatal size and density, and the responses are variable between species. In Chapter 2 of this thesis, data supporting the presence of larger stomata in lower densities in CAM *Clusia* plants compared with C3 *Clusia* plants were presented suggesting that this trait might reflect the fact that CAM plants are adapted to tolerate drought stress.

Russo et al. (2010) found a negative correlation between stomatal size and WUE in tropical plants that experience different nutrient availability, high humidity and low light irradiance. However, in the previous chapter of this thesis, I presented a positive relationship between stomatal size and WUE between 8 species of *Clusia*. Since larger stomata do not appear to be the best strategy for water preservation, the question is posed as to whether the larger stomata of CAM-performing *Clusia* plants respond faster (open/close) to environmental variables like light and humidity than those of C3 *Clusias*, and could this result in a higher rate of CO₂ intake and lower water loss? Assmann and Wang (2001) found that smaller stomata were more sensitive to a decrease in leaf water potential, whereas bigger stomata were more sensitive to the increase of leaf water potential. Furthermore, the correlation is opposite when width of guard cells was examined. Wider guard cells might confer a higher capacity to detect decreases in humidity, which is more important in dry environments. Also, in general, larger cells are a consequence of a larger genome (Beaulieu et al., 2008). One theory for CAM evolution

suggests genome duplication (Cushman, 2001). Large stomata may be a reflection of a larger CAM genome, so did the potential for greater water loss from larger stomata act as a selective pressure for CAM evolution? To address such questions, in this chapter I will evaluate and compare the responses of stomata to light signals in a C3 and a CAM species of *Clusia*.

Mechanisms that might underpin the contrasting responses to light that are known for CAM and C3 stomata (i.e. day-time stomatal closure in CAM plants as compared to day-time stomatal opening in C3 plants) will be examined. Stomatal opening is induced by light, including blue and red light. Blue light acts as a direct signal activating the plasma membrane H⁺-ATPase (Kinoshita et al., 2001; Briggs and Christie, 2002) driving K⁺ uptake. Red light acts as an energy source and drives photosynthesis in mesophyll and guard cell chloroplasts, thereby causing a decrease in internal CO₂ concentration which is also believed to act as a signal for stomatal movements (Roelfsema and Hedrich, 2005). Carotenoids, flavins and pterins are known as photoreceptors in plants (Horwitz and Berrocal, 1997) and the pigment zeaxanthin, which absorbs mainly blue light (Quinones et al., 1996), has also been proposed as a guard cell photoreceptor (Zeiger and Zhu, 1998; Zeiger et al., 2002; Talbott et al., 2003)

An investigation on stomatal responses to light in the facultative CAM plant *Mesembryanthemum crystallinum*, showed a loss of stomatal response to blue and white light (but not red; (Tallman et al., 1997). The same study also demonstrated an inhibition of the guard cell xanthophylls cycle during the light in CAM-performing *M. crystallinum* and suggested this as a key mechanism involved in the regulation of stomatal movements during the shift from C3 to CAM (Tallman et al., 1997). It has also been suggested that in CAM plants, the high affinity of PEPC for HCO₃ results in low CO₂ concentrations within the mesophyll (C_i) at night and that this is responsible for stomatal opening at night (Meidner H, 1968; Raschke et al., 1976). However, some authors (Farquhar et al., 1978; Wong et al., 1978; Morison and Jarvis, 1983; Ramos and Hall, 1983) state that the sensitivity of stomata to changes in C_i is low and in some cases stomata have been shown to be unresponsive to CO₂ in well watered plants but more responsive in the presence of water stress, ABA, Ca⁺ and changes in diurnal rhythms of light or temperature.

Changes in photoperiod length can also influence stomatal movements (Lee, 2010). Work with *Kalanchoë blossfeldiana*, showed that the induction of CAM by photoperiod (shorter days) coincided with the day/night reversal of stomatal movements, compared to C3 plants (Brulfert and Queiroz, 1982). Initial opening of stomata in the dark could be mediated by phytochrome in the form P_{fr} activating the plasma membrane H⁺ pumps (Taiz, 2002), with K⁺ entering the guard cells and malate being synthesized at the same time in the mesophyll via PEPC. Malate is transported to the guard cells and maintains the turgor pressure to keep stomata open. A study in *Portulacaria afra*, a C3/CAM

intermediate, demonstrated that stomatal guard cells responded to blue and red light in the C3 mode but the blue light response was lost when the plants performed CAM, suggesting that the signalling pathways involved in stomatal responses to light quality are modified and/or inhibited when CAM is induced in *P. afra* (Lee and Assmann, 1992). Another study (Talbot et al., 2002) demonstrated that the orchid *Papiphelidum* has stomata that responded to blue light but lacked a response to red light, probably due to the lack of guard cell chloroplasts for photosynthesis. This response was reversed by green light and far red light suggesting the involvement of phytochrome in the stomatal opening. Furthermore, the xanthophylls cycle was still found to be operating in the guard cells of this orchid. In conclusion, the direct response of stomata to blue light in CAM plants may have less to do with the xanthophylls cycle and more to do with the way photoreceptors like phytochrome and cryptochrome are linked to the circadian clock.

In CAM plants, the circadian clock controls net CO₂ uptake via post-transcriptional regulation of PEPC by its dedicated kinase (PEPC kinase; (Wilkins, 1992; Nimmo, 1998). Day/night changes in PEPC activation are important in directing carbon flux in the CAM pathway along with changes in stomatal behaviour, fluctuations in carbohydrate storage and organic acids content (Cushman, 2001). All of these processes are subject to circadian control (Borland and Taybi, 2004) and are also responsible for the high WUE exhibited by CAM plants (Drennan and Nobel, 2000). Thus, circadian control of CO₂ uptake and stomatal behaviour in CAM plants is likely a critical selective trait influencing fitness of these plants that typically inhabit water-limited environments.

The aim of this chapter was to evaluate and compare stomatal responses to blue (400-450 nm) and red (650-700nm) light in *Clusia rosea* a constitutive CAM plant and in *Clusia multiflora* a constitutive C3 plant. Furthermore, I will test the hypothesis that the circadian control of stomatal conductance and gas exchange in *Clusia* CAM plants is more robust than that in C3 plants.

In order to address the questions posed above, the following hypotheses were constructed:

H₁: The circadian control of stomatal conductance is more robust in CAM than in C3 *Clusia* plants

P₁: Since CAM species of *Clusia* have larger stomata than C3 species (Chapter 2) it is predicted that the clock will exert a stronger control over stomatal conductance in CAM plants, thereby reducing water loss and enhancing CO₂ uptake. In other words, the CAM *Clusia* will maintain a conserved rhythm and unaltered period of leaf gas exchange under constant light.

H₂: The circadian control of stomatal conductance in *Clusia* is mediated via photoreceptors rather than via metabolism (photosynthesis).

P₂: If the hypothesis is true, the circadian rhythm of leaf gas exchange in *Clusia* will be altered under blue light but will remain unaltered under red light. This is because the response to blue light is a direct light signal perceived via photoreceptors that changes the membrane potential causing the stomatal movements. On the other hand, stomatal movements in response to red light are believed to emanate from change in C_i due to photosynthesis in the mesophyll and guard cells. Furthermore, it is predicted that responses to blue light will be more marked in C3 than in CAM plants based on the well documented response of guard cells to light in C3 plants which open stomata during the day.

H₃: Circadian control of stomatal conductance is important to maintain high WUE in CAM *Clusia* (*C. rosea*) compared with C3 *Clusia* (*C. multiflora*).

P₃: Any alterations in rhythms of stomatal conductance under constant light conditions will have negative consequences on WUE (lower values). This effect is expected to be stronger in *C. rosea* than in *C. multiflora*, since water preservation is an central feature of CAM metabolism, and circadian control is central to the operation of CAM (Drennan and Nobel, 2000; Borland and Taybi, 2004).

H₄: Stomata of the CAM *Clusia* (*C. rosea*) respond differently to changes in light intensity in terms of speed of opening and closing, compared with stomata of the C3 *Clusia* (*C. multiflora*).

P₄: Initially it might be predicted that stomata of *C. rosea* respond more slowly to changes in light intensity compared to those of *C. multiflora*, because the CAM stomata are usually open during the dark and also because the larger guard cells of CAM stomata will take longer to experience changes in turgor pressures needed to open and close the pore. However, knowing, that stomata of some CAM plants have not lost the response to light (Talbot et al., 2002), it could also be possible that stomata of *C. rosea* have a faster response to changes in light intensity, due to the need to preserve water and maintain high water use efficiency.

3.2 Materials and methods

For the following experiments, the constitutive CAM plant, *Clusia rosea* and the constitutive C3 plant *Clusia multiflora* were compared. Cuttings of each species were taken from plants growing at Moorbank Botanic Garden, Newcastle University. Rooted cuttings that were between 1-2 years old and about 80cm -100cm in height were taken from Moorbank to a growth chamber with a 12 hour photoperiod, 65-75% relative humidity, 250-300 $\mu\text{molm}^{-2}\text{s}^{-1}$ light intensity at plant height and day/night

temperature of 27/18 °C. Plants were kept in those conditions for 2-4 weeks for acclimation before experiments commenced.

3.2.1 Gas exchange under different light regimes

Leaf gas exchange parameters that included net CO₂ uptake ($\mu\text{molm}^{-2}\text{s}^{-1}$), stomatal conductance ($\text{mmol m}^{-2}\text{s}^{-1}$) and transpiration rate ($\text{mmol m}^{-2}\text{s}^{-1}$) were measured using a compact mini cuvette system, Central Unit CMS-400 with BINOS- 100 infra-red gas analyzer, working in open mode (Walz GmbH, Effeltrich, Germany). A fully expanded leaf was clamped in the cuvette, ensuring it received full light of $250\mu\text{molm}^{-2}\text{s}^{-1}$. Temperature was tracked according to the conditions of the growth room or kept constant at 24°C under constant illumination for the circadian studies. Data were recorded every 15 minutes. The measurements were made under dark/light 24h cycles for two days before imposing the different light treatments. The treatments included two days under constant white light (400-700 nm), two days under constant red light or two days under constant blue light with temperature held at 24°C. The light treatments were imposed using an external adjustable fibre optic light source (KL 2500LCD, Schott, Mainz, Germany) giving $250\mu\text{molm}^{-2}\text{s}^{-1}$ in all the cases and employing Lee filters to impose blue (400-450 nm: filter number 165) and red (650-700nm: filter number 182) light, and far red light ($18\mu\text{molm}^{-2}\text{s}^{-1}$) treatment as well. In addition, low intensity blue light ($15\mu\text{mol m}^{-2}\text{s}^{-1}$) was applied after a period of 24-48 hours darkness, to evaluate the specific response of stomatal photoreceptors to the light (i.e. avoiding possible influence of photosynthetic metabolism on stomatal movements). Finally, to test if the reduced response of *C. multiflora* to red light was due to the absence of blue light stimuli, a mixture ($250\mu\text{molm}^{-2}\text{s}^{-1}$) of red light with a background of blue light (the same filter used before, Lee filters number 165 (400-450 nm covering all the sides of the cuvette) was examined. Each of the gas exchange profiles presented is representative of 2-3 replicated runs.

3.2.2 Speed of response of stomata to changes in light intensity

Measurements of gas exchange parameters were made for a complete 24 h light/dark cycle for leaves of *C. rosea* and *C. multiflora*. Leaves were then exposed to an external source of light ($250\mu\text{molm}^{-2}\text{s}^{-1}$) for 30 min during the dark period; at 23:00 h for *C. multiflora* and at 06:00 h for *C. rosea*. During the light period, the light was turned off for 30 min between 12:00-15:00 h for *C. multiflora* and between 18:00-19:00 h for *C. rosea*. Stomatal responses to light on and light off were tracked and

recorded at 1 minute intervals over a 30 minute period. The changes in stomatal conductance g_{H_2O} ($\text{mmolm}^{-2}\text{s}^{-1}$) and net CO_2 uptake ($\mu\text{molm}^{-2}\text{s}^{-1}$) were plotted and the slope of the linear part of curve was calculated as: $(d_{\text{max}} g_{H_2O} / dt (\text{mmolm}^{-2}\text{s}^{-1}))$ to provide an indication of the speed of closing and opening of stomata.

Finally, in order to establish if the guard cells of stomata in *Clusia* have chloroplasts, peels from the abaxial epidermis of leaves from eight species with contrasting photosynthetic physiologies (see chapter 2) were taken, using a sharp blade. The epidermal peels were mounted on a glass microscope slide with a drop of water plus cover slip on top and viewed under the fluorescence microscope (Leica DM RB). Pictures were taken at 40 X magnification.

3.3 Results

3.3.1 Gas exchange profiles under different light regimes

Patterns of stomatal conductance to water vapour (g_{H_2O}) and net CO_2 uptake were measured under light/dark cycles and then monitored under constant white light (Fig. 3.1). Stomatal conductance and net CO_2 uptake continued to oscillate in both species under constant white light. However, the timing of the rhythm was altered more in the CAM species (Figure 3.1 a,) compared to the C3 (Figure 3.1 b). Under constant white light, stomata remained open over the subjective day in the CAM species *C. rosea*, and the plants took up more CO_2 over the subjective day, compared to plants under the light/dark cycles (Fig. 3.1a). Also, stomatal conductance and CO_2 assimilation were closely coupled in the C3 *C. multiflora* but in the CAM species *C. rosea*, peaks in stomatal conductance seemed to precede peaks in net CO_2 assimilation under constant white light.

Under conditions of constant red light, *C. rosea* maintained coupled rhythms of net CO_2 uptake and g_{H_2O} however the C3 species did not maintain this rhythm and once stomata closed after 12 hours of red light, they did not re-open (Fig. 3.2). For the CAM species, red light elicited higher values of stomatal conductance to those measured under the preceding light/dark cycle and the period of maximal net CO_2 uptake was moved to the subjective day.

Under constant blue light ($250 \mu\text{mol m}^{-2}\text{s}^{-1}$), for the CAM species, net CO_2 uptake and g_{H_2O} continued to oscillate for over 48h and higher stomatal conductance and rates of net CO_2 uptake were measured during subjective day time compared to that under normal light/dark conditions (Figure 3.3 a). In contrast, the C3 species showed reduced rates of net CO_2 uptake and lower stomatal conductance

under blue light compared to those measured under the light/dark cycle and the rhythm was lost after approximately 24 hours in constant blue light (Figure 3.3b).

Switching from light/dark conditions to constant dark maintained oscillations in stomatal conductance in both species and in net CO₂ uptake in the CAM species (Fig. 3.4a, b). Moving then to constant low intensity (15 μmol m⁻²s⁻¹) blue light maintained the rhythm in stomatal conductance in both species whilst the rhythm in net CO₂ uptake was damped. Moving from darkness to low intensity blue light increased maximum stomatal conductance in the C3 species for the first 24 h cycle. In the CAM species, there was no change in maximal stomatal conductance when shifted from darkness to low intensity blue light, but stomata remained open for longer periods under constant low blue light, compared to the situation in constant darkness (Fig 3.4a).

Under constant red light, *C. multiflora* was unable to maintain a rhythm in stomatal conductance or net CO₂ uptake (see Fig 3.2b) To test that this loss in rhythm was due to the absence of blue light, the plants were shifted from light/dark to dark then to red (250 μmolm⁻²s⁻¹) with a blue background (Figure 3.5). Under constant red + blue light, *C. rosea* presented oscillations in both stomatal conductance and net CO₂ uptake with higher values of net CO₂ uptake and stomatal conductance compared to those in dark/light, but shifted to the subjective day (Figure 3.5 a). *C. multiflora* showed similar patterns in oscillations of stomatal conductance and net CO₂ uptake under constant red + blue light as in dark/light, but with much higher values for gH₂O and CO₂ uptake for the first 24 h in constant red+ blue light (Figure 3.5 b), supporting the initial idea of the necessity of a blue light to stimulate the C3 stomata to open. However, the oscillations in net CO₂ uptake and stomatal conductance became damped in the C3 species after 24 h of red + blue light.

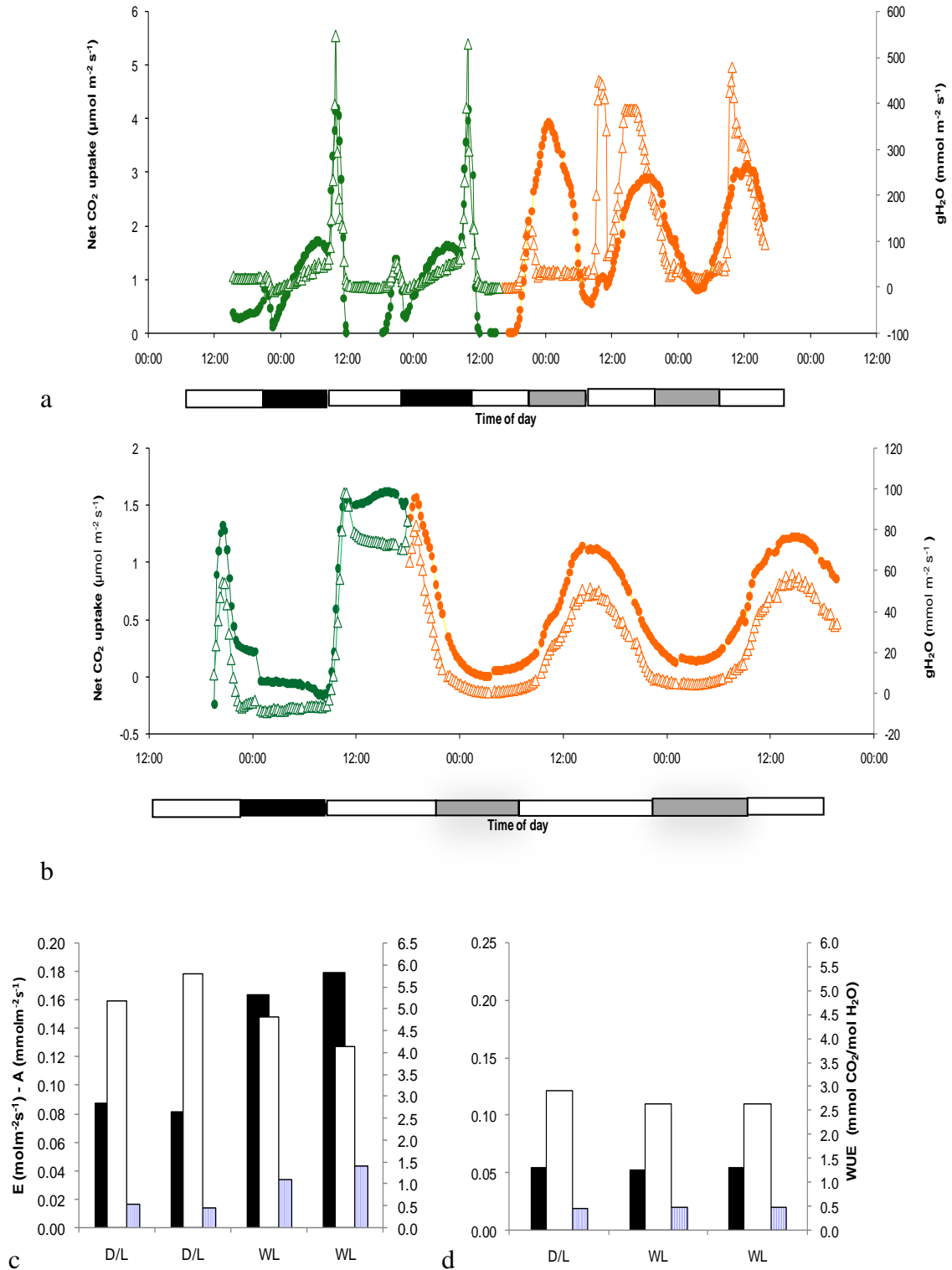


Figure 3.1. a, b Net CO₂ uptake ($\mu\text{mol m}^{-2}\text{s}^{-1}$ closed circles) and stomatal conductance gH₂O ($\text{mmol m}^{-2}\text{s}^{-1}$ open triangles) for *C. rosea* (a) and *C. multiflora* (b). Curves in green represent gas exchange under regular 12h dark/light; in orange under 24 h constant white light, both at $250 \mu\text{mol m}^{-2}\text{s}^{-1}$. On the x-axes, dark bars represent night, open bars day and grey bars subjective night. Integrated transpiration (molH_2O) CO₂ uptake (mmolCO_2) and instantaneous Water use efficiency ($\text{mmolCO}_2/\text{molH}_2\text{O}$) in *C. rosea* (c) and *C. multiflora* (d) for 24 h periods under Dark/light (D/L) followed by constant white light (WL). n=3

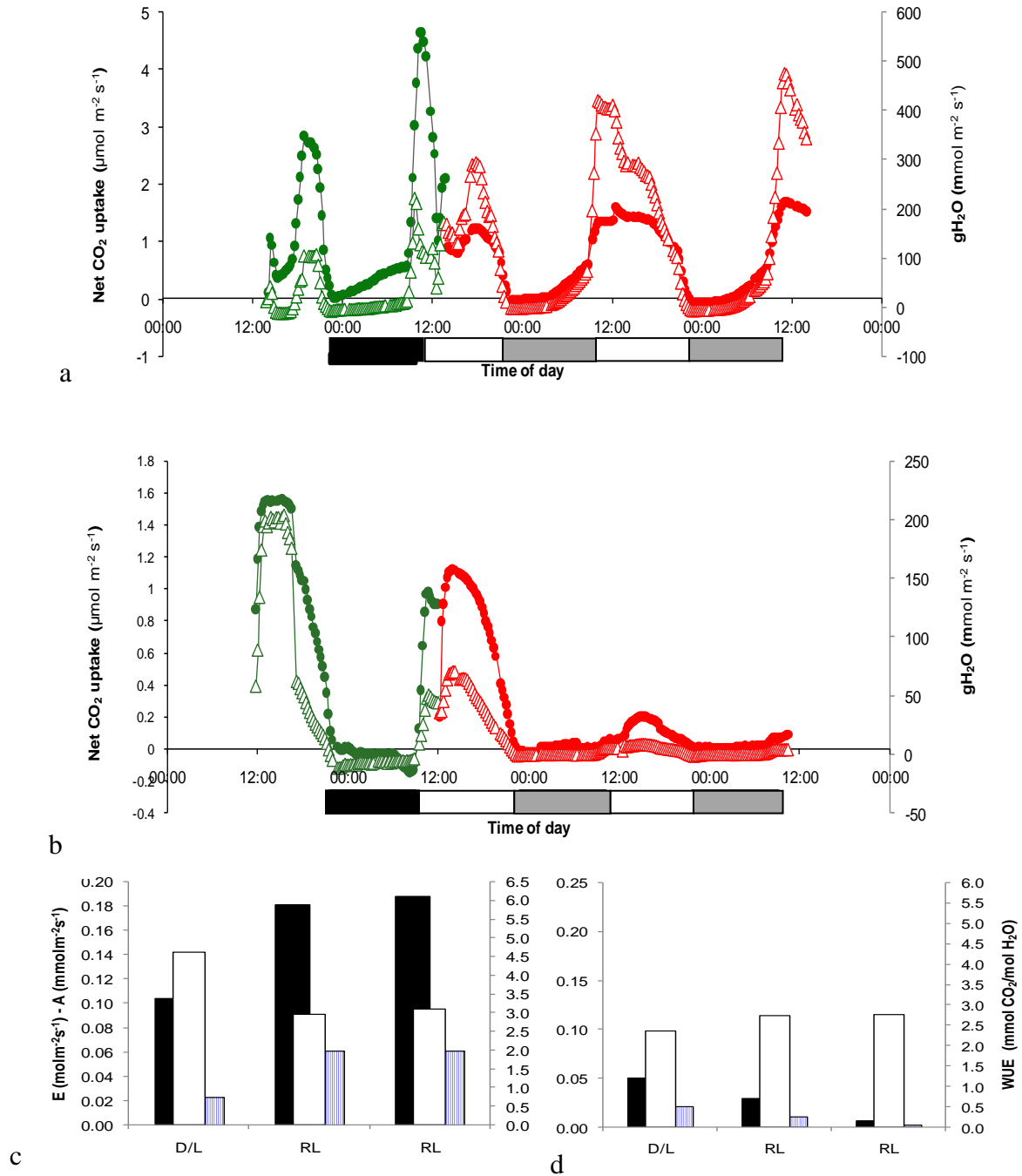


Figure 3.2. a,b Net CO₂ uptake ($\mu\text{mol m}^{-2}\text{s}^{-1}$ closed circles) and stomatal conductance $g\text{H}_2\text{O}$ ($\text{mmol m}^{-2}\text{s}^{-1}$ open triangles) for *C. rosea* (a) and *C. multiflora* (b). Curves in green represent gas exchange under regular 12h dark/light, in red under 24 h constant red light (650-700 nm), both at $250 \mu\text{mol m}^{-2}\text{s}^{-1}$. On the x-axes, dark bars represent night, open bars day and grey bars subjective night. c,d Integrated transpiration (molH_2O) CO₂ uptake (mmolCO_2) and instantaneous Water use efficiency ($\text{mmolCO}_2/\text{molH}_2\text{O}$) in *C. rosea* (c) and *C. multiflora* (d) for 24 h periods under Dark/light (D/L) followed by constant red light (RL). n=3

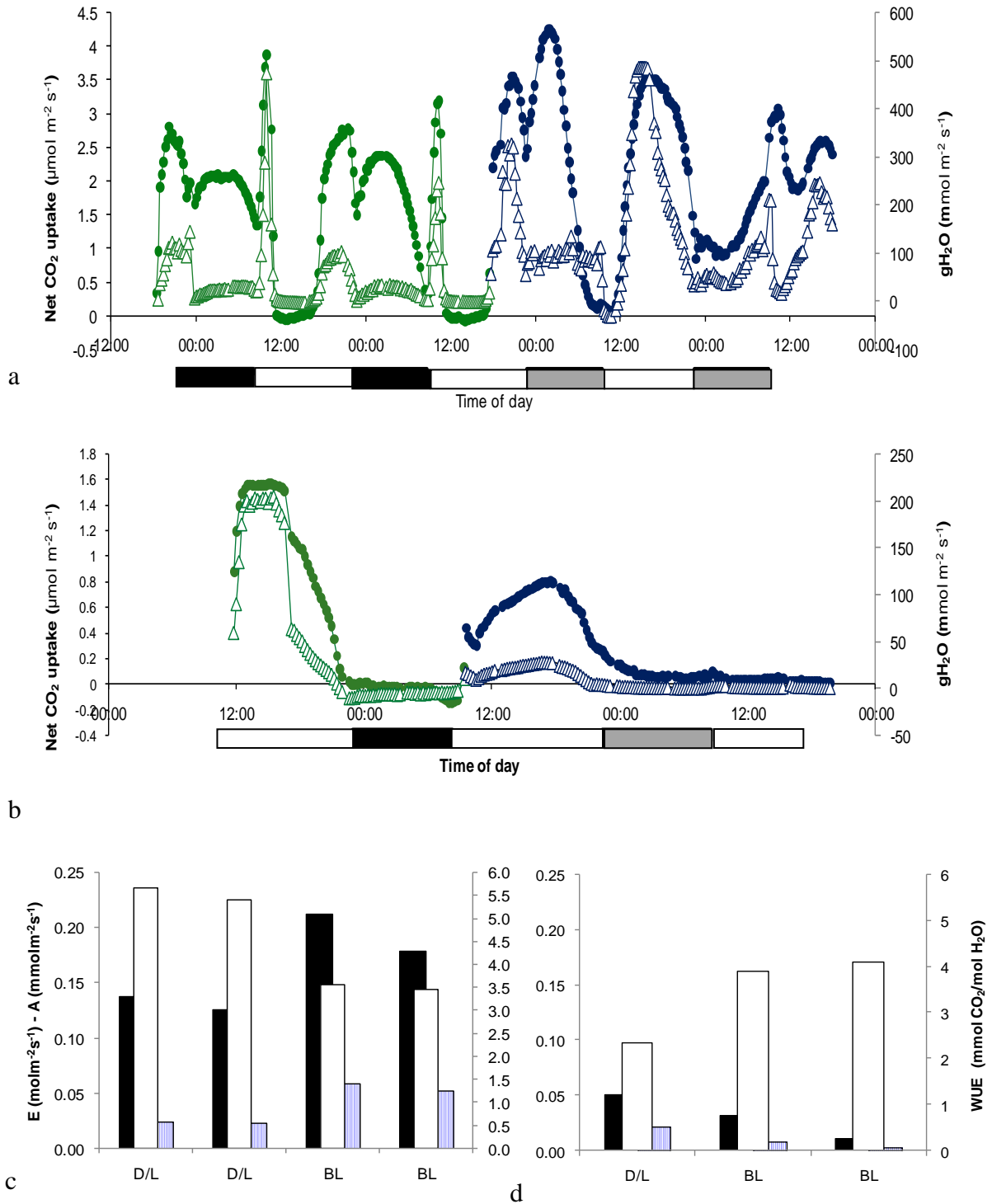


Figure 3.3. a,b Net CO₂ uptake (μmol m⁻²s⁻¹ closed circles) and stomatal conductance gH₂O (mmol m⁻²s⁻¹ open triangles) for *C. rosea* (a) and *C. multiflora* (b). Curves in green represent gas exchange under regular 12h dark/light, in blue under 24 h constant blue light (400-450 nm), both at 250 μmol m⁻²s⁻¹. On the x-axes the solid bars represent night, open bars day and grey bars subjective night. c,d Integrated transpiration (molH₂O) CO₂ uptake (mmolCO₂) and instantaneous Water use efficiency (mmolCO₂/molH₂O) in *C. rosea* (c) and *C. multiflora* (d) for 24 h periods under Dark/light (D/L) followed by constant blue light (BL) (250 μmolm⁻²s⁻¹). n=3

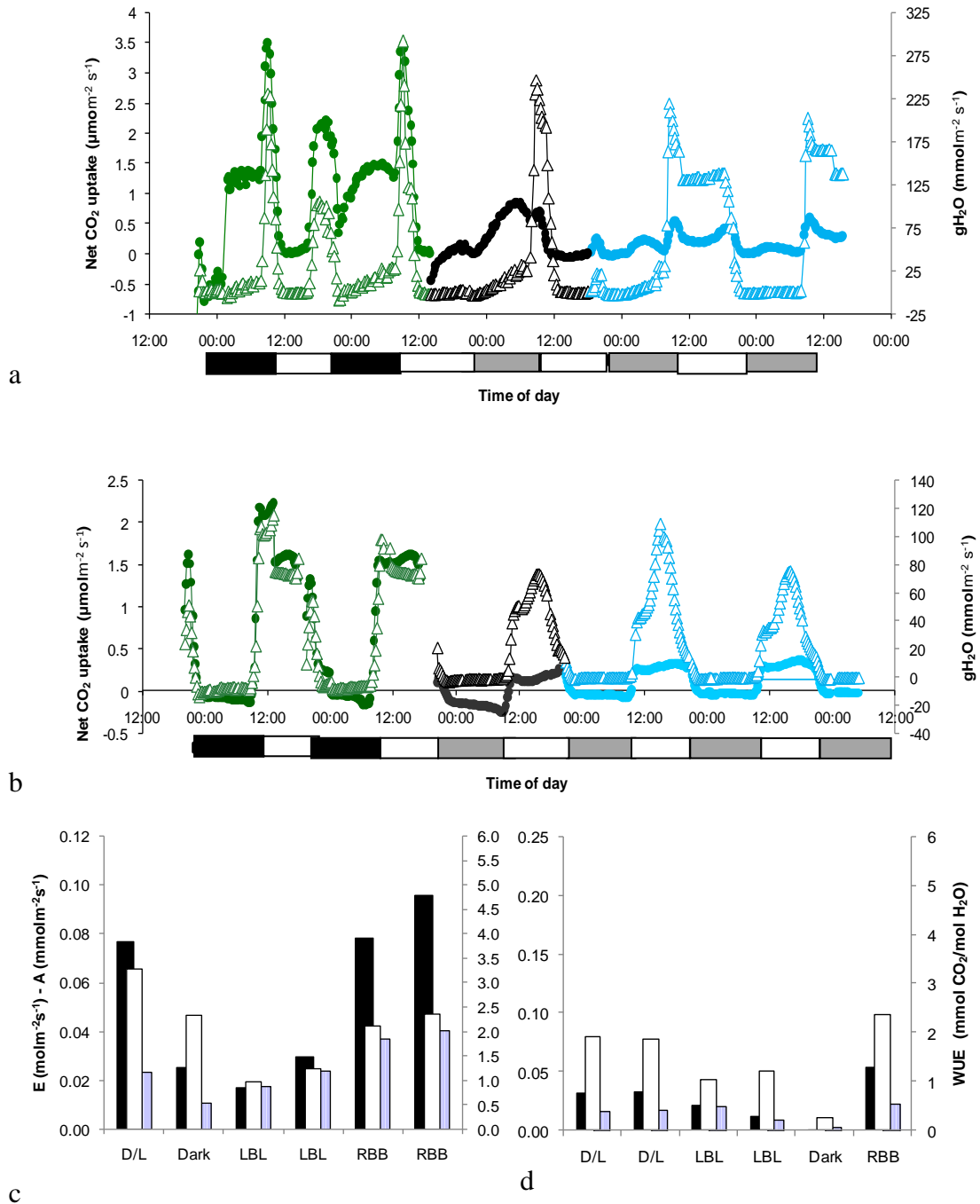


Figure 3.4 a,b Net CO₂ uptake (μmol m⁻²s⁻¹ closed circles) and Stomatal conductance gH₂O (mmol m⁻²s⁻¹ open triangles) for *C. rosea* (a) and *C. multiflora* (b). Curves in green represent gas exchange under regular 12h dark/light, in black under 24 h constant dark, in blue under 24 h constant low level blue light (400-450 nm; 15 μmol m⁻²s⁻¹), , On the x-axes the solid bars represent night, open bars day and grey bars subjective night. c,d Integrated transpiration (molH₂O) CO₂ uptake (mmolCO₂) and instantaneous Water use efficiency (mmolCO₂/molH₂O) in *C. rosea* (c) and *C. multiflora* (d) for 24 h periods under Dark/light (D/L) followed by constant low blue light (15 μmolm⁻²s⁻¹) (LBL), dark and red light (250 μmolm⁻²s⁻¹) with blue background (RBB). n=3

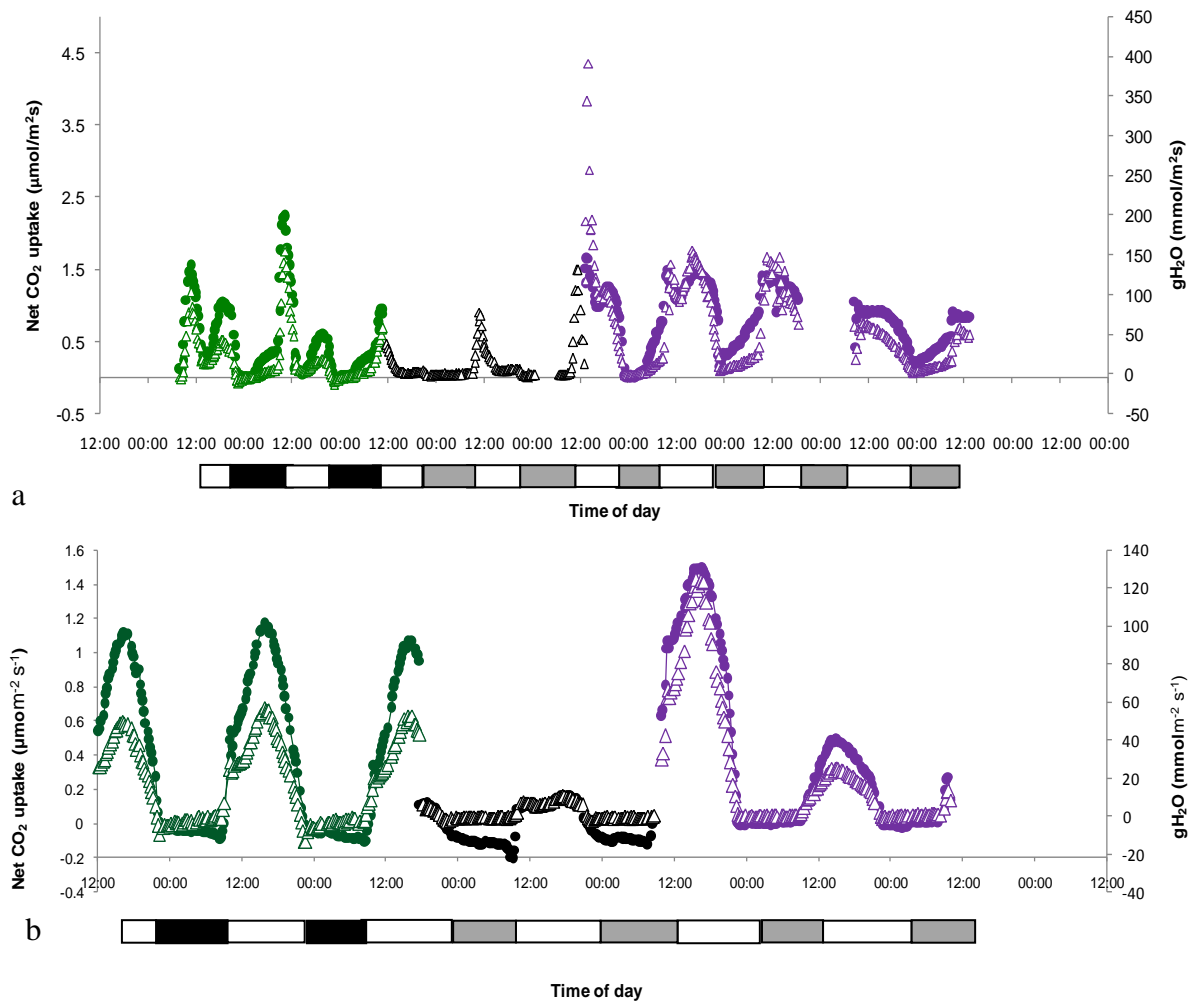


Figure 3.5 Net CO₂ uptake ($\mu\text{mol m}^{-2}\text{s}^{-1}$ closed circles) and stomatal conductance gH_2O ($\text{mmol m}^{-2}\text{s}^{-1}$ open triangles) for *C. rosea* (a) and *C. multiflora* (b). Curves in green represent gas exchange under regular 12h dark/light, next in black under constant dark, next in purple under constant 24 h red light ($250 \mu\text{mol m}^{-2}\text{s}^{-1}$) with a background of blue light. On the x-axes the solid bars represent night, open bars day and grey bars subjective night.

The distance between the maximum values for net CO₂ uptake and stomatal conductance were measured under 48 h dark/light and under the constant light regimes to establish period length and to see if there were alterations in period length in the CAM and C3 species under the contrasting light treatments. *C. multiflora* and *C. rosea* both presented a period of 24 h under the dark/light regime. *C. rosea* showed shorter periods under constant white, red and blue light, but *C. multiflora* presented a shorter period just under white light, and near to 24 h under red and blue light. Under low blue light *C. rosea* kept the same period of 24 h but *C. multiflora* presented a longer period 25 h (while the cycle rhythm was maintained Table 3.1).

Table 3.1. Distance in hours (period length) for peaks of net CO₂ uptake and stomatal conductance under regular 48 hour light/dark and under constant 48 hours, in white WI, red RI and blue BI light (250 μmol m⁻²s⁻¹) and low blue light (15 μmol m⁻²s⁻¹) for *C. rosea* and *C. multiflora*. Distance was measured during the first 48 hours under the light treatment and is the result of 3 replicates.

	<i>C. rosea</i>		<i>C. multiflora</i>	
	CO ₂ uptake (h)	Stomatal conductance (h)	CO ₂ uptake (h)	Stomatal conductance (h)
Dark/light	24	24	24	24
White light	17.5 ± 4.77	18	19	19
Red light	20.5 ± 4.84	21 ± 3.03	24	24
Blue light	16 ± 4.45	19	24	-
Low blue	24	24	25	25

It is interesting to know how circadian oscillations in net CO₂ uptake and stomatal conductance under the contrasting light regimes impacted on water use efficiency. WUE was calculated for 24 h periods under the different light regimes for both species (Table 3.2). Under the usual light/dark cycle, the CAM species presented a higher WUE (5.5 mmolCO₂/mol H₂O) compared to the C3 species (2.75 mmol CO₂/mol H₂O). However, under constant light conditions, the CAM *C. rosea* presented lower values of WUE compared to those under the standard day/night cycle with values obtained much closer to those of the C3 species *C. multiflora*. In the CAM species, alterations in the timing of net CO₂ uptake and stomatal conductance which shifted to the subjective day under constant light converted the CAM species into a ‘C3 species’ in terms of the preservation of water, at least for short periods. On the other hand, the C3 species *C. multiflora* showed lower values of WUE just under low blue light and darkness, whilst under the other light regimes (high intensity red or blue), the values for WUE were similar (white red with blue background) to those under dark/light cycle. The maintenance of WUE under constant light conditions in *C. multiflora* might be related to the robust control of period length (Table 3.1) in the C3 species compared to the CAM *C. rosea*.

Table 3.2 Water use efficiency (mmolCO₂/molH₂O) for a 24 h period, CO₂ uptake (A) and transpiration (E) for *C. rosea* and *C. multiflora* under different light regimes: Dark/light (D/L), constant white light(WL), constant red light (RL) and constant blue light (BL) (250 μmol m⁻²s⁻¹), low blue light (15 μmol m⁻²s⁻¹) (LBL) and red light (250 μmol m⁻²s⁻¹) with blue background (RBB).

<i>C. rosea</i>	E (mol H ₂ O m ⁻² s ⁻¹)	A (mmol m ⁻² s ⁻¹)	WUE (mmolCO ₂ /mol H ₂ O)
D/L	0.017	0.087	5.189
D/L	0.014	0.082	5.787
WL	0.034	0.163	4.823
WL	0.043	0.179	4.143
D/L	0.023	0.104	4.606
RL	0.061	0.181	2.945
RL	0.061	0.187	3.079
D/L	0.024	0.137	5.651
D/L	0.023	0.125	5.402
BL	0.059	0.212	3.570
BL	0.052	0.179	3.443
D/L	0.023	0.076	3.268
Dark	0.011	0.025	2.316
LBL	0.018	0.017	0.968
LBL	0.024	0.030	1.239
RBB	0.037	0.078	2.109
RBB	0.041	0.096	2.356
<i>C. multiflora</i>			
D/L	0.019	0.055	2.900
D/L	0.020	0.053	2.632
WL	0.020	0.054	2.628
D/L	0.022	0.051	2.351
RL	0.011	0.029	2.721
RL	0.002	0.006	2.757
D/L	0.022	0.051	2.351
BL	0.008	0.031	3.895
BL	0.003	0.011	4.110
D/L	0.016	0.031	1.910
D/L	0.017	0.033	1.875
LBL	0.021	0.022	1.037
LBL	0.010	0.012	1.208
Dark	0.003	0.001	0.258
RBB	0.023	0.054	2.356

3.3.2 Speed of response of stomata to light

To test the hypothesis that larger stomata respond more slowly to changes in light intensity (i.e. either switching lights off during the photoperiod or switching lights on during the dark), measurements of stomatal conductance and net CO₂ uptake were recorded every minute following lights off or on and the slope of the linear part of the response was estimated. The larger stomata of the CAM species *C. rosea* responded faster than stomata of the C3 species *C. multiflora* when lights were switched off (stomatal closure) or on (stomatal re-opening) during the photoperiod (Figs 3.8a,b, 3.9a,b Table 3.3). However, this difference between species in stomatal kinetics was not observed at night. Stomata of the C3 *C. multiflora* opened faster when an external light was applied during the night compared to when the light was reapplied following a period of darkness during the day (Table 3.3 and Figure 3.6). Moreover, in *C. multiflora*, turning the light on at night had a negligible effect on net CO₂ uptake suggesting that the stomatal response to light imposed at night in the C3 species was as a direct effect on photoreceptors rather than an indirect effect mediated via photosynthesis. Turning lights on during the dark period resulted in an increase in net CO₂ uptake in the CAM species but stomatal conductance showed either a slow increase (Fig 3.8c) or no change, followed by a drop then a gradual increase (fig 3.8d). When this artificially imposed light was subsequently turned off at night, net CO₂ uptake dropped rapidly then increased rapidly and continued to rise (Figs 3.8c,d) until the lights came on naturally in the growth room at the end of the dark period when both net CO₂ uptake and stomatal conductance declined in the CAM species (Figs 3.8 ,d). Such responses in the CAM species may be attributed to the operation of PEPC and/or some other internal signal that overrides responses to light treatments imposed at night/start of the day.

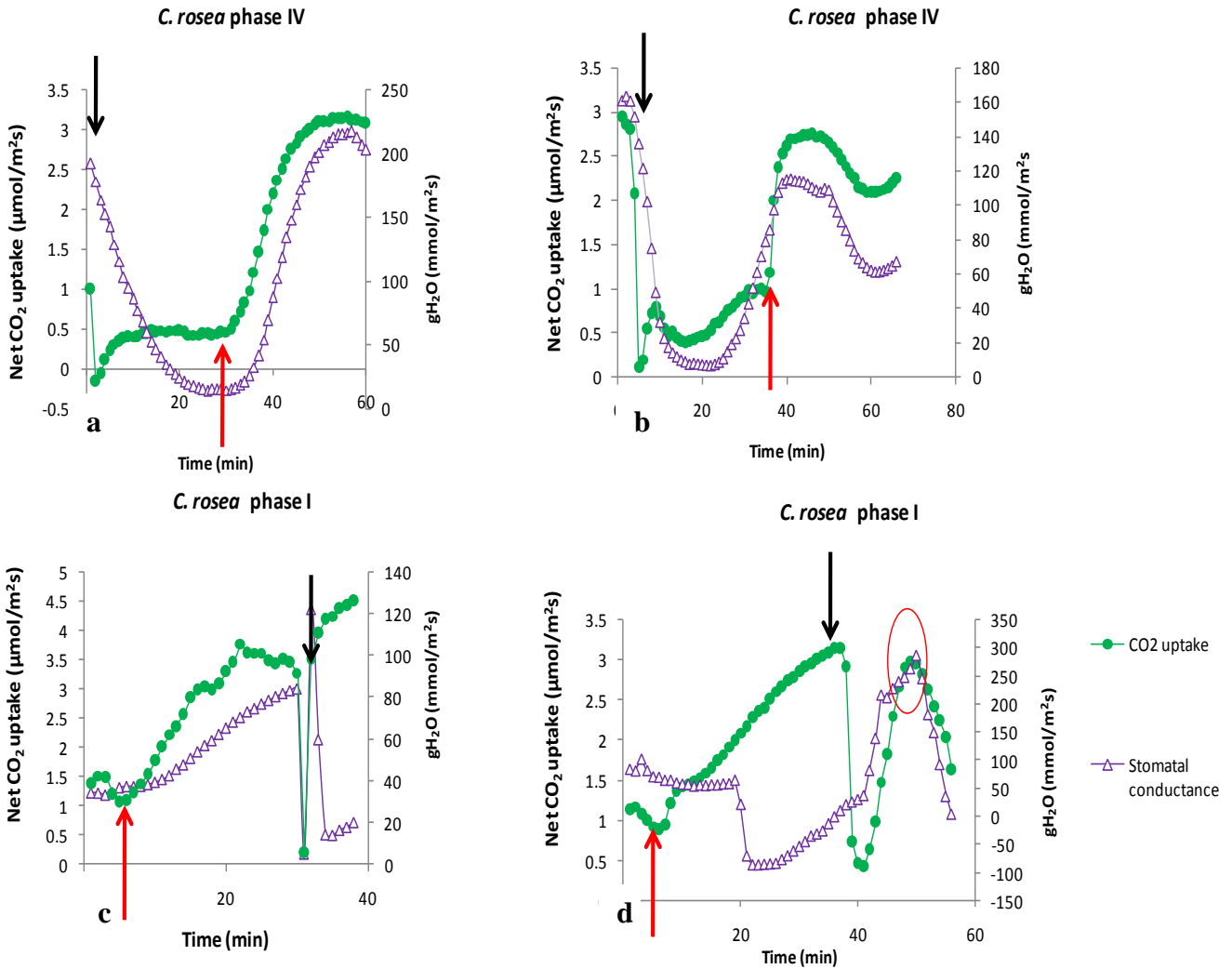


Figure 3.6. Changes in rates of net CO₂ uptake (closed circles) and stomatal conductance (open triangles) in the CAM species *C. rosea* after an external light source ($250 \mu\text{mol m}^{-2} \text{s}^{-1}$) was turned on (red arrows) and turned off (black arrows) either during the day (a-b) or night (c-d). Data were recorded at 1 minute intervals. In figure d the red circle highlights how the stomata closed after the external lights came on at the start of the photoperiod in the growth room. (For explanation of negative stomatal conductance values, see the text).

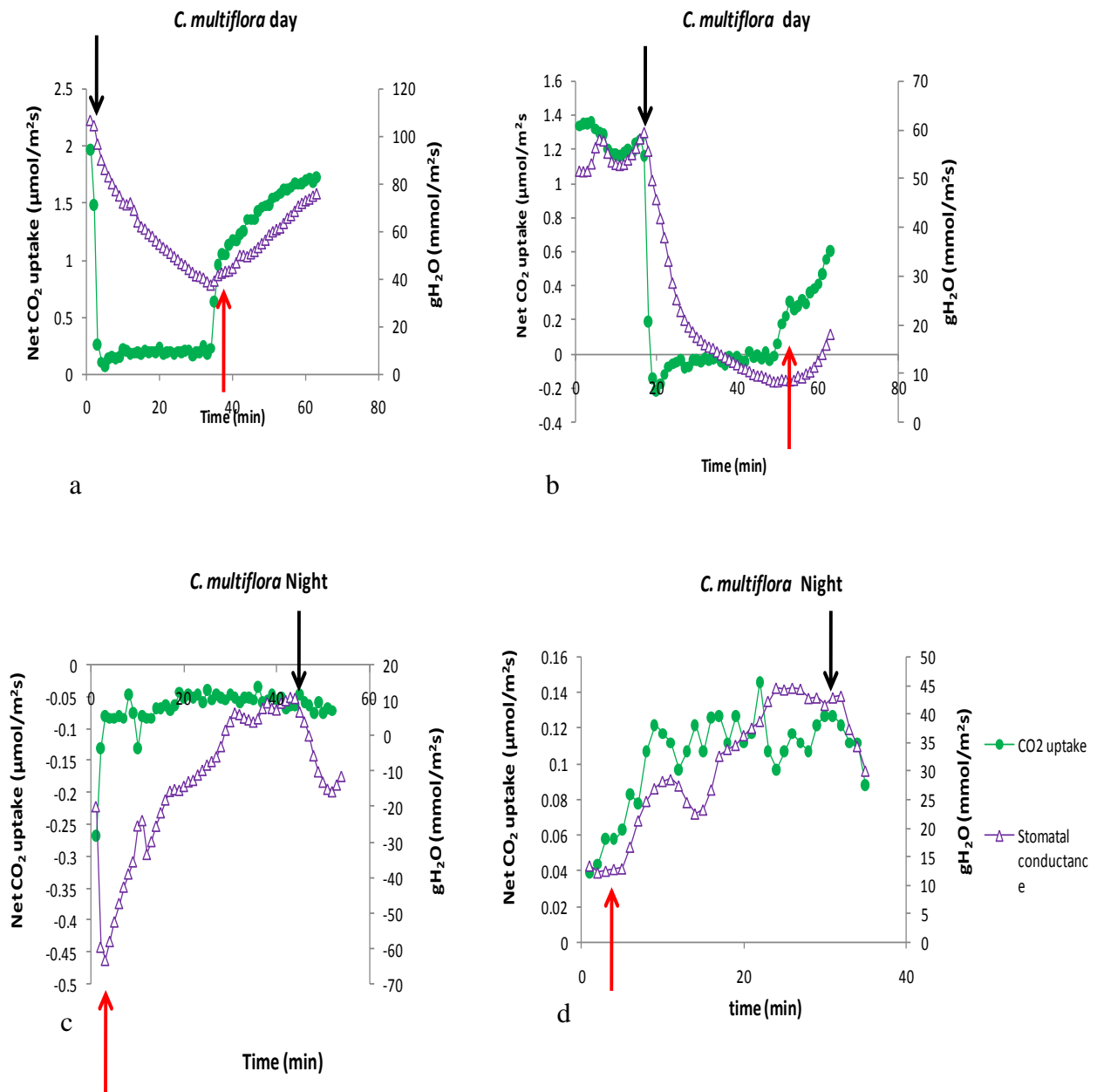


Figure 3.9. Changes in rates of net CO₂ uptake (closed circles) and stomatal conductance (open triangles) in the C₃ species *C. multiflora* after an external light source ($250 \mu\text{mol m}^{-2} \text{s}^{-1}$) was turned on (red arrows) and turned off (black arrows) either during the day (a 15:30, b 11:30) or night (c-d, 22:30-23:00). Data were recorded at 1 minute intervals. (For explanation of negative stomatal conductance values, see the text).

Table 3.3. Rates (slope of the linear part of the curves corresponding to figures 3.8 and 3.9) of stomatal opening after the light ($250 \mu\text{mol m}^{-2}\text{s}^{-1}$) was turned on and stomatal closing after the light was turned off during natural dark (phase I for *C. rosea* and night time for *C. multiflora*) and natural light (phase IV for *C. rosea* and day time for *C. multiflora*). Degree of opening and closing was indicated by stomatal conductance ($\text{gH}_2\text{O: mmol H}_2\text{O m}^{-2} \text{s}^{-1}$). Temperature was 21°C at night and 27°C during the day.

	<i>C. rosea</i>		<i>C. multiflora</i>	
	$\Delta \text{gH}_2\text{O: mmol H}_2\text{O m}^{-2} \text{s}^{-1}$		$\Delta \text{gH}_2\text{O: mmol H}_2\text{O m}^{-2} \text{s}^{-1}$	
	Phase IV	Phase I	Day	Night
Light on	7.66 (a)	2.87(c)	1.33(a)	4.94(c)
	6.5 (b)	-1.9 (d)	0.39(b)	2.2 2(d)
Light off	-11.89(a)	4.09(c)	-3.49(a)	-3.41(c)
	-17.39(b)	6.29(d)	-4.17(b)	-2.08(d)

3.3.3 Stomatal guard cell chloroplasts

There was evidence to indicate the presence of chloroplasts in guard cells of eight species of *Clusia* with contrasting photosynthetic physiologies. The species examined were *C. hilariana*, *C. rosea*, *C. alata*, *C. lanceolata*, *C. aripoensis*, *C. grandiflora*, *C. tocuchensis* and *C. multiflora*. Due to difficulties in obtaining good quality and thin epidermal peels from fresh leaves, the quality of the pictures is not enough to quantify the number of chloroplasts in the guard cells of the different species, or to compare with the number of chloroplasts in mesophyll cells. However, the fluorescence emission seems to be associated with guard cells in the leaves of all species, suggesting the presence of chloroplasts in guard cells of stomata of *Clusia* plants (Figure 3.8)

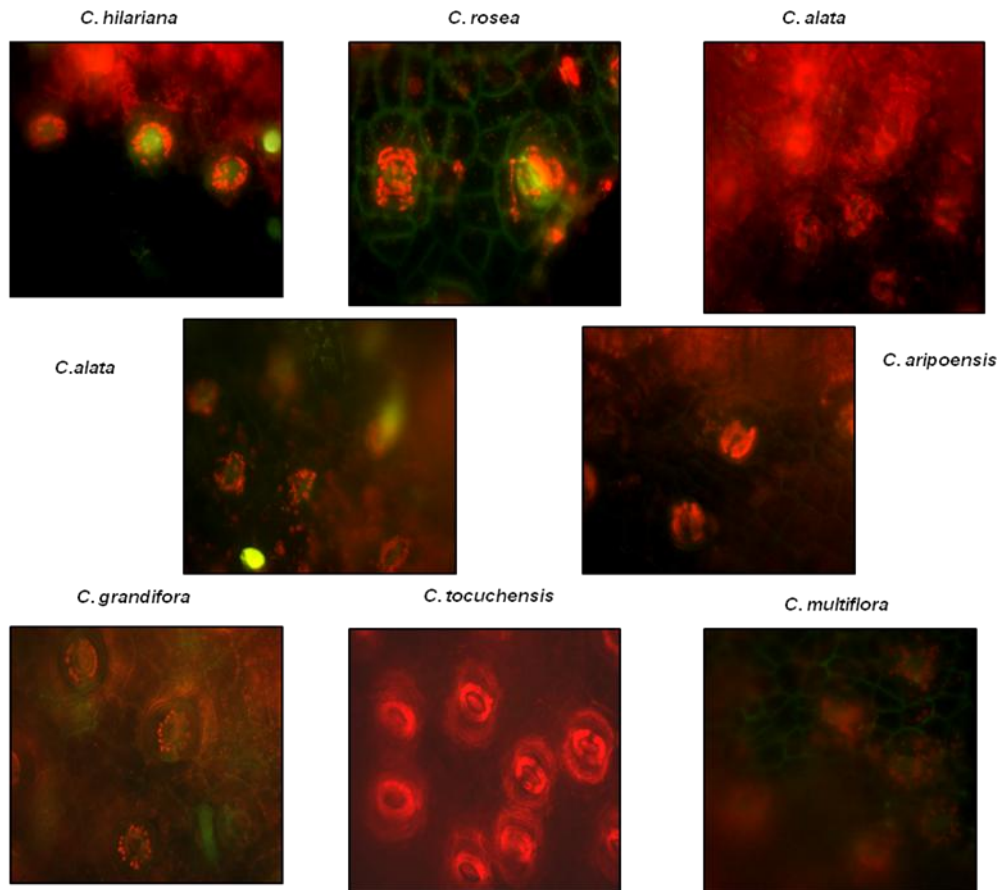


Figure 3.8 Pictures of epidermal peelings from the abaxial leaf surfaces of eight *Clusia* species under fluorescence microscope at 40x magnification. Bright dots in red indicate the presence of chloroplasts as a result of chlorophyll fluorescence. n=3

3.4 Discussion

3.4.1. Circadian control of stomatal conductance is more robust in the CAM *Clusia* compared to the C3 *Clusia*

Light intensity and temperature are some of the most influential environmental factors controlling circadian rhythms in plants (Bohn et al., 2001). Circadian oscillations in stomatal conductance and net CO₂ uptake were maintained for longer in the CAM *C. rosea* compared to the C3 *C. multiflora* under the contrasting light regimes so in that regard, hypothesis 1 was proved to be correct (i.e. more robust clock control over stomata in the CAM species). However, circadian control of stomatal conductance and net CO₂ uptake was more responsive to light quality in *C. rosea*, the CAM species, than in *C. multiflora*, the C3 species, in terms of shifts in period length. Under constant conditions of white light, red light and blue light, *C. rosea* presented a higher stomatal conductance

shifted to the day time and a higher integrated net CO₂ uptake during the subjective day compared to that measured under light/dark. *C. multiflora*, showed the same or lower values for stomatal conductance and CO₂ uptake under the continuous light regimes compared to dark/light. This suggests that the circadian clock in *C. rosea* is more responsive (in comparison to the *C. multiflora* clock) to light signals, which modify clock control over stomatal conductance and the CO₂ uptake rhythm.

It has been reported that PEPC is regulated by reversible phosphorylation in response to light in C3 and C4 plants but to a circadian oscillator in CAM plants through the control of PEPC kinase activity (Carter et al., 1991; Hartwell et al., 1996). It is also known that minimal PEPC activity corresponds to maximal C_i/C_a levels in CAM plants (Grams et al., 1997), and some studies report that PEPC activation remains rhythmical at different light intensities but variations in the light intensity can alter malate accumulation through C3 photosynthesis with subsequent effects on C_i/C_a ratios (Bohn et al., 2001). Alterations in PEPC activation status under constant light could be generating the shifts in net CO₂ uptake and stomatal conductance that are observed in *C. rosea* under the contrasting light regimes but not in *C. multiflora*. The involvement of PEPC and metabolites such as malate in modulating period length for stomatal conductance and net CO₂ uptake under different environmental scenarios could confer a degree of flexibility for the clock in CAM plants which may serve to optimise the use of resources under potentially limiting environments (Borland and Taybi, 2004).

In conclusion, with reference to hypothesis 1, circadian control of stomatal conductance was found to be more robust in the CAM species *C. rosea*, (as compared to the C3 *C. multiflora*) in terms of the maintenance of stomatal opening and closing under constant conditions of white, red and blue light. However, the CAM species showed a more flexible response to differences in light quality by altering period length and the timing of maximal stomatal conductance and net CO₂ uptake.

3.4.2. Circadian control of stomatal conductance is mediated via photosynthesis and by photoreceptors in *Clusia*

The role of chloroplasts in stomatal guard cells of C3 and C4 plants in the fixation of CO₂ is still in dispute. Some studies have reported that the reduction of CO₂ concentration in guard cell chloroplasts via the Calvin cycle is insignificant (Outlaw, 1989; Reckmann et al., 1990), whilst others have suggested that guard cell photosynthesis could play a key role in sensing changes in the environment and signalling these changes to adjust stomatal aperture (Outlaw, 1989; Goh et al., 1999). Lawson et al. (2002, 2003) found that chloroplasts in guard cells of *Commelina communis* and

Tradescantia albiflora responded to internal but not ambient CO₂ concentrations. In the present work, under constant red light a more robust rhythm of stomatal conductance and net CO₂ uptake was observed in the CAM species compared to the C3 species. Lower maximal values of net CO₂ uptake were observed under red light in both species but whilst stomatal conductance was also lower under red light (compared to white light) in *C. multiflora*, in *C. rosea* stomatal conductance was significantly higher under red light compared to values measured under white light. This result indicates that stomata of the CAM *C. rosea*, might respond to changes (depletion) in CO₂ concentrations in the mesophyll if PEPC remains active during the subjective day and/or there is both C3 and C4 photosynthesis occurring in the guard cells, which draw down C_i and elicit an increase in stomatal conductance under red light. In principle this is possible since chloroplasts are present in the guard cells of this species (Figure 3.8).

Ogawa et al. (1978) found that blue light elicits an increase in stomatal opening when given over a background of saturating red light. That the stomata of the C3 species *C. multiflora* showed a reduction in stomatal conductance under red light compared to white light, suggested that, in contrast to the CAM *C. rosea*, the C3 species required the blue light stimulus to open the stomata and maintain the circadian rhythm under constant red light. This was proved to be correct since supplying red light with a blue light background for a period of 24 h elicited an increase in stomatal conductance in the C3 species over that observed under white light. However, the response was damped beyond 24 h, perhaps due to an increase of CO₂ in the mesophyll.

Under constant blue light (250 $\mu\text{molm}^{-2}\text{s}^{-1}$) stomatal conductance and net CO₂ uptake were lower for *C. multiflora*, but higher for *C. rosea* compared to dark/light. Moreover, as found under constant white and red light conditions, in *C. rosea* blue light elicited a shift in the rhythms of gas exchange with maximal sustained rates of net CO₂ uptake and stomatal conductance shifted to the subjective day. Other studies (Sharkey, 1987; Zeiger, 1987, 1990) have demonstrated that stomata are more sensitive to low levels of blue and red light and those larger stomatal apertures are found under saturating blue as compared to saturating red light. The initial response of *C. rosea* to blue light (250 $\mu\text{molm}^{-2}\text{s}^{-1}$) was presumably a photosynthetic/metabolic response rather than a direct response of the blue light photoreceptor, due to the high light intensity imposed. Under low level blue light (15 $\mu\text{molm}^{-2}\text{s}^{-1}$), maximal stomatal conductance was increased (compared to that observed under darkness) in the C3 *C. multiflora* and the stomatal rhythm of opening and closing was maintained for at least 48 h, indicating the direct involvement of blue light photoreceptor(s) in circadian regulation of stomatal conductance in the C3 species. Whilst there was no increase in maximal stomatal conductance under low level blue light (compared to that observed under darkness) in the CAM *C. rosea*, stomatal behaviour was altered such that higher levels of stomatal conductance were maintained over the

subjective day and a robust rhythm of stomatal opening and closing was maintained for at least 48 h under low level blue light. This important observation indicates that the CAM *Clusia* has not lost the 'blue light' response that was reported for other CAM species (Lee and Assmann, 1992; Tallman et al., 1997). It is intriguing why the stomata of *C. multiflora* showed a very reduced response to high intensity blue light compared to the CAM *Clusia*. It has been proposed that the concentration of sugars (sucrose) and acids (malate) inside the guard cells is important for stomatal opening (Talbot and Zeiger, 1993). In the absence of red light for photosynthesis in the C3 guard cells, this accumulation of sugars and malate may be curtailed and this might interfere with stomatal opening. Also, with reduced rates of net CO₂ uptake in the mesophyll cells of *C. multiflora* under high intensity blue light internal CO₂ concentrations will stay stable (probably high) and stomatal conductance will be curtailed (Farquhar and Wong, 1984; Jarvis and Davies, 1998). A linear correlation between rates of guard cell and mesophyll photosynthesis has been found at the cellular level suggesting that guard cell photosynthetic activity can be a sensing mechanism connecting stomatal opening to mesophyll photosynthetic rate (Lawson et al., 2003). There may be other signals that are transduced from the mesophyll to the guard cells that link mesophyll photosynthesis with the control of stomatal opening (Kana and Miller, 1977; Lee and Bowling, 1995); (Wong et al., 1978).

In previous works ((Deitzer and Frosch, 1990) it has been shown that circadian rhythms in stomatal conductance are coupled with changes in CO₂ assimilation and this behaviour is attributed to stomatal factors in the majority of the cases. In the present work, changes in the rhythm of net CO₂ uptake were coupled with changes in stomatal conductance under all constant light regimes of both species but not under constant white light for *C. rosea* where peaks in stomatal conductance preceded the peaks in net CO₂ uptake. Whilst the period length and timing of major peaks in stomatal conductance and net CO₂ uptake were unaltered in the C3 species under constant light conditions, in the CAM species the timing and magnitude of peaks in stomatal conductance and net CO₂ uptake cycles changed after different light regimes were applied. With this result, it appeared that the stomata of *C. rosea* responded to light in terms of directly altered rates of photosynthesis and that some blue light photoreceptors were also implicated in circadian rhythm of stomatal conductance. Also, the response to light was not more marked in *C. multiflora* than in *C. rosea* as was predicted given the well documented response of guard cells to light in C3 plants which open stomata during the day. Although light may have direct (i.e. photoreceptor) and indirect (i.e. metabolic/photosynthetic) effects on stomatal behaviour, the processes may be coupled to each other via C_i; (Bohn et al., 2001). Thus, in terms of hypothesis 2, it appears that the circadian control of stomatal conductance in CAM *Clusia* plants is controlled by photoreceptors and photosynthesis as well as other metabolic processes (e.g. malate fluctuation).

3.4.3. Water use efficiency is altered under constant light regimes in CAM *Clusia* (*C. rosea*)

By restricting the major period of stomatal opening and net CO₂ uptake to the dark period when conditions are generally cooler and more humid than during the day, it has been proposed that the circadian clock plays a key role in optimising the WUE of CAM species (Borland et al., 2009). In comparing the integrated values for WUE over the 24 h light/dark cycle it was found that, as expected, the CAM species *C. rosea* showed a substantially higher WUE than the C3 *C. multiflora*. However, under the conditions of constant light (white, red, or blue) the CAM species *C. rosea* increased both stomatal conductance and net CO₂ uptake with the major periods for both CO₂ uptake and water loss shifted to the subjective day. This C3-like timing of the periods for net CO₂ uptake and water loss meant that under constant light, the CAM *C. rosea* showed a 24 h WUE that was comparable to that of the C3 *C. multiflora*.

A study (Woerner and Martin, 1999) in *Peperomia scandens* (Bowler et al., 1994) and *P. obtusifolia* (C3) reported higher WUE of the CAM species in relation to that of the C3 species under a range of environmental settings and suggested that factors such as stomatal density in addition to stomatal opening during night time in CAM, might be involved in the maintaining of high WUE in CAM compared to closely-related C3 plants. The data in chapter 2 indicated that whilst stomatal density was lower in the CAM *C. rosea* compared to the C3 *C. multiflora*, the stomatal complex (including the aperture) was larger in the CAM species. In this regard it can be observed that the maximal values of stomatal conductance, particularly under conditions of constant light, were significantly higher in the CAM *Clusia* than in the C3 *Clusia*. The alterations in the rhythm of stomatal conductance, especially in *C. rosea* probably due to the overstimulation of the large stomata under constant light caused a imbalance in transpiration and CO₂ uptake (the stomata opened more fully in response to light which resulted in an increase in water loss that was not compensated for by the increase in net CO₂ uptake) and the CAM *Clusia* was unable to maintain the same high level of WUE as in dark/light cycles. It is important to point out that all plants were maintained under well watered conditions so the finding that the increase in C gain under constant light was accompanied by greater water loss may have been acceptable in terms of maximising resource use. It would be interesting to determine if the clock elicited a greater control over WUE in the CAM *C. rosea* under conditions of constant light where water availability was limited.

Other studies have demonstrated that clock control over the phases of CAM can be modulated under different environmental conditions. (Winter et al., 2009) reported that changes in photon flux

density under natural conditions modulated the 24 h pattern and magnitude of net CO₂ uptake pattern in *C. rosea* under well watered conditions such that under low PFD the main period of net CO₂ uptake shifted from the night to the day (i.e. phase II) (Winter et al., 2009). That study demonstrated that the clock permits flexibility for modulating the day and night phases of CAM to modulate carbon gain but the implications for water use were not assessed. The present study indicates that by curtailing the major period of net CO₂ uptake to the night period, CAM in *Clusia* plays a key role in water conservation in dry environments.

3.4.4 Stomata of the CAM *Clusia* responded faster to changes in PFD imposed during the photoperiod compared to the C3 *Clusia*

Based on the anatomical studies presented in chapter 2 which indicated that CAM species of *Clusia* possess larger stomatal guard cells than C3 species of *Clusia* it was hypothesised that the stomata of the different photosynthetic types would exhibit different kinetics in terms of the speed of stomatal responses to changes in PFD. The data obtained indicated that the larger stomata of the CAM species *C. rosea* responded faster than stomata of the C3 species *C. multiflora* when lights were switched off (stomatal closure) or on (stomatal re-opening) during the photoperiod. This increased rate of response of the larger CAM stomata could be important for optimising carbon gain and water loss under changing environmental conditions at the start and end of the day. However, this difference between species in stomatal kinetics was not observed at night. Stomata of the C3 *C. multiflora* opened faster when an external light was applied during the night compared to when the light was reapplied following a short period of darkness during the day and the light-stimulated opening at night was independent of any change in net CO₂ uptake. Other studies (Mansfield, 1963; Mansfield and Heath, 1963; Kana and Miller, 1977) have shown that the stomata of C3 plants open faster in response to a light pulse when given after longer periods of dark, particularly when the light is given towards the end of the natural night (i.e. towards the start of the subjective day). Such findings indicate clock control of stomatal kinetics in C3 plants that appear to be independent of photosynthesis.

The stomatal responses to light imposed at night were more complex in the CAM *C. rosea*. When lights were switched on at night, net CO₂ uptake increased but stomatal conductance in the CAM species either remained unchanged or increased slowly. Such findings suggest day/night differences in the signals that link stomatal behaviour to changes in light. When the lights were turned off again at night, a drop in net CO₂ uptake was observed followed by a rapid increase in stomatal conductance, thus

as found for the C3 *Clusia* at night, stomatal opening was not closely coupled to photosynthesis/metabolism. It was also observed that as the external lights in the growth room came on naturally at the end of the night, both stomatal conductance and net CO₂ uptake declined in the CAM *C. rosea*, indicating that the day/night CAM rhythm could override the previous perturbations in dark/light perturbations.

Since stomatal responses to light were different in the CAM *Clusia* plant *C. rosea* with respect to the C3 *Clusia* plant. *C. multiflora* and circadian control might be behind these responses, it is interesting to explore inside the molecular mechanisms under this. In the next chapter the circadian expression of four photoreceptors phototropine 1, phototropine 2, phytochrome A and cryptochrome 2 in *C. rosea* and *C. multiflora* will be compared under the same light regimes (constant white, red, blue, dark and also far red) with the purpose of comparing physiological results from gas exchange patterns and molecular results from transcript abundance of those phototropins.

Chapter 4: Circadian regulation of the expression of photoreceptors in a C3 and CAM species of *Clusia*

4.1 Introduction

It has previously been hypothesized that light signals are involved in the inhibition of stomatal opening during the day in CAM plants or in the shift from diurnal to nocturnal opening in CAM plants (Tallman et al., 1997). A study in *Portulacaria afra* a C3/CAM plant, demonstrated that stomatal guard cells responded to blue and red light when C3 photosynthesis occurred, but this response was lost when the plants performed CAM, suggesting that the signalling pathways involved in stomatal responses to light are modified and/or inhibited when CAM is induced in *P. afra* (Lee and Assmann, 1992). Tallman et al., (1997) also showed that upon the induction of CAM in *Mesembryanthemum crystallinum* the formation of zeaxanthin and stomatal opening in response to blue and white light was lost. In chapter 3 of this thesis, more robust circadian control of stomatal conductance was noted in the CAM species *Clusia rosea* and stomatal conductance was more responsive to light quality in the CAM than in the C3 *Clusia*. Taken together, the findings described above suggest that the signals/mechanisms which link stomatal responses to the circadian clock and to differences in light quality have diverged in the different photosynthetic modes. The aim of this chapter is to establish if these divergent responses are linked to differences between C3 and CAM species of *Clusia* in the circadian control of the expression of photoreceptors implicated in blue and red light responses.

The direct response of stomata to blue light has been conferred to the action of **phototropine 1 and phototropine 2 (PHOT1 and PHOT2)**, blue light receptors that are located in the plasma membrane of the guard cells (Kinoshita et al., 2001; Sakamoto and Briggs, 2002). The PHOT receptors are membrane kinases that are activated by blue light (Briggs and Christie, 2002). Blue light prompts auto-phosphorylation of PHOT receptors, leading to activation of the H⁺-ATPase driving K⁺ uptake (Roelfsema and Hedrich, 2005). It has been reported that there is a functional redundancy between *phot1* and *phot2*, but it is possible that the sensitivity of each phototropin to light might be different. Experiments with mutants demonstrated that *phot2* seems to function just at high light intensity (Briggs et al., 2007). Kinoshita et al. (2001) showed that single *phot1* and *phot2* *Arabidopsis* mutants responded

to blue light opening the stomata, but the aperture was slightly less than the wild type and stomata in the double *phot1 phot2* mutant did not respond to blue light. In addition, the induction of stomatal opening through the activation of the ATP pump in the membrane of guard cells did not occur in the double *phot1phot2* mutant (Biggs et al 2005). The movement and accumulation of chloroplasts in mesophyll cells in *Arabidopsis* has been shown to be mediated by *phot1* irrespective of the blue light intensity, whilst *phot2* acted under low blue light fluence rates (Sakai et al., 2001; Kagawa and Wada, 2002; Wada et al., 2003). The movement of chloroplasts regulated by phototropins might be important in stomatal opening. Chloroplasts in mesophyll cells are accumulated under low blue light and this process is mediated by phototropins (Sakai et al., 2001). If chloroplasts are present in guard cells, chloroplast accumulation in the guard cells following the imposition of blue light might increase the photosynthetic activity (under red or white light) leading to accumulation of starch and sugars, changing the osmotic potential of guard cells and thus stimulating stomatal movements i.e. opening (Humble and Raschke, 1971; Mansfield, 1986; Serrano et al., 1988; Poffenroth et al., 1992) Work with the fern *Adiantum capillus-veneris*, showed that *phot1* but not *phot2*, is involved in chloroplast movement under blue light induction (Kagawa et al., 2004).

Photoreceptors also play a key role in transducing information about the external light environment to the circadian clock. Two families of photoreceptors implicated in this aspect of circadian rhythms, are the Phytochromes and Cryptochromes (McClung, 2000). **Phytochrome A (PHYA)**, encodes a pigment sensitive to red and far red light and in higher plants phytochrome is involved in the recognition of photoperiod length and in the regulation of circadian rhythms (Reed et al., 1994). PHYA responds to low levels of far red and red light and it is a photo labile molecule degrading after exposure to light (Toth et al., 2001). Some studies have reported conflicting results regarding *phyA* RNA accumulation in plants growing under dark/light cycles (Adam et al., 1994; Clack et al., 1994; Hauser et al., 1998). Recent work with microarrays in *Arabidopsis* show either rhythmic or arrhythmic changes in transcript abundance of *PhyA* (Harmer et al., 2000; Schaffer et al., 2001). Furthermore, a recent review (Lee, 2010) suggested that stomatal opening in CAM plants depends on circadian rhythms involving PHYA which could regulate ion fluxes and the electrical potential of the plasma membrane.

A further photoreceptor that could also be involved in stomatal opening is **cryptochrome 2 (CRY2)**. In principle, cryptochrome is a blue light photoreceptor that controls germination, photoperiodism and circadian rhythms in plants. The CRY2 protein presents quick degradation upon blue light exposure and works mainly under low light intensities (Lin et al., 1998). Furthermore, cryptochrome has been reported to play a role in concert with phytochrome to entrain the circadian clock (Somers et al., 1998). Photoreceptor-specific null mutants in *Arabidopsis* have provided evidence

for the molecular interactions between PHYA, PHYB and CRY1 (Ahmad et al., 1998) and its dependence on light quality and intensity in signalling pathways (Casal and Mazzella, 1998).

Some works have suggested that phototropins, phytochromes and cryptochromes act together in the induction of stomatal opening. Kasahara et al (2004), showed that the “*photA2photB1photB2-1* mutant” (*photA* and *photB* were named based on the deduced amino acids sequences of mRNA) of the moss *Physcomitrella patens* was unable to generate chloroplast movements and accumulation under red light. This unexpected result suggests that phototropins could be part of the signalling pathways for phytochrome-dependant chloroplast movements. Another study by (Mao et al., 2005) reported that CRY 1 and CRY 2 act in conjunction with PHOT1 and PHOT2 to mediate blue light induction of stomatal opening in *Arabidopsis*. This work also showed the role of another protein COP1 as a repressor of stomatal opening probably downstream of the signalling pathways of CRY and PHOT.

Nothing is currently known about the involvement of cryptochrome and little is known of the role of phytochrome (Talbot et al., 2003) or phototropins in stomatal movements in CAM plants. One way to start to tackle the role of photoreceptors in stomatal movements in CAM plants is to explore the way in which photoreceptors are linked to the clock in C3 and CAM plants. This can be approached by comparing 24 h patterns of transcript abundance of the different photoreceptors under different light regimes in closely related C3 and CAM species.

This chapter was thus centred on the following hypotheses:

H₁: The patterns of transcript abundance of *phot 1* and *phot 2* will be different in *C. multiflora* and *C. rosea* under 12h dark/12h light cycles and will present changes in response to different light regimes

P₁: Expression of these blue-light photoreceptors is predicted to be lower in the CAM species *C. rosea* compared with the C3 species *C. multiflora* in order to prevent stomatal opening during the day time in the CAM species. Given the reported lack of a blue light response in the stomata of CAM plants, it is predicted that transcript abundance of phototropins will be less affected by the imposition of different light regimes in the CAM compared to the C3 *Clusia*.

H₂ Circadian expression of photoreceptors will be more robust in *C. rosea* than in *C. multiflora*.

P_{2.1}: Transcript abundance of *cry2* and *phyA* is reported to vary at different points of the day/night cycle and peaks in abundance during the light period are expected (Toth et al., 2001) at least for *C. multiflora* the C3 species. The rhythm is believed to be controlled by the circadian clock (persists under constant light).

P_{2.2}: Circadian control of the expression of *phyA* and *cry2* might be stronger in *C. rosea* than in *C. multiflora*, based on previous results (Chapter 3) where circadian oscillations of carbon assimilation and stomatal conductance were maintained for longer in *C. rosea* under constant light regimes. Thus, the diel cycle of transcript abundance of these photoreceptors is expected to persist under constant light conditions in the CAM *Clusia*.

H₃: The amplitude of circadian oscillations in the transcript abundance of *cry2* and *phyA* will be more responsive to the imposition of different light regimes in the CAM compared to the C3 *Clusia*

P₃: Circadian expression of *phyA* might be altered under the imposition of constant red and far red light because of the sensitivity of this photoreceptor to those wavelengths (650-700nm and 700-800 nm). Expression of *cry2* might be altered under the imposition of constant blue light because of the sensitivity of this photoreceptor to those wavelengths (400-450 nm). Given that stomatal conductance of the CAM *Clusia* was more responsive than the C3 *Clusia* in responding to different light treatments (Chapter 3) might suggest that transcript abundance of *phyA* and *cry2* will be more responsive to light regime in the CAM compared to the C3 *Clusia*.

H₄: Alterations in the circadian rhythms at the gas exchange level (as noted in Chapter 3), will be reflected in diel changes in the content of leaf titratable acids.

P₄: Given that *C. rosea* presented alterations in the rhythm in stomatal conductance and CO₂ uptake under different constant light regimes, changes in the rhythm of accumulation of acids are expected, and also these changes are likely to present a concordant pattern with gas exchange. For the C3 species *C. multiflora*, non cyclical patterns in the accumulation of acids are predicted under the different light regimes.

4.2 Materials and methods

4.2.1 Plant material

The experiments described in this chapter were performed on excised leaves from 2-3 individual plants of the CAM species *Clusia rosea* and the C3 species *C. multiflora*. Plants were propagated and grown up as described previously (Chapters 2, 3).

4.2.2 Experimental set up: Light Treatments

Two leaves from two different individuals of each species were taken from plants in the growth room (12h/12h light/dark), cut in half to have enough material for all six light treatments and placed in moist petri dishes under constant white light (390-750 nm, $250 \mu\text{molm}^{-2}\text{s}^{-1}$), blue light (400-450 nm: Lee filter number 165 at $15 \mu\text{molm}^{-2}\text{s}^{-1}$) red light (650-700nm: Lee filter number 182 at $12 \mu\text{molm}^{-2}\text{s}^{-1}$) or far red light (70-800 nm: Lee filter number 87 at $18 \mu\text{molm}^{-2}\text{s}^{-1}$) for a total of 48 h at 24 °C. After the first 24 h under constant conditions, two leaf halves from different individuals of each species were sampled for RNA extraction and titratable acidity, at regular intervals over the remaining 24 h at 06:00, 10:00, 14:00 19:00, 23:00. The light treatments were imposed within a cabinet except for far red light, due to the small size of the filter 10cm*10cm, where an external adjustable fibre optilight source (KL 2500LCD, Schott, Mainz, Germany) was clamped to the cuvette with the leaf inside.

4.2.3 Genes selection and primers design

Based on a recently established EST database for *Clusia* http://xyala.cap.ed.ac.uk/Gene_Pool/Katherine_Shorrock (Katherine Shorrock, 2009), genes encoding four photoreceptors were chosen for study: Phototropins 1 and 2, Cryptochrome 2, and Phytochrome A (see table 4.1 for sequences and reference numbers from the database).

Table 4.1. DNA sequences of genes coding for four photoreceptors Cryptochrome 2, Phototropin 1, Phototropin 2 and Phytochrome A, a housekeeping Elongation factor α (control) and the correspondent reference number from the Clusia data base (Shorrock, 2009). Highlighted regions correspond to the segments against which primers were designed.

Gene	Sequence	Reference
<i>cry2</i>	ACACAACAAAATAAGAGTGATTGTTTCAAGTTTTCTGTAAAGTTCTGCTTCTCCTTGGGTGTGGGGTATGAAGTATTTCTGGATGCGGATTGAAAAGTGATATCCTAGGATGGCAGTATATTTACAGGGAGCCTGCCGGATGGCCATGAACTTGAACTGCTGTCCAAAGGTTCAAAGTTTGATCCAGAGGGTGAATATGTAAGACATTGGCTGCCTGAGCTAGCAAGGATGCCAACTGAATGGAGGATGCGCCTCTTACTGTTCTTAAAGCTGCTGGAAGTGGACTTGGGCCAGAACTATCCGAGTCTATTATTGACATGGATTGCTTACTGAAAGCTATATTTCAAGATGCGGGATTGGAAGCGGCTGCAAAATCATCTGATGCAAATGCAACTAGTGAAGTGGTTGACTGAAAAATTGGCGATTCCCATGGTGGTCTTAAAGGAGAAAGCTGTGTGTACCTGCCCGGGCGGCCCTCGAAAGGGCGAAGCAGTG	CC_MuF_004G08 CUC00039_1
<i>phot1</i>	ACAGATTGTTACACGGAGATCCCAAAAACAGATTGGGATCACATGAAGGTGCATATGAAATTAAGCGGCATCCTTTTTCAAGGCGCTAGTCCGCTACACGAATCCTCCTGAGCTTAAGGCTCCACTTTCCCAAGCGAAGCAGAAGAGGAAGCAGAACTCATTAAAGATCTACAAACAAATGTCTTCTAAATCAAGGACAAGACCATGAAACGTGTCTCGAAACCTCCCTCGATTGCGCTACGAAGGACTTGTCTTTTTATGGCAGCCAAGATGCTCCATCTTTGGATAAAAATCTAGGCTCTTGATAATGTTTGTGTGTATGTATGCTAATTTTGTGATACTCTTTTTTAGT	CC_MiF_011E05 MIC00386_1
<i>phot2</i>	ACCTAGCTAGCATAACTCACAAATTTTCAGGACTCCAAGAAAACATAACTTTCAAAAATCGTGAGCACTGAAGGAATTAAGGAGGATTCTGAGTGAACCGGATTACTGAATGCCATCAGAAGTTTGTGCTCATATAGGCAGAGTATGCTAGCGAAGAGATTTGCAGATAACAAGACAGTAAACAAAAGAAAGTATCTCTTCATTAAAGATATATGGACCTCAAGAGAATTATTTAAGAAAGAGTCTAATATGCTTAAATAATGATGGGTAATTATCACCAAAGAAAACCATCGACAATGGAGACA TAGTGTGCTTACCAGTGCCACCAAGCGCTACTGTGGCCAGTGCCTGTGA	CC_MuF_011 G04 CUC00375_1
<i>phyA</i>	ACTGAACGTCCCATTCATGAGCTTACCAGCTTCTGTGATAAGCAGACTGATGCCCTCGTCGGAAGCATCTCCATCACGTTTCAGCAACCCCTTCAGGTATCCCGCCACCTGCATGTGTTATCCTGAGTTGAAGATGAACAAGATGAACAGATTGTCTAATTTGGTAGCTGATAAGGTAAGCTGGCCTCCATTTGGGGTAAAAATTAAGTAAATAGCAAAAAGTCGGCTAACACCTGTTGAAAGCCATATAACGTTTCAGTCATGATCTTCTACTGCATCATTAGTAATTTGAATCCCTTTGCATTGCTTTTCATCATGACTTGACTTAAAACTTCACTCAGGGAAAACTCCACCATTCCAGATCCAAGTAGCCTTCAATGATGCTATCAAGATCCGAGTCAACAAGAGCGCTGGCACTGGGCACTAGTATGCAATAAGCTGCTTCTGTTCTACTCCCAACTCAGTACCTGCCCGGGCGGCCCTCGAAAGCTTCCACAGTG	CC_MuF_011 H04 CUC00382_1
<i>ef α</i>	ACAAGGGCCCCACTCTCCTTGATGCTTTGACTTAATCCAGGAGCCCAAGAGGCCCTCAGACAAGCCCTCCGTCTCCACCAAGATTGGTGGTATTGGAACCGTGCCAGTGGGACGTGTCGAGACTGGTATCCTGAAGCCTGGTATGGTTGTGACCTTTGGCCAACTGAAAATTAAGTCTGTTGAGATGCACCATGAGGCTCTCCAGGAGGCTCCTCCAGGAGACAATGTTGGATTCAATGTCAAAAGGATCTCAAGCGTGGTTTTGTTGCTTCCAACTCCAAGGATGATCCTGCCAAGGAGGCTGCCAACTTCACTCTCAGGTCATCCTGGCCAGATTGGTAACGGATATGCCCAAGTGCCTGACTGCCACACTGCCACATTGCTGTCAAGTTTGGCGAGATCTTGAATCCGATCAGGCAAGGAGCTTGAGAAGGAGCCCAAAATCTTGAAGAATGGGGATGCTGGATTGTGAAGATGATTCCACCAAGGTTGTGGAGACATTCTCCAGT	CC_MuR_003A12 CUC00133_2

Primers for the four photoreceptors and the elongation factor α were designed using the software Primer3 <http://frodo.wi.mit.edu/primer3/>, (see Table 4.2 for primer sequences).

Table 4.2 Primers used to amplify DNA fragments of four genes encoding for photoreceptors (Cryptochrome 2, Phototropin 1 – 2 Phytochrome A) and the housekeeping Elongation factor α in *C. Rosea* and *C. multiflora*. The software Primer 3 <http://frodo.wi.mit.edu/primer3/> was used to design the primers. The annealing temperature and the predicted size of the amplified products in base pairs are also shown.

Gene	Sequence	Annealing Temperature (°)	Product size (bp)
<i>cry2</i>	FW (5'-3')	60.08	155
	CCA GAG GTC CAA GGT TCA AA	60.11	
	RV (5'-3')		
<i>phot1</i>	TAG TTC TGG CCC AAG TCC AC		184
	FW (5'-3')	60.06	
	TAT CAA TTG GGC GCT AGT CC	60.34	
<i>phot2</i>	RV (5'-3')		199
	CTT CGT AGG CAA ATC GAG GA	59.77	
	FW (5'-3')	58.93	
<i>phy A</i>	GGC AGA GTA TGC TAG CGA AGA		166
	RV (5'-3')		
	TGT CTC CAT TGT CGA TGG TT		
<i>efα</i>	FW (5'-3')	60.07	299
	CCC TTT GCA TTG CTT TTC AT		
	RW (5'-3')	59.90	
<i>efα</i>	TGC ATA CTA GTG CCC AGT GC		299
	FW (5'-3')	59.26	
	TTAATCCAGGAGCCCAAGAG	59.86	
<i>efα</i>	RV (5'-3')		299
	GGATCATCCTTGGAGTTGGA		

4.2.4 RNA extraction

To assess the transcript abundance of photoreceptors *phot1*, *phot2*, *cry1*, *phyA*, under different light qualities leaf samples were taken at 06:00, 10:00, 14:00 19:00, 23:00 under different light treatments as describe in section 4.2.2 and snap frozen in liquid N₂ then stored at -80°C until RNA extraction and RT-PCR was performed. Frozen leaf samples were ground under liquid N₂ to a fine powder using a pestle and mortar. Exactly 1 ml of homogenisation buffer that comprised of : 0.5 M Tris-HCl buffer pH 8, 0.3 M LiCl, 10 mM DTT, 10 mM EDTA, 5 mM Urea, 3% (v/v) Nonidet- P 40 ,2% (w/v) PEG 20, 000, 2% (v/v) CTAB (amounts are showed in table 4.3) was placed in an RNase free centrifuge tube and heated to 65°C, then 0.3 g of ground plant tissue and 200 µl 2-mercaptoethanol were added and heated for 10 minutes. The sample was left at room temperature for 10 minutes, and was vortexed frequently to homogenise. The sample was then centrifuged at 15,700 g (13,000 rpm) at 4°C

for 10 min. Exactly 1 ml Tri-reagent (Helena Biosciences) was placed in an autoclaved micro-centrifuge tube, 700 µl supernatant was added and the mixture was left in the fume hood at RT for 10 min. The mixture was centrifuged at 15,700 g at 4°C for 10 min, the supernatant was removed and placed in a clean tube with 250 µl chloroform. The mixture was vortexed and left on ice for 5 min. The sample was then centrifuged at 15,700 g at 4°C for 10 min and 600 µl of the upper phase was transferred to a clean centrifuge tube. On ice, 250 µl precipitation solution containing: 1.20 M sodium chloride, 0.8 M sodium citrate in a total volume of 100 ml of DEPC H₂O and 250 µl isopropanol were added and the mixture was incubated at -20°C overnight to re-precipitate the RNA. Next day, the mixture was centrifuged at 15,700 g at 4 °C for 45 min and supernatant was removed. The remaining pellet was washed with 1 ml ice cold 70% ethanol and vortexed, and then centrifuged at 15,700 g at 4°C for 5 min. The supernatant was removed, followed by the ethanol and the centrifugation step was repeated. The remaining pellet was air dried in a fume hood for 1-2 min. On ice, RNA was re-suspended in 15 µl Tris (10 mM) + EDTA (1 mM), then heated for 15 min and vortexed before being left on ice for 1 hour. Finally, the sample was treated with 0.5 µl DNase and 1µl buffer per 10µl sample (here 0.75µl+1.5 µl), incubated for 15 minutes at room temperature and then the reaction was stopped with 1 µl 25 mM EDTA per 10 µl (here 1.5 µl). The sample was then heated to 65°C for 10 minutes. RNA concentrations were estimated using a spectrophotometer (Nanodrop ND1000, LabTech). In addition to concentration, A260/A280 was recorded to give an indication of RNA purity. Values of A260/A280 between 1.8-2.1 indicate highly pure RNA with very low levels of protein contamination (Glasel and Agarwal, 1995). Aliquots were stored at -80 °C.

Table 4.3 Amount of reagents comprising the homogenization buffer used for RNA extraction.

Reagent	Amount
TRIS-HCl	6.057 g
LiCl	2.119 g
DTT	1 ml
EDTA	0.3724 g
Urea	0.03 g
Nonidet-P40	3 g
PEG 20.000	2 g
CTAB	2 g
DEPC H ₂ O	100 ml

4.2.5 Sequencing of photoreceptors

Products from DNA amplification for all genes *cry2*, *pho1*, *pho2* and *phyA*, from both species, were sent to be sequenced by Genevision (<http://www.genevision.co.uk>) using Applied Biosystems BigDye® cycle chemistry. Analyses were performed on ABI 3730xl capillary sequencers. Exactly 10 µl of sample 3ng/ µl and 5 µl of a forward primer for each gene at 3.2 pmol/µl were used in all cases. A blast search was performed to verify the identity of the products (Table 4.5).

A clone was used to amplify phototropin 1 after difficulties in its identification using direct PCR products. The protocol used for this cloning consisted of: first, 0.2 µl of Taq DNA polymerase was added to PCR products and incubated at 72 °C for 10 min. Exactly 2 µl of this reaction, 3 µl of cloning buffer and 1 µl of vector were mixed and incubated at room temperature for 15 min. Exactly 2 µl of this reaction were added to a tube of *Escherichia coli* cells to amplify the DNA fragment. The *E. coli* cells were incubated in 3 ml of LB (2 g/100 ml diH₂O) and 3 µl of Kanamycin (50mg/ml) at 37°C and 200 rpm shaking overnight. The colonies were grown in 1.5% Agar in LB media and 20 µl of 2% Xgal in N-N Dimethylformamide, at 37°C during the night. The next day, white colonies were selected for plasmid extraction.

Plasmid extraction from culture was conducted as follows: 1.5 ml from culture were taken and centrifuged at 9,291 g (10,000 rpm) for 5 min. The supernatant was discarded and 250 µl of buffer P1 (Table 4.4) was added to the pellet and mixed with a pipette. Exactly 250 µl of buffer P2 (Table 4.4) was added and mixed by inverting 45 times; the reactions were incubated at room temperature for exactly 5 min. Then, 350 µl of buffer N3 (Table 4.4) was added and mixed by inverting, and resulting white mixture was then centrifuged at 15,700g for 10 min. The supernatant was transferred to an eppendorf tube with a filter and centrifuged at 15,700g for 1 min. The liquid at the bottom was removed and the filter washed with 700 µl of PE (Table 4.4). This mixture was centrifuged at 15,700g for 1 min and liquid at bottom removed. With the filter back in place this was centrifuged again at 13,000 for 1 min. The filter was transferred to a new 1.5 ml eppendorf and 50 µl of EB buffer (Table 4.4) was added at the top of the filter, this was incubated at room temperature for 1 min. The mixture was centrifuged at 15,700g for 2 min. The filter was discarded and the DNA at the bottom kept at -20 °C.

Table 4.4. Composition of the buffers comprising the kit QIAGEN® Plasmid Purification used for the plasmid extraction.

Buffer	Composition
Buffer P1 (resuspension buffer)	50 mM Tris·Cl, pH 8.0; 10 mM EDTA; 100 µg/ml RNase A
Buffer P2 (lysis buffer)	200 mM NaOH, 1% SDS (w/v)
Buffer N3 (neutralization buffer)	3.0 M potassium acetate, 15–25°C pH 5.5
Buffer PE (wash buffer)	1.0 M NaCl; 50 mM MOPS, pH 7.0; 15% isopropanol (v/v)
Buffer EB (elution buffer)	1.25 M NaCl; 50 mM Tris·Cl, pH 8.5; 15% isopropanol (v/v)

4.2.6 Reverse Transcriptase Polymerase Chain Reaction (RT-PCR)

Polymerase chain reaction (<http://pathmicro.med.sc.edu/pcr/realtime-home.htm>) is a widely used method that permits exponential amplification of DNA sequences (usually between 100 to 600 bases) from double stranded DNA. To amplify a pre-determined DNA fragment, a pair of primers of about 20 nucleotides each, need to be used. The primer sequence is complementary to one portion of the target fragment and is extended by DNA polymerase to make the copy of interest. This process of copying occurs several times in an exponential curve. Every time, before the next copy is made, the double stranded DNA must be separated. This is achieved by increasing the temperature without causing any damage to the DNA polymerase (Taq polymerase), due to its thermo-stability. After approximately 40 cycles of amplification, the product can be visualized in an agarose gel stained with ethidium bromide, a dye that binds the double stranded DNA intercalating between base pairs, irradiating UV fluorescence (<http://pathmicro.med.sc.edu/pcr/realtime-home.htm>).

Starting with an RNA molecule instead of DNA requires an extra step to the PCR methodology described above in order to do a reverse transcription from mRNA to complementary DNA (cDNA). Reverse Transcript PCR was used to amplify each gene using this protocol:

1. Reverse transcription at 50 °C for 30 min,
2. Separation at 94 °C for 2 min and
3. at 94 °C 30 sec more,
4. Annealing at 55 °C for 30 sec,
5. Extension at 72°C for 45 sec, then
6. Go to step 2, 30 times for all genes except for *PhyA* (25 cycles).
7. Finally an extension at 72°C for 5 min then samples were held at 4°C.

The RT-PCR reaction occurred in a master mix containing: 10 x reaction buffer (2.5 µl), 0.1 M DTT (2.5 µl), 2.5mM dNTP (2.5 µl), 50 mM MgCl₂ (1.25 µl), SuperScript (0.3 µl), RNase (0.15 µl), Taq DNA Polymerase (0.1 µl), Primers (1µl each), between 0.5 - 2 µl (depending on initial concentration) of RNA to get a final concentration of to 100 ng/µl for all four photoreceptors and elongation factor alpha made up to a final volume of 25 µl with DEPC H₂O.

Agarose Gels (1.5 %) were run at 100 V for 60 min to identify the products. A 6X orange Dye and 1000 bp lower range ladder were used to detect and determine product sizes. In addition, PCR products were sequenced to prove the identity of each gene in each plant species. To prevent bias in the interpretation of results from PCR an internal control gene is needed. A suitable control gene is one that remains unaffected (in terms of transcript abundance) by experimental conditions and any other external treatments so that the gene can be used for normalization of the expression patterns of the other genes (photoreceptors) being evaluated. Usually, constitutive genes required for the maintenance of basic cellular functions are chosen as PCR controls and are known as “housekeeping genes” (Nicot et al., 2005) Within the most common and more robust housekeeping genes in plants (Nicot et al 2005) is the Elongation factor alpha (*efa*) (Sturzenbaum and Kille, 2001; Dean et al., 2002), a protein transcription factor responsible for the delivery of aminoacyl tRNA to the ribosome, and nuclear exportation of proteins <http://www.ncbi.nlm.nih.gov/sites/entrez?Db=gene&Cmd=ShowDetailView&TermToSearch=1915>. Based on NCBI data bases for *A. thaliana* and the EST database for *Clusia* (Shorrock 2009) *ef α* was chosen as the control for PCR experiments.

An approximated quantification of RT-PCR products was made, based on the intensity of the band in the agarose gel. For this purpose, the software Quantity one[®] (Bio-Rad) was used and a quantitative value was given to each band. Plots of the relative abundance of the cDNA products at different times of the day and under different light regimes were made for comparative purposes (results none showed). Most of the results were concordant with the gels, but some did not reflect the real expression shown in the gels, due to inaccuracies of the software in estimating the intensity of the band

(i.e.: for Elongation factor which showed a very similar expression during the diel cycle in the gels, the plots looked as if the expression was different under dark/light, constant blue light and constant darkness) probably due to the quality of the pictures used in Quantity one[®] or due to errors in the quantification of the bands. Thus, although this tool allows an easier comparative representation of transcript abundance patterns, it was not very accurate and for this reason the graphs are not presented here.

4.2.7 Real time PCR

Even although PCR is the most sensitive method for monitoring changes in transcript abundance (in comparison to e.g. Northern blotting) and can differentiate between closely related mRNAs, with conventional PCR it is difficult to quantify the results (as described above). Thus, Real Time PCR was used, a method that is based on the same principles of PCR as described above, but independent of the number of cycles. Real time PCR uses SYBR green, a dye more fluorescent than ethidium bromide, that binds to double stranded DNA but not to single-stranded DNA. In addition, the ratio of fluorescence of SYBR green of a double strand to a single strand of DNA is much higher than the ratio for ethidium bromide <http://pathmicro.med.sc.edu/pcr/realtime-home.htm>. To quantify the amount of cDNA a threshold must be established in a plot of the number of cycles against relative fluorescence during the linear phase of the exponential amplification when the fluorescence starts to increase. From here, the machine calculates the Ct, which is the cycle when the fluorescence curve crosses a threshold (usually referred to as the time at which fluorescence intensity is greater than background fluorescence (Wong and Medrano, 2005) and this increases with a decreasing amount of template (Figure 4.1).

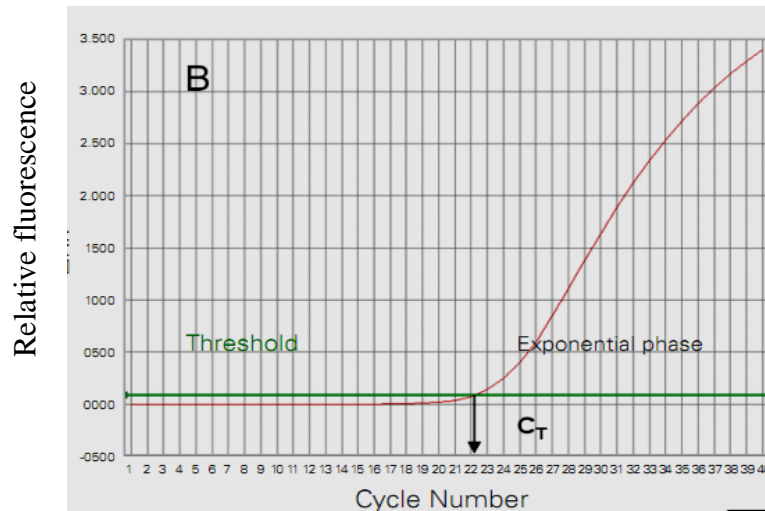


Figure 4.1. Setting the threshold (C_T) in a real time PCR reaction, which is based on the number of cycles (y-axis) when the fluorescence (x-axis) starts to increase and crosses the curve just before the exponential phase of fluorescence. Modified from (Biosystems, 2008).

To quantify the relative amount of mRNA from each gene with respect to a housekeeping control (in this case Elongation factor α), 5 series of 10 fold dilutions (100, 10, 1, 0.1, 0.01 ng/ μ l of RNA) were made for each gene (including the housekeeping gene) and a calibration curve was plotted (this curve must have a good negative correlation coefficient, Figure 4.1). The slope of the curve (3 replicates) was calculated and the amount of mRNA in relation to the control was estimated as follows:

1. $\Delta C_T = (\text{lowest } C_T - \text{highest } C_T) * -1$
2. Efficiency (E) = $10^{(-1/\text{slope})}$
3. Fold = $E^{(\Delta C_T)}$
4. True fold = Fold / Fold (control)

The true fold is an indication of the difference in expression of each sample (i.e. photoreceptor transcript abundance at different times of the day) normalized by the control. As mentioned before, the amplification of the double strand of DNA occurs in exponential way, samples with a difference in the concentration of cDNA (from mRNA) by a factor of 2 should be 1 cycle apart. Then in the case of the calibration curve, samples ten times more concentrated should be about 3.3 cycles apart from each other (<http://pathmicro.med.sc.edu/pcr/realtime-home.htm>).

Another important factor to take into account when dealing with real-time PCR is the certainty of product's purity. To know this the Opticon real time PCR machine determines a melting point of the product at the end of the cycles. This melting temperature of a DNA double helix depends on its base composition and length and it is expected that all products from a particular set of primers show the same melting point, otherwise errors from contamination, mis-priming or primer-dimer artefacts are occurring in the reaction (<http://pathmicro.med.sc.edu/pcr/realtime-home.htm>).

Real time PCR was performed using a commercial master mix, i.e. Brilliant[®] II SYBR[®] Green QRT-PCR Low ROX Master Mix, 1-step from Stratagene. This was applied to all the four photoreceptors and the housekeeping gene for RNA samples extracted at different times of the day and under different light regimes. The same primers as described above were used and good amplification was obtained for *phot1*, *phy A* and Elongation factor α . For the other two genes (*phot 2* and *cry2*), an unexpected calibration curve was observed. A matrix with different concentrations of forward and reverse primers was tested to see if results could be improved but without success. To get better results a new set of primers needed to be designed, but time constraints prevented this within the scope of this thesis.

4.2.8 Titratable acidity

Measurements of leaf titratable acidity were made using leaf tissue from samples taken at five different times of the day (6:00, 10:00, 14:00, 19:00, 23:00) under constant white light ($250 \mu\text{mol m}^{-2}\text{s}^{-1}$), constant dark, constant red light ($15 \mu\text{mol/m}^2\text{s}$), constant blue light ($15 \mu\text{mol m}^{-2}\text{s}^{-1}$) or constant far red light ($18 \mu\text{mol m}^{-2}\text{s}^{-1}$). About 200 mg of frozen leaf tissue (weight recorded using a Sartorius balance) was ground in liquid nitrogen using a pestle and mortar. Tissue was heated in 5ml 80% methanol at 80°C for 40 minutes. Exactly 1ml extract was then diluted with 2ml of distilled water and titrated against 0.005M NaOH to neutrality, using 3 drops of phenolphthalein as an indicator.

Number of moles (Z) H^+ in 5ml extract was calculated using the following equations:

$$Z (\text{moles H}^+) = \text{NaOH titre} \times 0.005/1000 \times 5$$

$$Z/\text{fwt} = \text{moles H}^+ \text{ g}^{-1}\text{fwt}$$

4.3 Results

4.3.1 DNA sequences of photoreceptors

Once the primers were designed and the PCR for each photoreceptor was done, cDNA resulting from the reaction was sent to be sequenced in order to prove the identity of the product. Each sequence was compared against a BLAST search in Arabidopsis and the identities of all products were confirmed.

Table 4.5. DNA sequences obtained using a pair of primers designed based on EST data base for *Clusia*, for four genes encoding for *cry2*, *phot1*, *phot2*, *phyA*, for *C. rosea* and *C. multiflora* a search in blast results in a match > 85%.

Species	Gene	Sequence
<i>C. rosea</i>	<i>Cry2</i>	CGCCTCTTACTGTTCTTAAAGCTGCTGGAGTGGACTTGGGCCAGAACTAAAG
	<i>Phot1</i>	CTTGAGGCAAATCGAGGAGGTTTCGAGACACGTTTCATGGTCTTGTCTTGTGTTTGTAGAACATTTCGTTT TTGTAGTTCGGGATCAATGAGTTTGTCTTCAATTTCTGCTTCGCTTGGGAAAAGTGGAAACCTTAAGCTCA GGAGGATTTCGTGTAGCGGACTAGCGCCCAATTGATAA
	<i>Phot2</i>	AAAAGAAGTATCTCTTCAATTAAGATATATGGACCTCAAGAGAATTATTTAAGAAAAGTTTAAGCAACTG TCATGCTTAAATAATGATGGTAATTATCACCAAAAGAAAACCATCGACAATGGAGACAAAACAGAC
	<i>PhyA</i>	TAGCTGTCAGATAACAGGAAAATGTAAGATAGTAATCAATAAGACAGAAAGAAGGTGCTGTGTCCATG TGGGACATGGCTACCTACTATGTTGCCATTCTACTCAGGATGCAGGAACAAGCTACAATTCAGTTTACA TAAAATCTTAAAACCTGAGAAAATAACTGTCACTGTTGCTCATATAGGCATGCATTGCAAAAAGAAGTATAA ATCCAACCTTTCACGCACTAGACCCATAAGAAATGAATGTAGGGAGACCTGCACTTCTTCCATTAGTAA GTTCTGTTTTTCAATGGCGAGTTTTAACATACCCTTCAATGATGCTATCAAGATCTGAGTCAATCAAGAAC AGTTGGCGCTGGCACTGGGCACTAGTATGCAAACTGTGAAAAGCAATGCAAAGGGATGAAAAGCAATG ATGAAAAGCAATGCAAAGGGATGAAAAGCAATGCAAAGGGATGAAAAGCAATGCAAAGGGATGAAAAGC AAGGGATGAAAAGCAATGCAAAGGGATGAAAAGCAATGCAAAGGGATGAAAAGCAATGCAAAGGGAT
<i>C. multiflora</i>	<i>Cry2</i>	CGCCTCTTACTGTTCTTAAAGCTGCTGGAGTGGACTTGGGCCAGAACTAATCT
	<i>Phot1</i>	GAAGGCAAATCGAGGAGGTTTTCGAGACACGATCATGGTCTTGTCTTGTGATTTAGAAGACATTTGTTG GTAGTTCGGGATCAATGAGTTTGTCTTCTTTCTGCTTCGCTTGGGAAAAGTGGAGCCTTAAGCTCAG CGTGTAGCGGACTAGCGCCCAATTGATAAAGGGCG
	<i>Phot2</i>	ACAAAAAGAAGTATCTCTTCAATTAAGATATATGGACCTCAAGAGAATTATTTAAGAAAAGTTTAAGCAA TCATGCTTAAATAATGATGGTAATTATCACCAAAAGAAAACCATCGACAATGGAGACAAA
	<i>PhyA</i>	TAGCTGTCAGATAACAGGAAAATGTAAGATAGTAATCAATAAGACAGAAAGAAGGTGCTGTGTCCATG TGGGACATGGCTACCTACTATGTTGCCATTCTACTCAGGATGCAGGAACAAGCTACAATTCAGTTTACA TAAAATCTTAAAACCTGAGAAAATAACTGTCACTGTTGCTCATATAGGCATGCATTGCAAAAAGAAGTATAA ATCCAACCTTTCACGCACTAGACCCATAAGAAATGAATGTAGGGAGACCTGCACTTCTTCCATTAGTAA GTTCTGTTTTTCAATGGCGAGTTTTAACATACCCTTCAATGATGCTATCAAGATCTGAGTCAATCAAGAAC AGTTGGCGCTGGCACTGGGCACTAGTATGCAAACTGTGAAAAGCAATGCAAAGGGATGAAAAGCAATG ATGAAAAGCAATGCAAAGGGATGAAAAGCAATGCAAAGGGATGAAAAGCAATGCAAAGGGATGAAAAGC AGGGATGAAAAGCAATGCAAAGGGATGAAAAGCAATGCAAAGGGATGAAAAGCAATGCAAAGGGAT

4.3.2 Gene expression

4.3.2.1 Phot1

Under a 24 h light/dark cycle, *phot1* presented the highest transcript abundance during the day for *C. rosea* (14:00) and *C. multiflora* (10:00; Fig. 4.2a). However, under constant white light this timing was changed to the end of the subjective day for *C. multiflora* and to the middle of the night for *C. rosea*. All other light treatments (red, far red, blue and darkness) resulted in a decrease in *phot1* transcripts in the CAM species to below the limits of detection. For the C3 species, blue light and constant darkness resulted in an increase in *photo1* transcripts which showed maximal abundance in subjective night (Fig. 4.2d,f).

4.3.2.2 Phot2

Under a 24 h light/dark cycle *phot2* transcript abundance was highest during the day for *C. rosea* but in the middle of the night for *C. multiflora* (Fig. 4.3.a). Under constant darkness *phot 2* transcripts were below the limit of detection for both species, except for *C. multiflora* where a band can be seeing at 23:00. *Phot 2* transcripts were below the limits of detection for both species under constant white, red or blue light but under far red the CAM species showed a clear pattern of transcript abundance being higher in subjective day compared to night (Fig. 4.3e).

4.3.2.3 Cry 2

Under a 24 h light/dark cycle, *cry2* presented higher transcript abundance at the end of the photoperiod/early night (19:00) for *C. rosea* but in the morning (at 10:00) for *C. multiflora* (Fig. 4.4 a). Under constant white light, the time of highest transcript abundance in *C. rosea* was similar to that under light/dark but in *C. multiflora* was delayed compared to that noted in light/dark (Fig. 4.4.b the end of photoperiod in *C. multiflora*). Under constant red or far red light (Fig 4.4c, e), timing of maximum transcript abundance was similar to that noted under light/dark in both species (i.e. late photoperiod in the CAM species, early photoperiod in C3). Blue light resulted in increased transcript abundance in *cry2* in the subjective night in both species (Fig. 4.4d). Under constant darkness, *cry2* showed enhanced

expression compared to that under light/dark in the C3 species (Fig. 4.4d) but could not be detected in the CAM species.

4.3.2.4 PhyA

Under a 24 h light/dark cycle, transcript abundance of *phyA* increased over the first part of the day, declined over the latter part of the day then started to increase in the dark in both species (Fig. 4.5a). This rhythm was maintained under constant far-red light in both species (Fig. 4.5 e). Red light resulted in an increase in transcript abundance in the CAM species but not in the C3 (Fig. 4.5c) whilst blue light and constant darkness stimulated *phyA* transcript abundance in the C3 (but not the CAM species).

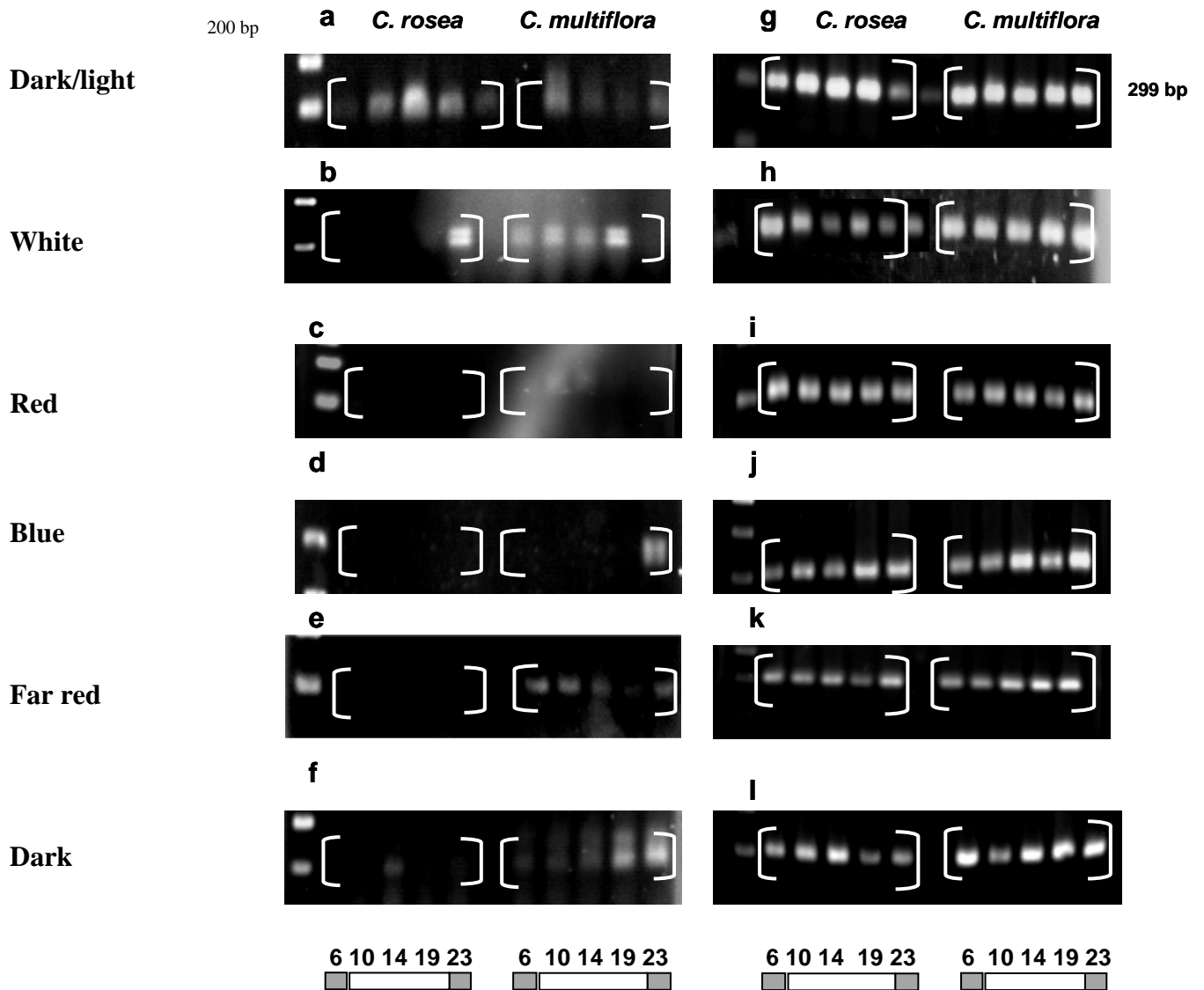


Figure 4.2. Electrophoresis gels showing transcript abundance of Phototropin 1 (product size = 184 bp) (a-f) at five different times (6am, 10am, 14pm, 19pm, 23pm) bars under figures represent subjective night in grey and subjective day in white for *C. rosea* (left) and *C. multiflora* (right) of a 24 h cycle (times shown at the bottom), under different light treatments: **a.** 12 h dark/light, **b.** constant white light $250 \mu\text{mol m}^{-2}\text{s}^{-1}$, **c.** constant red light $15 \mu\text{mol m}^{-2}\text{s}^{-1}$, **d.** constant blue light $15 \mu\text{mol m}^{-2}\text{s}^{-1}$, **e.** constant far red $18 \mu\text{mol m}^{-2}\text{s}^{-1}$ light and **f.** constant dark. On the right hand side of all gels, the PCR control Elongation factor α is shown under the corresponding light treatments (g-l).

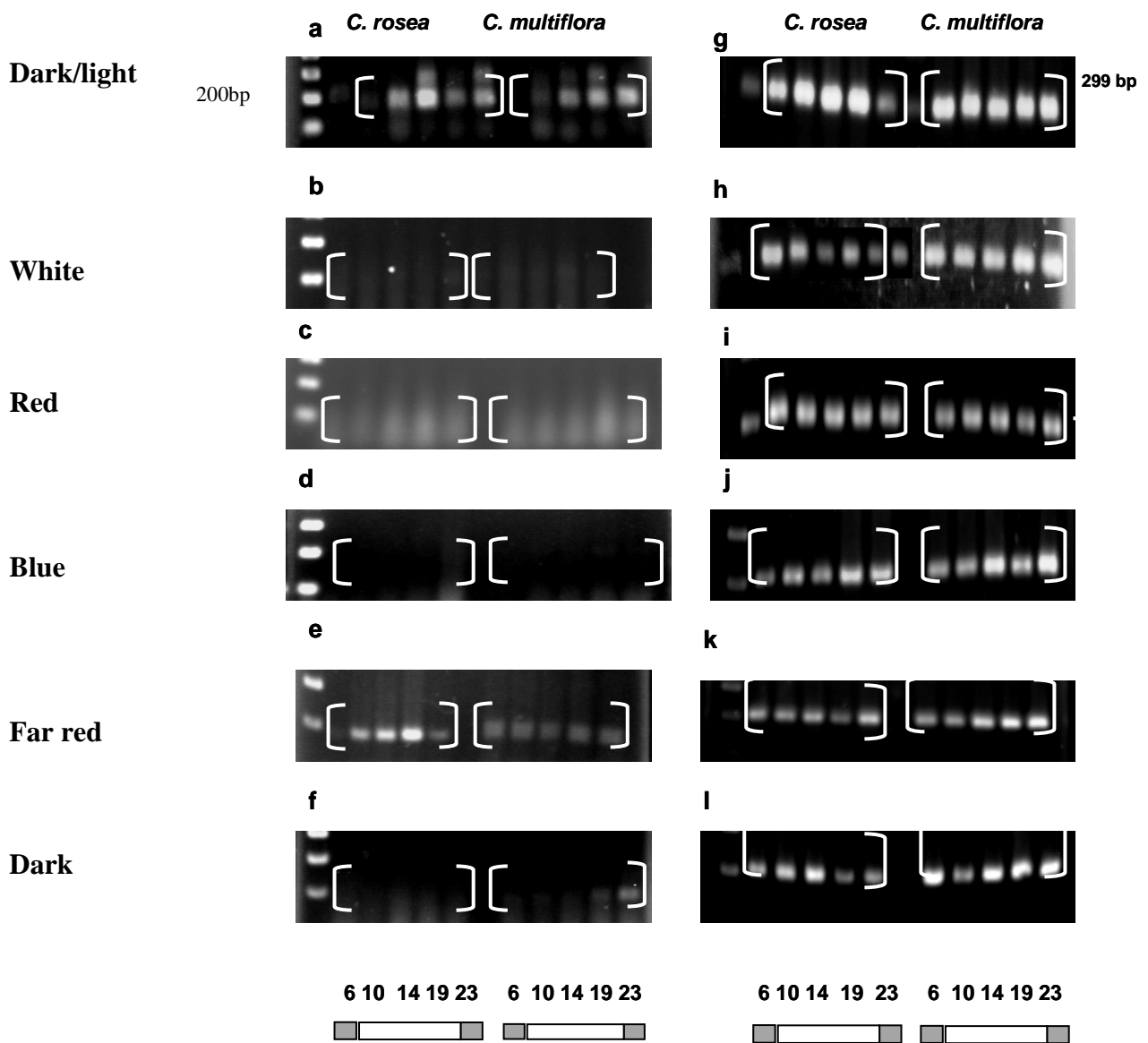


Figure 4.3. Electrophoresis gels showing transcript abundance of Phototropin 2 (product size = 199 bp) (a-f) at five different times (6am, 10am, 14pm, 19pm, 23pm) bars under figures represent subjective night in grey and subjective day in white for *C. rosea* (left) and *C. multiflora* (right) of a 24 h cycle (times shown at the bottom), under different light treatments: **a.** 12 h dark/light, **b.** constant white light $250 \mu\text{mol m}^{-2}\text{s}^{-1}$, **c.** constant red light $15 \mu\text{mol m}^{-2}\text{s}^{-1}$, **d.** constant blue light $15 \mu\text{mol m}^{-2}\text{s}^{-1}$, **e.** constant far red $18 \mu\text{mol m}^{-2}\text{s}^{-1}$ light and **f.** constant dark. On the right hand side of all gels, the PCR control Elongation factor α is shown under the corresponding light treatments (g-l).

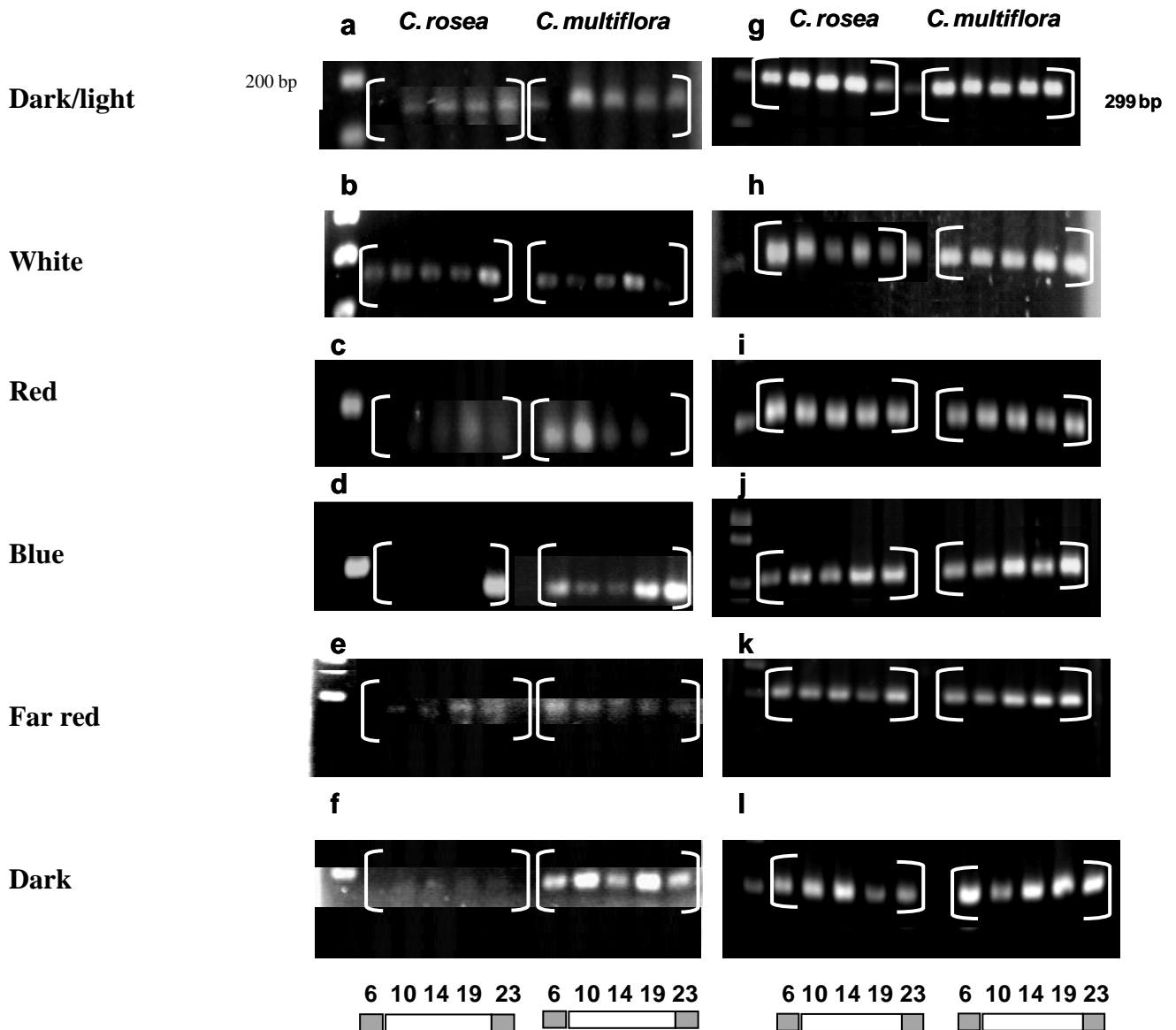


Figure 4.4 Electrophoresis gels showing transcript abundance of Cryptochrome 2 (product size = 155 bp) (a-f) at five different times (6am, 10am, 14pm, 19pm, 23pm) under figures represent subjective night in grey and subjective day in white for *C. rosea* (left) and *C. multiflora* (right) of a 24 h cycle (times shown at the bottom), under different light treatments: **a.** 12 h dark/light, **b.** constant white light $250 \mu\text{mol m}^{-2}\text{s}^{-1}$, **c.** constant red light $15 \mu\text{mol m}^{-2}\text{s}^{-1}$, **d.** constant blue light $15 \mu\text{mol m}^{-2}\text{s}^{-1}$, **e.** constant far red $18 \mu\text{mol m}^{-2}\text{s}^{-1}$ light and **f.** constant dark. On the right hand side of all gels, the PCR control Elongation factor α is shown under the corresponding light treatments (g-l).

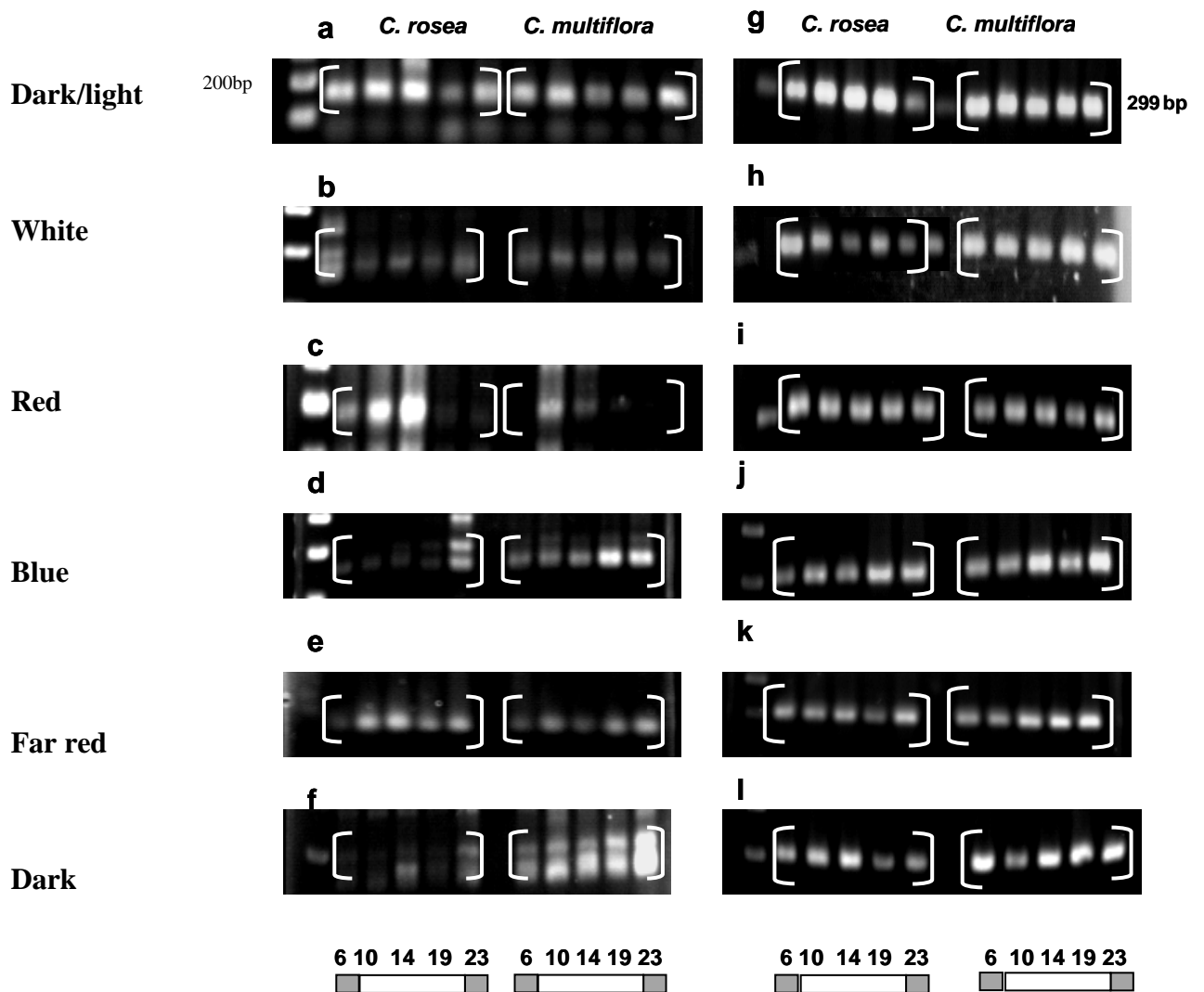


Figure 4.5. Electrophoresis gels showing transcript abundance of Phytochrome A (product size = 166bp) (a-f) at five different times (6am, 10am, 14pm, 19pm, 23pm) bars under figures represent subjective night in grey and subjective day in white for *C. rosea* (left) and *C. multiflora* (right) of a 24 h cycle (times shown at the bottom), under different light treatments: **a.** 12 h dark/light, **b.** constant white light $250 \mu\text{mol m}^{-2}\text{s}^{-1}$, **c.** constant red light $15 \mu\text{mol m}^{-2}\text{s}^{-1}$, **d.** constant blue light $15 \mu\text{mol m}^{-2}\text{s}^{-1}$, **e.** constant far red $18 \mu\text{mol m}^{-2}\text{s}^{-1}$ light and **f.** constant dark. On the right hand side of all gels, the PCR control Elongation factor α is shown under the corresponding light treatments (g-l).

Table 4.6 Time of the highest expression for four photoreceptors: Cryptochrome 2, Phototropin 1-2, Phytochrome A under different light regimes (12h dark/12h light, constant white 250 $\mu\text{mol m}^{-2}\text{s}^{-1}$, constant red and constant blue 15 $\mu\text{mol m}^{-2}\text{s}^{-1}$, constant far red 18 $\mu\text{mol m}^{-2}\text{s}^{-1}$, constant darkness) for *C. rosea* and *C. multiflora*. Highlighted in yellow is the subjective day and in grey the subjective night.

	Dark/light		White		Red		Blue		Far red		Dark	
	<i>C. rosea</i>	<i>C. multiflora</i>										
Cry 2	19	10	23	19	19	10	23	23	19	6	14	19
Pho 1	14	10	23	19	-	10	-	23	-	19	14	23
Pho 2	14	23	-	-	23	19	-	-	19	6	14	23
Phy A	14	23	6	10	14	6	23	19	14	23	14	23

4.3.4 Real time PCR

In order to quantify in a more precise way the transcript abundance for all the four genes in *C. rosea* and *C. multiflora* under a 24 h dark/light cycle and the different constant light regimes, Real Time PCR was adopted. However, it proved to be extremely difficult to optimize the method for all the genes and just two of the photoreceptors (*pho1* and *phyA*) and the housekeeping (Elongation factor α) gave good and reproducible amplification under dark/light conditions. Calibration curves were performed to test the primer efficiency for the genes and are presented below. A high negative correlation between mRNA concentration and C_T was expected, nevertheless just three of the genes showed the expected pattern.

Differences in the amount of mRNA at different times of the day under a 24 h dark/light cycle and corrected by the control elongation factor alpha α (where the level, represented by C_T , was equal for all the times, Fig 4.7c) were estimated for *phot1* and *phyA*. *Phot1* presented a higher transcript abundance during the day for both species but peaks in transcript abundance appeared earlier in the C3 species (as also found in the PCR gels (see Fig 4.2a). *Phot1* transcripts were more abundant in *C. rosea* compared to *C. multiflora*. Phytochrome A presented the highest transcript abundance during the night in both species with levels of transcripts considerably higher in *C. rosea* compared with *C. multiflora*.

In order to test the primers and define if it was a limitation of the reaction due to this, a matrix of concentrations for reverse and forward primers (0.04 μM , 0.08 μM , 0.24 μM , 0.4 μM) were used, however different set of primers concentrations did not improve (lower C_t) the reactions and the best combination of concentrations was the one used before (0.2 μM). Thus it was concluded that concentration was not the issue but primer length or GC content; could be important. To test this, a new set of primers needed to be designed and all the reactions performed again. However, due to time constraints these modifications weren't done and checked. For *phot1* and *phyA*, calibration curves gave slopes near to -3.33 (-3.07, E=111% and -1.89, E= 238% respectively) and a negative relationship ($R^2=0.530$ and $R^2=0.569$ respectively) and for housekeeping, Elongation factor α ($R^2= 0.66$, E= 81%). Such a high efficiency >100% for *phot1* and *phyA* and low efficiency < 100% for *ef α* could be due to inaccuracies in the serial sample dilutions of the standards resulting from a consistent excess or shortage of sample when pipeting (Applied Bio systems), differences in C_T between samples 10 fold dilutions apart were lower than 3.33 (i.e.: ΔC_T in *phot1* = 2.64) or higher than 3.33 (i.e.: ΔC_T in *ef α* = 4.26). These results revealed that the efficiency of the reaction is not as high as is required for accurate quantification of mRNA, but it can give us an idea of the differences in the transcript abundance with the samples at different times of the day relative to the control.

There are some other possible reasons why real time PCR did not work well for all genes (<http://www.appliedbiosystems.com/absite/us/en/home/support/tutorials/realtime-pcr-trouble-shooting-guide.html>): RNA may have contained inhibitory compounds such as an excess of protein, chlorophylls, contaminants as phenol (which is the case of some *Clusia* plants, Shorrocks, 2009). High acidity was thought to be a potential problem for extracting good quality RNA from *Clusia* but checking pH of extractions revealed it to be 7.5. The quantity and quality of RNA were analyzed using a Nanodrop to try and avoid contamination and inhibition during the PCR. Values for the ratio A_{260}/A_{280} were between 1.8 and 2 in most of the cases, indicating good quality samples. However, it has been suggested that the NanoDrop can give overstated values if the sample is contaminated with phenol or ethanol. Using a bioanalyzer could be helpful to confirm the quality of the sample and verify or discard an inhibitory problem. In the first case, a purification of the RNA would need to be done, testing a different RNA extraction protocol. Time constraints prevented this approach.

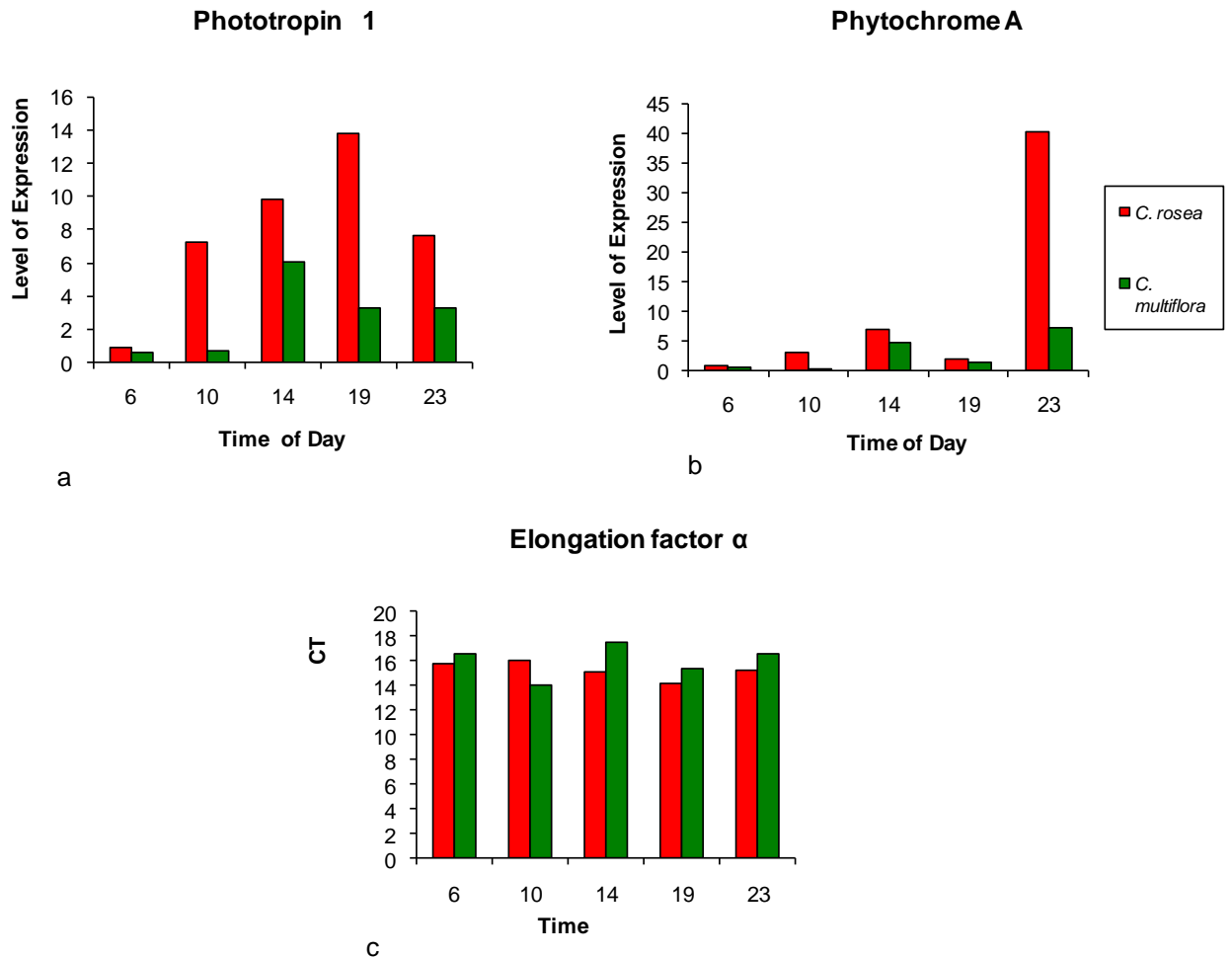


Figure 4.6. Relative change in the transcript abundance of Phototropin 1 (a) and Phytochrome A (b), at different times of the day under a regular dark/light cycle and corrected by the control Elongation factor α where similar C_T were present for all the samples in both species (c) in *C. rosea* (Gehrig et al., 1998) and *C. multiflora* (Poffenroth et al., 1992), using Real Time PCR.

4.3.5 Titratable acidity

Measurements of leaf titratable acidity under different light regimes were taken to examine if and how the contrasting light regimes impacted on the CAM cycle. Under the dark/light regime, *C. rosea* showed a typical CAM acid fluctuation, having a high acid content in the morning and low in the afternoon (Figure 4.8 a). The CAM fluctuation in titratable acids was preserved under constant white light ($250 \mu\text{mol m}^{-2}\text{s}^{-1}$, Fig. 4.8 b). However, under constant dark the acid fluctuation pattern was reversed, presenting a higher acid content at mid day in *C. rosea* (Figure 4.8 d). Under constant blue light ($15 \mu\text{mol m}^{-2}\text{s}^{-1}$) the amount of acids was high during the whole 24 h cycle (Figure 4.8 e). Under

constant red and far-red light regimes ($18 \mu\text{mol m}^{-2}\text{s}^{-1}$), acid levels showed a slight dip in the middle of the day (Figure 4.8 c, f). The C3 species *C. multiflora* presented a light/dark pattern of titratable acid fluctuations opposite to that of *C. rosea*, being low in the morning and showing a peak at the end of the day (19:00; Figure 4.8 a). This pattern was also observed under constant white light and, but to a lesser extent, under constant red light. Under constant darkness (Figure 4.8 d), constant blue light (Figure 4.8 e) and constant far red light (Figure 4.8 f) the levels of acids in the C3 species were low and did not show any appreciable fluctuation. Yellow and brown spots were noted in leaves of *C. rosea* under constant blue and constant far red light, and under constant darkness, whole leaves of *C. rosea* turned yellow, indicating possible loss of chlorophyll (figure 4.7).

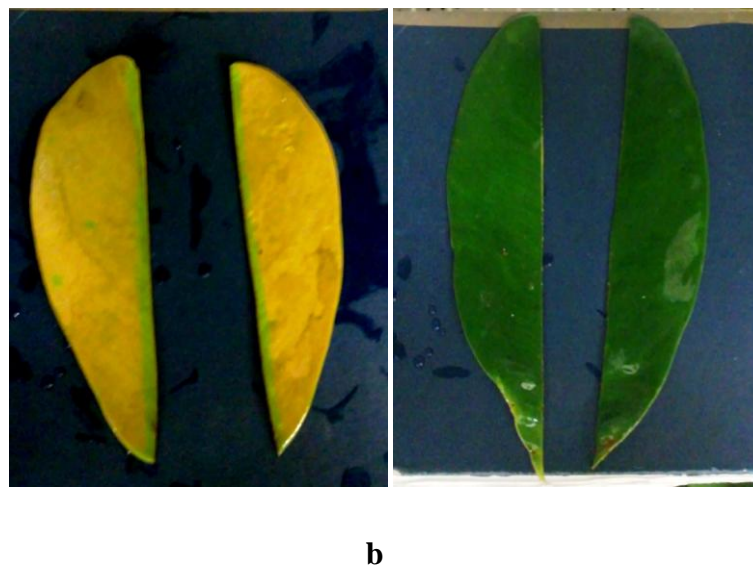


Figure 4.7. Leaves of *C. rosea* a. and *C. multiflora* b. after 48 h in constant darkness. The image shows how almost the whole leaf of *C. rosea* has a yellow colour compared with leaves of *C. multiflora*, possibly due to the accumulation of acids in the CAM plant. Constant darkness resulted in high background acid levels in *C. rosea* (see Fig 4.15). Brown spots were also observed on leaves of the CAM species under constant blue and far red light, where the background acids content was also higher than under light/dark or constant white light.

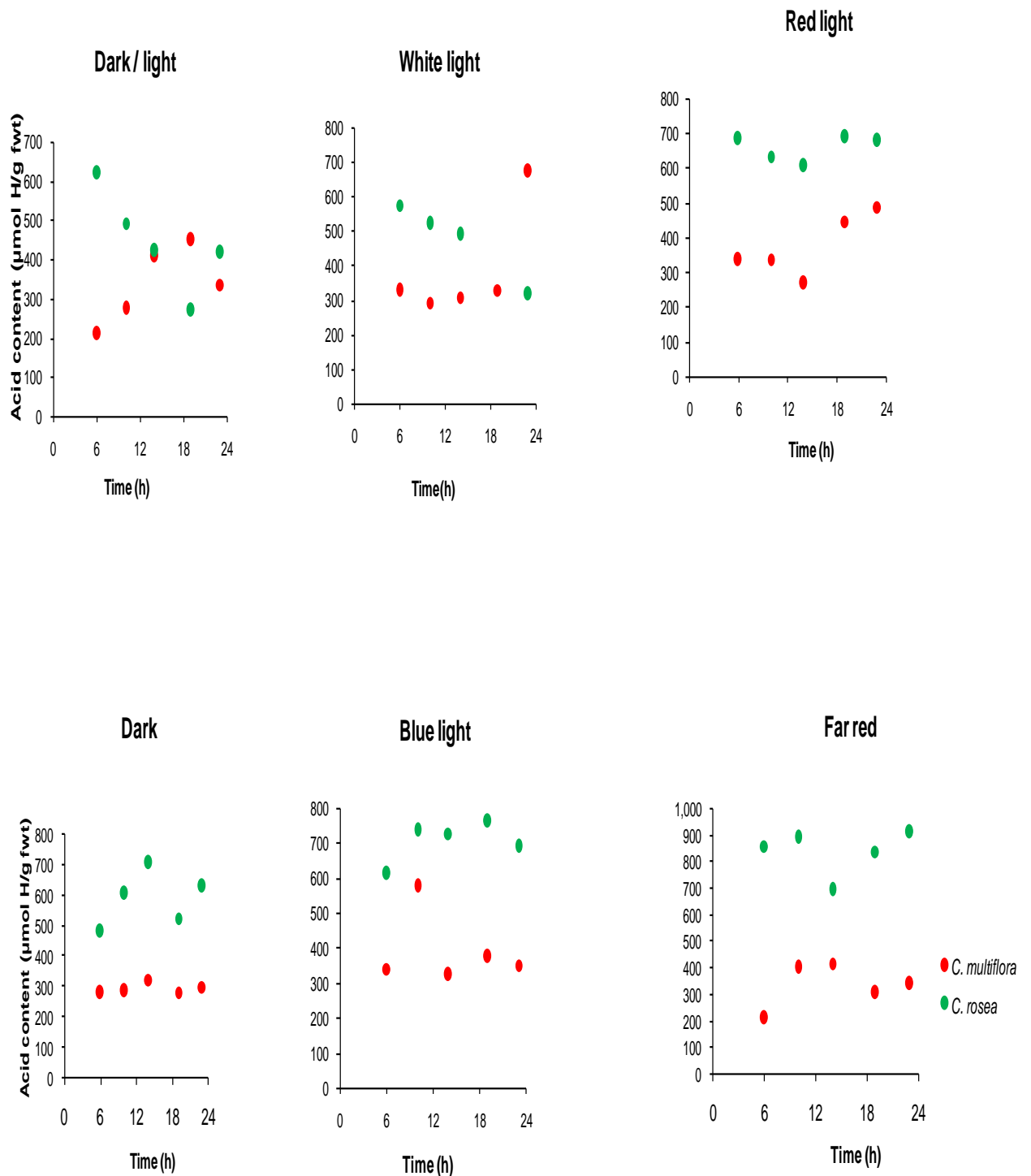


Figure 4.8. Titratable acid content ($\mu\text{moles H}^+/\text{g fwt}$) for *C. multiflora* (red circles) and *C. rosea* (green circles) at five points over 24 hours cycles under dark/light (a), constant white light $250 \mu\text{mol m}^{-2}\text{s}^{-1}$ (b), constant red light $15 \mu\text{mol m}^{-2}\text{s}^{-1}$ (c), constant dark (d), constant blue light $15 \mu\text{mol m}^{-2}\text{s}^{-1}$ (e), and constant far red $18 \mu\text{mol m}^{-2}\text{s}^{-1}$ (f).

4.4 Discussion

4.4.1 Transcript abundance of *phot1* and *phot2*

Phototropins have been implicated in mediating the blue-light opening response of stomata in *Arabidopsis* (Briggs and Christie, 2002; Christie, 2007). A study with *Arabidopsis* proved that the Ser-851 is the site of autophosphorylation for phototropins under blue light and this is the primary step to signalling several physiological events that include stomatal opening. The reported lack of a blue-light response in CAM stomata suggested that CAM and C3 species of *Clusia* would exhibit differences in: a) transcript abundance of *phot1* and *phot2*, b) the level of control exerted by the circadian clock over *phot1* and *phot2* transcripts and c) the response of *phot1* and *phot2* to different light treatments. The diel expression patterns of the phototropins were found to differ in all of these aspects between *C. rosea*, the CAM species and *C. multiflora* the C3 species, thus supporting hypothesis 1. Contrary to expectations, the relative abundance of both phototropins under the usual 24 h light/dark cycle appeared to be highest in the CAM species – this was confirmed for *phot1* using real-time PCR where transcript abundance was up to 10 fold higher in *C. rosea* compared to *C. multiflora* at times of peak expression. Transcript abundance of the phototropins varied under light/dark cycles but also under constant white light (*phot 1*), indicating a possible diel oscillation of this gene in *Clusia* species. This is in contrast to *Arabidopsis* where microarrays have not given any indication of circadian control of *phot1* or *phot2* (<http://www.arabidopsis.org>). Transcript abundance of *phot1* presented a peak during the day in both *Clusia* species whilst *phot2* had a peak in abundance during the day in *C. rosea* but during the night in *C. multiflora*.

Studies with *Arabidopsis* mutants have indicated that stomata of *phot1* or *phot2* mutants have a reduced blue light response and the double mutant *phot1 phot2* completely lacks the blue light response for stomatal opening (Kinoshita et al., 2001; Kasahara et al., 2004)). However, there are no published examples relating transcript abundance of *phot1* or *phot2* with the magnitude of stomatal opening, in *Arabidopsis* mutants although the protein abundance of cryptochrome has been related with the degree of stomatal aperture (Mao et al., 2005). Localization and abundance of phototropin determined by green fluorescence protein-fusions in leaves and in guard cells has been related to its importance in the blue light transduction signalling for leaf expansion and stomatal movements (Sakamoto and Briggs, 2002). It is interesting to note that the highest transcript abundances of *phot1* and *phot2* occurred in the middle of the photoperiod in the CAM *Clusia*, at the time when the stomata were shut. Under constant white light, *phot2* transcripts were not detected in the CAM *Clusia* and peak abundance of *phot1* shifted to the subjective night, but stomatal conductance under the same treatment did not follow the same pattern,

presenting a peak during the subjective morning (around 10:00 h; see Chapter 3) in *C. rosea*, In *C. multiflora* the maximal abundance of *phot1* was at the end of the subjective day (19:00 h), and again does not correspond with the timing of maximal stomatal conductance for the same treatment (peak at 14:00 h; see Chapter 3). That the timing of maximum transcript abundance of *phot1* or 2 did not correlate with the timing of maximal stomatal conductance in either *Clusia* species suggests the involvement of post-transcriptional regulation of phototropins that could include the involvement of an inhibitory signal or a negative feedback regulation in the transcription of the PHOT proteins (McClung 2000; (Millar and Kay, 1991).

Since phototropins serve as blue-light receptors for stomatal opening it was of interest to compare the impact of low fluency blue light on transcript abundance of these photoreceptors in the CAM and C3 *Clusias*. Several studies have demonstrated the increase in the abundance of phototropins (protein content) after blue light exposition (Sakai et al., 2001; Inoue et al., 2008). Blue light resulted in a decline of *phot1* transcript abundance in the CAM species whilst in the C3 species there was an increase in *phot1* transcripts. This observation is of interest in light of results from Chapter 3 which indicated a greater magnitude of response in stomatal conductance in the C3 compared to the CAM *Clusia* under low fluency blue light, suggesting divergent responses in the pathways linking phototropin transcription to blue light in the different photosynthetic modes.

There were differences in the 24 h patterns of expression between *phot1* and *phot2* and in the responses of *phot1* and *phot2* to the different light treatments, implying that there is not a redundancy in the function of these photoreceptors in *Clusia*. The highest transcript abundance of *phot2* during the night in the C3 *Clusia* under dark/light could be related with the sensitivity of *phot2* to low blue light (Sakai et al., 2001; Kagawa and Wada, 2002; Wada et al., 2003; Biggs et al 2005) and its importance in sensing these wavelengths of light early at dawn. There were also alterations in the transcript abundance of *phot1* and *phot2* under different light regimes which varied between the C3 and CAM species, again highlighting the possibility that transcriptional regulation of phototropins could be a key mechanism underpinning the divergent responses of stomata to light in C3 and CAM species.

In general, transcripts of *phot2* were reduced after the imposition of the various constant light regimes might be due to constant autophosphorylation of phototropins 1 and 2, which is reversible in darkness (Christie, 2007), and which could result in a down-regulation in transcription of the proteins. Similar results have been reported for *phot1* under constant blue light in *Arabidopsis* (Sakamoto and Briggs, 2002). It is known that transcription of some genes related to the photosynthetic apparatus is regulated by light, for example stability and turnover of thylakoid protein complexes is regulated by phosphorylation via redox-sensitive kinases in the thylakoid membranes. These mechanisms involve negative feedback at the level of translation level through binding of excess protein to the 5'

untranslated region of the chloroplast mRNA (Minai et al., 2006). Another example is the activity of the MBP kinase in tobacco cells which is regulated by post-translational phosphorylation of tyrosine residues (Susuki and Shinshi, 1995).

The response of *phot2* to far red light only in the CAM species was unexpected. As far as we know, there are no works reporting responses to red/far red light mediated by phototropins in higher plants. However, Kawai et al. (2003) reported an unconventional response to red light inducing phototropism and chloroplasts moving in the fern *Adiantum capillus-veneris*, which is mediated by chimaeric photoreceptor PHY3 that is sensitive to blue light and red/far red light. The authors suggested that this photoreceptor which exists among several ferns species had a central role in the divergence and proliferation of fern species under low light canopy conditions. The increase of transcript abundance of *phot2* at the end of the subjective day in *C. rosea* under far-red light is difficult to explain, and could be due to an experimental error which introduced a leak of blue or white light to a portion of one of the leaves used for the RNA extraction. However, it is important to consider the presence of other isoforms of known photoreceptors present in this CAM plants especially when the response to light might be different. Also, it is interesting to notice that the titratable acids oscillations under far red light for *C. rosea* were maintained and are very similar to those under constant red light and darkness. This pattern was different to those of the acids under constant white and constant blue light, making it more difficult to elucidate which photoreceptor is mediating the responses to different light regimes and supporting the idea that there is a coordinated division of labour among different photoreceptors to control processes like stomatal opening, CO₂ assimilation and acid turnover in CAM plants.

4.4.2 Transcript abundance of photoreceptors implicated in transducing light inputs to the circadian clock

Cryptochrome 2 is a photoreceptor sensitive to low and high intensity blue light and Phytochrome A is a photoreceptor sensitive to low intensity red light. The two photoreceptors belong to two families of photoreceptors implicated in the light signal transduction to the circadian clock in plants, giving information about the length of the photoperiod and thus allowing the plant to entrain physiology and biochemistry to the diel oscillation (Somers et al., 1998). Based on previous results (Chapter 3) where circadian oscillations of carbon assimilation and stomatal conductance were maintained for longer in *C. rosea* under constant light regimes, it was hypothesised that a stronger control of circadian expression of *cry2* and *phyA* transcripts would be observed in *C. rosea* than in *C. multiflora*. It was also

hypothesised that transcript abundance of *cry2* and *phyA* would be more responsive to changes in light quality *C. rosea* compared to *C. multiflora*.

The transcript abundances of both *phyA* and *cry2* varied over the light/dark cycle and under constant light, indicating circadian control of both photoreceptors in the C3 and CAM *Clusias*. Both *cry2* and *phyA* presented a peak of transcripts during the day under dark/light as was expected based on literature reports for C3 species, according with the second prediction of hypothesis 2. *C. rosea* showed peaks of expression during the day for both *cry2* and *phyA*, which were altered under constant white and constant blue light when the time of maximum expression was shifted to the subjective night. Maximal stomatal conductance under constant blue light for *C. rosea* was reached during the early morning (8:00-10:00, see Chapter 3), so it was predicted that the highest transcript abundance of *cry2* would precede the maximal stomatal conductance. Such a scenario would have suggested a peak in the transcript abundance at 6:00 for *C. rosea* and at 14:00 for *C. multiflora* however this was not observed, suggesting again, the involvement of more than one photoreceptor in stomatal movements and probably also more than one mechanism (photosynthesis, direct light responses and circadian control) for the control of stomatal opening. Under red, far red and darkness the pattern of transcript abundance was the same as during dark/light. Changes in the transcript abundances of both *cry2* and *phyA* were expected under low blue light since previous work (Somers et al 1998) reported the sensitivity of both *phyA* and *cry2* in *Arabidopsis* to low fluence blue light as a means of entrainment and to give signals to the clock.

For *cry2*, the C3 species *C. multiflora* presented peaks of transcript abundance during the day under the conventional light/dark cycle as well as under constant white light, red light and dark. However, this was shifted to the night under constant blue light. Previous reports on *Arabidopsis* have similarly shown that *cry2* transcripts peaked during the day under dark/light and showed a modified pattern of abundance under low blue light. Interestingly, *phyA*, expression was also modified under low blue light in the C3 *Clusia*, with timing of maximum abundance shifting to the end of photoperiod and continuing into the subjective night. Previous studies have indicated the possible interaction between *cry2* and *phyA* in higher plants and ferns in the response to low blue light specially controlling photomorphogenesis. However, it is not clear which is the role of phytochromes by itself or in conjunction with other photoreceptors mediating signals from blue light (Batschauer, 1996; Ahmad, 1997; Ahmad, 1998; Briggs and Huala, 1999). The down-regulation of *cry2* and *phyA* under constant white light and up-regulation under constant darkness in *C. rosea* and *C. multiflora* has been reported before in *Arabidopsis* (Thot et al 2001). Furthermore, several authors (Clark et al 1994, Ahmad and Cashmore 1993, Lin et al 1998) have reported no changes in the accumulation of mRNA of these photoreceptors caused by light; this discrepancy may be due to differences in experimental setups or to the responses of different plant species. *Cry2* responded to blue light in both C3 and CAM species. That this blue light

response has not been lost in the CAM species suggests the importance of *cry2* in controlling circadian processes.

Real time PCR indicated the presence of more (eight times more at 23:00h) transcripts for *phyA* in the CAM *Clusia* compared to the C3 species. Moreover, the CAM *Clusia* exhibited more robust oscillations in *phyA* transcripts under red and far red light as compared to the C3 species, with both peaking at around 14:00 in the CAM species. It is interesting to note that the CAM species exhibited more robust control of stomatal conductance under constant red light, compared to the C3 species. Thus, the way in which *phyA* is linked to the clock could be a point of divergence between the C3 and CAM *Clusias*.

In general, in terms of changes in the time of expression of *cry2* and *phyA* under constant light regimes, there were no notable differences between *C. rosea* and *C. multiflora*. Transcript abundance of both genes was altered under constant light regimes in both species. Even when in some cases this variation in transcript abundance seemed to be related to gas exchange patterns, is very likely that more genes are involved in the control of stomatal movements and responses to light (i.e.: *cry1*, *phyB*). Thus, hypothesis 3 was not supported, since the amplitude of the oscillations in the transcript abundances of *cry2* and *phyA* do not seem to be more responsive to light in *C. rosea* than in *C. multiflora*.

Finally, it is important to remember that the photoreceptors examined in this chapter were transcribed from RNA extracted from the whole leaf. RNA extracted exclusively from stomatal guard cells may have revealed C3 and CAM differences between photoreceptor expressions but this approach was beyond the scope of this thesis.

4.4.3 Quantification of photoreceptor abundance and responses to light using real time PCR

Real time PCR was intended to quantify the amount of mRNA of *cry2*, *phot1*, *phot2* and *phyA* at different times of the day under the contrasting light regimes for both species. However, reliable results were obtained just for two of the photoreceptors. Real time PCR is a precise method to quantify mRNA but it is not easy to optimize, due to the high sensitivity of the assay and the several steps that can introduce experimental error (Wong and Medrano 2005). There is also considerable probability of non-specific interactions and the primers designed need to be very specific. Given its sensitivity, real time PCR assays can detect gene expression differences as small as 23% between samples (Gentle et al., 2001). Despite the care taken with primer design (and primers were blasted against mRNA references

sequences), a single melting peak was not attained for two of the photoreceptors of this investigation (*cry2*, *phot2*) and the calibration curve also demonstrated that efficiency of the PCR was not high enough (*cry2* E = -99%, *phot2* E = -98%). Due to the fact that some genes were amplified better than others during real time PCR, that mRNA samples used were the same for all, that the dilutions were done at the same time and that three replicates were used in each case, failures of the reactions are probably a consequence of primer inefficiency rather than as a result of sample contamination or consistent errors in the serial dilutions of the standard curve.

Although real-time PCR was used with some confidence on *phot1*, *phyA* and the housekeeping elongation factor some discrepancies were found when compared with the gel images of the same genes. This may be attributed to low efficiency of the primers, or errors when the baseline is set during the early exponential phase of the real time reaction which can generate differences in the amplification efficiency and produce minor variations in Ct values (Giulietti et al., 2001). An overview of real-time quantitative PCR was given in terms of applications to quantify cytokine gene expression (Giulietti et al., 2001). For example, after 26 cycles a 5% variation in amplification efficiency can result in a 2-fold change of PCR product abundance (Freeman et al., 1999). In conclusion, despite several efforts to quantify differences in the transcript abundance of the four photoreceptors *cry2*, *phot1*, *phot2*, *phyA* under dark/light cycles in *C. rosea* and *C. multiflora*, it was not possible to perform good quality real time PCR reactions. A different set of primers needs to be designed to perform real time PCR.

4.4.4 CAM expression in detached leaves under contrasting light regimes

Monitoring the amount of titratable acids over a 24 h cycle is a useful indicator of CAM and illustrates how expression of the pathway was influenced in the detached leaves subjected to the various light regimes. The CAM species *C. rosea* presented a typical CAM pattern of acid fluctuation, with high levels of titratable acids detected early in the morning and low levels measured at the end of the day. Under constant white light, there was a peak of acid content at the subjective morning just before the acids started to be broken down. This pattern was similar but less pronounced to the pattern observed under dark/light and indicates circadian regulation of the CAM cycle under white light (see also Chapter 3). The fluctuation in acids was lost in all other light regimes in *C. rosea*. It is worth remembering that the blue, red and far red light treatments imposed in this chapter were of low fluence (i.e. $15 \mu\text{mol m}^{-2}\text{s}^{-1}$) and thus not comparable to the higher fluence light treatments imposed in Chapter 3. Under the low

fluence light treatments and constant darkness, the acid content was high during the whole 24 h cycle in *C. rosea*, some instances of the appearance of brown/necrotic patches were evident in the CAM (but not the C3) species. Similar findings have been reported for the CAM bromeliad, *Aechmea maya*, under low light intensities with the necrotic lesions attributed to cell death that resulted from over-acidification of the cytosol (Ceusters et al 2010). Modifications in the acid cycle in *C. rosea* under low levels of irradiance might be related to perturbation of the circadian control of PEPC kinase (Bohn et al 2001, Carte et al 1991) and/or to an inability to decarboxylate malic acid under low levels of light (Borland et al., 2000; Borland and Taybi, 2004; Lüttge, 2004). Moreover, maintaining leaves at a constant temperature of 24 °C (which is higher than the usual night-time temperature of 20°C given to *Clusia*) may have impacted on the transport of malate across the tonoplast (Betley and Smith 1993, Ratajczak et al 1994) and storage in the vacuole (Lüttge and Smith 1994, Kluge et al 1991). High concentrations of malic acid in the cytosol may have resulted in feed-back inhibition of PEPC in the cytoplasm (Kluge et al 1981, Nimmo et al 1984,1989), thereby changing the CAM rhythm and acid fluctuations.

The C3 species *C. multiflora* presented some fluctuations in acids under the different light treatments but the patterns were not consistent with CAM. Changes in acids could result from perturbations in other metabolic processes but further analysis of this phenomenon was outside the scope of this thesis.

(<http://www.appliedbiosystems.com/absite/us/en/home/support/tutorials/realtime-pcr-trouble-shooting-guide.html>)

Chapter 5: General Discussion

Several authors have indicated the close relationship between leaf anatomical characteristics (i.e. succulence) and the ability to perform CAM photosynthesis. The CAM requirement for large vacuoles contributes to lower air airspace in the mesophyll, and in addition, previous studies have indicated that in general more succulent species show lower stomatal density than less succulent species (Sayed, 1998; Lüttge et al., 2007). Based on those observations, the aim of this thesis was to investigate the possible advantages and constraints imposed by leaf anatomical traits, including stomatal anatomy and density, in the performance of CAM photosynthesis. The genus *Clusia* was the subject of study since it has a remarkable photosynthetic plasticity, with species performing obligate C₃, C₃/CAM intermediary and obligate CAM photosynthesis (Brulfert et al., 1975; Lüttge, 2006) and is thus an excellent model to study the evolution of CAM..

5.1. Leaf anatomical traits are related to the magnitude of CAM in *Clusia*

In general, close relationships were found between the magnitude of CAM photosynthesis in eight species of *Clusia* and six anatomical traits (stomatal size, stomatal density, IAS, % Lmes/area, cell size, SLA) at leaf level. The data collected for *Clusia* were generally in agreement with those presented by Nelson and Sage (2008) who considered a much broader taxonomic range of CAM species (i.e. across 14 plant families). Within the eight species of *Clusia*, a negative relationship between the degree of CAM and IAS (internal air space), % Lmes/area (length of mesophyll surface exposed to air) and SLA (specific leaf area) was found. Given this result, it was hypothesized that the presence of PEPC protein would be more abundant in the spongy mesophyll due to its proximity with the sub-stomatal cavities, thus serving to optimize uptake of CO₂. However, PEPC was found in higher density in the palisade mesophyll cells as was Rubisco. The increased availability of light in the palisade mesophyll would help to optimise the energetic of CO₂ uptake via Rubisco, a feature that could be important in counteracting the high energetic cost of CAM. However, the localisation of most PEPC in the palisade mesophyll cells also implies a more protracted route for CO₂

to travel from the sub-stomatal cavities to the site of maximal PEPC activity. Carbonic anhydrase (CA) is also necessary to convert CO₂ and water to bicarbonate before it can be made available for PEPC. It would be of future interest to localize and estimate the amount of CA in the mesophyll of closely related C3 and CAM species. Co-localization of both carboxylation enzymes in the palisade mesophyll could signify a strategy to improve decarboxylation efficiency during the day, allowing direct transfer of CO₂ from acid breakdown to Rubisco, within the same cell, offsetting diffusion limitations of CO₂ across the leaf.

The lower intercellular air space in the mesophyll of the CAM *Clusia* leaves was due to the highly packed cells but also due to the larger cell size. Cell size was significantly larger in the palisade mesophyll as the degree of CAM increased. In addition, as the magnitude of CAM increased, pore area (taken as the aperture, and calculated using the equation: Area ellipse: [(major axis/2)*(minor axis/2)]* π) was found to be significantly larger and stomata were found in lower densities on the abaxial surface of leaves. Unexpectedly, stomatal guard cell size (area) did not show a clear relationship with the degree of CAM, but still the maximal pore area (aperture) was found in the constitutive CAM species. Having larger stomata in lower densities might be a strategy to improve resource use in water limitation environments, since high rates of photorespiration have been reported in guard cells (Srivastava et al., 1995), and even when the relationship between the degree of CAM and guard cell size was not very clear, CAM *Clusia* plants still have on average slightly larger guard cells compared with C3 *Clusia* (CAM = 917.3 μm^2 C3 = 767.7 μm^2). Taken together these results raise the question if having larger cells is a consequence of the necessity to fit a bigger genome inside. It has been proposed that CAM may have evolved from C3 photosynthesis via a duplication of genes required for the metabolic necessities of the CAM pathway (Cushman and Bohnert, 1996). However, it is also possible that the larger mesophyll cell size of CAM *Clusia* reflects the need to accommodate large vacuoles for acid and water storage.

5.2 Genome size and correlation with anatomical traits in *Clusia*

It has been demonstrated in previous work that there is a positive relationship between genome size and epidermal and guard cell areas, and a negative relationship

with stomatal density in Angiosperms (Beaulieu et al., 2008). Increases in the genome size could alter the water use efficiency, since larger cells dictated by the necessity of accommodating a bigger genome, will lead to bigger stomata in lower densities (Beaulieu et al., 2008). Since larger cells (e.g. palisade, mesophyll and guard cells) were found in *C. rosea* compared with *C. multiflora*, it was decided to measure the genome size of 10 species of *Clusia* with contrasting photosynthetic physiologies. Samples collected from plants grown at Moorbank were sent to the Jodrell Laboratory, Royal Botanic Gardens, Kew for genome analyses performed by Dr. Ilia Leitch and Dr. Jaume Pellicer, following the protocol described in Annex 4. 2C DNA amounts in pg (Table 5.1) were found to be positively related to stomatal guard cell size ($r^2 = 0.468$; Figure 5.1). However, there was no correlation between genome size and palisade or spongy mesophyll cell size or with the level of CAM expression.

The constitutive CAM species *C. rosea* contained almost double the amount of genomic DNA compared to the CAM *Clusia* plants and 3 fold more than the C3/CAM *C. lanceolata* (Table 1). This result suggested polyploidy in the case of *C. rosea* (I. Leitch personal communication and thus root tip samples for each of the 10 *Clusia* species were fixed in 3:1 ethanol: acetic acid and then sent to Kew for chromosome counting. *C. rosea* had the highest (almost double) amount of CDNA within the species of *Clusia* studied and seems to be a polyploidy, since this species has more chromosomes than the other *Clusia* we tested which were diploid, figure 5.2 There is just one published study reporting chromosome counts in 5 species of *Clusia* (Cruz et al., 1990), including some constitutive CAM species. Whilst this study did not reveal any polyploidy, there were differences in the number of chromosomes at the Clusiaceae family level. Other work reported the occurrence of adventitious embryos in *C. rosea* and *C. minor* (Maguire, 1976), which is generally a common phenomenon in polyploidy. These studies suggested that polyploidism might be important in the evolution of the Guttiferae (Clusiaceae) family (Cruz et al 1990). In spite of these findings, in general, stomatal guard cell size was not highly correlated with either stomatal pore aperture in *Clusia* plants, or with the degree of CAM. Thus, the larger genome of *C. rosea* compared with other *Clusia* species, even with those which also are constitutive CAM, appears to be something of an anomaly.

Table 5.1. Amounts of 2C DNA in pg and standard deviations (SD) for 10 species of *Clusia* with different type of photosynthesis, guard cell size presented a relation with the amount of 2C DNA ($r^2 = 0.468$). Estimations of 2C DNA were done at Jodrell Laboratory Royal Botanic Gardens, Kew, by Dr. I. Leitch and Dr. J. Pellice.

Species	Photosynthesis type	Guard Cell size (μm^2)	2C DNA amount (pg)	SD
<i>C. hilariana</i>	CAM	879.18	4.05	0.02
<i>C. alata</i>	CAM	623.93	4.32	0.01
<i>C. rosea</i>	CAM	1248.82	6.70	0.03
<i>C. lanceolata</i>	C3/CAM	447.6	3.70	0.01
<i>C. aripoensis</i>	C3/CAM	754.56	3.35	0.00
<i>C. minor</i>	C3/CAM		3.98	0.01
<i>C. grandiflora</i>	C3	879.18	3.32	0.00
<i>C. tocuchensis</i>	C3	710.52	4.54	0.01
<i>C. multiflora</i>	C3	713.28	4.30	0.00
<i>C. palmicida</i>	C3		3.49	0.02

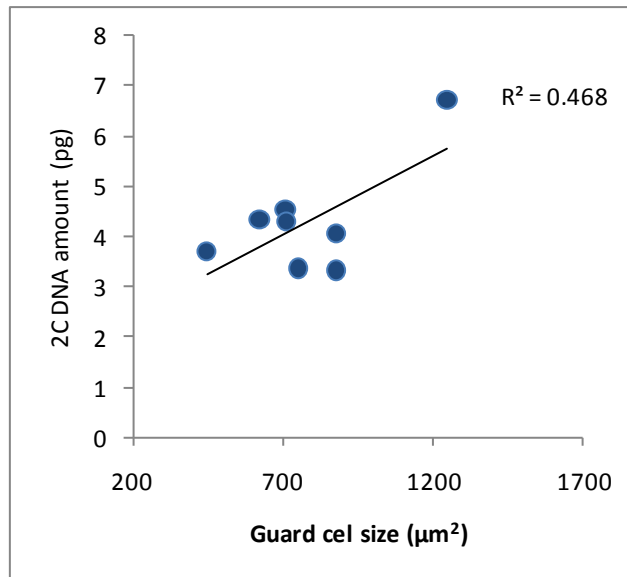
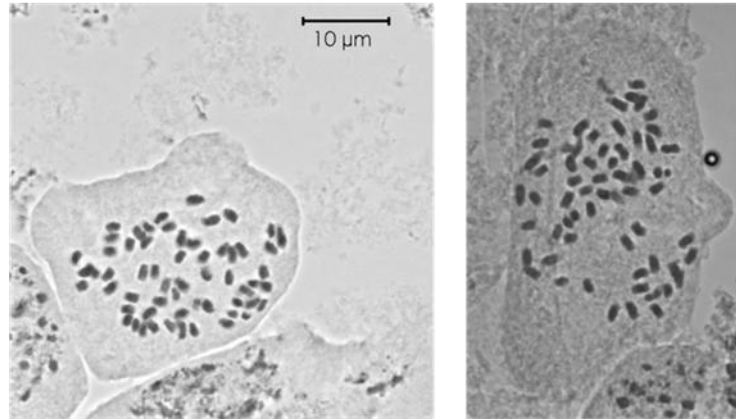


Figure 5.1. Positive relationship between stomatal guard cell size (area μm^2) and 2G DNA amount (pg) for eight species of *Clusia*. Estimations of 2C DNA were done at Jodrell Laboratory Royal Botanic Gardens, Kew, by Dr. I. Leitch and Dr. J. Pellice.

Clusia multiflora

2C = 4.3 pg

2n = c. 60



Clusia rosea

2C = 6.7 pg,

2n = ??
(much > 60)

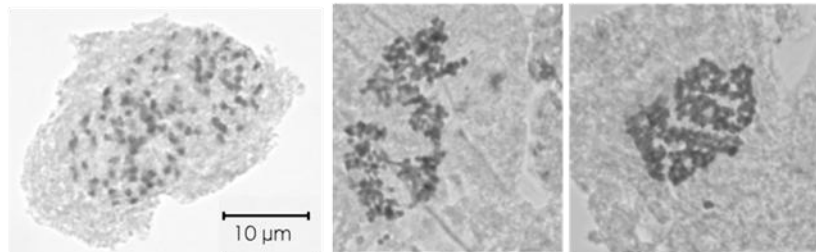


Figure 5.2. Chromosome preparation of *C. multiflora* and *C. rosea* by Jaume Pellicer (Dec. 2010). It was possible to count the chromosome number in *C. multiflora*, affirming the diploid, but poorer preparations in *C. rosea* prevented accurate counting of chromosomes, although there did appear to be more than in the C3 species. (All images at the same magnification).

CAM is believed to have evolved as a means of optimising plant water use efficiency, and the possession of larger stomatal apertures (and indeed larger stomatal guard cells in the case of the constitutive CAM species *C. rosea*) is difficult to reconcile with this. Thus, it was hypothesised that the larger stomata of the CAM *C. rosea* would respond faster to changes in the environment and be subject to more robust circadian control compared to those of a constitutive C3 *Clusia*. These ideas were explored further in Chapter 3.

5.3 Circadian control of stomatal conductance is more robust in CAM than in C3 *Clusia* plants and is mediated via photoreceptors rather than via metabolism

The circadian clock is believed to play a key role in coordinating the metabolic processes that underpin CAM (Hartwell et al., 1996; Nimmo, 1998, 2003; Hartwell, 2005) Light is a critical factor in gating responses of the circadian clock to changes in

environmental conditions and it has also been proposed that the day-time closure of stomata in CAM plants is due to a loss of light-regulated stomatal conductance (Lee and Assmann, 1992). Stomata respond to light via two main mechanisms: a metabolic response to red light which induces photosynthesis (lowering the internal CO₂ concentrations, which is believed to act as a signal for stomatal movements (Roelfsema and Hedrich, 2005) and a direct response to blue light which causes depolarization of the guard cells membranes and changes in osmotic potential, thereby generating stomatal opening. To establish if the stomata of CAM plants which are open during the night, still respond to light, and to examine if circadian oscillations in net CO₂ uptake and stomatal conductance are disrupted by changes in light regime, gas exchange measurements were made over 48 hours under constant light regimes (e.g. white light, blue light, red light and darkness). *C. rosea* a constitutive CAM plant, and *C. multiflora*, a constitutive C3 plants were compared and were found to respond differently to variation in light regimes. Contrary to expectations, stomata in the CAM *Clusia* had not lost the blue light response; oscillations of stomatal conductance and CO₂ assimilation were maintained under constant blue light but shifted in the time of peak responses (compared to under white light). On the other hand, the C3 species *C. multiflora* showed a damped oscillation of CO₂ assimilation under constant blue light and both CO₂ assimilation and stomatal conductance were damped under constant red light. The CAM species, *C. rosea* maintained circadian oscillations in net CO₂ uptake and stomatal conductance under constant red light but the peaks in both were now shifted to the subjective day, compared to responses under white light. In conclusion, both species responded differently to light and circadian control of stomatal conductance was found to be mediated by both photoreceptors and metabolism, the latter including photosynthesis and, in the case of the CAM *Clusia*, PEPC activation status.

The CAM *Clusia* showed a decrease in water use efficiency under constant light regimes, probably as a consequence of the increase in stomatal conductance during the subjective light period which generated high rates of transpiration that were not compensated for by net CO₂ assimilation. This was not the case for the C3 *C. multiflora* and indicates the importance of the maintenance of circadian control over the larger stomata in the CAM *Clusia*.

Given the finding that the response of stomata to different wavelengths of light has not been lost in CAM species of *Clusia*, and remembering the importance of the maintenance of circadian control in the conservation of water, the kinetic responses of

the larger CAM stomata to changes in the environment were assessed. It has been reported previously that wider guard cells can better sense a decrease in humidity, but might have slower responses to changes in water potential compared to smaller guard cells (Assmann and Wang, 2001). In this thesis it was hypothesized that CAM species of *Clusia* with larger stomata (higher maximal aperture) than C3 species have a stronger control over stomatal conductance and will maintain a conserved rhythm to maintain high WUE. It was proposed that stomata of the CAM *C. rosea* would respond differently (perhaps faster) to changes in light intensity in terms of speed of opening and closing, compared with stomata of the C3 *C. multiflora*. This hypothesis was corroborated by recording the changes in stomatal conductance every minute over a 30 minute period in response to changes in turning lights on or off. The larger stomata of *C. rosea* responded faster during the photoperiod compared with those of *C. multiflora*, but not during the night. The results suggest that the more rapid responses in the stomata of the CAM species might be important for optimising carbon gain and reducing water loss under changing environmental conditions at the start and end of the day. Several studies have suggested that in dry environments smaller stomata respond faster to water stress and high density stomata maximize the CO₂ diffusion under optimal conditions for photosynthesis. However, this does not appear to be the case in *Clusia*, where larger stomata of *C. rosea*, the CAM plant, responded faster to light compared with smaller stomata of *C. multiflora*, the C3 plant, under non water stressed conditions. Furthermore, the larger guard cells of *C. rosea* appear to be related to the necessity of accommodating a bigger genome yet this does not confer a disadvantage for this plant since CAM confers a with higher WUE compared with the C3 plant. On the other hand, smaller stomata in higher densities could result in a good strategy for *C. multiflora* inhabiting dry and very exposed environments, with less of a selective pressure for CAM.

Following on from these findings, it was decided to probe the molecular mechanisms underpinning the contrasting responses of stomata to light noted in the C3 and CAM species of *Clusia*.

5.4 Circadian control of photoreceptors may represent a point of divergence between C3 and CAM in *Clusia*

Phototropins are photoreceptors involved directly in the blue light signalling in the guard cell for stomatal opening. Cryptochrome is another well studied photoreceptor involved in the circadian control of different processes in response to blue light. Phytochrome is a red/far red chromophore involved in the recognition of photoperiod length and in the regulation of circadian rhythms (Reed et al., 1994). Some works have suggested that phototropins, phytochromes and cryptochromes act together in the induction of stomatal opening. Kasahara et al (2004), demonstrated the impossibility of mobilized and accumulated chloroplasts, lowering the photosynthetic efficiency, in the “*photA2photB1photB2-1* mutant” of the moss *Physcomitrella patens* under red light, implying that phototropins could be part of the signalling pathways for phytochrome-dependant chloroplast movements. Also (Mao et al., 2005) reported that CRY 1 and CRY 2 act in conjunction with PHOT1 and PHOT2 to mediate blue light induction of stomatal opening in *Arabidopsis*.

Based on the contrasting responses of stomatal conductance and CO₂ assimilation in *C. rosea* and *C. multiflora* observed under different light regimes, differences between the species in the transcript abundance of phototropins under regular 24h dark/light and under different light treatments were predicted. Results from real time PCR showed a 5 fold higher abundance (of *pho1*) under regular 24h light/dark for *C. rosea*, compared with *C. multiflora*. The species also differed in terms of the timing of peak expression of phototropins, the level of control exerted by circadian clock over the transcripts and the response of transcript abundance to different light regimes. Variations in the transcript abundance of phototropins over the diel cycle under different light treatments were not correlated with the patterns of stomatal conductance observed under the same light treatments, indicating possible post-transcriptional regulation of phototropins, including inhibitory signals or negative feedback, in the control of the functioning of these photoreceptors.

The level of control exerted by the circadian clock over the transcript abundance for phototropins appeared to differ between the C3 and CAM *Clusia*. Moreover, the diel patterns of expression under different light regimes was found to be different when comparing *phot 1* and *phot 2* in *C. multiflora*, supporting the idea of a non identical sensitivity and non-redundant function of these phototropins as has been tested before in previous work on the C3 species *Arabidopsis* (Nakasako et al., 2008). In the CAM *C.*

rosea, *phot1* and *phot2* responded very similarly to blue, far red and darkness. Transcripts of *phot1* were not detected under constant red and white light in the CAM *Clusia*, and the same occurred for *phot2* but under constant white and blue light. This might indicate a different function of the two phototropins, with *phot1* more sensitive to low light intensities, and *phot 2* to higher irradiances. Furthermore, *phot 2* seemed to be degraded or not expressed under high irradiances (constant white light and blue light) in both plants. These results demonstrated that the phototropin response has not been lost in CAM plants but there is a divergence in the functions of *phot 1* and *phot 2* at some point in the *Clusia* CAM and the *Clusia* C3. It is possible that the appearance of evolutionary variants like isoforms of the known photoreceptors or even different photoreceptors is part of the mechanisms underpinning divergence between photosynthetic modes in the *Clusia* genus. On the other hand, *cry2* seemed to respond rather similarly in the C3 and CAM *Clusia* although the amplitude of the oscillations in the transcript abundance and the responsiveness to light was lower in *C. rosea* than in *C. multiflora* for *cry2*. *Cry2* may warrant further investigation as a component of the changed blue-light response that has been reported for CAM versus C3 stomata.

Transcript abundance of *phyA*, also showed contrasting patterns (almost opposite) in both species, under all light treatments. Transcript abundance of *phyA* was 7 fold higher for *C. rosea* than for *C. multiflora* under 24h dark/light cycles. Could this be another point of divergence between the two photosynthetic modes? It would be of future interest to explore phytochromes in more detail in closely related C3 and CAM systems, given the proposed importance of phytochromes in circadian control.

In conclusion, the response of stomata to light in *Clusia* plants must be mediated by a coordinated labour and cross-talk between different photoreceptors which exert control over CO₂ assimilation, acid turnover and water use.

5.5 Other findings related to the main hypotheses of the thesis

5.5.1 Vein density

Given the observed differences in the size of stomatal apertures and density of stomata between CAM and C3 species of *Clusia* it is important to consider the implications for transpirational water loss, taking into account the diffusion limitations

inside the mesophyll of succulent leaves which might constitute a barrier for water vapour movement. The hydraulic apparatus is expected to play an important role in the movement of water across the leaf, from delivery to the leaf via the mid-vein to the sites of transpirational loss (i.e. the stomata). For that reason leaf vein density was estimated and compared between the constitutive CAM plant *C. rosea* and the constitutive C3 plant *C. multiflora* following the methods described in Annex 3.

Differences between leaf vein densities were observed between species. When grouping together primary and secondary veins, the density was slightly lower in *C. rosea* (0.72 mm/mm^2) than in *C. multiflora* (0.8 mm/mm^2), although this difference was not statistically significant ($p = 0.896$). However, it is clear that primary vein is higher than secondary vein, but these differences are not significant between species either ($p=0.126$).

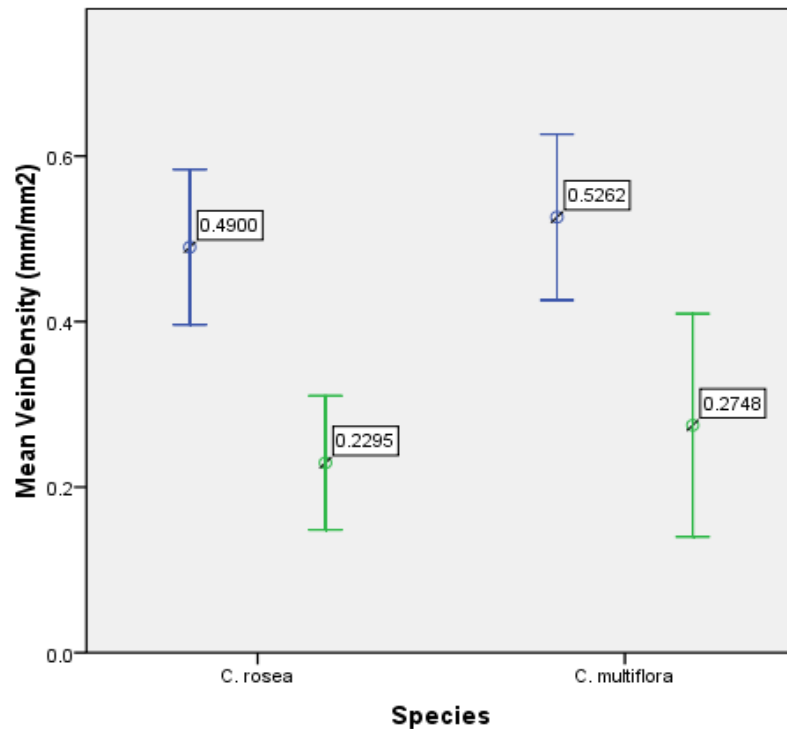


Figure 5.3. Mean values (mm/mm^2) and errors bars at 95% CI of primary vein density in blue and secondary vein density in green for leaves of *C. rosea* $n=61$ and *C. multiflora*. $n=47$.

Based on these results, it could be suggested that the C3 *C. multiflora* with a higher primary and secondary vein density has a higher potential to conduct water through the mesophyll compared to the CAM *C. rosea*. It has been reported previously that increased vein density is an adaptation to arid environments; *Acacia* in areas with

lower precipitation presented a higher primary vein density compared with plants of the same genus in places with higher precipitation (Sommerville et al., 2010) and with higher irradiance (Roth-Nebelsick, 2001; Sage, 2004). Better water movement and less water stress appears to result from having a superior network connecting tissues from xylem to mesophyll (McKown and Dengler, 2009). Sage et al (2004) suggested that higher vein density is a strategy to improve water status by increasing water supply relative to the evaporative surface of the leaf. However, having in mind the higher specific leaf area (SLA) and higher stomatal densities of C3 *Clusia* species compared to CAM *Clusia*, higher vein densities in the C3 *Clusia* could signify a higher potential for water transpiration and might be reflected in the lower water use efficiency in the C3 compared with the CAM *Clusia*. This potential disadvantage might be counteracted by the smaller stomata in the C3 plant. In addition, the higher cost of having more stomata and more veins might be offset by making the most of the high light irradiance (Sage, 2004; Sack and Frole, 2006). In previous works, sun-establishing species were found to have in addition to higher vein density, a thicker palisade (Popma et al., 1992; Kenzo et al., 2004)). Furthermore, Sack et al (2006), suggested that the higher vein density of sun-establishment species means lower hydraulic resistance for water supply to larger stomata, allowing high gas exchange rates and perhaps high growth rate, which could compensate for the cost of constructing more veins. It has also been observed that higher vein density is related with mesophyll cell size (McKown and Dengler, 2009), which is not the case in the two *Clusia* species examined here (*C. rosea* had larger mesophyll cells compared to *C. multiflora*). Increased vein density is an early anatomical change which is suggested to be a precondition for evolving the C4 photosynthetic pathway from C3 (Sage, 2001; McKown et al., 2005; McKown and Dengler, 2007; McKown and Dengler, 2009). On the other hand, the slightly lower vein density found in *C. rosea* compared to *C. multiflora* could be attributed to the difficulty in picking out minor veins in the thicker-leaved CAM species (Figure 5.3).

Mechanical models that simulate the hydraulic systems of real leaves, have demonstrated that after a certain point increasing leaf thickness does not influence the hydraulic conductance. Thus, to invest in more veins could signify a waste of energy for succulent plants, since it is more important to reduce the distance between veins and epidermis or veins to stomata (Brodribb et al., 2007). Results from the present study do not provide conclusive information about the length of secondary veins, especially in the CAM *Clusia* species. It is possible that the amount and length of secondary veins

(reflected in the density) is being underestimated due to the poor resolution of the pictures. Also, the densities recorded for both *Clusia* species are notably lower compared with values reported by other works (McKown and Dengler, 2009), suggesting a general underestimation of the total vein density. It would be very interesting to test these hypothesis in more species of *Clusia* since it has been demonstrated that photosynthetic efficiency is directly related to hydraulic conductance (McKown and Dengler, 2009). Attempts to understand the constraints on water transport must include vein patterns as well as stomatal control and morphological characteristics of the mesophyll (Noblin et al., 2008). Having information about the hydraulic system would give us a better and more complete understanding of the leaf anatomical relationships with the photosynthetic mode within *Clusia*.

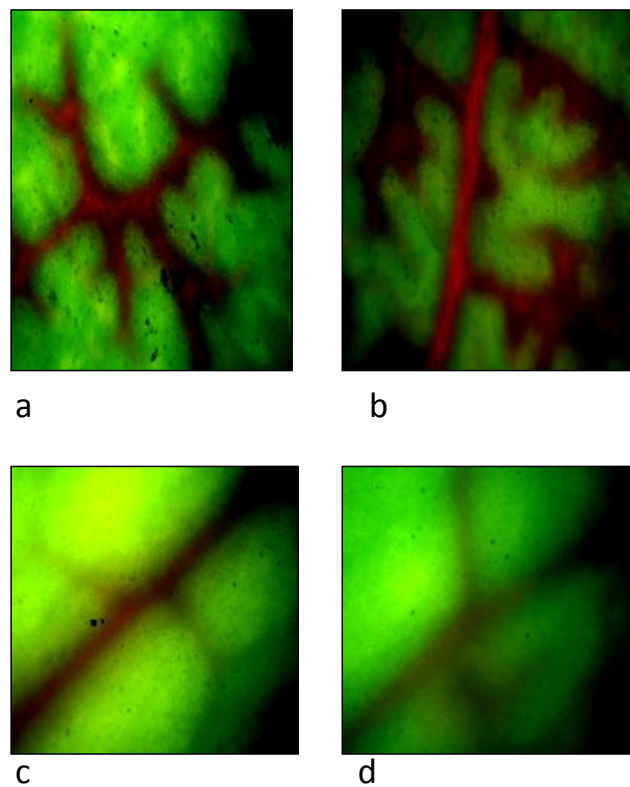


Figure 5.4. Pictures of leaves showing veins in red, from *C. multiflora* (a, b) and *C. rosea* (c, d) treated and stained with 1% Safarin under light microscopy 5X magnification.

5.4 Technical challenges encountered in studying *Clusia*

Throughout the course of the research underpinning this thesis a number of technical difficulties were encountered when trying to apply standardised anatomical, biochemical and molecular methods to *Clusia*. These difficulties are described below, along with suggested guidelines for future improvements.

A key result from the thesis was demonstrating a close relationship between certain leaf anatomical traits and the degree of CAM photosynthesis. Such relationships have not previously been reported for *Clusia* and may ultimately give better insight on mechanisms underpinning evolutionary divergence between C3 and CAM. Immunolocalization techniques have been used before in *Clusia* to examine the localization throughout the mesophyll of PEPC and PEPCK (Borland et al., 1998). Research conducted as part of the present thesis sought to actually quantify the amount of PEPC and Rubisco proteins through different layers of the leaf mesophyll of C3 and CAM species of *Clusia* proteins via Immuno-gold staining. Unfortunately it was not possible to determine the localization and density of PEPC and Rubisco proteins in *C. multiflora* or *C. tocuchensis*, possibly due to the high content of phenolics in these species which could have interfered with the recognition of the antibodies (E. Olmos personal communication). Also, the presence of latex, and the thickness of the *Clusia* leaves make resin penetration difficult, leaving the tissue very weak and in some cases damaged after fixation and sectioning which is noticeable under electron microscopy. For species like *Clusia* with very thick leaves, the content of latex and phenolic implies a trade off between penetration of the resin and conservation of the tissue, versus sensitivity of the antibodies. In order to deal with the high phenolic content of some *Clusia* leaves, it may be necessary to try a different resin (E. Olmos personal communication), but due to time constraints this was not possible in the present thesis. However, good tissue preservation and immunogold localisation was achieved using a constitutive CAM plant *C. rosea* and a very weak inducible CAM, *C. aripoensis*, making possible some comparisons between species that show different photosynthetic physiologies (see section 2.3.1 Figure 2.3)

At the molecular level, the work reported in the thesis gave new insights for *Clusia*. Real time PCR is a valuable technique to quantify transcript abundance and is becoming more popular than reverse transcript (RT) PCR. The aim of quantifying the transcript abundance of four photoreceptors under regular light/dark conditions was to validate results from RT PR and also to optimize the primers to be used in the future.

However, despite several attempts, just two of the photoreceptors (*pho1*, *phyA*) were amplified by real time PCR, whilst the other two genes (*pho2*, *cry2*) did not give accurate results, which might be due to the primers specificity. It is probably necessary to design new primers, taking into account the higher sensitivity of the SYBR green and real time PCR compared to that of RT-PCR. It is possible that some primers were designed against a low complexity sequence, and are not very specific for the gene in question. For example in the case of *cry2* the sequence used to design the primer is quite short; to solve the problem it is necessary to select another region of the sequence (difficult in this case because there is only one sequence available for *Clusia* in the EST data base constructed by Shorrocks 2009). An alternative would be to try a longer primer with higher melting temperature (T_m) to increase specificity. Also the length of the amplicon could be a problem in this case; the primers for *cry2* were designed to amplify a product of 155 bp, and the literature recommends amplicons between 50-150 bp. Finally, the efficiency ratio between the target gene and the reference gene should be 1 and this it was not the case in our experiments. Future work should consider the use of software (i.e.: primer express) to design real time PCR experiments.

The research described in the thesis is the first to explore the responses to light quality in two species of the same genus with contrasting modes of photosynthesis. It was discovered that the CAM *Clusia* responded differently to blue and red light compared with the C3 *Clusia* and it was also shown that the response of stomata to blue light has not been lost in *C. rosea* the constitutive CAM plant. Future studies need to focus on the light responses of the actual stomatal guard cells, in order to be able to relate light-quality induced changes in water/CO₂ regulation to light-quality effects on stomatal movements. Cryo-sectioning techniques which enable the extraction of RNA from guard cells are a most promising technique at the moment. To be able to isolate RNA specifically from guard cells in order to examine the expression of photoreceptors will give more compelling evidence about the involvement of these photoreceptors in stomatal movements in C3 and CAM species. Since photoreceptors have several functions within the plant including leaf growth, phototropism, etc. more localised studies of gene expression at the cellular level are required. Nevertheless, the transcript abundance measurements of *cry 2* and *phyA* at the leaf level could provide further information about circadian control than if these genes were just assessed within the guard cells. Experiments at the levels of leaf and guard cells need to be conducted in closely related C3 and CAM species. To better explore the circadian expression of

photoreceptors under different light treatments, longer periods of exposure to light would be ideal, in order to assess the robustness of transcript oscillations through time. Such destructive sampling would require a lot of plant material and a lot of suitable environmental space within which to impose the different light treatments. Because of these limitations, the present work used experiments with excised leaves which could not support more than 48 hours detached from the plant.

5.5 New perspectives and further experiments

Plants within the genus *Clusia* possess outstanding plasticity in their mode of photosynthesis and are thus an interesting model with which to examine the evolution of CAM photosynthesis. Only 7% of the angiosperms perform CAM photosynthesis, which might imply that CAM presents constraints and limitations to e.g. growth, reproductive success, and competition. However, it has been proven that CAM plants are very successful under certain environmental conditions, such as high irradiance, water stress and low CO₂ concentrations. Moreover, recent work has highlighted the high productivity of certain CAM plants despite the higher energetic costs of the mechanism compared to C3 (Borland et al 2009; 2011). The physiological basis of high WUE in CAM plants has been described previously in several works and genes implicated in the C3-CAM transition have been suggested from studies conducted on *Mesembryanthemum crystallinum* (Cushman et al., 2008). *M. crystallinum* is a good model for molecular work because of its relatively small genome size and ease of growth. However, in *M. crystallinum* CAM is induced via the imposition of salinity stress, a factor which might obscure changes in gene expression that are specific to CAM from those that are associated with acclimation to salinity. With regard to *Clusia* a recent EST data base was constructed from libraries of transcripts produced from droughted leaves of a constitutive CAM species (*C. multiflora*) and a facultative CAM species (*C. minor*; (Shorrocks, 2009). This study has provided a way with which to dissect out genes implicated in general drought acclimation from those specifically associated with CAM. This important resource allows comparative molecular studies on various aspects of CAM.

The contrasting patterns in leaf anatomy and stomatal responses to light reported here for two species of *Clusia* with different modes of photosynthesis, provide more insight in understanding the mechanisms that underpin CAM. Now it is clear that leaf

anatomy is strongly related with CAM within closely related species in a single genus. However, to fully understand the molecular bases of those relationships and the performance of CAM, it would be ideal to be able to genetically modify *Clusia* in order to evaluate the implications of different photoreceptors in gas exchange mechanisms and their relationship with drought tolerance. There are no reports of successful transformation of *Clusia* and due to the size and relatively slow growth rates of *Clusia*, genetic modification approaches will be difficult in this species. However, other CAM plants as *Kalanchoe fedstchenkoi* are easier to modify genetically and mutants with modified photoreceptor expression could be created in this species and the implications for stomatal conductance assessed. Another approach to examining the role of different photoreceptors in stomatal regulation in CAM plants would be to evaluate the transcript abundance of photoreceptors in the stomatal guard cells in *C. multiflora* and *C. rosea*. At the whole leaf level differences were found in the transcripts of four photoreceptors under different light treatments. Also it was evident that the response of stomata to blue light has not been lost in the CAM species *C. rosea* since it maintained circadian oscillation in gas exchange and shifted the maximal stomatal conductance to subjective day under low intensity blue light (Chap 3). Moreover, it seems that *C. rosea* does not need the specific blue light stimuli to open the stomata as was found on as the C3 species *C. multiflora*. Stomata of *C. rosea* were also more sensitive to blue light, as stomata opened under high blue light without a background of red (perhaps because that high intensity ($250 \mu\text{mol m}^{-2}\text{s}^{-1}$) also stimulates photosynthesis). The C3 species *C. multiflora* needed both red and blue light to open stomata. This result may be due to the need of a higher depletion in CO_2 internal concentrations driven by photosynthesis in response to red light. It is still not entirely clear if the response to blue light in *C. rosea* is positive, since stomata opened during the subjective day as they did under constant darkness but at a lower magnitude. Then it is possible that photoreceptors of *C. rosea* are transmitting a negative signal from light to shut the stomata, and in the absence of light, the signal is not transmitted and the stomata are open. To evaluate this hypothesis it would be necessary to work at the level of the stomatal guard cells. In addition to cryosectioning of guard cells and RNA extraction, another possibility is to use green fluorescence protein (GFP) techniques to mark specific genes within the guard cells. For this purpose it would be necessary to isolate epidermis from the rest of the mesophyll, from leaves previously subjected to different light treatments. However, this approach presents two main problems: previous attempts to do molecular work at the guard cell

level have faced difficulties related to isolation of guard cells in *Arabidopsis* due to their small size (Pandey et al., 2002) and species such as *Clusia* do not allow for easy removal of epidermis strips. However, other CAM plants such as *Kalanchoe* have easily peelable epidermis and are easier to transform with GFP compared to *Clusia*, indicating that this species would be a good model for exploring the molecular basis of stomatal function in CAM plants. The idea would be to mark some photoreceptors (making a recombinant gene) with green fluorescence protein and introduce the construct to the plants via a vector. Transformed plants would be placed for at least 48 hours (more if leaves don't suffer any damage) under the different light treatments, and then the epidermis would be peeled, trying to isolate it from mesophyll. The epidermis could be checked under the fluorescence microscope for the presence of any of the GFP-tagged genes in stomatal guard cells. It would be interesting as well, to continue the circadian experiments on photoreceptor gene expression over longer periods of time under different light regimes. However, the complication with this type of experiment is the potential leaf damage (brown spots) that can occur; in this work, yellow and brown spots were noted in leaves of *C. rosea* under constant blue and constant far red light, and under constant darkness whole leaves of *C. rosea* turned yellow, indicating possible loss of chlorophyll (chapter 4 figure 4.7). To counteract this effect it would be better to isolate and culture stomatal guard cells and then conduct *in vitro* experiments exposing the cells to different light treatments. However, *in vitro* culturing of guard cells can present some difficulties due to their totipotentiality; once the epidermal cells are cleaned from the culture, the guard cells can become undifferentiated and can even form calli (Hall et al., 1996). In this case it would be necessary to culture both kind of cells (epidermal pavement cells and stomatal guard cells) and then separate the cell types by flow cytometry or sorting or just differentiating the cells by morphology under the microscope to make Immuno-staining assays for identifying protein expression. Due to these constraints it could be worthwhile to optimize a technique for separating the epidermis of *Clusia* plants from the rest of the mesophyll in order to isolate guard cells. There is as well the possibility to work with another CAM plant like *Kalanchoe*, which is easier to grow and modify genetically.

Microarrays or Elisais for photoreceptors at leaf and stomatal guard cell level could be another interesting technique to use, to obtain more information about the transcriptional regulation of certain genes in response to light in CAM and C3 species of

Clusia. Elisas and western blots could also provide information about some possible post-transcriptional regulation of photoreceptors.

Currently, several studies suggest that genes involved in circadian control are also responsible for stomatal movements (Somers et al., 1998). However, further work that allows the identification of genes involved in stomatal control in CAM plants in the direct (if it exists) response to light could start a program of research on how modifying stomatal responses in C3 crops could make them more tolerant/resistant to drought. The expression of some photoreceptors in CAM plants first needs to be proved at stomatal guard cell level. It is difficult to create knockouts of some genes if those play key functional roles, because the plants would be dysfunctional. Moreover, it is almost impossible to test the role of just one gene or protein in the stomatal movements in CAM plants, because several genes and proteins act in conjunction to control gas exchange in response to different factors such as light and CO₂ concentrations. Then to be able to modify other plants of economic interests in order to get higher WUE, I believe that the next step is to test *in vitro* the response of those photoreceptors in CAM plants. For example, it would be feasible to create a *Kalanchoe* knockout of *pho1* and another of *pho2*, put the plants under different light treatments, (low and high blue light), and measure stomatal conductance and other gas exchange parameters. The stomatal guard cells could also be isolated and cultured from those plants to measure the changes in the electric potential in the culture media and guard cell membrane, as an indication of depolarization of the guard cell membrane under different light treatments, and compare it with the control wild type. This experiment could give us an indication of the different roles of both phototropins 1 and 2 in stomatal movements in CAM plants. Knowing this, it would be possible to create a mutant of the phototropin that responded more to high blue light irradiancy (i.e.: *phot2*) and restrict the stomatal opening to the time of the day when the blue light is less intense, i.e. dusk and dawn, and thus lessen the transpiration. However, in this case it is very possible that CO₂ internal concentrations will override the effect of light on stomata and manage the movements, but still it would be worth to test this in CAM plants. Similarly, other experiments could be done with cryptochromes and phytochromes, although the complications could be superior, since both genes are implicated in circadian processes.

In summary one of the overarching aims of this thesis was to give an advance in the knowledge of functional CAM anatomy and stomatal regulation. Such aims can provide a platform for implementing this knowledge in improving the water use

efficiency of current crops and helping the conservation of natural ecosystems, using abandoned lands or desert habitats for plant cultivation instead of deforesting valuable habitats for agricultural activities

5.6 Final conclusions – key findings of the thesis

- Leaf morphological traits: specific leaf area (SLA), internal air space in the mesophyll (%IAS), length of mesophyll per area exposed to air ($L_{mes}/area$) and stomatal density are negatively related with the magnitude of CAM whereas cell size and stomatal pore area are positive related with CAM. This has strong implications for leaf anatomy in the evolution of CAM.
- Circadian oscillations in stomatal conductance and net CO_2 uptake were maintained for longer in the CAM *C. rosea* compared to the C3 *C. multiflora* under the contrasting light regimes (i.e. more robust clock control over stomata in the CAM species).
- The circadian clock in *C. rosea* is more responsive (in comparison to the *C. multiflora* clock) to light signals, which modify clock control over stomatal conductance and the CO_2 uptake rhythm.
- The stomata of *C. rosea* responded to light directly altering rates of photosynthesis and some blue light photoreceptors were also implicated in the circadian rhythm of stomatal conductance, confirming that blue light response has not been lost in the CAM species. Also as cry2 is the photoreceptor implied in circadian rhythms and is sensitive to blue light, this result highlights the importance of this gene product in controlling circadian processes.
- Circadian control of stomatal conductance in CAM *Clusia* plants is controlled by both photoreceptors directly and photosynthesis indirectly, as well as other metabolic processes (e.g. malate fluctuations).
- Patterns of transcript abundance of *phot 1* and *phot 2* were different in *C. multiflora* and *C. rosea* under 12h dark/12h light cycles and presented changes in

response to different light regimes. The relative abundance of both phototropins under the usual 24 h light/dark cycle appeared to be highest in the CAM species.

- The transcript abundances of both *phyA* and *cry2* varied over the light/dark cycle and under constant light, indicating circadian control of both photoreceptors in the C3 and CAM *Clusias*.
- There were differences in the 24 h patterns of expression between *phot1* and *phot2* and in the responses of *phot1* and *phot2* to the different light treatments, implying that there is not a redundant function between them.
- The CAM species exhibited more robust control of stomatal conductance under constant red light, compared to the C3 species. Thus, the way in which *phyA* is linked to the clock could be a point of divergence between the C3 and CAM *Clusias*.
- Transcript abundance of *cry2* and *phyA* was altered under constant light regimes in both species. However, the amplitude of the oscillations in the transcript abundances of *cry2* and *phyA* do not seem to be more responsive to light in *C rosea* than in *C. multiflora*. Even when in some cases variation in transcript abundance seemed to be related to gas exchange patterns, is very likely that more genes are involved in the control of stomatal movements and responses to light (i.e.: *cry1*, *phyB*).

Appendix 1: Gas exchange measurements

Net CO₂ uptake

Measurement of net CO₂ uptake is a direct alternative, non destructive method of measuring carbon gain, compared to the traditional method of harvesting, drying and weighing plant material. An advantage of this technique is the ability to identify the relative contribution of the four phases of the CAM cycle to total carbon gain.

The Walz CMS-400 Compact Minicuvette System

Net CO₂ uptake was measured using the bench-top Walz CMS-400 Compact Minicuvette system (Heinz Walz, Effeltrich, Germany), with an integral BINOS-100 infrared gas analyser (IRGA). The system was operated in open (differential) mode, with no addition of CO₂ to the flow of air through the system to compensate for CO₂ taken up during photosynthesis.

Air was collected from outside the building and passed through a buffering chamber to reduce fluctuation in CO₂ concentration. The air was then saturated with water vapour, before passing through the input humidity control unit (Walz Cold Trap KF-18/2), cooling the input gas to a predetermined dew point temperature, using the Peltier effect, controlled humidity. This temperature was set manually at dawn and dusk, to a level lower than growth room temperature to avoid condensation within the apparatus.

The air flow was then passed into the central unit, where it was split between two parallel paths, the measuring gas path and the reference gas path, each having a pump, mass flow meter and electronic flow rate control; maintaining the gas flow at approximately 400 ml min⁻¹, allowing sufficient air to pass over.

The leaf surface to prevent a build up of humidity in the leaf chamber, and thus maintain adequate boundary layer conductance which might affect calculations of assimilation (Long and Hallgren, 1993).

The measuring gas stream passed through the sealed leaf cuvette, whilst the reference gas passed through a compensation vessel with the same path length and volume as that taken by the measuring gas. Thus both gas flows reached the IRGAs at the same time, eliminating any differences in measurement due to fluctuations in input CO₂ concentration. Differential zero point measurements eliminated any drift between the zero points of the measuring gas and reference systems. These corrections were achieved by stopping the flow of measuring gas and splitting the

reference gas flow into two, passing this gas through both the reference gas and measuring gas low IRGAs.

Infra-red (IR) gas analysis relies on the principle that hetero-atomic gas molecules absorb radiation at specific IR bands, each gas having a characteristic absorption spectrum. Gas molecules with two identical atoms, such as O₂ and N₂, do not absorb IR radiation and hence do not interfere with the measurement of CO₂. However, the absorption spectrum of H₂O does interfere with the measurement of CO₂ and so the gas stream was cooled prior to measuring CO₂ in the BINOS-100, to remove water vapour by condensation. In most IRGAS, IR radiation from heated metal or alloy source is passed through a gas chamber in which the gas being analysed flows continuously. A change in the concentration of this gas will alter the radiation leaving the chamber.

Measurements using the Walz CMS-400 System

An intact *Clusia* leaf was placed in the leaf cuvette, maintaining leaf position and orientation. Balance measuring and reference gas flows confirmed the leaf chamber was sealed. The leaf was allowed to acclimate to chamber conditions for one to two hours before gas exchange measurements began. At the start of the study, data was logged over 48 hours for a random sample of pineapple leaves, to ensure that sufficient time was allowed for gas exchange to stabilise before measurements were taken. Data was logged every 15 minutes and differential zero point measurements taken every 10 data collection periods. Data was downloaded onto IBM compatible computer and analysed using DIAGAS software supplied by Walz.

CO₂ and H₂O concentrations were determined using the BINOS-100 IRGA. Gas flow rates, leaf temperature, chamber relative humidity and incident PDF were all measured directly by the walz CMS-400 System. Net CO₂ uptake was determined using the difference in CO₂ mole fractions between gas entering and leaving the leaf cuvette (equation 1.1). This approach follows the work of von Caemmerer and Farquhar (1981).

$$A = \frac{u_m(c_e - c_o)}{s}$$

Equation 1.1

Where

A= net rate of CO₂ uptake per unit leaf area (μmol m⁻²s⁻¹).

Um = molar flow rate (mol s⁻¹)

S = leaf area (m^2)

$C_e - C_o$ = difference in mole fraction between CO_2 entering and leaving the leaf cuvette.

However, C_e and C_o are equivalent to the reference gas and the measuring gas CO_2 mole fractions, respectively, so the term $(C_e - C_o)$ is effectively the CO_2 ppm differential between the reference and measuring gas flows. The molar gas flow (U_m) is calculated from the volumetric flow rate (U_v ; $\text{m}^3 \text{s}^{-1}$), using gas laws, and the relationship that one mole of an ideal gas has a volume of 0.0224 m^3 at 273.15 K and 101.3 kPa (equation 1.2 (Holum, 1994)).

$$U_m = \frac{U_v \times 273.15 \times p}{0.0224 \times 101.3 \times T} \quad \text{Equation 1.2}$$

Where p is atmospheric pressure (kPa) and T is temperature (K).

Appendix 2: Image J - How to estimate IAS and Lmes/area

First a duplicate image was created (right hand click and select duplicate). On this duplicated image, the next step was to click on - *Process – find edges*, *Process – binary – make binary*, to make the airspaces visible and these were then selected using the fill tool – *bucket of paint*- or by hand using the paint brush tool, After this, these areas were selected using the wand tool and holding the shift key down the areas appeared in yellow. Once the areas were selected the image was converted into a mask – *edit – selection – create mask* (This creates an image that just has the selected areas on it). Then, the image was threshold – *image – adjust – threshold* (this is like a density slice, and was used to be sure the selected areas are in red). The threshold image can be altered using the sliding bar if necessary. The individual particles/areas were measured using – *Analyze – measure particles*. The results were displayed in a separate window and the corresponding area numbers were mapped onto the image.

Appendix 3: Stomata dimensions

Measures of stomata dimensions in μm for eight species of *Clusia*. The measures have been made based on the diagram in figure 2.2 b, and stomatal pore area was calculated assuming the pore as an ellipse with a constant minor axis = pore length, at different apertures, and maximal aperture as major axis;

$$\text{Area ellipse: } [(\text{major axis}/2) * (\text{minor axis}/2)] * \pi$$

Specie	pore length (um)	PGD (um)	Pore width (um)	Guard cell length (um)	Pore area (um ²)
<i>C. alata</i>	23.21	28.46	10.93	26.39	199.32
	20.59	33.15	8.84	33.68	142.96
	22.19	36.15	10.10	28.28	176.03
	20.32	30.22	9.02	30.07	143.99
	20.43	26.67	5.67	29.83	90.92
	22.37	33.01	12.71	30.19	223.38
	22.19	27.58	11.35	30.41	197.77
	18.93	33.58	6.11	26.20	90.87
	20.63	26.91	5.99	26.28	97.08
	20.71	28.44	6.84	28.50	111.22
	18.89	28.67	2.13	30.33	31.66
	19.96	31.48	4.03	30.01	63.09
	18.58	30.17	8.33	28.68	121.45
	21.64	30.37	3.30	29.53	56.08
	20.92	28.65	10.88	28.99	178.68
	17.92	32.32	10.35	25.71	145.63
	18.19	31.56	10.44	29.24	149.09
	20.65	27.97	9.48	25.64	153.68
	18.06	29.69	9.82	27.20	139.24
	19.97	29.16	11.66	29.51	182.92
	16.92	30.62	8.68	27.04	115.29
	21.24	28.81	9.02	29.96	150.45
	18.64	27.72	8.45	29.32	123.64
	21.34	26.72	12.45	30.86	208.61
	17.69	27.23	7.85	27.40	109.05
	17.78	31.38	9.47	29.75	132.25
	19.85	30.28	7.91	29.03	123.35
	18.31	33.35	7.25	28.36	104.23
	14.52	28.76	11.24	26.40	128.16
	16.07	23.33	8.84	26.67	111.51

	17.16	27.02	12.88	29.41	173.57
	18.17	29.79	13.53	26.55	193.13
	17.30	29.19	14.76	29.31	200.55
	20.95	28.38	15.42	32.20	253.74
	15.48	26.09	13.65	24.81	165.87
	15.39	32.21	14.01	22.54	169.37
	17.71	27.75	13.00	29.07	180.81
	16.66	27.17	13.67	25.00	178.86
	22.13	32.05	9.25	28.00	160.80
	18.19	29.08	13.27	27.81	189.60
	14.92	31.87	9.37	26.89	109.79
	13.65	25.19	9.80	27.55	105.11
	20.85	31.47	10.80	31.45	176.89
	17.35	25.17	6.60	27.58	89.94
	17.33	27.38	7.80	30.25	106.17
	16.23	28.37	7.27	29.52	92.66
	17.09	29.38	9.35	27.04	125.45
	19.53	29.78	9.43	26.52	144.63
	15.85	23.91	7.25	25.70	90.21
	18.38	28.26	8.83	26.25	127.49
	12.47	27.10	9.11	24.16	89.22
	17.77	28.63	6.13	25.63	85.47
	18.21	27.31	13.17	28.82	188.35
	14.45	23.73	11.22	26.20	127.30
	12.32	29.41	11.95	24.04	115.57
	18.75	26.16	13.54	31.04	199.33
	19.58	24.83	14.17	28.21	217.81
<i>c. hilarana</i>	24.03	34.18	0.75	37.89	14.16
	24.87	32.00	2.83	34.60	55.26
	26.17	26.76	6.37	39.36	130.89
	23.03	35.98	6.44	41.26	116.45
	22.27	29.91	3.18	34.89	55.70
	19.46	26.74	2.58	35.54	39.39
	16.60	26.56	4.49	30.88	58.52
	18.50	24.50	4.17	34.17	60.54
	21.19	26.44	8.35	33.82	139.03
	18.44	30.26	5.67	31.87	82.10
	21.54	31.10	2.22	36.31	37.62
	22.00	23.50	1.51	31.34	26.07
	23.30	30.89	14.01	35.95	256.40
	24.50	28.67	12.50	39.13	240.55
	22.74	30.79	4.47	36.53	79.87
	23.11	29.77	8.13	35.74	147.54
	24.66	31.37	12.98	38.70	251.37

	21.74	31.21	11.05	37.69	188.73
	23.45	32.49	6.13	34.68	112.90
	18.23	31.73	4.36	34.14	62.43
	17.84	27.28	3.30	37.28	46.24
	13.79	28.31	4.25	34.19	46.01
	21.93	29.83	6.47	36.05	116.78
<i>C. rosea</i>	20.03	28.86	8.53	37.23	134.21
	17.41	26.49	8.14	36.82	111.35
	11.87	28.70	5.85	35.88	54.54
	20.30	27.61	9.65	38.15	153.84
	20.80	26.49	8.20	35.04	133.93
	20.18	29.56	10.73	37.27	170.12
	18.66	25.42	8.31	36.42	121.76
	25.31	30.99	14.45	37.55	287.29
	18.86	27.77	11.34	35.28	167.90
	18.93	28.29	9.26	36.15	137.66
	15.77	19.56	8.15	31.99	101.00
	22.98	28.88	10.36	38.10	186.97
	19.10	24.24	9.95	33.61	149.20
	14.61	25.66	6.56	39.17	75.28
	13.79	29.01	7.57	36.68	81.94
	15.14	29.55	5.94	40.63	70.64
	24.01	27.36	12.02	37.65	226.57
	21.14	27.22	11.68	36.34	193.98
	15.64	30.57	7.13	37.53	87.56
	11.04	27.81	6.04	33.70	52.34
	18.09	26.17	9.36	34.46	132.97
	22.63	28.34	10.35	39.97	183.96
	15.23	25.66	7.17	38.70	85.69
	14.33	25.51	5.34	38.67	60.07
	17.50	25.37	8.17	34.17	112.34
	11.49	23.61	5.67	30.46	51.17
<i>C. lanceolata</i>	16.25	21.25	6.88	23.25	87.74
	19.47	19.00	5.55	24.72	84.92
	19.46	19.35	6.85	23.59	104.71
	16.79	18.70	4.93	23.05	64.96
	19.95	19.14	5.13	27.49	80.33
	18.31	18.62	5.71	25.52	82.11
	19.89	16.68	4.96	24.76	77.46
	17.34	18.10	3.25	22.01	44.25
	19.53	17.44	4.85	23.07	74.30
	18.51	18.25	5.27	23.53	76.62
	15.83	17.75	5.00	20.83	62.18

	19.69	20.91	7.17	22.84	110.83
	16.42	17.10	3.52	20.13	45.33
	21.84	20.67	9.42	26.50	161.55
	20.34	18.86	4.70	23.53	75.04
	17.43	19.95	6.40	23.80	87.63
	17.91	17.57	3.56	23.03	50.04
	17.14	19.30	4.38	22.10	58.88
	14.37	20.13	4.85	23.05	54.78
	15.09	18.37	3.48	22.37	41.27
	19.28	21.69	7.95	28.07	120.42
	22.08	20.37	5.67	26.33	98.30
	17.45	18.69	6.17	25.04	84.50
	20.29	16.25	4.25	25.20	67.73
	14.79	17.63	5.25	21.03	60.93
	17.67	19.09	4.42	22.43	61.32
<i>C. aripoensis</i>	11.86	25.00	4.14	33.84	38.54
	13.40	25.19	4.49	32.99	47.24
	13.44	31.50	4.76	32.22	50.21
	14.24	27.75	4.74	36.58	52.99
	14.47	25.01	5.83	31.25	66.30
	12.13	26.98	4.07	31.47	38.77
	12.53	26.50	4.04	27.72	39.70
	13.37	26.00	4.37	29.79	45.86
	12.26	28.61	3.89	32.00	37.44
	11.51	22.70	5.03	30.58	45.43
	14.43	23.80	4.44	30.44	50.32
	20.80	28.60	12.03	33.18	196.54
	12.67	29.82	5.32	28.44	52.90
	19.69	20.81	7.11	30.45	109.91
	14.32	31.21	6.96	33.07	78.26
	19.68	23.56	10.81	30.12	167.18
	24.43	23.41	9.52	35.89	182.66
	11.44	25.66	5.38	30.80	48.30
	22.23	31.81	10.18	30.94	177.71
	14.42	28.92	5.59	33.35	63.33
	12.73	28.24	5.68	34.00	56.77
	10.99	24.97	3.85	32.11	33.20
	21.37	26.76	11.79	34.06	197.84
	10.36	28.39	4.30	28.18	35.01
	13.51	26.42	6.02	34.41	63.87
<i>c. grandiflora</i>	21.14	30.99	8.45	33.31	140.29
	24.16	31.64	7.21	37.10	136.85
	21.93	37.54	11.11	32.07	191.30

	21.52	33.92	10.44	30.44	176.38
	21.61	28.14	8.80	32.25	149.35
	19.75	29.26	9.10	28.99	141.08
	21.72	32.35	9.33	35.54	159.05
	23.26	32.51	9.46	33.93	172.69
	21.26	31.96	14.68	34.37	245.14
	21.11	28.71	8.80	33.85	145.89
	15.03	32.85	12.96	31.66	153.01
	22.59	32.13	10.74	31.38	190.53
	22.08	28.74	11.63	34.15	201.69
	18.49	26.55	8.38	32.96	121.62
	20.95	32.70	8.05	34.96	132.47
	16.39	29.90	6.38	30.53	82.16
	19.80	32.09	7.62	31.42	118.44
	18.04	31.90	4.86	34.04	68.83
	19.34	30.49	6.71	37.37	101.88
	22.78	31.18	8.91	37.76	159.37
	20.41	28.68	5.86	33.87	93.87
	20.60	27.53	3.66	34.71	59.18
	23.76	28.00	7.09	36.66	132.24
	19.19	32.79	8.06	31.83	121.37
	18.27	29.24	5.66	29.17	81.16
<i>C. tocuchensis</i>	15.10	21.37	4.25	30.53	50.42
	11.21	20.54	4.17	30.14	36.72
	19.78	22.17	8.34	27.72	129.50
	19.01	21.85	8.14	29.16	121.53
	15.79	22.22	8.18	25.56	101.47
	14.76	20.22	5.13	27.51	59.52
	13.45	21.95	4.32	25.24	45.68
	16.29	18.31	1.88	26.01	24.05
	17.48	22.29	1.25	24.62	17.16
	16.85	20.00	8.67	25.51	114.66
	17.37	21.21	7.18	26.58	97.94
	18.60	19.23	4.38	27.77	63.92
	16.89	20.74	5.59	26.09	74.14
	18.39	21.23	11.77	27.62	169.95
	12.57	21.14	5.59	26.17	55.14
	15.60	19.46	5.62	26.10	68.82
	16.01	20.01	6.20	27.37	77.98
	16.93	22.67	6.67	27.52	88.61
	18.00	21.86	7.92	25.38	111.94
	13.83	21.54	6.75	25.30	73.38
	13.87	19.23	5.60	26.16	61.05
	12.78	22.36	4.10	29.60	41.17

	15.44	17.58	7.47	28.29	90.58
	12.30	20.79	3.59	24.83	34.68
	19.32	20.67	7.17	26.08	108.79
	18.50	22.75	8.75	26.95	127.12
	13.52	20.65	5.34	24.58	56.72
	20.85	22.24	9.61	27.03	157.28
	17.61	26.44	11.47	26.45	158.57
	18.53	22.28	10.16	26.52	147.88
	13.34	22.07	8.16	23.30	85.46
C. multiflora	19.33	30.32	5.77	31.90	87.63
	17.50	26.60	6.17	31.01	84.75
	12.92	32.70	7.08	27.45	71.82
	11.47	30.51	2.24	26.95	20.15
	12.98	28.99	4.04	31.16	41.14
	7.85	29.00	2.15	24.56	13.25
	17.04	28.18	2.06	35.95	27.58
	12.84	27.93	2.43	29.21	24.46
	12.62	34.70	4.30	36.19	42.63
	10.89	28.14	2.76	31.98	23.58
	8.54	26.41	3.44	27.47	23.04
	9.23	27.55	4.19	24.04	30.38
	10.43	29.21	4.96	30.42	40.66
	10.43	30.66	4.26	30.83	34.88
	14.33	28.23	8.85	31.29	99.55
	12.29	29.65	6.01	31.12	57.97
	10.81	23.81	3.15	25.42	26.70
	8.41	24.58	3.01	30.48	19.85
	10.41	24.94	5.39	27.76	44.02
	11.79	22.98	3.55	33.13	32.81
	6.94	25.24	3.01	25.54	16.38
	9.80	27.70	4.30	33.14	33.11
	9.22	32.93	4.26	29.49	30.84
	16.15	24.94	4.50	25.95	57.10
	11.32	28.67	6.17	28.76	54.83
	14.67	22.92	4.26	29.88	49.07
	10.90	21.99	3.50	29.34	29.99
	11.45	27.94	3.26	30.39	29.32
	11.93	32.57	8.19	36.34	76.70
	18.34	30.99	3.91	28.51	56.35
	9.13	27.22	4.03	26.66	28.88
	10.52	30.38	6.31	28.47	52.11
	10.15	25.63	6.56	30.15	52.33
	7.85	27.32	5.20	27.01	32.08
	12.70	25.81	6.58	29.61	65.60

	11.97	28.00	9.36	26.80	87.99
	11.72	27.75	6.08	31.28	55.98
	7.42	31.33	5.53	28.00	32.25
	11.95	27.20	6.87	28.47	64.43
	16.37	27.53	8.75	28.31	112.46
	16.25	29.25	6.67	32.62	85.14
	16.16	28.03	6.71	29.63	85.14
	16.01	24.85	6.79	32.05	85.38
	10.80	30.09	5.03	28.37	42.67
	14.09	33.71	9.75	28.97	107.91
	11.05	29.96	5.93	27.61	51.44
	9.55	29.35	5.67	29.89	42.49
	10.00	31.57	6.80	30.50	53.43
	7.79	26.34	4.78	27.41	29.21
	13.20	29.48	7.85	24.44	81.34
	10.00	29.03	7.18	27.33	56.36
	13.40	28.83	7.34	31.16	77.21
	10.09	28.40	5.83	27.90	46.23
	18.03	31.02	6.97	32.24	98.74
	11.79	27.84	5.94	31.01	54.95
	10.98	29.88	6.36	30.25	54.89
	18.83	29.18	8.97	34.21	132.67
	15.34	30.42	5.76	30.00	69.34
	10.55	26.25	5.77	35.02	47.81
	14.36	29.99	6.27	34.86	70.68
	14.47	29.57	8.25	35.32	93.76
	11.36	28.57	6.13	28.17	54.68
	10.50	27.80	6.89	30.13	56.79
	15.06	28.07	4.27	28.82	50.49
	13.50	27.79	6.76	32.25	71.64
	11.79	32.17	7.59	31.87	70.31
	13.66	33.44	9.22	35.10	98.89

Appendix 4: Calculated values for Stomatal conductance GH₂O

Calculated values for GH₂O for eight species of *Clusia* using the equation below (Lawson et al 1998), values of stomata pore area (taken as a 2/3 of pore length), and pore depth have been converted to meters to use the same units for all the variables. a=mean formula mass of air, b= effective diffusion coefficient, c= stomatal density, d=pore area, e= pore depth, e= end correction.

	mean formula mass of air (mmol m ⁻³)	diffusion coefficient (m ² s ⁻¹)	stomatal density (N stomata m ⁻²)	pore area (m ²)	pore depth (m)	end correction (m)	(a*b*c*d)	(e+f)	GH ₂ O (mmolm ⁻² s ⁻¹)
<i>alata</i>	40900	0.0000249	1.1987E+08	1.91E-10	1.35E-05	7.797E-06	2.33E-02	2.13372E-05	1092.768486
<i>hilariana</i>	40900	0.0000249	7.4030E+07	2.28E-10	1.15E-05	8.519E-06	1.72E-02	1.99691E-05	860.810391
<i>rosea</i>	40900	0.0000249	1.0400E+08	1.67E-10	1.09E-05	7.291E-06	1.77E-02	1.81809E-05	972.873616
<i>lanceolata</i>	40900	0.0000249	1.2620E+08	1.71E-10	9.88E-06	7.378E-06	2.20E-02	1.72577E-05	1273.486991
<i>aripoensis</i>	40900	0.0000249	1.2825E+08	1.16E-10	8.24E-06	6.077E-06	1.52E-02	1.43165E-05	1058.281344
<i>grandiflora</i>	40900	0.0000249	1.3400E+08	2.22E-10	8.00E-06	8.406E-06	3.03E-02	1.64062E-05	1846.595393
<i>tocuchensis</i>	40900	0.0000249	1.4491E+08	1.73E-10	1.06E-05	7.421E-06	2.55E-02	1.80607E-05	1413.615873
<i>multiflora</i>	40900	0.0000249	1.1811E+08	1.03E-10	1.57E-05	5.726E-06	1.24E-02	2.13759E-05	579.584134

$$G_s = \frac{(\text{mean formula mass of air}) \times (\text{effective diffusion coefficient}) \times (\text{Stomatal density}) \times (\text{pore area})}{(\text{pore depth}) + (\text{end correction})}$$

Equation used to calculate theoretical stomatal conductance (Lawson et al 1998), mean formula of air was taken as 40.9 mol m⁻³ at 25°C, effective diffusion coefficient for water vapour in air is 2.49 x 10⁻⁵ m² s⁻¹ at 25°C (Jones 1992). Pore area was calculated assuming the pore as an ellipse with a constant minor axis, pore length, at different apertures, and maximal aperture as major axis. Finally an end correction = (pore area/ π)^{0.5} (Nobel 1991) was applied.

Appendix 5: Vein density estimation (adapted from McKown and Dengler, 2009).

To assess the amount of veins per area, leaves were excised from the base of the petiole and immediately put in water, then treated with a solution of 15% w/v sodium hydroxide (NaOH) in ethanol for several days (2-5) until all the chlorophyll was gone and the leaf was completely dark brown, nearly black, after this, washes with water to clean the NaOH residues were done and the leaf was transferred to bleach (sodium hypochlorite) for 24 hours or until it was clear, before the tissues start to disintegrate. After this, the leaf was stained with 1% saffarin in ethanol (modified from (McKown and Dengler, 2009)) at this point, the tissue was very delicate and easily broken, then careful manipulation was needed.

To estimate the vein density, pieces of the treated leaf as described above, were put under the light microscope and pictures were taken at the lower magnification 5x. Using image J the length of the primary and secondary veins was measured in a known area of 62.6 mm² and then added for each category to calculate length of vein (mm) per mm² of leaf. Primary veins were considered the larger and thicker veins which cross the leaf (Hickey, 1979) leaf architecture working group in (McKown and Dengler, 2009) and secondary veins those which arise from the primary and were more thinner, no other vein category was identifiable due to the thickness of the leaf.

Appendix 6: Collection and fixation of plant material for chromosome counting (Dr. I. Leitch and Dr. J. Pellice at Jodrell Laboratory Royal Botanic Gardens, Kew, by).

Root tips from very young plants were used for DNA amount estimations. Using clean forceps, healthy roots were removed from soil in the morning (better metaphases) and immediately placed in a glass collecting bottle, half filled with distilled water, around 5 -10 roots were collected in a 5 ml tube. Once the roots were in the laboratory, they were pre-treated by placing in a solution of 8 hydroxyquinoline (previously a 2mM solution was prepared with distilled water and incubated at 60°C bath with constant swirling) at fume hood and leave at room temperature for 3 hours. After this roots were fixed by transferring into a fresh solution of 3:1 ethanol: acetic acid. Roots were left at room temperature for up to 24 hours and then transfer to the fridge. Then fixed roots were sent to the laboratory in Kew for chromosome count.

References

- Abe H, Yamamoto KT, Nagatani A, Furuya M** (1985) Characterization of green tissue-specific phytochrome isolated immunochemically from pea-seedlings. *Plant and Cell Physiology* **26**: 1387-1399
- Adam E, Szell M, Szekeres M, Schaefer E, Nagy F** (1994) The developmental and tissue-specific expression of tobacco phytochrome-A genes. *Plant Journal* **6**: 283-293
- Adams P, Nelson DE, Yamada S, Chmara W, Jensen RG, Bohnert HJ, Griffiths H** (1998) Growth and development of *Mesembryanthemum crystallinum* (Aizoaceae). *New Phytologist* **138**: 171-190
- Ahmad M, Cashmore AR** (1993) HY4 gene of *A-thaliana* encodes a protein with characteristics of a blue-light photoreceptor. *Nature* **366**: 162-166
- Ahmad M, Jarillo JA, Smirnova O, Cashmore AR** (1998) The CRY1 blue light photoreceptor of *Arabidopsis* interacts with phytochrome A in vitro. *Molecular Cell* **1**: 939-948
- Ahmad MC, AR** (1997) The blue-light receptor cryptochrome 1 shows functional dependence on phytochrome A or phytochrome B in *Arabidopsis thaliana*. *Plant Journal* **11**: 421-427
- Ahmad MJ, JA; Smirnova** (1998) The CRY1 blue light photoreceptor of *Arabidopsis* interacts with phytochrome A in vitro. *Molecular Cell* **1**: 939-948
- Alba R, Kelmenson PM, Cordonnier-Pratt MM, Pratt LH** (2000) The phytochrome gene family in tomato and the rapid differential evolution of this family in angiosperms. *Molecular Biology and Evolution* **17**: 362-373
- Arakaki Mn, Christin P-A, Nyffeler R, Lendel A, Eggli U, Ogburn RM, Spriggs E, Moore MJ, Edwards EJ** (2011) Contemporaneous and recent radiations of the world's major succulent plant lineages. *Proceedings of the National Academy of Sciences* **108**: 8379-8384
- Assmann SM** (1993) Signal-Transduction in Guard-Cells. *Annual Review of Cell Biology* **9**: 345-375
- Assmann SM, Shimazaki K-i** (1999) The Multisensory Guard Cell. Stomatal Responses to Blue Light and Abscisic Acid. *Plant Physiol.* **119**: 809-816
- Assmann SM, Wang XQ** (2001) From milliseconds to millions of years: guard cells and environmental responses. *Current Opinion in Plant Biology* **4**: 421-428
- Ball E, Hann J, Kluge M, Lee HSJ, Luttge U, Orthen B, Popp M, Schmitt A, Ting IP** (1991) Ecophysiological comporment of the tropical CAM-tree *Clusia* in the field. *New Phytologist* **117**: 483-491
- Ball E, Hann J, Kluge M, Lee HSJ, Luttge U, Orthen B, Popp M, Schmitt A, Ting IP** (1991) Ecophysiological Comporment of the Tropical Cam-Tree *Clusia* in the Field .2. Modes of Photosynthesis in Trees and Seedlings. *New Phytologist* **117**: 483-491
- Batschauer AR, M; Kaiser, T; et al.** (1996) Blue and UV-A light-regulated CHS expression in *Arabidopsis* independent of phytochrome A and phytochrome B. *Plant Journal* **9**: 63-69
- Beaulieu JM, Leitch IJ, Patel S, Pendharkar A, Knight CA** (2008) Genome size is a strong predictor of cell size and stomatal density in angiosperms. *New Phytologist* **179**: 975-986

- Benzing DH** (1987) Vascular epiphytism - taxonomic participation and adaptive diversity. *Annals of the Missouri Botanical Garden* **74**: 183-204
- Berner RA** (1994) GEOCARB II; a revised model of atmospheric CO₂ over Phanerozoic time. *Am J Sci* **294**: 56-91
- Biosystems A** (2008) *In Applied Biosystems*, Vol 2011. Printed in the USA. 05/2008 Publication 136AP01-01
- Black CC** (1973) Photosynthetic carbon fixation in relation to net CO₂ uptake. *Annual Review of Plant Physiology and Plant Molecular Biology* **24**: 253-286
- Black CC, Chen JQ, Doong RL, Angelov MN, Sung SJS** (1996) Alternative carbohydrate reserves used in the daily cycle of crassulacean acid metabolism. *In* SJ Winter K, eds, ed, *Crassulacean acid metabolism: biochemistry, ecophysiology and evolution*, Vol 114. New York: Springer, Berlin, Heidelberg, pp 31-45
- Blatt MR** (2000) Cellular signaling and volume control in stomatal movements in plants. *Annual Review of Cell and Developmental Biology* **16**: 221-241
- Bohn A, Geist A, Rascher U, Luttge U** (2001) Responses to different external light rhythms by the circadian rhythm of Crassulacean acid metabolism in *Kalanchoe daigremontiana*. *Plant Cell and Environment* **24**: 811-820
- Borland AM, Dodd AN** (2002) Carbohydrate partitioning in crassulacean acid metabolism plants: reconciling potential conflicts of interest. *Functional Plant Biology* **29**: 707-716
- Borland AM GH, Maxwell C, Broadmeadow M S J, Griffiths N M, Barnes J. D.** (1992) On the Ecophysiology of the Clusiaceae in Trinidad - Expression of CAM in *Clusia-Minor* L During the Transition from Wet to Dry Season and Characterization of 3 Endemic Species. *New Phytologist* **122**: 349-357
- Borland AM, Griffiths H** (1990) The regulation of CAM and respiratory recycling by water-supply and light regime in the C3-CAM intermediate *Sedum-telephium*. *Functional Ecology* **4**: 33-39
- Borland AM, Griffiths H** (1992) Properties of Phosphoenolpyruvate carboxylase and carbohydrate accumulation in the C3-CAM intermediate *Sedum-Telephium* L grown under different light and watering regimes. *Journal of Experimental Botany* **43**: 353-361
- Borland AM, Griffiths H, Broadmeadow MSJ, Fordham MC, Maxwell C** (1994) Carbon-isotope composition of biochemical fractions and the regulation of carbon balance in leaves of the C3 crassulacean acid metabolism intermediate *Clusia minor* L growing in Trinidad. *Plant Physiology* **106**: 493-501
- Borland AM, Griffiths H, Hartwell J, Smith JAC** (2009) Exploiting the potential of plants with crassulacean acid metabolism for bioenergy production on marginal lands. *Journal of Experimental Botany* **60**: 2879-2896
- Borland AM, Griffiths H, Maxwell C, Broadmeadow MSJ, Griffiths NM, Barnes JD** (1992) On the ecophysiology of the Clusiaceae in Trinidad - expression of CAM in *Clusia-Minor* L during the transition from wet to dry season and characterization of 3 endemic species. *New Phytologist* **122**: 349-357
- Borland AM, Griffiths H, Maxwell C, Fordham MC, Broadmeadow MSJ** (1996) CAM induction in *Clusia minor* L. during the transition from wet to dry season in Trinidad: the role of organic acid speciation and decarboxylation. *Plant, Cell & Environment* **19**: 655-664
- Borland AM, Maxwell K, Griffiths H** (2000) Ecophysiology of Plants with Crassulacean Acid Metabolism. *In* vCSe Leegood R. C. STD, ed,

- Photosynthesis: Physiology and Metabolism. Kluwer Academic Publishers, Netherlands, pp 583-605
- Borland AM, Taybi T** (2004) Synchronization of metabolic processes in plants with Crassulacean acid metabolism. *Journal of Experimental Botany* **55**: 1255-1265
- Borland AM, Tecsli LI, Leegood RC, Walker RP** (1998) Inducibility of crassulacean acid metabolism (CAM) in *Clusia* species; physiological/biochemical characterisation and intercellular localization of carboxylation and decarboxylation processes in three species which exhibit different degrees of CAM. *Planta* **205**: 342-351
- Bowler C, Vancamp W, Vanmontagu M, Inze D** (1994) Superoxide-dismutase in plants. *Critical Reviews in Plant Sciences* **13**: 199-218
- Boxall SF, Foster JM, Bohnert HJ, Cushman JC, Nimmo HG, Hartwell J** (2005) Conservation and divergence of circadian clock operation in a stress-inducible Crassulacean acid metabolism species reveals clock compensation against stress. *Plant Physiology* **137**: 969-982
- Briggs WR, Christie JM** (2002) Phototropins 1 and 2: versatile plant blue-light receptors. *Trends in Plant Science* **7**: 204-210
- Briggs WR, Huala E** (1999) Blue-light photoreceptors in higher plants. *Annual Review of Cell and Developmental Biology* **15**: 33-62
- Briggs WR, Tseng T-S, Cho H-Y, Swartz TE, Sullivan S, Bogomolni RA, Kaiserli E, Christie JM** (2007) Phototropins and Their LOV Domains: Versatile Plant Blue-Light Receptors. *Journal of Integrative Plant Biology* **49**: 4-10
- Brodribb TJ, Feild TS, Jordan GJ** (2007) Leaf maximum photosynthetic rate and venation are linked by hydraulics ($1[W][OA]$). *Plant Physiology* **144**: 1890-1898
- Brodribb TJ, Holbrook NM** (2003) Stomatal closure during leaf dehydration, correlation with other leaf physiological traits. *Plant Physiology* **132**: 2166-2173
- Brulfert J, Guerrier D, Queiroz O** (1975) Photoperiodism and enzyme rhythms: Kinetic characteristics of the photoperiodic induction of Crassulacean acid metabolism. *Planta* **125**: 33-44
- Brulfert J, Kluge M, Guclu S, Queiroz O** (1988) Combined effects of drought, daylength and photoperiod on rapid shifts in the photosynthetic pathways of *Sedum spectabile*, a CAM species. *Plant Physiology and Biochemistry* **26**: 7-16
- Brulfert J, Queiroz O** (1982) Photoperiodism and crassulacean acid metabolism .3. different characteristics of the photoperiod-sensitive and nonsensitive isoforms of phosphoenolpyruvate carboxylase and crassulacean acid metabolism operation. *Planta* **154**: 339-343
- Buckley TN** (2008) The role of stomatal acclimation in modelling tree adaptation to high CO₂. *Journal of Experimental Botany* **59**: 1951-1961
- Burger A** (2008) Mexico and agaves: moving from tequila to ethanol in: <http://www.renewableenergyworld.com/rea/news/story?id%453265>. In,
- Carter PJ, Nimmo HG, Fewson CA, Wilkins MB** (1991) Circadian-rhythms in the activity of a plant protein-kinase. *Embo Journal* **10**: 2063-2068
- Casal JJ, Mazzella MA** (1998) Conditional synergism between cryptochrome 1 and phytochrome B is shown by the analysis of phyA, phyB, and hy4 simple, double, and triple mutants in *Arabidopsis*. *Plant Physiology* **118**: 19-25
- Cashmore A** (1998) The cryptochrome family of blue/UV-A photoreceptors. *Journal of Plant Research* **111**: 267-270
- Casson S, Gray JE** (2008) Influence of environmental factors on stomatal development. *New Phytologist* **178**: 9-23

- Celaya RB, Liscum E** (2005) Phototropins and associated signaling: Providing the power of movement in higher plants. *Photochemistry and Photobiology* **81**: 73-80
- Cerling T. E. WY, Quade Jay** (1993) Expansion of C4 ecosystems as an indicator of global ecological change in the late Miocene. *Nature* **361**: 344 - 345
- Cerling TE, Wang Y, Quade J** (1993) Expansion of C4 ecosystems as an indicator of global ecological change in the late miocene. *Nature* **361**: 344-345
- Ceulemans R, Mousseau M** (1994) Tansley review no-71 - effects of elevated atmospheric CO₂ on woody-plants. *New Phytologist* **127**: 425-446
- Chapin FS, Rincon E, Huante P** (1993) Environmental responses of plants and ecosystems as predictors of the impact of global change. *Journal of Biosciences* **18**: 515-524
- Christie JM** (2007) Phototropin Blue-Light Receptors. *Annual Review of Plant Biology* **58**: 21-45
- Christie JM, Reymond P, Powell GK, Bernasconi P, Raibekas AA, Liscum E, Briggs WR** (1998) Arabidopsis NPH1: A flavoprotein with the properties of a photoreceptor for phototropism. *Science* **282**: 1698-1701
- Clack T, Mathews S, Sharrock RA** (1994) The phytochrome apoprotein family in arabidopsis is encoded by 5 genes - the sequences and expression of phy D and phy E. *Plant Molecular Biology* **25**: 413-427
- Clack T, Mathews S, Sharrock RA** (1994) THE PHYTOCHROME APOPROTEIN FAMILY IN ARABIDOPSIS IS ENCODED BY 5 GENES - THE SEQUENCES AND EXPRESSION OF PHYD AND PHYE. *Plant Molecular Biology* **25**: 413-427
- Clifford SC, Black CR, Roberts JA, Stronach IM, Singletonjones PR, Mohamed AD, Azamali SN** (1995) The effect of elevated atmospheric CO₂ and drought on stomatal frequency in groundnut (*Arachis hypogaea* (l)). *Journal of Experimental Botany* **46**: 847-852
- Conti S, Smirnoff N** (1994) Rapid triggering of malate accumulation in the C3/CAM intermediate plant sedum-telephium - relationship with water status and phosphoenolpyruvate carboxylase. *Journal of Experimental Botany* **45**: 1613-1621
- Crayn DM, Winter K, Smith JAC** (2004) Multiple origins of crassulacean acid metabolism and the epiphytic habit in the Neotropical family Bromeliaceae. *Proceedings of the National Academy of Sciences of the United States of America* **101**: 3703-3708
- Cruz ND, Sellito-Boaventura YM, Sellito YM** (1990) Cytological studies of some species of the genus *Clusia* L. (Guttiferae). *Rev. Basil Genet.* **12**: 335-345
- Cunningham SA, Summerhayes B, Westoby M** (1999) Evolutionary divergences in leaf structure and chemistry, comparing rainfall and soil nutrient gradients. *Ecological Monographs* **69**: 569-588
- Cushman JC** (2001) Crassulacean acid metabolism. A plastic photosynthetic adaptation to arid environments. *Plant Physiology* **127**: 1439-1448
- Cushman JC, Bohnert HJ** (1996) Transcriptional activation of CAM genes during development and environmental stress. *Crassulacean Acid Metabolism* **114**: 135-158
- Cushman JC, Bohnert HJ** (1999) Crassulacean acid metabolism: Molecular Genetics. *Annual Review of Plant Physiology and Plant Molecular Biology* **50**: 305-332
- Cushman JC, Borland AM** (2002) Induction of Crassulacean acid metabolism by water limitation. *Plant Cell and Environment* **25**: 295-310

- Cushman JC, Meyer G, Michalowski CB, Schmitt JM, Bohnert HJ** (1989) Salt stress leads to differential expression of 2 isogenes of phosphoenolpyruvate carboxylase during crassulacean acid metabolism induction in the common ice plant. *Plant Cell* **1**: 715-725
- Cushman JC, Tillett RL, Wood JA, Branco JM, Schlauch KA** (2008) Large-scale mRNA expression profiling in the common ice plant, *Mesembryanthemum crystallinum*, performing C-3 photosynthesis and Crassulacean acid metabolism (CAM). *Journal of Experimental Botany* **59**: 1875-1894
- Cutter JM, Rains, D.W., Loomis, R.S.** (1977) The importance of cell size in the water relations of plants. *Physiol Plant* **40**: 255–260
- Dean JD, Goodwin PH, Hsiang T** (2002) Comparison of relative RT-PCR and northern blot analyses to measure expression of beta-1,3-glucanase in *Nicotiana benthamiana* infected with *Colltotrichum destructivum*. *Plant Molecular Biology Reporter* **20**: 347-356
- Deitzer GF, Frosch SH** (1990) Multiple action of far-red light in photoperiodic induction and circadian rhythmicity. *Photochemistry and Photobiology* **52**: 173-179
- Devlin PF** (2002) Signs of the time: environmental input to the circadian clock. *Journal of Experimental Botany* **53**: 1535-1550
- Devlin PF, Kay SA** (2000) Cryptochromes are required for phytochrome signaling to the circadian clock but not for rhythmicity. *Plant Cell* **12**: 2499-2509
- Diaz M, HaagKerwer A, Wingfield R, Ball E, Olivares E, Grams TEE, Ziegler H, Luttge U** (1996) Relationships between carbon and hydrogen isotope ratios and nitrogen levels in leaves of *Clusia* species and two other *Clusiaceae* genera at various sites and different altitudes in Venezuela. *Trees-Structure and Function* **10**: 351-358
- Dodd AN, Borland AM, Haslam RP, Griffiths H, Maxwell K** (2002) Crassulacean acid metabolism: plastic, fantastic. *Journal of Experimental Botany* **53**: 569-580
- Drennan PM, Nobel PS** (2000) Responses of CAM species to increasing atmospheric CO₂ concentrations. *Plant Cell and Environment* **23**: 767-781
- Eckert M, Kaldenhoff R** (2000) Light induced stomatal movement of selected *Arabidopsis thaliana* mutants. *Journal of Experimental Botany* **51**: 1435-1442
- Edmunds LN, Jr.** (1988) Cellular and molecular bases of biological clocks. Models and mechanisms for circadian timekeeping. *Cellular and molecular bases of biological clocks. Models and mechanisms for circadian timekeeping.*: i-xix, 1-497
- Ehleringer JR, Cerling TE** (1998) C₃ and C₄ Photosynthesis. *In* PHAMaDJG Canadell, ed, *Encyclopedia of Global Environmental Change, Vol Volume 2, The Earth system: biological and ecological dimensions of global environmental change.* John Wiley & Sons, Ltd, , Chichester, pp 186–190
- Ehleringer JR, Monson RK** (1993) Evolutionary and Ecological Aspects of Photosynthetic Pathway Variation. *Annual Review of Ecology and Systematics* **24**: 411-439
- Evans JR, Voncaemmerer S, Setchell BA, Hudson GS** (1994) The relationship between CO₂ transfer conductance and leaf anatomy in transgenic tobacco with a reduced content of Rubisco. *Australian Journal of Plant Physiology* **21**: 475-495

- Farquhar GD, Dubbe DR, Raschke K** (1978) Gain of feedback loop involving carbon-dioxide and stomata - theory and measurement. *Plant Physiology* **62**: 406-412
- Farquhar GD, Wong SC** (1984) An empirical-model of stomatal conductance. *Australian Journal of Plant Physiology* **11**: 191-209
- Fejes E, Nagy F** (1998) Molecular analysis of circadian clock-regulated gene expression in plants: features of the 'output' pathways. *In* MAe Lumsden PJ, ed, *Biological Rhythms and Photoperiodism in Plants*. BIOS Scientific Publishers, Oxford, pp 99–118
- Fondom NY, Castro-Nava S, Huerta AJ** (2009) Seasonal variation in photosynthesis and diel carbon balance under natural conditions in two *Peperomia* species that differ with respect to leaf anatomy. *Journal of the Torrey Botanical Society* **136**: 57-69
- Franco A, Herzog B, Hubner C, de Mattos E, Scarano F, Ball E, Luttge U** (1999) Diurnal changes in chlorophyll a fluorescence, CO₂-exchange and organic acid decarboxylation in the tropical CAM tree *Clusia hilariana*. *TREE PHYSIOLOGY* **19**: 635-644
- Franks PJ, Drake PL, Beerling DJ** (2009) Plasticity in maximum stomatal conductance constrained by negative correlation between stomatal size and density: an analysis using *Eucalyptus globulus*. *Plant, Cell & Environment* **32**: 1737-1748
- Franks PJ, Farquhar GD** (2007) The Mechanical Diversity of Stomata and Its Significance in Gas-Exchange Control. *Plant Physiol.* **143**: 78-87
- Freeman WM, Walker SJ, Vrana KE** (1999) Quantitative RT-PCR: Pitfalls and potential. *Biotechniques* **26**: 112-+
- Garnier E, Laurent G** (1994) Leaf Anatomy, Specific Mass and Water-Content in Congeneric Annual and Perennial Grass Species. *New Phytologist* **128**: 725-736
- Gay AP, Hurd RG** (1975) Influence of light on stomatal density in tomato. *New Phytologist* **75**: 37-46
- Gehrig HH, Aranda J, Cushman MA, Virgo A, Cushman JC, Hammel BE, Winter K** (2003) Cladogram of Panamanian *Clusia* based on nuclear DNA: Implications for the origins of crassulacean acid metabolism. *Plant Biology* **5**: 59-70
- Gehrig HH, Heute V, Kluge M** (1998) Toward a Better Knowledge of the Molecular Evolution of Phosphoenolpyruvate Carboxylase by Comparison of Partial cDNA Sequences. *Journal of Molecular Evolution* **46**: 107-114
- Gentle A, Anastasopoulos F, McBrien NA** (2001) High-resolution semi-quantitative real-time PCR without the use of a standard curve. *Biotechniques* **31**: 502-+
- Gibeaut DM, Thomson WW** (1989) Leaf ultrastructure of *Peperomia-obtusifolia*, *Peperomia-campotricha*, and *Peperomia-scandens*. *Botanical Gazette* **150**: 108-114
- Gibson AC** (1982) The anatomy of succulence. *In* GM Ting IP, eds, ed, *Crassulacean acid metabolism*. American Society of Plant Physiologists, Rockville
- Gil F** (1986) Origin of Cam as an Alternative Photosynthetic Carbon Fixation Pathway. *Photosynthetica* **20**: 494-507
- Giuliano G, Hoffman NE, Ko K, Scolnik PA, Cashmore AR** (1988) A light-entrained circadian clock controls transcription of several plant genes. *Embo Journal* **7**: 3635-3642

- Giulietti A, Overbergh L, Valckx D, Decallonne B, Bouillon R, Mathieu C** (2001) An overview of real-time quantitative PCR: Applications to quantify cytokine gene expression. *Methods* **25**: 386-401
- Givnish TJ** (1988) Adaptation to sun and shade - a whole-plant perspective. *Australian Journal of Plant Physiology* **15**: 63-92
- Glasel JA, Agarwal D** (1995) Anti-idiotypic antibodies that mimic opioids. *Methods in Molecular Biology; Antibody engineering protocols*: 183-201
- Goh CH, Schreiber U, Hedrich R** (1999) New approach of monitoring changes in chlorophyll a fluorescence of single guard cells and protoplasts in response to physiological stimuli. *Plant Cell and Environment* **22**: 1057-1070
- Gorton HL, Williams WE, Assmann SM** (1993) Circadian-rhythms in stomatal responsiveness to red and blue-light. *Plant Physiology* **103**: 399-406
- Grams TEE, HaagKerwer A, Olivares E, Ball E, Arndt S, Popp M, Medina E, Luttge U** (1997) Comparative measurements of chlorophyll a fluorescence, acid accumulation and gas exchange in exposed and shaded plants of *Clusia minor* L and *Clusia multiflora* H B K in the field. *Trees-Structure and Function* **11**: 240-247
- Grams TEE, Herzog B, Luttge U** (1998) Are there species in the genus *Clusia* with obligate C-3-photosynthesis? *Journal of Plant Physiology* **152**: 1-9
- Griffiths H** (1992) Carbon isotope discrimination and the integration of carbon assimilation pathways in terrestrial CAM plants. *Plant, Cell & Environment* **15**: 1051-1062
- Griffiths H, Cousins AB, Badger MR, von Caemmerer S** (2007) Discrimination in the Dark. Resolving the Interplay between Metabolic and Physical Constraints to Phosphoenolpyruvate Carboxylase Activity during the Crassulacean Acid Metabolism Cycle. *Plant Physiol.* **143**: 1055-1067
- Griffiths H, Cousins AB, Badger MR, von Caemmerer S** (2007) Discrimination in the dark. Resolving the interplay between metabolic and physical constraints to phosphoenolpyruvate carboxylase activity during the crassulacean acid metabolism cycle. *Plant Physiology* **143**: 1055-1067
- Griffiths H, Helliker B, Roberts A, Haslam RP, Girnus J, Robe WE, Borland AM, Maxwell K** (2002) Regulation of Rubisco activity in crassulacean acid metabolism plants: better late than never. *Functional Plant Biology* **29**: 689-696
- Gustafsson MHG, Bittrich V** (2002) Evolution of morphological diversity and resin secretion in flowers of *Clusia* (Clusiaceae): insights from ITS sequence variation. *Nordic Journal of Botany* **22**: 183-203
- Hall A, Kozma-Bognar L, Toth R, Nagy F, Millar AJ** (2001) Conditional circadian regulation of PHYTOCHROME A gene expression. *Plant Physiol.* **127**: 1808-1818
- Hall RD, RiksenBruinsma T, Weyens G, Lefebvre M, Dunwell JM, Krens FA** (1996) Stomatal guard cells are totipotent. *Plant Physiology* **112**: 889-892
- Harmer SL, Hogenesch JB, Straume M, Chang H-S, Han B, Zhu T, Wang X, Kreps JA, Kay SA** (2000) Orchestrated transcription of key pathways in *Arabidopsis* by the circadian clock. *Science* **290**: 2110-2113
- Hartwell J** (2005) The co-ordination of central plant metabolism by the circadian clock. *Biochemical Society Transactions* **33**: 945-948
- Hartwell J, Smith LH, Wilkins MB, Jenkins GI, Nimmo HG** (1996) Higher plant phosphoenolpyruvate carboxylase kinase is regulated at the level of translatable mRNA in response to light or a circadian rhythm. *Plant Journal* **10**: 1071-1078

- Hauser BA, Cordonnier-Pratt MM, Pratt LH** (1998) Temporal and photoregulated expression of five tomato phytochrome genes. *Plant Journal* **14**: 431-439
- Hennessey TL, Field CB** (1991) Circadian-rhythms in photosynthesis - oscillations in carbon assimilation and stomatal conductance under constant conditions. *Plant Physiology* **96**: 831-836
- Herzog B, Hoffmann S, Hartung W, Luttge U** (1999) Comparison of photosynthetic responses of the sympatric tropical C-3 species *Clusia multiflora* H. B. K. and the C-3-CAM intermediate species *Clusia minor* L. to irradiance and drought stress in a phytotron. *Plant Biology* **1**: 460-470
- Hetherington AM, Woodward FI** (2003) The role of stomata in sensing and driving environmental change. *Nature* **424**: 901-908
- Hickey LJ** (1979) A revised classification of the architecture of dicotyledonous leaves. . In CL Metcalfe CR, editors, ed, *Systematic anatomy of leaf and stem, with a brief history of the subject. Anatomy of the dicotyledons*, Ed 2nd Vol 1. Oxford University press, New York, pp 25-39
- Hillman WS, Koukkari WL** (1967) Phytochrome effects in nyctinastic leaf movements of *Albizia julibrissin* and some other legumes. *Plant Physiology* **42**: 1413-&
- Holtum JAM, Aranda J, Virgo A, Gehrig HH, Winter K** (2004) delta C-13 values and crassulacean acid metabolism in *Clusia* species from Panama. *Trees-Structure and Function* **18**: 658-668
- Holtum JAM, Winter K, Weeks MA, Sexton TR** (2007) Crassulacean acid metabolism in the ZZ plant, *Zamioculcas zamiifolia* (Araceae). *Am. J. Bot.* **94**: 1670-1676
- Holum JR** (1994) *Fundamentals of General, Organic and Biological Chemistry*,
- Horwitz BA, Berrocal GM** (1997) A spectroscopic view of some recent advances in the study of blue light photoreception. *Botanica Acta* **110**: 360-368
<http://pathmicro.med.sc.edu/pcr/realtime-home.htm>. In, Vol 2011
- Humble GD, Raschke K** (1971) Stomatal opening quantitatively related to potassium transport - evidence from electron probe analysis. *Plant Physiology* **48**: 447-&
- Inoue S, Kinoshita T, Matsumoto M, Nakayama KI, Doi M, Shimazaki K** (2008) Blue light-induced autophosphorylation of phototropin is a primary step for signaling. *Proceedings of the National Academy of Sciences of the United States of America* **105**: 5626-5631
- Jarvis AJ, Davies WJ** (1998) The coupled response of stomatal conductance to photosynthesis and transpiration. *Journal of Experimental Botany* **49**: 399-406
- Johnson CH, Golden SS** (1999) Circadian programs in cyanobacteria: Adaptiveness and mechanism. *Annual Review of Microbiology* **53**: 389-409
- Johnson CH, Golden SS, Kondo T** (1998) Adaptive significance of circadian programs in cyanobacteria. *Trends in Microbiology* **6**: 407-410
- Johnson CH, Hiroshige T, Honma K-i** (1992) Phase response curves: what can they tell us about circadian clocks? Circadian clocks from cell to human. *Proceedings of the Fourth Sapporo Symposium on Biological Rhythm*. August 21-23, 1991.: 209-246
- Johnson E, Bradley M, Harberd NP, Whitelam GC** (1994) Photoresponses of light-grown phyA mutants of *Arabidopsis* - phytochrome-a is required for the perception of day length extensions. *Plant Physiology* **105**: 141-149
- Jones HG** (1992) *Plants and microclimate: a quantitative approach to environmental plant physiology*. Cambridge University Press

- Kagawa T, Kasahara M, Abe T, Yoshida S, Wada M** (2004) Function analysis of phototropin2 using fern mutants deficient in blue light-induced chloroplast avoidance movement. *Plant and Cell Physiology* **45**: 416-426
- Kagawa T, Wada M** (2002) Blue light-induced chloroplast relocation. *Plant and Cell Physiology* **43**: 367-371
- Kaiser H** (2009) The relation between stomatal aperture and gas exchange under consideration of pore geometry and diffusional resistance in the mesophyll. *Plant, Cell & Environment* **32**: 1091-1098
- Kana TM, Miller JH** (1977) Effect of photoperiod on stomatal opening in *Vicia-faba*. *Plant Physiology* **60**: 803-804
- Kasahara M, Kagawa T, Sato Y, Kiyosue T, Wada M** (2004) Phototropins Mediate Blue and Red Light-Induced Chloroplast Movements in *Physcomitrella patens*. *Plant Physiol.* **135**: 1388-1397
- Kasahara M, Swartz TE, Olney MA, Onodera A, Mochizuki N, Fukuzawa H, Asamizu E, Tabata S, Kanegae H, Takano M, Christie JM, Nagatani A, Briggs WR** (2002) Photochemical properties of the flavin mononucleotide-binding domains of the phototropins from *Arabidopsis*, rice, and *Chlamydomonas reinhardtii*. *Plant Physiology* **129**: 762-773
- Kawai H, Kanegae T, Christensen S, Kiyosue T, Sato Y, Imaizumi T, Kadota A, Wada M** (2003) Responses of ferns to red light are mediated by an unconventional photoreceptor. *Nature* **421**: 287-290
- Kendrick RE, Kronenberg, G.H.M.** (1994) *Photomorphogenesis in plants*. Kluwer Academic Publishers, Dordrecht
- Kenzo T, Ichie T, Yoneda R, Kitahashi Y, Watanabe Y, Ninomiya I, Koike T** (2004) Interspecific variation of photosynthesis and leaf characteristics in canopy trees of five species of Dipterocarpaceae in a tropical rain forest. *Tree Physiology* **24**: 1187-1192
- Kinoshita T, Doi M, Suetsugu N, Kagawa T, Wada M, Shimazaki K** (2001) phot1 and phot2 mediate blue light regulation of stomatal opening. *Nature* **414**: 656-660
- Kinoshita T, Emi T, Tominaga M, Sakamoto K, Shigenaga A, Doi M, Shimazaki K** (2003) Blue-light- and phosphorylation-dependent binding of a 14-3-3 protein to phototropins in stomatal guard cells of broad bean. *Plant Physiology* **133**: 1453-1463
- Kircher S, Kozma-Bognar L, Kim L, Adam E, Harter K, Schafer E, Nagy F** (1999) Light quality-dependent nuclear import of the plant photoreceptors phytochrome A and B. *Plant Cell* **11**: 1445-1456
- Kluge M, Brulfert J, Lipp J, Ravelomanana D, Ziegler H** (1993) A comparative-study by delta-c-13-analysis of crassulacean acid metabolism (CAM) in *Kalanchoe* (crassulaceae) species of Africa and Madagascar. *Botanica Acta* **106**: 320-324
- Kluge M, Brulfert J, Ravelomanana D, Lipp J, Ziegler H** (1991) Crassulacean acid metabolism in *Kalanchoe* species collected in various climatic zones of Madagascar - a survey by delta-c-13 analysis. *Oecologia* **88**: 407-414
- Kluge M, I. P. TING.** (1987) *CAM: analysis of an ecological adaptation*. Springer-Verlag, Berlin.
- Kluge M, Razanoelisoa B, Brulfert J** (2001) Implications of genotypic diversity and phenotypic plasticity in the ecophysiological success of CAM plants, examined by studies on the vegetation of Madagascar. *Plant Biology* **3**: 214-222

- Kluge M, Razanoelisoa B, Ravelomanana D, Brulfert J** (1992) In situ studies of Crassulacean Acid Metabolism in *Kalanchoe-Beharensis* Delcastillo, Drake, a Plant of the Semiarid Southern Region of Madagascar. *New Phytologist* **120**: 323-334
- Kozlowski TT, Pallardy SG** (2002) Acclimation and adaptive responses of woody plants to environmental stresses. *Botanical Review* **68**: 270-334
- Kreps JA, Kay SA** (1997) Coordination of plant metabolism and development by the circadian clock. *Plant Cell* **9**: 1235-1244
- Kuiper PJ** (1964) Dependence upon wavelength of stomatal movement in epidermal tissue of *Senecio odoris*. *Plant Physiology* **39**: 952-955
- Laemmli UK** (1970) CLEAVAGE OF STRUCTURAL PROTEINS DURING ASSEMBLY OF HEAD OF BACTERIOPHAGE-T4. *Nature* **227**: 680-&
- Lakin-Thomas PL** (2000) Circadian rhythms - new functions for old clock genes? *Trends in Genetics* **16**: 135-142
- Landrum J** (2002) Four succulent families and 40 million years of evolution and adaptation to xeric environments: What can stem and leaf anatomical characters tell us about their phylogeny? *TAXON* **51**: 463-473
- Lüttge U** (2004) Ecophysiology of Crassulacean Acid Metabolism (CAM). *Annals of Botany* **93**: 629-652
- Laws EA, B. N, Popp, R. R., Bidigare, U. Riebesell, S. Burkhardt, and S. G. Wakeham** (2001) Controls on the molecular distribution and carbon isotopic composition of alkenones in certain haptophyte algae. *Geochem. Geophys. Geosyst* **2**
- Lawson T, James W, Weyers J** (1998) A surrogate measure of stomatal aperture. *Journal of Experimental Botany* **49**: 1397-1403
- Lawson T, Lefebvre S, Baker NR, Morison JIL, Raines CA** (2008) Reductions in mesophyll and guard cell photosynthesis impact on the control of stomatal responses to light and CO₂. *Journal of Experimental Botany* **59**: 3609-3619
- Lawson T, Oxborough K, Morison JIL, Baker NR** (2002) Responses of photosynthetic electron transport in stomatal guard cells and mesophyll cells in intact leaves to light, CO₂, and humidity. *Plant Physiology* **128**: 52-62
- Lawson T, Oxborough K, Morison JIL, Baker NR** (2003) The responses of guard and mesophyll cell photosynthesis to CO₂, O₂, light, and water stress in a range of species are similar. *Journal of Experimental Botany* **54**: 1743-1752
- Lawson T, Weyers J, A'Brook R** (1998) The nature of heterogeneity in the stomatal behaviour of *Phaseolus vulgaris* L. primary leaves. *Journal of Experimental Botany* **49**: 1387-1395
- Lee DM, Assmann SM** (1992) Stomatal responses to light in the facultative crassulacean acid metabolism species, *Portulacaria-Afra*. *Physiologia Plantarum* **85**: 35-42
- Lee HSJ, Lüttge U, Medina E, Smith JAC, Cram WJ, Diaz M, Griffiths H, Popp M, Schafer C, Stimmel KH, Thonke B** (1989) Ecophysiology of xerophytic and halophytic vegetation of a coastal alluvial plain in northern Venezuela .3. *Bromelia-humilis* jacq, a terrestrial CAM bromeliad. *New Phytologist* **111**: 253-271
- Lee HSJ, Schmitt AK, Lüttge U** (1989) The Response of the C₃-CAM Tree, *Clusia rosea*, to Light and Water Stress. *Journal of Experimental Botany* **40**: 171-179
- Lee JS** (2010) Stomatal opening mechanism of CAM plants. *Journal of Plant Biology* **53**: 19-23

- Lee JS, Bowling DJF** (1995) Influence of the Mesophyll on Stomatal Opening. *Australian Journal of Plant Physiology* **22**: 357-363
- Lin CT, Ahmad M, Cashmore AR** (1996) Arabidopsis cryptochrome 1 is a soluble protein mediating blue light-dependent regulation of plant growth and development. *Plant Journal* **10**: 893-902
- Lin CT, Yang HY, Guo HW, Mockler T, Chen J, Cashmore AR** (1998) Enhancement of blue-light sensitivity of Arabidopsis seedlings by a blue light receptor cryptochrome 2. *Proceedings of the National Academy of Sciences of the United States of America* **95**: 2686-2690
- Long SP, Hallgren JE** (1993) Measurement of CO₂ assimilation by plants in the field and laboratory. *In* SJ Hall DO, Bolhar-Nordenkamp HR, Leegood RC, Long SP, eds, ed, *Photosynthesis and productivity in a changing environment: a field and laboratory manual*. Chapman and Hall, London, pp 129–167
- Lüttge U** (1999) One morphotype, three physiotypes: Sympatric species of *Clusia* with obligate C-3 photosynthesis, obligate CAM and C-3-CAM intermediate behaviour. *Plant Biology* **1**: 138-148
- Lüttge U** (1987) Carbon-dioxide and water demand - crassulacean acid metabolism (CAM), a versatile ecological adaptation exemplifying the need for integration in ecophysiological work. *New Phytologist* **106**: 593-629
- Lüttge U** (2000) Light-stress and crassulacean acid metabolism. *Phyton-Annales Rei Botanicae* **40**: 65-82
- Lüttge U** (2002) CO₂-concentrating: Consequences in crassulacean acid metabolism. *Journal of Experimental Botany* **53**: 2131-2142
- Lüttge U** (2004) Ecophysiology of Crassulacean Acid Metabolism (CAM). *Annals of Botany* **93**: 629-652
- Lüttge U** (2006) Photosynthetic flexibility and ecophysiological plasticity: questions and lessons from *Clusia*, the only CAM tree, in the neotropics (vol 171, pg 7, 2006). *New Phytologist* **171**: 683-683
- Lüttge U** (2007) *Clusia*: a woody neotropical genus of remarkable plasticity and diversity.
- Lüttge U** (2008) Stem CAM in arborescent succulents. *Trees-Structure and Function* **22**: 139-148
- Lüttge U, Duarte HM, Scarano FR, de Mattos EA, Cavalin PO, Franco AC, Fernandes GW** (2007) Physiological ecology of photosynthesis of five sympatric species of Velloziaceae in the rupestrian fields of Serra do Cipo, Minas Gerais, Brazil. *Flora* **202**: 637-646
- Lüttge U, Gustafsson MHG, Winter K, Bittrich V** (2007) Diversity, Phylogeny and Classification of *Clusia*. *In* *Clusia*, Vol 194. Springer Berlin Heidelberg, pp 95-116
- Maguire B** (1976) Apomixis in genus *Clusia* (Clusiaceae) - preliminary-report. *Taxon* **25**: 241-244
- Mansfield TA** (1963) Length of night as a factor determining stomatal behaviour in Soybean. *Physiologia Pl* **16**: 523
- Mansfield TA** (1986) The physiology of stomata: new insights into old problems. *In* FS JF Sutcliffe, JE Dale, eds, ed, *Plant Physiology: A Treatise*, Vol 9. Academic Press, New York, pp 155-224
- Mansfield TA, Heath OVS** (1963) Studies in stomatal behaviour. IX. Photoperiodic effects on rhythmic phenomena in *Xanthium pennsylvanicum*. *J. Exp. Bot.* **14**: 334

- Mao J, Zhang YC, Sang Y, Li QH, Yang HQ** (2005) A role for Arabidopsis cryptochromes and COP1 in the regulation of stomatal opening. *Proceedings of the National Academy of Sciences of the United States of America* **102**: 12270-12275
- Martinocatt S, Ort DR** (1992) Low-temperature interrupts circadian regulation of transcriptional activity in chilling-sensitive plants. *Proceedings of the National Academy of Sciences of the United States of America* **89**: 3731-3735
- Maxwell K** (2002) Resistance is useful: diurnal patterns of photosynthesis in C-3 and crassulacean acid metabolism epiphytic bromeliads. *Functional Plant Biology* **29**: 679-687
- Maxwell K, VonCaemmerer S, Evans JR** (1997) Is a low internal conductance to CO₂ diffusion a consequence of succulence in plants with crassulacean acid metabolism? *Australian Journal of Plant Physiology* **24**: 777-786
- McClung CR** (1997) Regulation of catalases in Arabidopsis. *Free Radical Biology and Medicine* **23**: 489-496
- McClung CR** (2000) Circadian rhythms in plants: a millennial view. *Physiologia Plantarum* **109**: 359-371
- McKown AD, Dengler NG** (2007) Key innovations in the evolution of Kranz anatomy and C-4 vein pattern in Flavea (Asteraceae). *American Journal of Botany* **94**: 382-399
- McKown AD, Dengler NG** (2009) Shifts in leaf vein density through accelerated vein formation in C-4 Flaveria (Asteraceae). *Annals of Botany* **104**: 1085-1098
- McKown AD, Moncalvo JM, Dengler NG** (2005) Phylogeny of Flaveria (Asteraceae) and inference of C-4 photosynthesis evolution. *American Journal of Botany* **92**: 1911-1928
- McWatters HG, Bastow RM, Hall A, Millar AJ** (2000) The ELF3 zeitnehmer regulates light signalling to the circadian clock. *Nature* **408**: 716-720
- Medina E, Aguiar G, Gomez M, Aranda J, Medina JD, Winter K** (2006) Taxonomic significance of the epicuticular wax composition in species of the genus *Clusia* from Panama. *Biochemical Systematics and Ecology* **34**: 319-326
- Meidner H MeT** (1968) *Physiology of stomata*. McGraw Hill., London
- Messinger SM, Buckley TN, Mott KA** (2006) Evidence for involvement of photosynthetic processes in the stomatal response to CO₂. *Plant Physiology* **140**: 771-778
- Millar AJ, Kay SA** (1991) Circadian control of CAB gene-transcription and messenger-RNA accumulation in Arabidopsis. *Plant Cell* **3**: 541-550
- Minai L, Wostrikoff K, Wollman F, Choquet Y** (2006) Chloroplast biogenesis of photosystem II cores involves a series of assembly-controlled steps that regulate translation. *Plant Cell* **18**: 159-175
- Morison JIL, Gallouet E, Lawson T, Cornic G, Herbin R, Baker NR** (2005) Lateral diffusion of CO₂ in leaves is not sufficient to support photosynthesis. *Plant Physiology* **139**: 254-266
- Morison JIL, Jarvis PG** (1983) Direct and indirect effects of light on stomata .2. in *Commelina-communis* l. *Plant Cell and Environment* **6**: 103-109
- Motomura H, Yukawa T, Ueno O, Kagawa A** (2008) The occurrence of crassulacean acid metabolism in *Cymbidium* (Orchidaceae) and its ecological and evolutionary implications. *Journal of Plant Research* **121**: 163-177
- Nakahira Y, Baba K, Yoneda A, Shiina T, Toyoshima Y** (1998) Circadian-regulated transcription of the psbD light-responsive promoter in wheat chloroplasts. *Plant Physiology* **118**: 1079-1088

- Nakasako M, Zikihara K, Matsuoka D, Katsura H, Tokutomi S** (2008) Structural basis of the LOV1 dimerization of Arabidopsis phototropins 1 and 2. *Journal of Molecular Biology* **381**: 718-733
- Nelson EA, Sage RF** (2008) Functional constraints of CAM leaf anatomy: tight cell packing is associated with increased CAM function across a gradient of CAM expression. *Journal of Experimental Botany* **59**: 1841-1850
- Nelson EA, Sage TL, Sage RF** (2005) Functional leaf anatomy of plants with crassulacean acid metabolism. *Functional Plant Biology* **32**: 409-419
- Nicot N, Hausman JF, Hoffmann L, Evers D** (2005) Housekeeping gene selection for real-time RT-PCR normalization in potato during biotic and abiotic stress. *Journal of Experimental Botany* **56**: 2907-2914
- Nimmo GA, Nimmo HG, Fewson CA, Wilkins MB** (1984) Diurnal changes in the properties of phosphoenolpyruvate carboxylase in *Bryophyllum* leaves - a possible covalent modification. *Febs Letters* **178**: 199-203
- Nimmo GA, Nimmo HG, Hamilton ID, Fewson CA, Wilkins MB** (1986) Purification of the phosphorylated night form and dephosphorylated day form of phosphoenolpyruvate carboxylase from *Bryophyllum-fedtschenkoi*. *Biochemical Journal* **239**: 213-220
- Nimmo HG** (1998) Circadian regulation of a plant protein kinase. *Chronobiology International* **15**: 109-118
- Nimmo HG** (2003) How to tell the time: the regulation of phosphoenolpyruvate carboxylase in Crassulacean acid metabolism (CAM) plants. *Biochemical Society Transactions* **31**: 728-730
- Nishio JN, Ting IP** (1987) Carbon Flow and Metabolic Specialization in the Tissue Layers of the Crassulacean Acid Metabolism Plant, *Peperomia camptotricha*. *Plant Physiology* **84**: 600-604
- Nobel PS** (1988) *Environmental Biology of Agaves and Cacti*. Cambridge University Press., New York
- Nobel PS** (1991) *Physicochemical and environmental plant physiology*. Academic Press, San Diego
- Noblin X, Mahadevan L, Coomaraswamy IA, Weitz DA, Holbrook NM, Zwieniecki MA** (2008) Optimal vein density in artificial and real leaves. *Proceedings of the National Academy of Sciences of the United States of America* **105**: 9140-9144
- Ogawa T, Ishikawa H, Shimada K, Shibata K** (1978) Synergistic action of red and blue-light and action spectra for malate formation in guard cells of *Vicia-faba* l. *Planta* **142**: 61-65
- Osmond B, Maxwell, K., Popp, M., Robinson, S.** (1999) On being thick: Fathoming apparently futile pathways of photosynthesis and carbohydrate metabolism in succulent CAM plants. *In* BJ Burrell M, Kruger N (eds), ed, *Plant Carbohydrate Biochemistry*. BIOS, Oxford, pp 183-200
- Osmond CB** (1978) Crassulacean Acid Metabolism - Curiosity in Context. *Annual Review of Plant Physiology and Plant Molecular Biology* **29**: 379-414
- Outlaw WH** (1989) Critical-examination of the quantitative evidence for and against photosynthetic CO₂ fixation by guard-cells. *Physiologia Plantarum* **77**: 275-281
- Pandey S, Wang XQ, Coursol SA, Assmann SM** (2002) Preparation and applications of Arabidopsis thaliana guard cell protoplasts. *New Phytologist* **153**: 517-526
- Pearson PN, Palmer MR** (2000) Atmospheric carbon dioxide concentrations over the past 60 million years. *Nature* **406**: 695-699

- Piechulla B** (1999) Circadian expression of the light-harvesting complex protein genes in plants. *Chronobiology International* **16**: 115-128
- Pilgrim ML, McClung CR** (1993) Differential involvement of the circadian clock in the expression of genes required for ribulose-1,5-bisphosphate carboxylase oxygenase synthesis, assembly, and activation in *Arabidopsis-thaliana*. *Plant Physiology* **103**: 553-564
- Pipoly J, Kearns DM, Berry PE.** (1998) *Clusia*, Vol 4. Berry PE, Holst BK, Yatskievych K, eds., St Louis, MO, USA
- Pittendrigh CS** (1981) Circadian systems: general perspective. *In* J Aschoff, ed, ed, *Biological rhythms: handbook of behavioral neurobiology.*, Vol 4. New York: Plenum Press, pp 57-80
- Poffenroth M, Green DB, Tallman G** (1992) Sugar concentrations in guard-cells of *Vicia-faba* illuminated with red or blue-light - analysis by high-performance liquid-chromatography. *Plant Physiology* **98**: 1460-1471
- Poffenroth M, Green DB, Tallman G** (1992) Sugar Concentrations in Guard Cells of *Vicia faba* Illuminated with Red or Blue Light : Analysis by High Performance Liquid Chromatography. *Plant Physiology* **98**: 1460-1471
- Poorter H, Niinemets U, Poorter L, Wright IJ, Villar R** (2009) Causes and consequences of variation in leaf mass per area (LMA): a meta-analysis (vol 182, pg 565, 2009). *New Phytologist* **183**: 1222-1222
- Popma J, Bongers F, Werger MJA** (1992) Gap-dependence and leaf characteristics of trees in a tropical lowland rain-forest in Mexico. *Oikos* **63**: 207-214
- Pyankov VI, Kondratchuk AV, Shipley B** (1999) Leaf structure and specific leaf mass: the alpine desert plants of the Eastern Pamirs, Tadjikistan. *New Phytologist* **143**: 131-142
- Quail PH, Boylan MT, Parks BM, Short TW, Xu Y, Wagner D** (1995) Phytochromes - photosensory perception and signal-transduction. *Science* **268**: 675-680
- Quarrie SA, Jones HG** (1977) Effects of abscisic-acid and water stress on development and morphology of wheat. *Journal of Experimental Botany* **28**: 192-&
- Quinones MA, Lu ZM, Zeiger E** (1996) Close correspondence between the action spectra for the blue light responses of the guard cell and coleoptile chloroplasts, and the spectra for blue light-dependent stomatal opening and coleoptile phototropism. *Proceedings of the National Academy of Sciences of the United States of America* **93**: 2224-2228
- Radoglou KM, Jarvis PG** (1990) Effects of CO₂ enrichment on 4 poplar clones .1. growth and leaf anatomy. *Annals of Botany* **65**: 617-626
- Ramirez SR, Gravendeel B, Singer RB, Marshall CR, Pierce NE** (2007) Dating the origin of the Orchidaceae from a fossil orchid with its pollinator. *Nature* **448**: 1042-1045
- Ramos C, Hall AE** (1983) Effects of photon fluence rate and intercellular CO₂ partial-pressure on leaf conductance and co₂ uptake rate in *Capsicum* and *Amaranthus*. *Photosynthetica* **17**: 34-42
- Raschke K, Pierce M, Popiela CC** (1976) Abscisic-acid content and stomatal sensitivity to CO₂ in leaves of *Xanthium-strumarium* l after pretreatments in warm and cold growth chambers. *Plant Physiology* **57**: 115-121
- Raven JA, Spicer, R.A** (1996) The Evolution of Crassulacean acid metabolism. *In* SJ Winter K, (eds.), ed, *Crassulacean acid metaboism: Biochemistry, ecphysiology and evolution*. Berlin: Springer-Verlag

- Reckmann U, Scheibe R, Raschke K** (1990) Rubisco activity in guard-cells compared with the solute requirement for stomatal opening. *Plant Physiology* **92**: 246-253
- Reed JW, Nagatani A, Elich TD, Fagan M, Chory J** (1994) Phytochrome-a and phytochrome-B have overlapping but distinct functions in Arabidopsis development. *Plant Physiology* **104**: 1139-1149
- Roberts S, Griffiths H, Borland AM, Reinert F** (1996) Is crassulacean acid metabolism activity in sympatric species of hemi-epiphytic stranglers such as *Clusia* related to carbon cycling as a photoprotective process? *Oecologia* **106**: 28-38
- Roelfsema MRG, Hedrich R** (2005) In the light of stomatal opening: new insights into 'the Watergate'. *New Phytologist* **167**: 665-691
- Roth-Nebelsick A** (2001) Heat transfer of rhyniophytic plant axes. Review of Palaeobotany and Palynology **116**: 109-122
- Russo SE, Cannon WL, Elowsky C, Tan S, Davies SJ** (2010) Variation in leaf stomatal traits of 28 tree species in relation to gas exchange along an edaphic gradient in a Bornean rain forest. *Am. J. Bot.* **97**: 1109-1120
- Sack L, Frole K** (2006) Leaf structural diversity is related to hydraulic capacity in tropical rain forest trees. *Ecology* **87**: 483-491
- Sage R** (2002) Are crassulacean acid metabolism and C-4 photosynthesis incompatible? *Functional Plant Biology* **29**: 775-785
- Sage RF** (2001) Environmental and evolutionary preconditions for the origin and diversification of the C4 photosynthetic syndrome. *Plant Biol (Stuttg)* **3**: 202,213
- Sage RF** (2004) The evolution of C4 photosynthesis. *New Phytologist* **161**: 341-370
- Sakai T, Kagawa T, Kasahara M, Swartz TE, Christie JM, Briggs WR, Wada M, Okada K** (2001) Arabidopsis *nph1* and *npl1*: Blue light receptors that mediate both phototropism and chloroplast relocation. *Proceedings of the National Academy of Sciences of the United States of America* **98**: 6969-6974
- Sakamoto K, Briggs WR** (2002) Cellular and Subcellular Localization of Phototropin 1. *Plant Cell* **14**: 1723-1735
- Salomon M, Christie JM, Knieb E, Lempert U, Briggs WR** (2000) Photochemical and mutational analysis of the FMN-binding domains of the plant blue light receptor, phototropin. *Biochemistry* **39**: 9401-9410
- Salomon M, Knieb E, von Zeppelin T, Rudiger W** (2003) Mapping of low- and high-fluence autophosphorylation sites in phototropin 1. *Biochemistry* **42**: 4217-4225
- Salvador ML, Klein U, Bogorad L** (1993) Light-regulated and endogenous fluctuations of chloroplast transcript levels in *Chlamydomonas* - regulation by transcription and RNA degradation. *Plant Journal* **3**: 213-219
- Sancar A, Thompson C, Thresher RJ, Araujo F, Mo J, Ozgur S, Vagas E, Dawut L, Selby CP** (2000) Photolyase/cryptochrome family blue-light photoreceptors use light energy to repair DNA or set the circadian clock. *Cold Spring Harbor Symposia on Quantitative Biology* **65**: 157-171
- Sayed O** (1998) Succulent plants inhabiting desert depressions in eastern Arabia were predominantly leaf succulents exhibiting a variety of adaptations. *Journal of arid environments* **40**: 177-189
- Scarano FR** (2009) Plant communities at the periphery of the Atlantic rain forest: Rare-species bias and its risks for conservation. *Biological Conservation* **142**: 1201-1208
- Scarano FR, Duarte HM, Franco AC, Geßler A, de Mattos EA, Nahm M, Rennenberg H, Zaluar HLT, Lüttge U** (2005) Ecophysiology of selected tree species in different plant communities at the periphery of the Atlantic Forest of

- SE Brazil I. Performance of three different species of *Clusia* in an array of plant communities. *Trees - Structure and Function* **19**: 497-509
- Schaffer R, Landgraf J, Accerbi M, Simon V, Larson M, Wisman E** (2001) Microarray analysis of diurnal and circadian-regulated genes in *Arabidopsis*. *Plant Cell* **13**: 113-123
- Schmitt AK, Lee HSJ, Luttge U** (1988) The response of the C3-CAM tree, *Clusia-rosea*, to light and water-stress .1. gas-exchange characteristics. *Journal of Experimental Botany* **39**: 1581-1590
- Serrano EE, Zeiger E, Hagiwara S** (1988) Red-light stimulates an electrogenic proton pump in *Vicia* guard-cell protoplasts. *Proceedings of the National Academy of Sciences of the United States of America* **85**: 436-440
- Shalitin D, Yang HY, Mockler TC, Maymon M, Guo HW, Whitelam GC, Lin CT** (2002) Regulation of *Arabidopsis* cryptochrome 2 by blue-light-dependent phosphorylation (vol 417, pg 763, 2002). *Nature* **418**: 447-447
- Sharkey TD, Ogawa T** (1987) *Stomatal response to light*. Stanford University Press., Stanford, CA
- Sharkey TD, Raschke K** (1981) Effect of light quality on stomatal opening in leaves of *Xanthium-strumarium* L. *Plant Physiology* **68**: 1170-1174
- Sharrock RA, Clack T** (2002) Patterns of expression and normalized levels of the five *Arabidopsis* phytochromes. *Plant Physiology* **130**: 442-456
- Sharrock RA, Quail PH** (1989) Novel phytochrome sequences in *Arabidopsis-thaliana* - structure, evolution, and differential expression of a plant regulatory photoreceptor family. *Genes & Development* **3**: 1745-1757
- Shimazaki KI, Doi M, Assmann SM, Kinoshita T** (2007) Light regulation of stomatal movement. *Annual Review of Plant Biology* **58**: 219-247
- Shimazaki Y, Pratt LH** (1985) Immunochemical detection with rabbit polyclonal and mouse monoclonal-antibodies of different pools of phytochrome from etiolated and green avena shoots. *Planta* **164**: 333-344
- Shinomura T, Nagatani A, Chory J, Furuya M** (1994) The induction of seed-germination in *Arabidopsis-thaliana* is regulated principally by phytochrome-b and secondarily by phytochrome-A. *Plant Physiology* **105**: 773-773
- Shipley B** (1995) Structured Interspecific Determinants of Specific Leaf-Area in 34 Species of Herbaceous Angiosperms. *Functional Ecology* **9**: 312-319
- Shorrocks K** (2009) *Physiological and molecular aspects of drought resistance in Clusia*. Newcastle University, Newcastle upon Tyne
- Silvera K, Santiago LS, Cushman JC, Winter K** (2009) Crassulacean acid metabolism and epiphytism linked to adaptive radiations in the Orchidaceae. *Plant Physiology* **149**: 1838-1847
- Sipes DL, Ting IP** (1985) Crassulacean Acid Metabolism and Crassulacean Acid Metabolism Modifications in *Peperomia-Camptotricha*. *Plant Physiology* **77**: 59-63
- Smith JAC, Ingram J, Tsiantis MS, Barkla BJ, Bartholomew DM, Betej M, Pantoja O, Pennington AJ** (1996) Transport across the vacuolar membrane in CAM plants. *Crassulacean Acid Metabolism* **114**: 53-71
- Smith JAC, Luttge U** (1985) Day-night changes in leaf water relations associated with the rhythm of crassulacean acid metabolism in *Kalanchoe-daigremontiana*. *Planta* **163**: 272-282
- Smith JAC, Winter K** (1996) Taxonomic distribution of Crassulacean acid metabolism. *Crassulacean Acid Metabolism* **114**: 427-436

- Smith WK, Hughes NM** (2009) Progress in Coupling Plant Form and Photosynthetic Function. *Castanea* **74**: 1-26
- Somers DE, Devlin PF, Kay SA** (1998) Phytochromes and cryptochromes in the entrainment of the Arabidopsis circadian clock. *Science* **282**: 1488-1490
- Sommerville KE, Gimeno TE, Ball MC** (2010) Primary nerve (vein) density influences spatial heterogeneity of photosynthetic response to drought in two Acacia species. *Functional Plant Biology* **37**: 840-848
- Srivastava A, Lu Z, Zeiger E** (1995) Modification of guard cell properties in advanced lines of Pima cotton bred for higher yields and heat resistance. *Plant Science* **108**: 125-131
- Sturzenbaum SR, Kille P** (2001) Control genes in quantitative molecular biological techniques: the variability of invariance. *Comparative Biochemistry and Physiology B-Biochemistry & Molecular Biology* **130**: 281-289
- Suetsugu N, Mittmann F, Wagner G, Hughes J, Wada M** (2005) A chimeric photoreceptor gene, NEOCHROME, has arisen twice during plant evolution. *Proceedings of the National Academy of Sciences of the United States of America* **102**: 13705-13709
- Susuki K, Shinshi H** (1995) Transient activation and tyrosine phosphorylation of a protein kinase in tobacco cells treated with a fungal elicitor *The Plant Cell* **7**: 639-647
- Swartz TE, Corchnoy SB, Christie JM, Lewis JW, Szundi I, Briggs WR, Bogomolni RA** (2001) The photocycle of a flavin-binding domain of the blue light photoreceptor phototropin. *Journal of Biological Chemistry* **276**: 36493-36500
- Taiz L, Zeiger, Eduardo.** (2002) *Plant Physiology*, Ed Third Edition. Sinauer Associates, Sunderland, MA
- Talbott LD, Shmayevich IJ, Chung YS, Hammad JW, Zeiger E** (2003) Blue light and phytochrome-mediated stomatal opening in the npq1 and phot1 phot2 mutants of Arabidopsis. *Plant Physiology* **133**: 1522-1529
- Talbott LD, Zeiger E** (1993) Sugar and organic-acid accumulation in guard-cells of vicia-faba in response to red and blue-light. *Plant Physiology* **102**: 1163-1169
- Talbott LD, Zhu JX, Han SW, Zeiger E** (2002) Phytochrome and blue light-mediated stomatal opening in the orchid, *Paphiopedilum*. *Plant and Cell Physiology* **43**: 639-646
- Tallman G, Zhu JX, Mawson BT, Amodeo G, Nouhi Z, Levy K, Zeiger E** (1997) Induction of CAM in *Mesembryanthemum crystallinum* abolishes the stomatal response to blue light and light-dependent zeaxanthin formation in guard cell chloroplasts. *Plant and Cell Physiology* **38**: 236-242
- Taybi T, Nimmo HG, Borland AM** (2004) Expression of phosphoenolpyruvate carboxylase and phosphoenolpyruvate carboxylase kinase genes. implications for genotypic capacity and phenotypic plasticity in the expression of crassulacean acid metabolism. *Plant Physiol.* **135**: 587-598
- Teeri JA, Tonsor SJ, Turner M** (1981) Leaf thickness and carbon isotope composition in the crassulaceae. *Oecologia* **50**: 367-369
- Ticha I** (1982) PHOTOSYNTHETIC CHARACTERISTICS DURING ONTOGENESIS OF LEAVES .7. STOMATA DENSITY AND SIZES. *Photosynthetica* **16**: 375-471
- Ting IP** (1985) Crassulacean Acid Metabolism. *Annual Review of Plant Physiology* **36**: 595-622

- Tokuhisa JG, Daniels SM, Quail PH** (1985) Phytochrome in green tissue - spectral and immunochemical evidence for 2 distinct molecular-species of phytochrome in light-grown *Avena-sativa* l. *Planta* **164**: 321-332
- Toth R, Kevei E, Hall A, Millar AJ, Nagy F, Kozma-Bognar L** (2001) Circadian clock-regulated expression of phytochrome and cryptochrome genes in *Arabidopsis*. *Plant Physiol.* **127**: 1607-1616
- Troughton JH, K. A. Card and C. H. Hendy** (1974) Photosynthetic pathways and carbon isotope discrimination by plants, Vol 73
- Vaasen A, Begerow D, Hampp R** (2006) Phosphoenolpyruvate carboxylase genes in C3, crassulacean acid metabolism (CAM) and C3/CAM intermediate species of the genus *Clusia*: rapid reversible C3/CAM switches are based on the C3 housekeeping gene. *Plant, Cell & Environment* **29**: 2113-2123
- Vaasen A, Begerow D, Luttge U, Hampp R** (2002) The genus *clusia* L.: Molecular evidence for independent evolution of photosynthetic flexibility. *Plant Biology* **4**: 86-93
- Van den Eynden V, Oatham MP, Johnson W** (2008) How free access internet resources benefit biodiversity and conservation research: Trinidad and Tobago's endemic plants and their conservation status. *Oryx* **42**: 400-407
- Vargas-Soto J, Andrade J, Winter K** (2009) Carbon isotope composition and mode of photosynthesis in *Clusia* species from Mexico. *Photosynthetica* **47**: 33-40
- Vendramini F, Diaz S, Gurvich DE, Wilson PJ, Thompson K, Hodgson JG** (2002) Leaf traits as indicators of resource-use strategy in floras with succulent species. *New Phytologist* **154**: 147-157
- Vile D, Garnier E, Shipley B, Laurent G, Navas ML, Roumet C, Lavorel S, Diaz S, Hodgson JG, Lloret F, Midgley GF, Poorter H, Rutherford MC, Wilson PJ, Wright IJ** (2005) Specific leaf area and dry matter content estimate thickness in laminar leaves. *Annals of Botany* **96**: 1129-1136
- Von Caemmerer S, Farquhar GD** (1981) Some relationships between the biochemistry of photosynthesis and the gas exchange of *Phaseolus-vulgaris* cultivar hawkesbury-wonder leaves. *Planta (Heidelberg)* **153**: 376-387
- Von Caemmerer S, Griffiths H** (2009) Stomatal responses to CO₂ during a diel Crassulacean acid metabolism cycle in *Kalanchoe daigremontiana* and *Kalanchoe pinnata*. *Plant Cell and Environment* **32**: 567-576
- von Caemmerer S, Lawson T, Oxborough K, Baker NR, Andrews TJ, Raines CA** (2004) Stomatal conductance does not correlate with photosynthetic capacity in transgenic tobacco with reduced amounts of Rubisco. *Journal of Experimental Botany* **55**: 1157-1166
- Wada M, Kagawa T, Sato Y** (2003) Chloroplast movement. *Annual Review of Plant Biology* **54**: 455-468
- Webb A** (1998) Stomatal rhythms. In MA Lumsden P, eds, ed, *Biology rhythms and photoperiodism in plants*. Bios Scientific, Oxford, UK, pp 69 – 80
- Weyers JDB, Johansen LG** (1985) Accurate estimation of stomatal aperture from silicone-rubber impressions. *New Phytologist* **101**: 109-115
- Wilkins MB** (1992) Circadian-rhythms - their origin and control. *New Phytologist* **121**: 347-375
- Wilson PJ, Thompson K, Hodgson JG** (1999) Specific leaf area and leaf dry matter content as alternative predictors of plant strategies. *New Phytologist* **143**: 155-162

- Winter K, Aranda J, Holtum JAM** (2005) Carbon isotope composition and water-use efficiency in plants with crassulacean acid metabolism. *Functional Plant Biology* **32**: 381-388
- Winter K, Garcia M, Holtum JAM** (2008) On the nature of facultative and constitutive CAM: environmental and developmental control of CAM expression during early growth of *Clusia*, *Kalanchoe* and *Opuntia*. *Journal of Experimental Botany* **59**: 1829-1840
- Winter K, Garcia M, Holtum JAM** (2009) Canopy CO₂ exchange of two neotropical tree species exhibiting constitutive and facultative CAM photosynthesis, *Clusia rosea* and *Clusia cylindrica*. *Journal of Experimental Botany* **60**: 3167-3177
- Winter K, Holtum JAM** (2002) How closely do the delta C-13 values of crassulacean acid metabolism plants reflect the proportion of CO₂ fixed during day and night? *Plant Physiology* **129**: 1843-1851
- Winter K, Medina E, Garcia V, Mayoral ML, Muniz R** (1985) Crassulacean acid metabolism in roots of a leafless orchid, *Campylocentrum-tyrridion garay* and *dunsterv.* *Journal of Plant Physiology* **118**: 73-78
- Winter K, Smith JAC** (1996) Crassulacean acid metabolism: Current status and perspectives. *Crassulacean Acid Metabolism* **114**: 389-426
- Winter K, Smith JAC** (1996) An introduction to crassulacean acid metabolism. Biochemical principles and ecological diversity. *Crassulacean Acid Metabolism* **114**: 1-13
- Winter K, Wallace BJ, Stocker GC, Roksandic Z** (1983) Crassulacean acid metabolism in australian vascular epiphytes and some related species. *Oecologia* **57**: 129-141
- Witkowski ETF, Lamont BB** (1991) Leaf specific mass confounds leaf density and thickness. *Oecologia* **88**: 486-493
- Woerner AC, Martin CE** (1999) Mechanistic basis of differences in water-use efficiency between a CAM and a C-3 species of *Peperomia* (Piperaceae). *New Phytologist* **144**: 307-312
- Wong ML, Medrano JF** (2005) Comment on Wong and Medrano's "Real-time PCR for mRNA quantification" - Response. *Biotechniques* **39**: 484-485
- Wong SC, Cowan IR, Farquhar GD** (1978) Leaf conductance in relation to assimilation in *Eucalyptus-pauciflora* sieb ex spreng - influence of irradiance and partial-pressure of carbon-dioxide. *Plant Physiology* **62**: 670-674
- Woodward FI, Lake JA, Quick WP** (2002) Stomatal development and CO₂: ecological consequences. *New Phytologist* **153**: 477-484
- Yulin LI1, Douglas A. JOHNSON2, Yongzhong SU1, Jianyuan CUI1, and Tonghui ZHANG1** (2005) Specific leaf area and leaf dry matter content of plants growing in sand dunes. *Bot. Bull. Acad. Sin* **46**: 127-134
- Yulin LI, Douglas A. Johnson, Yongzhong SU, Jianyuan CUI, and Tonghui Zhang** (2005) Specific leaf area and leaf dry matter content of plants growing in sand dunes. *Bot. Bull. Acad. Sin* **46**: 127-134
- Zeiger E** (1990) Light perception in guard-cells. *Plant Cell and Environment* **13**: 739-744
- Zeiger E, Hepler PK** (1977) Light and stomatal function - blue-light stimulates swelling of guard cell protoplasts. *Science* **196**: 887-889
- Zeiger E, Iino, M., Shimazaki, K. and Ogawa, T.** (1987) The blue-light responses of stomata: mechanism and function. Stanford University Press, Stanford, CA.

- Zeiger E, Talbott LD, Frechilla S, Srivastava A, Zhu JX** (2002) The guard cell chloroplast: a perspective for the twenty-first century. *New Phytologist* **153**: 415-424
- Zeiger E, Zhu JX** (1998) Role of zeaxanthin in blue light photoreception and the modulation of light-CO₂ interactions in guard cells. *Journal of Experimental Botany* **49**: 433-442
- Zhang N, Portis AR** (1999) Mechanism of light regulation of Rubisco: A specific role for the larger Rubisco activase isoform involving reductive activation by thioredoxin-f. *Proceedings of the National Academy of Sciences of the United States of America* **96**: 9438-9443
- Zhong HH, Resnick AS, Straume M, McClung CR** (1997) Effects of synergistic signaling by phytochrome A and cryptochrome1 on circadian clock-regulated catalase expression. *Plant Cell* **9**: 947-955
- Zotz G** (2004) How prevalent is crassulacean acid metabolism among vascular epiphytes? *Oecologia* **138**: 184-192
- Zotz G, Hietz P** (2001) The physiological ecology of vascular epiphytes: current knowledge, open questions. *Journal of Experimental Botany* **52**: 2067-2078